Utilizing Riverine Ecosystem for Optimal Benefits

Thesis submitted in partial fulfilment of the requirements

For the award of the degree of

DOCTOR OF PHILOSOPHY

by

Gaurav Talukdar

Department of Civil Engineering

Indian Institute of Technology Guwahati

Guwahati – 781 039, Assam, India

September 2022

Utilizing Riverine Ecosystem for Optimal Benefits

Thesis submitted in partial fulfilment of the requirements

For the award of the degree of

DOCTOR OF PHILOSOPHY

in

Civil Engineering

by

Gaurav Talukdar

(Roll No. 166104104)

Under the supervision of

Prof. Arup Kumar Sarma

Prof. Rajib Kumar Bhattacharjya

Department of Civil Engineering

Indian Institute of Technology Guwahati

Guwahati – 781 039, Assam, India

September 2022

Dedicated

To my beloved Parents, my friends

&

Mentors

INDIAN INSTITUTE OF TECHNOLOGY GUWAHATI

DEPARTMENT OF CIVIL ENGINEERING

STATEMENT

I do hereby declare that the content embodied in this thesis entitled **"Utilizing Riverine Ecosystem for Optimal Benefits"** is the result of investigation carried out by me at Department of Civil Engineering, Indian Institute of Technology Guwahati, Guwahati, India under the guidance of Prof. Arup Kumar Sarma and Prof. Rajib Kumar Bhattacharjya.

In keeping with the general practice of reporting scientific observations, due acknowledgements have been made wherever the work described is based on the findings of others investigators.

September 2022

Gaurav Talukdar

Roll No. 166104104

Department of Civil Engineering

Indian Institute of Technology Guwahati

Guwahati, Assam, India

INDIAN INSTITUTE OF TECHNOLOGY GUWAHATI

DEPARTMENT OF CIVIL ENGINEERING

CERTIFICATE

This is to certify that the work described in this thesis entitled **"Utilizing Riverine Ecosystem for Optimal Benefits"** by **Mr. Gaurav Talukdar (Roll No. 166104104)** for the award of **Doctoral of Philosophy** is an authentic record of the results obtained from the research work carried out under our supervision in the Department of Civil Engineering, Indian Institute of Technology Guwahati, India and this work has not been submitted elsewhere for a degree.

Dr. Arup Kumar Sarma
Professor
Department of Civil Engineering
Indian Institute of Technology Guwahati
Guwahati -781039, Assam, India

Dr. Rajib Kumar Bhattacharjya
Professor
Department of Civil Engineering
Indian Institute of Technology Guwahati
Guwahati – 781039, Assam, India

Acknowledgements

The tenure in IIT Guwahati as a PhD student has been an amazing and challenging experience for me which I will cherish in my journey to Life. It is full of my patience, support and encouragement from numerous individuals. I take my utmost pleasure to express my deepest gratitude to each and every one who supported me in several ways to complete my PhD Dissertation.

The first and foremost gratitude to my supervisors Prof. Arup Kumar Sarma and Prof. Rajib Kumar Bhattacharjya for their patience, valuable suggestions, motivation and constant support throughout my research work. I earnestly thank them for their humbleness, spending their valuable time and effort for imbibing scientific temperament and appreciable work ethics in me.

I would like to express my sincere gratitude to all my doctoral committee members Prof. Sudip Talukdar, Prof. Sachin K Kakoty and Prof. Bimlesh Kumar for their encouragement and insightful advice during my seminars and progress reviews that has led to the successful completion of my thesis.

I would also like to highly express my heartfelt gratitude to Prof. Sharad Gokhale, Head, Department of Civil Engineering for his help and support and also believing in me for carrying out my research work. I highly appreciate the ex-head of the department Prof. Chandan Mahanta and office bearers in the Department of Civil Engineering for imparting the facilities to carry out the research.

I want to express my appreciation to the Ministry of Human Resources Development, Government of India, for their support in the form of Ph.D. scholarship through IIT Guwahati.

I would also like to express my gratitude towards Center for Instrument Facility (CIF), IIT Guwahati for allowing me to carry out various experiments in their laboratory, and their staffs for helping me to access various instrument for my PhD work.

I will be always grateful to my friends and lab mates at IIT Guwahati Dr. Arup Jyoti Borah, Dr. Gurpreet Singh Sodhi, Ms. Gloria Narayan, Dr. Ashutosh Sharma, Dr. Gilbert Hinge, Dr. Sagarika Patowary, Dr. Bandita Barman, Dr. Pulendra Dutta, Dr. Jayshree Hazarika, Mr. P K Sarma, Ms. Dipima Sarma, Anupal, Dipsikha, Bhaswatee, Jeffrey, Tufa, Anurag,

Satheesh, Vishnu, Vijay and Shakti Di for their help, love and support. Without their help and support it would have been difficult to carry forward my work patiently. I would like to thank Amit, Dhruba, Priyam and Bikul, for helping me in smoothly conducting my laboratory experiments. I would also like to specially thank Bazal Haque for his immense help in accompanying me while conducting the field visits.

I am grateful to Hostel Affairs Board (HAB), Hostel Mess committee (HMC), Dibang, Students Affairs Board (SAB), IITG Gymkhana Sports Board for believing in me and making me part of it. I am very much thankful and obliged to work under them and able to represent my institute with zeal and enthusiasm.

I am also grateful to the IIT Guwahati Volleyball Team, IIT Guwahati Football Team, IIT Guwahati Cricket Team, PhD Premier League (PPL) Cricket Team, Football Team, SPARDHA Team, and all my friends for their believe and support in working as a team. I would also like to thank my friends, seniors and juniors of Dibang, Disang and Kapili hostel.

At last but not the least, I am highly indebted to my parents, Mr. Ashok Chandra Talukdar (Baba), Mrs. Rumjum Talukdar (Ma), my brother and his family for all sacrifices they have made for my better future, to have faith in me and giving me freedom to take my own decision. I also thank the rest of my family and fraternity outside IIT Guwahati. I would like to thank Almighty for his blessings and giving patience and strength to carry out my research in good health.

Sincerely

Gaurav Talukdar

Abstract

The intrinsic value of nature provides a variety of benefits in the form of ecosystem services that support the world economy and advance social and economic well-being. Since rivers have always been an important component of the landscape, riverscapes are just as important as landscapes. Since the beginning of time, it has provided various environmental benefits to thrive life within it. The complex interdependence between humans and nature is achieved by analyzing, modelling, quantifying, and valuing the degree to which humans are connected and benefitted from the ecosystem. Ecosystem services are now poised to provide real solutions to the problem of how to sustainably manage natural resources.

In large braided river systems around the world, there are various activities carried out along the floodplain. The floods bring fresh sediments along with them and deposits downstream. This process of aggravation and deposition of sediments due to the flow of water in the river leads to the formation of sandbars. The extent and characteristics of sandbars vary over the years due to the varying river morphology, making it difficult for researchers to conduct investigations in the river. This study attempts to understand the riverine ecosystem, particularly the sandbars within the Brahmaputra River, and the economic benefit derived from its utilization in agriculture and farming activities. The Brahmaputra River exhibits complex morphological characteristics due to wider braided river width, high flow, and sediment variability with erodible banks. A two-dimensional (2D) hydrodynamic model MIKE 21C was developed to determine the area available in the sandbar under different flow conditions. It can also be understood that increased urbanization has led to diminished mainland agricultural activities. The rapidly growing populations and rising food consumption necessitate either expansion of agricultural farmlands or sufficient production gains from existing resources. Riverine sandbars provide additional fertile landmass that could support farming and agricultural practices to cope with the rising food demand amidst urbanization.

The research encompasses land-use change using historical data and geospatial information. Intensive field investigations, questionnaire surveys, and data collection were done to determine current practices within the ecosystem. The questionnaire survey revealed various aspects of economic benefits, practices of sandbar cultivation, beneficial produce, difficulties faced, and willingness among farmers to expand sandbar cultivation. Satellite images were derived at decadal scales to determine the change in the land-use land

cover (LULC) within the Brahmaputra River in Assam, India. The analysis showed that the percentage of vegetated sandbars has increased and the percentage of non-vegetated sandbars has decreased during the years 1976-80 to 2016-17. Furthermore, it was found that the area under cropland and vegetated sandbar varied seasonally. The temporal variation of the vegetation status of crops grown in different sandbars was analyzed using the Normalized Differential Vegetative Index (NDVI). The interannual variation of NDVI values indicated the change in the crop cultivation period as well as different phases of growth and shifting of cropping patterns in the sandbars of the Brahmaputra River.

The study was carried out by gathering both primary and secondary data. To study the characteristics of sediments within the sandbars, a total of 126 samples from 42 sandbar locations were collected from the surface (topsoil), sub-soil (Upto depth of 30 cm), and bottom soil (30–100 cm depth). The samples were categorized as newly formed sandbars, vegetated sandbars, and cultivated sandbars and tested in the laboratory for the presence of nutrients and minerals. The experimental observations and field studies revealed that the vegetated and cultivated sandbars consist of silty and loamy soils, favoring agriculture and the newly formed sandbars were devoid of silt and clay, which can be utilized for growing crops like groundnut and some other vegetables, which requires sandy loam or clay loam soil. Although it was seen that sandbar activities had been carried out in a few sandbars within the Brahmaputra River, however, utilizing all possible agricultural land optimally is essential to alleviate the threat of food security and for the socio-economic development of society. As crop planning involves several possible and valuable objectives, which may or may not conflict with each other, a choice of judicious cropping pattern and temporal adjustments therein may be a useful strategy to minimize the possible crop damages and maximize economic returns and productivity. The uncertainties associated with the agricultural system were also handled through inexact multi-objective fuzzy programming optimization approaches, which could enable decision-makers to plan the cropping pattern ahead of time, thereby decreasing crop damage and economic losses. A substantial component of the uncertainty in agricultural productivity comes from seasonal variability linked to inter-annual climate fluctuations. The water level fluctuations could significantly impact crop growth within the sandbars. The seasonal forecasts were helpful in farmers' decision-making process as they predicted the expected streamflow in the near future. The historical information of the recent past events provided valuable information for future flows. To evaluate the economic losses an optimally planned riverine agricultural area

would suffer if the flow variation exceeds a certain threshold, a damage estimation model was developed. The model could comprehend the losses under fluctuating water level in different seasons in subsequent years that was found to vary between 5 and 34 percent in the study. With the practice of sandbar cropping and farming in riverine environments, farmers and dwellers need to understand risk and have risk management skills to better anticipate problems and reduce consequences. The study proposed a risk assessment approach for helping the decision-making process at a local level, addressing risks that affect agricultural areas near rivers, particularly the sandbars.

This study provides a framework for integrating modelling techniques with optimization approaches in an agricultural system under uncertainties within riverine ecosystems. The study shows the immense potential of utilizing the sandbars of large rivers to sustain food demands, alongside developing links between land-use change, ecosystem behaviour, and socio-economic development. The research works provide a vision towards utilizing the landmasses formed due to hydrological processes and morphological changes within the rivers around the globe that could sustain the food demand of the ever-increasing population.

Keywords: Riverine ecosystem; Mathematical modeling; Geospatial techniques; Optimization; Damage estimation; Risk assessment

Contents

List of Figures

List of Tables

List of Symbols

$	U.S. Dollar
%	Percentage
μ_k	membership function of the K^{th} objective function
μ_l	membership function of the L^{th} objective function
A_a	Available area under p, q, r, o
A_a	Available area
A_d	Damage area, i.e., the difference between the area at *t=1* and *t'=t+1*
A_d	Damage area
CC_{ij}	Cost of cultivation or cost of production (Rs/Ha)
D_{ana}	Duration of potential analogue
D_f	forecast duration
MP_{ij}	Market price (Rs/Kg),
N_{ana}	number of potential analogues
X_{ij}, A_{ij}	Area under i^{th} activity during the j^{th} season (Ha),
Y_{ij}	Crop yield (Kg/Ha)
Z_t	Total benefit (Rs)
$a_f(m)$	Forecast anomalies
$a_{p,b}$	Vector of the streamflow anomalies for the potential analogue with rank *b*
$a_p(k)$	Flow anomaly for each month *k*
a_t	Monthly anomalies
f^*	Fuzzy goals
m_{mon}	Monthly mean
q_t	Streamflow data
s_{mon}	Monthly standard deviation
₹	Rupees
≅	fuzziness
μ	fraction to which the existing area can be increased/decreased
C_s	coefficient of skewness

DC	Damage coefficient
DF	Damage factor
i	Types of activities/crop types
I	Total activities/crops
j	Season of the year
J	Total season
o, p, q, r	Water depth at 0 (dryland), 0-0.1m. 0.1-0.2m, 0.2-0.3m, respectively
t	time
C	coefficient of the objective function
L	lower limits
U	upper limits
d	Water depth
ω	weight coefficients

List of Abbreviations

1-D	One-Dimensional
2-D	Two-Dimensional
AD	Advection Dispersion
AD	Anderson-Darling
AI	Artificial Intelligence
ANN	Artificial Neural Network
ANUFLOOD	Australian National University Flood-Loss Adjustment And Abatement Computer Package
CASI	Compact Airborne Spectrographic Imager
CCHE	Center For Computational Hydroscience And Engineering
CFD	Computational Fluid Dynamics
CGA	Cumulative Genetic Algorithm
CLUE-S	Conversion of Land Use and its Effects at Small regional extent
CRIDA	Central Research Institute For Dryland Agriculture
CS	Chi-Square
DB	Dam break
DEFRA	Department for Environment, Food and Rural Affairs
DFO	Dartmouth Flood Observatory
DGPS	Differential Global Positioning System
DHI	Danish Hydraulic Institute
DM	Decision-Makers
DP	Dynamic Programming
DWOPER	Dynamic Wave Operational Model
EA	Evolutionary Algorithms
EB	Entrepreneurial Behaviour
ECDF	Empirical Cumulative Distribution Function
EDX/EDS	Energy-Dispersive X-Ray Spectroscopy
EVI	Enhanced Vegetation Index
F	Forest Cover
FAO	Food And Agriculture Organization
FDAP	Flood Damage Analysis Package

FESEM	Field Emission Scanning Electron Microscope
FFA	Flood Frequency Analysis
FHRC	Flood Hazard Research Centre
FLDWAV	Flood wave Routing Model
FLODSIM	Flood Damage Simulation
FMOLP	Fuzzy Multiobjective Linear Programming
FP	Fuzzy Programming
GDP	Gross Domestic Product
GEV	Generalized Extreme Value
GIS	Geographic Information System
GoA	Government of Assam
GP	Goal Programming
GPS	Global Positioning System
GVA	Gross Value Added
HA	Historical Analogues
HD	Hydrodynamic
HEC-RAS	Hydrologic Engineering Center-River Analysis System
HYV	High Yield Varieties
ICPR	International Commission For The Protection Of The Rhine
ILP	Inexact Linear Programming
IMOFLP	Inexact Multiobjective Fuzzy Linear Programming
IPP	Integer Programming models
IRS	Indian Remote Sensing
IS	Indian Standard
ITLUM	Integrated Transportation and Land-Use Model
JCPDS	Joint Committee on Powder Diffraction Standard
KS	Kolmogorov-Smirnov
KVK	Krishi Vigyan Kendra
LBV	Lower Brahmaputra Valley
LEM	Landscape Evolution Models
LISS	Linear Imaging Self Scanning Sensor
LN	Log-Normal
LP	Linear Programming

LULC	Land-Use And Land Cover
MACO	Multi-Type Ant Colony Optimization
MEA	Millennium Ecosystem Assessment
MLC	Maximum Likelihood Classification
MLUA	Multi-Site Land Use Allocation
MOEA	Multiobjective Evolutionary Algorithms
MOLP	Multiobjective Linear Programming
MOLU	Multi Objective Optimization Of Land Use
MSE	Mean Square Error
MT	Mud transport
NDVI	Normalized Differential Vegetative Index
NDWI	Normalized Differential Water Index
NESAC	North Eastern Space Applications Centre
NIR	Near Infrared
NLP	Nonlinear Programming
NSGA	Non-Dominated Sorting Genetic Algorithm
NVS	Non-Vegetated Sandbars
OLI	Operational Land Imager
PA	Particle Analysis
PAD	Peace-Athabasca Delta
PF	Persistence Flow
PSA	Particle size analysis
PSO	Particle Swarm Optimization
ReLU	Rectified Linear Unit
RISAT	Radar Imaging Satellite
RMSE	Root Mean Square Error
RR	Rainfall Runoff
RS	Remote Sensing
SA	Simulated Annealing
SCADE	Silsoe College Agricultural Drainage Evaluation
SLUA	Single Land Use Allocation Model
SMOLA	Sustainable Multiobjective Land Use Allocation
SO	Structure Operation

SRH	Sedimentation And River Hydraulics
SRI	System Of Rice Intensification
SSC	Suspended Sediment Concentration
SSM	Sustainable Soil Management
ST	Sediment Transport
SVM	Support Vector Machines
SWIR	Short Wave Infrared
TIRS	Thermal Infrared Sensor
TM	Thematic Mapper
TS	Total Station
USDA	United States Department Of Agriculture
USGS	United States Geological Survey
UTM	Universal Transverse Mercator
VS	Vegetated Sandbars
W-AI	Wavelet-Artificial Intelligence
WB	Waterbody
WGS	World Geodetic System
XRD	X-Ray Diffraction

1

Introduction

1.1 General

Nature's intrinsic worth delivers a wide range of advantages in the form of ecosystem services that fuel the global economy and promote human and social well-being (MA 2005, Kumar 2010). Tourism, forestry, agriculture, and the food and beverage industries are all sustained by nature, and they provide possibilities for recreation, cultural inspiration, and spiritual fulfillment. Riverscapes are just as essential as landscapes since rivers have always been a vital part of the landscape. The river system includes the shifting riverbeds, banks, woodlands, marshes, backwaters, and meadows of its floodplains. Rivers transport dissolved minerals, sediment, and nutrient-rich detritus from living and dead plants and animals. The diversity of rivers varies spatially across countries as well as in different seasons. Seasonal and annual variations in the amount of sediments and nutrients carried downstream could be significant, and such depositions over time improve the river's use in a variety of ways. Near the rivers, a diverse range of flora and fauna, plants, and animals thrive. It provides environmental services that have drawn humanity to them since the dawn of time. Figure 1.1 shows a schematic diagram of human dependency on river-floodplain systems.

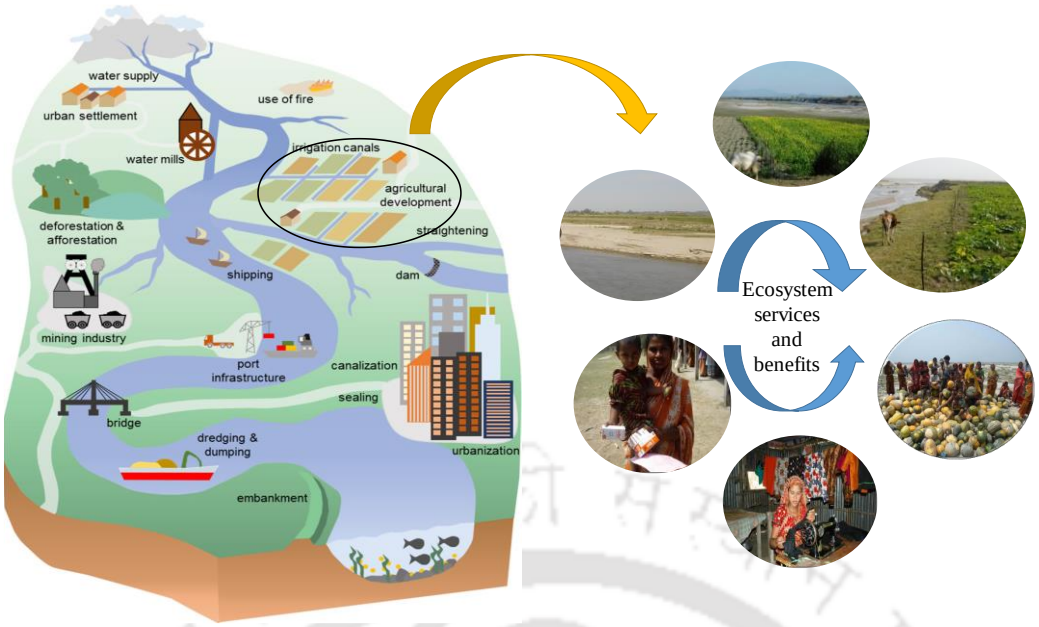

Figure 1.1: Schematic diagram of human dependency on river–floodplain systems (Maaß, 2019)

Large river systems around the world, such as the Mekong, the Brahmaputra, and the Mississippi, provide a vast array of services that benefit human well-being. The Brahmaputra is the fourth largest river in the world in terms of average flow discharge, whereas the river ranks 22nd in terms of the drainage area (Sarma and Acharjee 2018). It is a massive braided river that flows through China, India, and Bangladesh (Tandon and Sinha, 2007). High discharge, variable morphology, high bed aggradations, and severe erosion describe the river. In Assam's floodplains, it maintains a huge braiding in significant segments. Millions of people are dependent on this river for their livelihood, and land is extremely valuable within the river. The dwellers residing in the floodplains rely on the normal flood to bring fresh sediments to the floodplains favouring agriculture and farming. As a result, the river has been used for a variety of purposes, including agriculture, aquaculture, grazing, transportation, drinking, and washing. The river is governed by both high and low flows resulting in tremendous modifications in the bed.

1.2 Riverine Ecosystem and its services

Humanity is rediscovering an important interdependent relationship between humans and nature. The concept of the riverine ecosystem makes this interdependence apparent and quantitative, which is achieved by analysing, modelling, quantifying and valuing the degree to which humans are connected and benefitted from the ecosystems (Nicholls et al., 2018). The riverine ecosystem encompasses ecological, social, and economic processes (ecosystem functions) that interconnect organisms (ecosystem structure), including

humans, over some time period (Stanford et al., 2017). It provides a range of services that are of fundamental importance to human well-being, health, livelihood, and survival (Costanza et al. 1997; MEA 2005; de Groot et al. 2014). Ecosystem services are now poised to provide real solutions to the problem of how to sustainably manage natural resources. The Millennium Ecosystem Assessment (MEA) identified four major categories of ecosystem services: provisioning, regulating, cultural, and supporting services. Understanding these complex interactions between ecosystems and humans is important to detect the impact of changes in stressors on river ecosystems and their scope of utilization. Feeding the future world population sustainably and satisfactorily requires accessibility to resources of adequate quantity and quality (Sonneveld et al., 2018). Although utilizing the vast natural resources could be beneficial, but its over-exploitation could lead to serious implications towards adverse conditions in the health of the ecosystem. Ecosystems provide direct provisions for humans through processes of cultivation, food, and fibre. It regulates the environment through the absorption and processing of pollutants. Fisher et al. (2009) suggest that ecosystem services are the aspects of ecosystems used actively or passively to generate human well-being and do not necessarily relate to specific ecosystem functions. Therefore, there is a complex set of relationships between intermediate, final services, and benefits derived from ecosystems. Figure 1.2 shows a complex interaction of the ecosystem and its services.

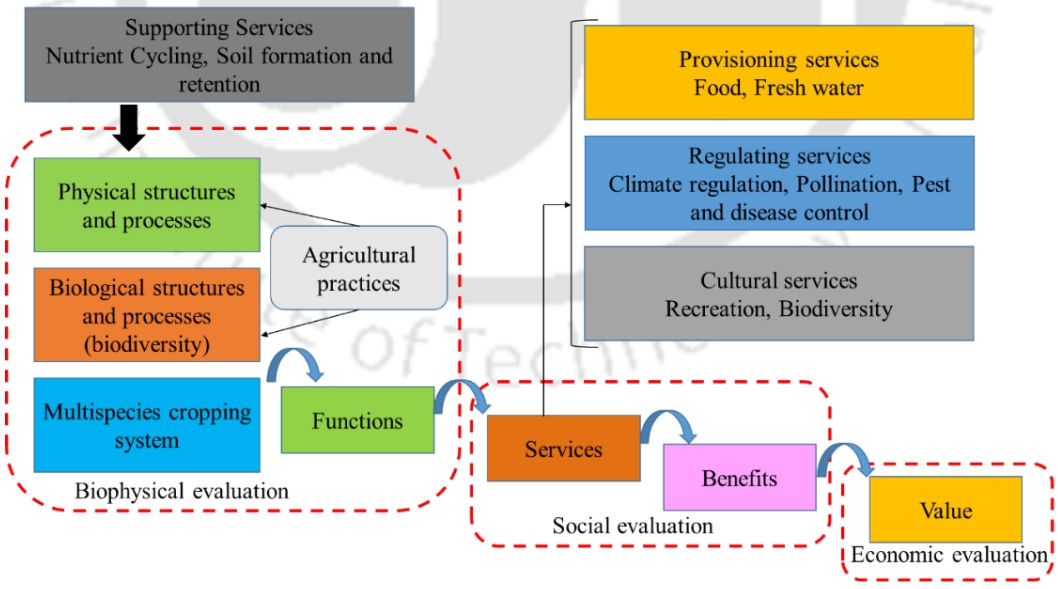

Figure 1.2: Cascade of ecosystem services in agricultural systems. Adapted from Haines-Young and Potschin (2010). The classification of services is taken from the Millennium Ecosystem Assessment (2005). "Physical structures and processes" also encompass physical and chemical structures and processes.

1.3 Utilization of riverine sandbars

In large braided river systems around the world, various activities are carried out along the floodplain. The floods bring fresh sediments along with them and deposits downstream. Hence, the river system has been used for various beneficial purposes, particularly the sandbars. The formation of sandbars is basically because of the sediment transport and flow of the river. This decides the rate of sediment deposition and erosion adding to the formation of the sandbars. During the flood and its recession afterward, the debris flowing with water stabilizes sandbars to initialize the plant growth. Sandbar utilization for performing farming and agricultural activities is a unique challenge within a riverine ecosystem. Large dynamic braided rivers like the Brahmaputra River undergoes flood every year during the monsoon period and pose a certain risk to agriculture and farming activities. The huge volume of water flow and sediment deposition leads to change in the morphology of the river. However, once the floodwater recedes, the river provides numerous opportunities for various activities. The floodplains and sandbars of the river are inhibited by the poor community, who are dependent primarily on agriculture for their livelihood (Chakraborty, 2013). Nevertheless, the proper utilization of such resources is complex and needs to be dealt with optimally, considering the seasonal and spatial land variability. Moreover, increased urbanization has led to diminished land availability for agricultural activities. To meet the increasing demand for food, agricultural production needs to be increased. Many researchers have emphasized that water, energy, and food are under stress, and their demand will increase significantly in the upcoming decades (El-Gafy et al., 2017; Endo et al., 2015). Agriculture is the prime user of land and water resources, essential for food production (Sadeghi et al., 2020), and its sustainability requires efficient management of these resources in an optimal way (Garg and Dadhich, 2014). Figure 1.3 shows the agriculture structure and the interdependence of cropping and farming activities.

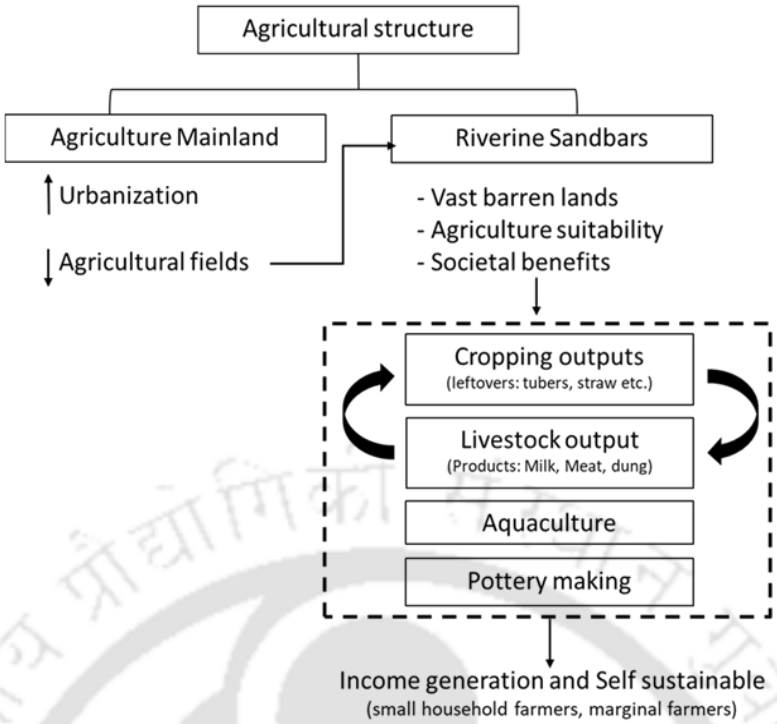

Figure 1.3: The agricultural framework in reference to sandbar activities and their interrelation.

1.4 Motivation of the study

It is commonly accepted that the ecosystem's services help society in terms of well-being; however, how these advantages are divided in society is yet unknown. The ability of offered services to improve human well-being is dynamic and path dependent. Rural livelihoods are diverse in geography and time, and rural communities rely on a variety of ecosystem services to make a living. The Brahmaputra River in Assam gives numerous chances and has become a source of income for a variety of people. Its sediment loads and transport patterns have an impact on the region's ecology and agriculture. Thousands of hectares of sandbars emerge every year after the monsoon when the water level in the rivers reduces. The extent and characteristics of sandbars vary year to year due to the unpredictable geomorphology of rivers, making it difficult for researchers to conduct investigations in the river. As a result, utilising this riverine land for diverse activities for the welfare of mankind is critical and should be researched. Hydro climatic disturbances could adversely affect the agricultural systems within the ecosystem. Excess water could lead to flooding of the entire crop area and scanty rainfall could lead to drought-like condition. The changing flow conditions, extreme events, frequency and magnitude of floods due to streamflow variation could cause challenges to farmers and threaten food security.

To address the challenges faced while utilizing the sandbars, the thesis work encompasses land-use change using historical data and geospatial information. Intensive field investigations, questionnaire surveys, and data collection were done to determine current practices within the ecosystem. Because of the large land mass within the river's planform, a more planned strategy to utilize these sandbars is required to get maximum advantage while minimizing disruption to the river's ecology. As a result, an optimum framework for allocating land for agricultural, farming, and non-farming uses has been devised. The streamflow parameter is significant for crop planning and crop damage since the riverine ecosystem is surrounded by water bodies. The development of better and more reliable numerical methodologies, efficient computing power, and innovative topographic survey techniques has envisaged the reliability on modelling studies. The creation of a damage assessment model has made it possible to analyze agricultural damage caused by water level fluctuations in a systematic way. The model assesses the actual benefit obtained from the agricultural planning process after accounting for potential economic losses. While undertaking agricultural activities in sandbars, there always exists a potential danger of crop damage due to the unpredictable streamflow conditions. However, forecasting approaches and statistical procedures, which have been principally detailed in the research work, can be utilized to predict future events and reduce the severity of such risks to certain extent.

1.5 Research objectives

Studies on the sandbars of the Brahmaputra River are limited, and they are required to draw considerable advantages, taking into account land use, challenges faced by dwellers, present practices, generated benefits, and other pertinent factors. Based on the necessity of the research, the following objectives are formulated.

1. Hydrodynamic model study of a riverine ecosystem to understand impacts of temporal variation in flow.

2. Socio-economic study of dwellers residing within the floodplain of a large river system and their challenges in adaptation to climate change.

3. Development and application of optimization model for land-use planning in general and riverine ecosystem in particular.

1.6 Organization of the thesis

Based on the broad objectives defined above, the entire work of the thesis has been divided into several phases and is described in different chapters as presented below.

Chapter 1 contains a brief introduction to the riverine ecosystem and the services provided for the benefit of humankind. It is followed by motivation, defining the objectives of the research and organization of the relevant chapters in the thesis.

Chapter 2 gives a systematic and detailed literature review which focuses on the past works done on utilizing the riverine floodplains and areas within the ecosystem and to have an up-to-date knowledge on various themes relevant to the study. The critical assessment of the literature stating the need for the present study has been discussed. Finally, the scope of the present work has been stated.

Chapter 3 describes a detailed description of the study area, the dynamics of sandbars and current practices performed in the sandbars. The details of field investigation, data collection, surveys and interviews performed along the riverine sandbars have been discussed.

Chapter 4 comprises of land-use land cover change (LULC) detection over the Brahmaputra River using the unsupervised classification technique. The cropping pattern change analysis has also been performed using different vegetation indices.

Chapter 5 contains the governing equations and model description of the 2-D hydrodynamic model. The model formulation and application for simulation of flows under different scenarios have also been presented in this chapter.

Chapter 6 reports a detailed investigation of sandbars along with sediment collection has been performed within the Brahmaputra River. The sandbars have been categorized into different classes and characterization of the sediments for analysing the mineral content and nutrients have been performed using XRD, EDX and particle size distributions.

Chapter 7 contains developing an optimization framework to determine the optimal cropping pattern considering the uncertainties associated with the agricultural systems and to increase the net agricultural benefits and crop production. The crop types and information, model inputs and complexities in determining land availability have been presented in this chapter.

Chapter 8 deals in short term flow forecasting and trend analysis for understanding the dynamics and behaviours of hydrological and climatic variables over a long-term period. Forecasting river streamflow is necessary for optimizing agricultural land for multiple crops in a riverine environment and is also of much significance in improving crop production and farmers' income under uncertainties.

Chapter 9 provide the details of the damage estimation model created for calculating the possible economic loss due to crop damage. Two distinct cases of loss estimation at varying water levels have been discussed.

Chapter 10 documents the agricultural risk assessment and risk associated with such practices. The flood frequency analysis involved the probability distributions in building the exceedance probability–discharge curves and loss-frequency curves for flood risk assessment and are documented in this chapter

Chapter 11 presents the major conclusions from the thesis work. The major outcomes of the present research work, the scope, and recommendations for future study are discussed.

2

Literature Review

2.1 Introduction

River landscapes have provided us with numerous benefits and served as areas for settlement, production and infrastructure for several thousands of years. Although the riverine ecosystem provides several opportunities, the related destructions, losses, and risks cannot be overlooked. The importance of river landscapes could be understood by taking into account the ecosystem services concept, where the significance of the ecosystem for the supply of services and its utilization for the benefit of humankind is important. This idea emphasizes the connection between various ecosystem-influencing factors and the availability of their functions as they relate to the delivery of services to humans. The many varied advantages that ecosystems offer to individuals are referred to as ecosystem services and constitute the interface between ecosystems and human wellbeing. The objective of the literature review is to give a critical summary of available research relevant to the study in understanding the processes taking place within the ecosystem. It comprises modeling studies on the riverine ecosystem, application of Remote Sensing (RS) and Geographic Information System (GIS) in hydrological studies and land-use change detection, optimization approaches, flood risk assessment, and socio-economic study on agriculture and allied sectors.

2.2 Modelling studies on riverine ecosystem

The development of better and more reliable numerical methodologies, efficient computing power, and innovative topographic survey techniques has substantially improved the hydrodynamic modelling of hydrological events in recent years. This progress has drive

the use of one dimensional (1-D) and two-dimensional (2-D) models in flow simulations with ability to reproduce the processes with greater accuracy and reliability.

2.2.1 Need of model study

For a vast braided river system, the conventional methodologies of field measurements and experimental investigations are very expensive, time-consuming, and challenging to comprehend river flow dynamics and morphology. Numerical models offer the chance to get around these restrictions of conventional methods. Different numerical models, such as CCHE2D Flood (Ying et al. 2004), LISFLOOD-FP (Bates and De Roo 2000), HEC-RAS and TELEMAC-2D (Baldassarre et al. 2009), and MIKE FLOOD (Patro et al. 2009), have been used in various studies for flood inundation. The 1950s saw the beginning of the use of mathematical models to explore morphological processes, together with correlations with empirical functions from experimental studies (Akhtar M. P., 2011). Thus, in the 1970s and afterward, the use of 1D and 2D models was expanded and deepened.

The MIKE 21C model was developed for simulating the 2D flows and morphological changes in rivers (Morianou et al., 2016). For dynamic 1D flow simulation in rivers, several commercially available software packages such as FLDWAV, DWOPER, MIKE-11, ISIS, etc., have also been widely used. The outcomes of the 1D model, however, fall short of giving accurate information on the flow simulation under extensive flooding. In order to solve these challenges, 2D models were first developed by Cunge et al. (1980) and Laura and Wang (1984). Subsequently, different schemes were developed to address the 2D flow equations. 2D flow simulation models like MIKE 21 (DHI, 2007) and TELEMAC-2D (Horrit and Bates, 2001) are frequently used. To understand the braided and meandering configuration of the rivers, several researchers have constructed 2D models (Enggrob and Tjerry, 1999; Lien et al., 1999; Jang and Shimizu, 2007). These models, which primarily concentrate on simplified geometry, have some drawbacks when utilised with intricate arrangements. In Assam, the Brahmaputra River is heavily intertwined with alluvial sandbars at both the central and near bank portions. In addition to seasonal flooding, the river also carries fresh sediments. These facilitate the utilization of the riverine ecosystem for the benefit of the people, enhancing them for cropping, agriculture, and various farming practices.

Over the last few decades, there has been extensive use of models for studying the river history, understanding and utilization of the river and its processes. According to Hallouin

et al. (2018), the major issues with using diverse models, such as hydrological, ecological, and environmental ones, for different classes of work are in ensuring that they are used properly and productively. In order to understand the processes that makeup ecosystem functions, from hydrology to ecology, including climate change and water quality, model studies had been conducted by a variety of scientific disciplines. These studies were useful in anticipating ecosystem services. Coulthard and Weil (2012) studied different classes of models (Landscape evolution models (LEM)), meander models, alluvial architecture models, cellular models, CFD models) for analysing the river history and found that model study provides us with the knowledge of fluvial changes, assessing hypotheses, challenging current ideas and some new questions on behavior of rivers.

Pietroniro et al. (2000) combined satellite data with a hydrodynamic model (HD) to evaluate changes in the hydrological and ecological ecology of the Peace-Athabasca delta (PAD) of northeast Alberta. They analysed the Landsat, Radarsat, and SPOT imageries and calibrated with the HD model. The researchers were able to assess the changes in the flow regulation and also emphasized on the need of climate change study.

Ji et al. (2002) developed a 1D time-dependent hydrodynamic, sediment, and hazardous model to examine the Blackstone River's silt, water quality, and heavy metal levels. The simulation of three storm occurrences was successful, and numerical analyses were also carried out to determine the effects of the sources of contaminants and the suspension of silt. They came to the conclusion that the proposed model would be a helpful tool for sediment study and metal transfer.

Shrestha and Nestmann, (2009) discussed the advantages of model study and its capabilities in handling uncertainties. Two traditional models-the HD model and the Muskingum-Cunge hydrologic model, as well as two data-driven models-the ANN and fuzzy network system-were used for the study. They came to the conclusion that all the models generate good outcomes, with the HD model performing satisfactorily in handling uncertainties except for the statistical performance, which was better accomplished by the other three models.

In order to estimate the hourly water level, Panda et al. (2010) compared the performance of the ANN approaches with that of MIKE 11 model. The researchers came to the conclusion that ANN can precisely estimate water levels at downstream sites of a river

reach using a time series of water level data from upstream locations and an appropriate lag period.

Conner and Tonina (2014) evaluated the effects of limited bathymetry data on 2D models in a large river system at different discharges. According to the researchers, the bathymetric data for 2D modelling in a large river should be collected at a cross-section density of 1 times the average channel width or less and 0.5 times for complex geometry.

Hu et al. (2015) created a 2D hydrodynamic model to investigate the properties of rivers and lakes. The model well illustrated features like the different flow regimes, annular branches, etc. They agreed that in terms of accuracy, the 2D model is preferable to the current 1D and nested 1D-2D models.

Salunkhe et al. (2018) used the CCHE 2D (Center for Computational Hydroscience and Engineering) hydrodynamic model to estimate the flood risk associated with the River Brahmaputra embankment breaching in the Lakhimpur District of Assam. The model was run under several discharge scenarios, and the results showed spatial variation in water depth and velocity. The study concluded that the derived information could be utilised to map flood hazards.

Singh et al., (2020) adopted the Hydrodynamic modelling technique for the identification of flood vulnerability zones during high discharge release from the Durgapur barrage in the lower Damodar river of eastern India.

Talukdar et al., (2021) implemented a hydrologic-hydraulic model for mapping the flood caused by the Baitarani River of Odisha, India. Flood inundation was simulated using the FLO-2D model and based on the flow depth, hazard zones were specified using the MAPPER tool of the hydraulic model. The result of the study exhibited the hydraulic model as a utile tool for generating inundation maps.

In large braided rivers like the Brahmaputra River, there have been various mathematical studies carried out on the basin and its tributaries (Dutta and Sarma, 2021; Kalita and Sarma, 2018). Dutta and Sarma (2020) used hydrological modelling to manage water resources of the data-scarce Brahmaputra basin. Patowary and Sarma (2017) developed a modified hydrodynamic model for routing unsteady flow in a river having a piedmont zone. Baruah and Sarma (2021) carried out an ecological flow assessment using a hydrological and hydrodynamic routing model in the Bhogdoi river in Assam, India. To interpret the

phenomenon of change in flow characteristics in a mining pit, Barman et al., (2019) studied the impact of sand mining on alluvial channel flow characteristics. Hence, the studies necessitated the understanding of the hydro-morphological parameters such as the streamflow, water level etc. to better understand the changes taking place at different zones as well as different seasons in such braided rivers.

2.2.2 Application of modelling tools for various studies

MIKE 11 is a 1D software package developed by Danish Hydraulic Institute (DHI), Denmark, to simulate flows and water levels, sediment transport in floodplains and rivers, irrigation canals and reservoirs. It is complemented by wide range of additional modules like the Hydrodynamic (HD) module, rainfall-runoff (RR) module, structure operation (SO) module, dam break (DB) module, advection-dispersion (AD) module, sediment transport (ST) module, Ecolab module and GIS extension. It solves the 1D Saint Venant's equation using the finite difference implicit scheme. Various researchers have used the MIKE 11 open-channel flow simulation. Stronska et al., (1999) developed a flood forecasting tool by simulating the flow in the Odra River using the MIKE 11 model. Sole and Zuccaro (2005) simulated a flood wave propagation using the MIKE 11 model for Albenga city in Italy. Doulgeris et al., (2012) used the MIKE 11-HD module to simulate the unsteady flow of the Strymonas River and to apply management rules based on the water level of Lake Kerkini. Girbaciu et al., (2016) applied the MIKE 11 model for water quality modelling of Bega River and captured the evolution of pollutant sources at both spatial and temporal scales. Nandy et al., (2020) performed a quantitative assessment of hydrodynamic impacts due to varying streamflow on the backwater deposits over the Damodar River in India.

MIKE 21 is a 2D free surface flow modelling system developed by the Danish Hydraulic Institute (DHI), Denmark, which simulates variations in water levels and flows, sediment dynamics, water quality, and ecology in response to a variety of forcing functions in the coastal areas, rivers, seas, lakes, and estuaries, etc. Various researchers have applied the MIKE 21 model and performed simulations in their studies. A brief review of the previous works reported on it is presented below:

As a hydrodynamic model for hydraulics and its associated phenomena in estuaries, lakes, rivers, etc., Warren and Bach (1992) specified MIKE 21. They came to the conclusion that

the model could replicate water quality, eutrophication, advection-dispersion, heavy metals, sediment transport, and hydrodynamics.

Somes et al. (1999) carried out a numerical simulation of flow within a wetland using the MIKE 21 model. They discovered that the flow-controlled criteria are hydraulic roughness, water depth and vegetation. However, calibration results showed that eddy viscosity plays a dominating role and flow in wetlands are influenced by inertia than friction.

Jørgensen and Edelvang, (2000) monitored the simulation of suspended matter concentration in dredged sediment spills during the construction of the Oresund Link during 1995-2001 using MIKE 21 Particle Analysis (PA) /Mud Transport (MT). Although MIKE 21 results had less spatial detail than RS data, they were compared to the results of a Compact Airborne Spectrographic Imager (CASI) in a plume to see the suspended matter concentration and discover a fair agreement.

Hassan and Dibike (2000) used MIKE21C to simulate the flows at the confluence of the rivers, Ganga and Jamuna in Bangladesh. The study showed the potential of the model in simulating river dredging and navigation studies.

For modelling the water depth and flood inundation extent during the monsoon season in the Mahanadi River basin of Odisha, Patro et al. (2009) employed the MIKE FLOOD model. When compared to remote sensing imageries, the model's ability to understand the pattern of flood inundation produced good results.

Kadam and Sen, (2012) used a quasi-2D model, MIKE-FLOOD for simulating the flow in Ajoy River in West Bengal. The flood inundation extent was compared with the Dartmouth Flood Observatory (DFO) flood map. The roughness coefficient was adjusted to have an agreement between the observed and simulated depths. The final value of the roughness coefficient was found to be 0.03 as a global value and also suggested that bathymetry is an important input for MIKE 21 hydrodynamic setup.

Sravanthi et. al., (2015) used the MIKE21 MT (Mud transport) model to examine the sediment transport along the central Kerala coast utilising wind, tide, bathymetry, and satellite-derived sediment concentration data. While comparing the simulated suspended sediment concentration (SSC) with satellite SSC, the study showed that river input and tidal currents controls the sediment dynamics.

Morianou et. al. (2016) simulated the water depth, silt transport, and flow velocity in the Greek river Koiliaris using the MIKE 21C model. The simulation made use of time series discharge data, a surface elevation map, and suspended sediment concentration data. The researchers concluded that the MIKE 21C model can effectively monitor extreme events with substantial sediment movement because there was a good agreement between the simulation results and field data.

Nigussie and Altunkaynak (2019) studied the effect of flood risk on urbanization using the MIKE 21 FM model. The results of the study showed that unrestricted urbanization in the watershed could lead to increased inundation of the land area. However, improving drainage system could reduce the risk to flooding.

Kanga et al., (2020) investigated the sediment flow and its spatio-temporal variation by quantifying the suspended sediment concentration (SSC) and water depth conditions using modelling studies and geoinformatics in a tidal estuary in West Bengal, India. The suspended sediment concentration was found higher in the pre-monsoon season than in the monsoon season. The study aided in an integrative system approach for managing diverse coastal environments.

2.3 Application of Geographic Information System (GIS) in land-use change detection

Real-time assessment of activities carried out within riverine ecosystems is crucial, and the use of remote sensing and GIS techniques can help overcome these challenges. Land-use and land cover (LULC) change results from complex interaction of social, ecological and geological processes and understanding the causes and their influences have piqued the interest of a wide range of researchers (Seto and Kaufmann, 2003; Santillan et al., 2012; Twisa and Buchroithner, 2019). In today's world, hydrological studies cannot be carried out without the ease of remote sensing and GIS.

2.3.1 Spatio temporal variation in land-use land cover

LULC classification techniques are developed to classify, map, quantify, and monitor the extent of environmental changes. To classify and quantify identified land use changes, most research works on LULC have relied on either supervised or unsupervised classification algorithms (Chamling and Bera, 2020). Satellite imagery can give precise information

regarding local, regional, and global LULC. Some of the previous works dealing with use of RS and GIS has been presented below:

Jayaraman et al., (1997) emphasized the role of space technology in analysing and managing the vulnerability of natural disasters around the world. Satellite-based Global Positioning System (GPS), disaster warning system, data collection platforms, etc. can be widely applied for various studies.

The advancement in remote sensing has made the studies in LULC at less time and cost and with better accuracy, with GIS providing a suitable platform for data analysis, update and retrieval (Cihlar, 2000). Thus LULC mapping has become one of the most important applications of remote sensing (Lo and Choi, 2004).

Piao et al., (2003) analysed the interannual variations and trends in NDVI and classified them into different classes based on climate variables. They found that settlements and cultivation practices have affected the vegetative cover of the region.

Vanwambeke et al., (2012) studied the changes in the rural landscape in Vidzeme in Latvia for last 20 years. The study found that increased forest cover was the most important land cover change in the study area. Between 1992 and 2007, the percent of forest cover loss was about 8.3 %, whereas the percent of forest cover gain was 17.1 %. The conversion of agricultural to forest cover accounted for 15.71 % of the 17.1 %.

Gandhi et al., (2015) employed NDVI threshold values ranging from 0.1 to 0.5 to help policymakers comprehend the importance of vegetation analysis and forecast future scenarios. They found that human activities have affected the landscape which includes intensified agriculture, reduced forest land and loss in biodiversity.

Pathan et al., (2021) conducted an assessment of spatial and temporal changes in the LULC types, vegetation cover and landmass in Majuli river Island, Assam, India. It was found that the vegetation cover had decreased by around 7.56 % i.e., around 102.8 km2. This large change in vegetation area has resulted in the conversion of these vegetation and agricultural sectors to barren land, built-up regions, and water bodies.

2.4 Socio economic status of dwellers residing within the floodplain of large rivers

Socio economic behavior can be defined as the study on how a society progress, regress or remains constant because of the local or regional economy. It is merely the behavior interactions among the individuals and groups. It is the relationship between the economic science and social ethics, dignity and philosophy. The people residing and practicing the process of cultivation and farming has the tendency to follow the procedures of their forefathers. It's their belief that they are blessed to carry out such practices and generally do not tend to get deviated or try something different than their traditional or conventional way. However, such traditional practice does not bring scope to adaptive measures to climate change. As can be seen and based on study, it has been found that climate change has serious impact on today's agriculture and farming practices. Farmers need to adapt to different modes of practice and identify the risk of extreme events on agriculture.

2.4.1 Socio economic impact on livelihood

Kumar and Narayanswamy (2000) performed a study on Entrepreneurial Behaviour (EB) to identify the socioeconomic features of farmers who adopted sustainable agriculture in India on the basis of age group, formal education level, large land holdings, and organisational participation. The EB of farmers varied with different age groups with young farmers had higher EB indices than middle-aged and elderly farmers.

Noorivandi et al. (2009) conducted research on the socioeconomic attitudes of farmers about the use of sustainable soil management (SSM) practices by Iranian wheat producers. The findings showed that 69% of respondents indicated moderate soil sustainability, 16% indicated unsustainably, and the remaining respondents indicated sustainable soil. Income, social involvement, education level, farmer perception, technical expertise, land size, crop production, loan rate, and SSM index all show a strong association with one another.

Shirur and Rana (2017) investigated the entrepreneurial behaviour of the farmers to understand mushroom farming across the state of Karnataka. The survey revealed that self-reliance, training, and cosmopolitanism, in addition to academic qualifications and participation in extensions, also contribute to the EB of the respondents.

Singh et al. (2017) examined the socioeconomic traits, and farming practises of 60 farmers through a questionnaire survey. According to the research, 3.33 percent of respondents

were female and 96.67 percent were men. For 88.33 percent of farmers, agriculture was their primary source of income. Farmers have adopted integrated agricultural practises, which comprise crop + dairy, crop + poultry, crop + beekeeping, etc., etc. The most common type of farming was found to be crop + dairy, followed by crop + fruits, beekeeping, floriculture, and forestry. This kind of agricultural technique reduced crop failure risk, increased employment opportunities, and reduced production costs.

2.4.2 People awareness to changing climate and adaptation

Climate change study in the Indian subcontinent has indicated changes in the mean, extremes and variability of several key parameters such as land temperature, precipitation, monsoon etc. (Mujumdar, 2008; Sarma and Hazarika, 2014, Barman and Bhattacharjya, 2020). A study conducted by Hazarika and Sarma (2017) on the impact of climate change on temperature and precipitation in the Northeastern part of India revealed an increasing trend in temperature and an increase in extreme events. Malhi et al., (2020) in their study reported that ecosystems are rapidly changing due to climate change. The drivers for such changes are not limited to temperature but also associated changes in precipitation, CO2 concentration, water balance and frequency and magnitude of extreme events which influences global food production. Reduction in agricultural benefits is encouraging farmers to migrate to an urban area in search of jobs, thereby promoting urban expansion and reduction in agricultural products (Lavorel et al., 2020). Therefore, utilizing all possible agricultural land optimally is essential to alleviate the threat to food security and to encourage farmers not to change their livelihood.

The impact of climate change may vary from region to region, and agriculture and food security are predicted to be significantly impacted by climate change (Anderson et al., 2020). The adaptation strategies include altering land and cropping practices as well as the development of enhanced varieties of crops such as high yield varieties (HYV) seed and water-resistant varieties. A healthy agricultural production demands suitable soil, favorable climate, adequate irrigation facilities, scientific methods, workforce, and market reach. Thus, in order to boost this sector, proper agricultural management practices with an objective of higher net returns with the best utilization of local resources should be implemented.

In order to evaluate crop yield, pest-related crop loss, and the effect of the agroecosystem on the tropical environment, Aggarwal et al. (2006) used the dynamic crop model InfoCrop.

The model was able to take into account variations in yield, emissions of CO2, CH4, and N2O, trends in soil organic carbon, etc. The relationship between growing output, tactics, and the possibility for global warming was also examined using the model. The researchers came to the conclusion that the response of the model to changing inputs is comparable to that of the field and useful for assessing crop production prospects and comprehending environmental inputs.

Guiteras (2009) conducted research on the impact of climate change on Indian agriculture. The researcher discovered that between 2010 and 2039, the major agricultural output would decrease by 4.5 to 9 percent, and between 2070 and 2099, it would decrease by about 25 percent.

In a research, Panda (2010) discussed cross-border migration, which is a significant effect of climate change in Bangladesh. In the near future, this will have destabilizing effects on socioeconomics, the environment, and politics. If no plans are made for such climate migrants, the risk to the nation will increase.

Sugirtharam (2012) conducted research among Sri Lankan farmers to learn about their socioeconomic status and awareness to changing climate. According to the study, 61 percent of farmers are aware of the increasing trend of floods and droughts, while 70 percent of farmers were aware of the changing climate pattern. Additionally, it was shown that 43% of farmers use innovative agronomic paddy cultivation techniques, such as altering the cultivation season, recycling drainage water, and employing tolerant crop varieties.

The effects of climate change are unparalleled in magnitude, ranging from changing weather patterns that endanger food production to increasing sea levels that increase the likelihood of catastrophic flooding. Through focus groups and questionnaire surveys, Dhanya and Ramachandran (2015) conducted research on farmers' perceptions of climate change, its effects, and adaption strategies. Farmers believed that variables contributing to climate change included rising temperatures, dry spells, decreased soil moisture, and delayed onset. Short-term crops like vegetables, legumes, etc., were grown as adaptation measures discarding major cereal production.

According to Shahid and Piracha (2016), in underdeveloped nations, a lack of understanding is a significant barrier to climate change adaptation. Given Pakistan's unique

and unusual combination of socio-political factors, the research places its findings in the context of Pakistan's ability to deal with the negative effects of climate change.

Raghuvanshi et. al., (2017) carried out a study about the awareness of the changing climate among farmers in Uttarakhand. The study indicated that farmers are aware of the changing climate and reported that unpredictable rainfall, declined agriculture yield, temperature increase, industrialization, overpopulation, etc. were some of the indicators of climate change. However, the impacts faced were crop failures, flooding, and migration to other places.

Tripathi and Mishra (2017) attempted to gather information on climate change from farmers of Uttar Pradesh using content analysis and group information. According to the study, farmers are able to recognise climatic changes and are aware of the risk posed by extreme weather and climate unpredictability. Farmers have revised the sowing and harvesting times, practised short-term cultivation, altered crop pattern, etc. as adaptations to various methods.

Banerjee and Kumar (2018) proposed Independent Component Analysis (ICA) based spatiotemporal analysis of hydrological components to understand the interdependencies of the large-scale hydrologic processes occurring in India. The authors suggested that these results can be used to improve the assessment and forecasting of hydrologic variables for improved water resource management by directly incorporating them into physically-based and statistical hydrological modelling.

The transformative adaptation method to mitigating climate change in the socio-ecological system was discussed by Fedele et al. (2019). Researchers examined how ecological, social, and social-ecological systems responded to climate change and came to the conclusion that transformative adaptations exhibited path-shifting, creative, multiscale, persistent, system-wide, and restructuring traits.

Chausson et al., (2020) studied the effectiveness of nature-based interventions in building resilience to climate change worldwide. The approaches involved Ecosystem-based Adaptation (EbA), ecosystem-based disaster risk reduction, natural infrastructure, green and blue infrastructure, and forest and landscape restoration.

The effect of climate change can be seen on different aspects of food security i.e. availability, access and absorption. According to the former director of International

Central Research Institute for Dryland Agriculture (CRIDA), Hyderabad, climate change affects around 4-9% of Indian agriculture every year, which leads to around 1.5% loss of Gross Domestic Product (GDP). By the end of the year 2030, yields in wheat and rice will decrease by 6-10%. However, crops like soybean, potatoes and mustard will have a neutral or near positive effect.

2.5 Optimization approaches for land-use planning

An optimization model is a mathematical model that maximizes or minimizes a particular objective function without violating the constraints. The objective function, constraints and decision variables are the components of an optimization model. The decision variables can be related to the activity levels/choices, constraints to the resource limitation and objective functions to the performance metrics. The problems are defined by the nature of the objective function and constraints. Various optimization models are being developed for special purposes based on priorities and need. Land-use optimization is a complex process in the areas of research and is a prime topic in the era of land-use planning. Land use involves the management of the natural environment in a systematic way without affecting it and preventing conflicts. However, for this, proper planning of land use must be affirmed. It can be achieved by systematic assessment of the land potential as well as socioeconomic conditions for the best land-use options. FAO defines land-use planning as the process of examining socioeconomic and physical aspects and motivating land users to meet society's goals in order to increase sustainable output (FAO, 1993). In the early 1960s, multi-regression models based on statistics and mathematics began to include spatial factors (Chen et al., 2014). But with the development of GIS and computer technology, optimization modelling and land-use allocation have become more common (Arciniegas et al., 2011). Several optimization approaches and algorithms have been proposed by various researchers for land allocation (Sethi et al., 2006), irrigation (Huang et al., 2012; Mahmoodi and Rafiee, 2020), water allocation (Raju and Kumar, 1999; Guo et al., 2014), and reservoir operation planning (Kumari and Mujumdar, 2017). The classical optimization techniques used for planning and management of land and water resources include linear programming (Zhang and Guo, 2014), nonlinear programming (2015; Li et al., 2017), dynamic programming (Macian-Sorribes et al., 2017) and hierarchical optimization techniques (Li et al., 2015).

2.5.1 Optimization studies on land-use

Aerts et. al., (2003) addressed the multi-site land-use allocation (MLUA) using spatial optimization techniques by developing integer programming (IP) models. The approach was acceptable for a lower grid size of approximately 50×50. When compared to various heuristic methods, the Integer Programming models (IPP) applied to the MLUA problems demonstrated good agreement in efficacy but inconvenience in terms of higher solution time.

With the aim of maximising the profit, Hassan et al. (2005) employed a linear programming model to identify the best cropping pattern utilising various crops. By using the optimal pattern rather than the existing ones, they discovered a significant increase in acreage, crop production, and income level.

Zielinska et al. (2008) used the Sustainable Multiobjective Land-use Allocation (SMOLA) spatial optimization technique for long-term land-use allocation that encourages efficient use of urban space. They discovered that the model helps with a trade-off analysis between generating a variety of options and optimising diverse objectives.

Maoh and Kanaroglou (2009) created a simulation model called the Integrated Transportation and Land-Use Model (ITLUM), to predict the future of urban planning and sustainability. The goal was to maximize economic gains while minimizing social and environmental effects.

Zhang et. al., (2010) designed a system for spatial optimal agricultural land-use considering the food consumption and land-use suitability. The whole region has been divided into various subzones, with targets allotted to each subzone. They found that by sub-zoning, every crop has enough land as well as there is a fragmental pattern of land use.

Osaki and Batalha (2014) proposed a decision support system for improving agricultural planning under risk conditions. It selects the best production proportion of each product that yields higher returns with lower risks. The researchers suggested that crop insurance policies can be taken up based on the region's production.

Memmah et al. (2015) conducted a review of the literature on the application of metaheuristics to optimise agricultural land usage. The researchers have come to a variety of findings on how well the strategy works depending on the problem. Such an approach relies more on previous usage and appeal than on the characteristics of the problem while

solving it. The stakeholders' trade-offs for the best land-use pattern at various scales can also benefit from this. However, merging of parallelization techniques with hybrid metaheuristic approach will be a challenge in the future.

For the management of sustainable land use in a semi-arid environment, Rao et al. (2018) developed an imprecise multi-objective optimization model combined with an ecosystem services evaluation model. The researchers came to a conclusion that when compared to traditional land use patterns, adopting an optimal strategy produced more advantages from both an ecological and an economic standpoint.

Wu et al., (2020) explored the ecosystem service values by integrating a linear optimization model with CLUE-S model (Conversion of Land Use and its Effects at Small regional extent) to develop an ecological land-use planning indicator in the Jiangsu province of China. The results showed that the spatial distribution of the ecosystem's services supply, flow, and demand could be understood.

2.5.2 Optimization studies on riverine ecosystem

In recent years, crop optimization has received considerable attention, and mathematical models have been developed and widely used to maximize net benefits. However, with an increase in the rate of urban expansion resulting in diminished agricultural land resources, the riverine ecosystem provides ample opportunities in this context. A study conducted by Prashnani et al. (2019) revealed that vast areas of stable vegetated sandbars prevail within the Brahmaputra River in Assam, India, and these sandbar areas have been continuously increasing over the years. The vegetated sandbars increased from 173 thousand Hectares in 1988 to 225 thousand Hectares in 2018. To receive higher productivity and net return, conventional farming practices need to be replaced with innovative techniques. A study undertaken by Khatun et al. (2017) stated the practice of pumpkin cultivation in the sandbars of the Jamuna river in Bangladesh gave high yields and returns, and with increased production, it can be exported to different places.

Pape et al. (2010) used coupled cross-coast bathymetry and neural network models to study the predictability of offshore sandbar migration. By observing the net offshore migration over a time span of 1-4 years, they were able to characterise the sandbar behaviour. However, the study also noted that linear models are superior to intricate nonlinear models

to forecast long-term sandbar behaviour, even though offshore migration is challenging over a longer period of time.

Rahman and Reza (2011) conducted research and discovered some of the factors that facilitated the poor to access the Sandbars in Bangladesh for cropping. According to the findings of their investigation, sandy soil with enough silt is ideal for the cultivation of tobacco and maize. Additionally, sandbars devoid of silt are not used since they are unsuitable for farming.

Noman et. al., (2014) studied the process of sandbar cropping and its scope with the basis of constraints faced by the farmers by performing interview surveys in riverine areas of Bangladesh. They considered age, agricultural knowledge, annual family income, and literacy as some of the constraints for their study. It was observed from their study that farmers received fewer market prices during peak time of harvest. The researchers concluded that the scope of sandbar cropping can be improved with the mix cultivation of different crops supported by food security.

Barbour et al., (2016) reviewed the use of optimisation for ecosystem management in river systems and highlighted the challenges in formulating the objectives, developing the model and applying it to ecosystem management. It was derived that decision-making may become more open, taken into consideration the views of several stakeholders, and uncover knowledge gaps for future research with the use of optimization.

Nahar et. al., (2017) encouraged the sandbar cropping practices for analysing the profit by the cultivation of sweet guard production. The socio-economic wellbeing of the dwellers involved in this practice was found satisfactory. It is always possible to increase the income, employment, and overall standard of living of farmers through such activities, as well as to make it possible for women to take part in them.

In the Qiantang Estuary in China, Xie et al. (2017) looked into the morpho-dynamic behaviour of sandbars using morphological models. A sensitivity analysis was done on the annual and seasonal fluctuation of discharges. The high concentration of suspended silt is what causes the fluctuations in bed level. The middle of the bar erodes during high and low flows, while the top of the bar repeatedly shifts toward the land and the sea. Nevertheless, there is a sediment exchange both upstream and downstream of the bar.

In order to maximise the financial gain, Zhai et al. (2020) used optimization techniques to analyse the amount of sand and gravel mining necessary to preserve the stability, health, and security of the river system, as well as its ability to prevent flooding. The relationship between quantity, pricing, and demand and supply determined how much money was made by mining river sand and gravel. However, detailed analysis was suggested as the river characteristics are dynamic and there could be specific restrictions to health and safe operation of river ecosystems.

2.6 Agriculture loss estimation and risk assessment

Flood damage has increased during the past few decades, and because of climate change and expanding vulnerability, additional increases are anticipated in certain regions (Kreibich et al., 2015). Flood-related economic losses around the world were more than $60 billion in 2016 and average of around $50 billion annually for the past ten years (Benfield, 2016). Flood loss estimation is an important component in risk mapping, risk analysis and risk oriented flood design. However, studies on flood loss modelling especially in the agricultural sector has not gained much attention where flood damage comprises loss of crops, as well as damage to agricultural buildings, contents, and machinery, and soil erosion and loss of livestock (Dutta et al., 2003). Assessments of agricultural losses can provide an approximation of the financial provisions required for farmers' compensation, particularly in the context of cost-benefit analyses.

2.6.1 Economic impact on agriculture and allied sectors

Kuhlmann, (2010) studied the variation of economic losses due to crop damages in different growing seasons and found that crops suffer more or less damage according to its development stage, which could be identified by the month and duration of inundation.

Ding et al. (2011) analyzed the impacts of droughts on irrigated and rain fed agriculture and found that severe droughts have historically resulted in huge socio-economic losses in agriculture and resulted in significant reduction in crop production.

Martin-Ortega et al., (2012) mentioned that the methods used to estimate direct economic losses in the agricultural sector are based on crop production function and market prices. In addition, these input could be integrated into water resources model to analyze the

economic impact physical, environmental and institutional features of the system (Harou et al., 2009, Ward and Pulido-Velazquez, 2012).

Kilimani et al., (2017) proposed a framework to analyze the economic impact of drought that could potentially aid managers in decision making regarding water scarcity in drought prone zones. They concluded that econometric approaches are accurate ways to determine the economic impact of droughts.

Singh et al., (2020) studies the impact of COVID-19 pandemic on agriculture and allied sectors in India. The study found that although the harvesting of major seasonal food crops was completed in some parts, but the crops were damaged due to lack of laborers for cutting and storing the produce. The dairy farming produce such as milk and meat were mostly affected. Farmers need to adopt the e-channel for marketing and advisory for farm and farm produce in addition to creating awareness.

2.6.2 Risk associated with floodplain agriculture, risk perception and communication

It has been recognized that the structural measures of flood protection cannot fully eliminate inundations (Kundzewicz, 1999). Holistic approaches incorporating societal analysis together could be useful in assessment and mitigation of floods. It is currently recommended to take a multifaceted strategy to managing flood risk, with a greater emphasis on non-structural measures such as better land-use planning, relocation, flood proofing, flood forecasting and warning, and insurances (Bradford et al., 2012). In order to manage flood risk, perception of risk at the individual and societal levels is a crucial social factor that affects how people react to flood warnings and initiatives to improve community preparation.

Brown and Damery, (2002) found that flood risk management measures in Europe have failed due to overlooking of public perceptions in policy making. Numerous warnings were rendered ineffective due to the authorities' ignorance of the public's perception of risk.

Terpstra (2010) argues that improving campaigns will need taking the public's perception of risk into account. Understanding how the general public conceptualizes risk is therefore essential to the success of flood risk control measures.

According to Buchecker et al. (2015), people have a poor tolerance for losses caused by natural disasters, which has increased the need for state-sponsored risk reduction measures.

They found that People's acceptance of risk or risk (in)tolerance appears to be a key explanatory element in addition to risk perception and effectiveness.

Holdstead et al., (2017) found that implementation of flood management plans depends on the risk of flooding in the famers agricultural farms. If farmers are not "bothered by flooding", they are less likely to put natural flood management strategies into action.

Anderson and Renaud (2021) suggested that using nature to address societal issues like the danger of natural disasters is frequently very successful and can provide a wide range of co-benefits. In contrast to the conventional grey measurements that practitioners and the general public frequently rely on the method is still seen as innovative, in contexts of risk.

Individuals and communities must be aware that they are at danger of flooding before taking action to increase their flood resilience. Therefore, a key element of efficient flood risk management is awareness. High levels of preparedness will aid in improving the response to a flood and fostering community resilience, which will lessen the negative effects (Paton et al., 2006).

2.7 Critical appraisal of literature review

The ecosystem service concept is a promising avenue to inform riverine ecosystem management and decision-making processes. Riverine ecosystems are home to a wide variety of biodiversity and play a significant role in supporting people's livelihoods and traditions by offering them a variety of advantages, such as access to food, water, and recreational spaces (FAO, 2015). The knowledge of ecosystem services offers a comprehensive and flexible framework to assess the various ways ecosystems contribute to human well-being, making it a possible path to effective riverine management.

Literature review revealed various studies being conducted on the benefits as well as disadvantages of ecosystem services. Majority of the studies could be found focussing on the ecological significance of theses service, however understanding the social, economic and cultural perspectives are equally important. Overall, provisioning and regulating services were quantified most often, while cultural and supporting ecosystem services were less frequently measured (Hanna et al., 2018). Floodplains support rich ecosystems and provide critically important benefits to people. Sandbars in particular provide numerous benefits in terms of economic benefits as well as coping with the urbanized expansion and diminished mainland agriculture. Quantifying the ecosystem services at play on riverscapes

is a key step towards being able to talk about them among different actors, compare management options in a systematic way, and use information about ecosystem services to help make informed decisions.

Therefore, the current research involves a holistic approach to understanding the benefits derived from ecosystem services by incorporating hydrological components, geospatial techniques, damage assessment approach and decision making in an optimal way.

3

Study Area and Data Acquisition

3.1 Introduction

The Brahmaputra River is a dynamic braided river originating from the Manasarovar Lake in the Kailash range of the Himalayas. It is a transboundary river flowing through Tibet, India, and Bangladesh, meeting the Ganga River in Bangladesh, and finally falling into the Bay of Bengal. The river basin extends over a catchment area of 5,80,000 Sq. Km lying in Tibet, India, Bangladesh, and Bhutan, with a land cover of 1,94,413 Sq. Km in India. The Brahmaputra River lies between 95°23'5.94" to 89°49'14.29" East longitudes and 27°49'15.82" to 25°43'40.38" North latitudes in the state of Assam. It drains through many varied and diverse habitats across its course of about 2900 km. The river flows from east to west in India and from north to south in Bangladesh. In its lower reaches, the river's bed gradient is very gradual. There is a great diversity in the physicochemical aspect of the soils of the Brahmaputra basin. In the floodplains, the soil is primarily alluvial and red loamy and also comprises of sandy, clayey, and laterite types. The sand content of upland soil is less than 28% at the surface and decreases at further depths (Talukdar et al., 2004). The silt content ranges from 30-75% in the basin. The clay content increases from a depth of 28 to 49 cm in the soil of the middle, eastern, and western parts of the basin with increased rainfall. The organic matter in the soils increases with an increase in the rainfall amount and decreases with an increase in temperature (Chakravarty et al., 1978). Illite and Kaolinite are significant minerals found in clay fractions of the soils in the basin (Karmakar 1985). The Brahmaputra basin experiences a typical climate with varying temperatures and

rainfall. The climate of the basin is humid with rainfall being moderate to high. It is mainly influenced by both southwest monsoons from the Bay of Bengal and the surrounding hills of the Assam Himalayas, the lower Himalayas, and the Assam plateau. The southwest monsoon brings the precipitation from May to September. The mean temperature varies between 10-15°C in the winter and 30-40°C in the summer.

3.2 Site Description

Assam is located in the north-eastern part of India, south of the Eastern Himalayas along the Brahmaputra and Barak River valleys lying between 89°46' to 96°01' East longitude and 24°03' to 27°58' North latitude. It is considered the land of agriculture, and more than 60% of the population is engaged in this sector. In Assam, agriculture and its allied sectors play a pivotal role in socio-economic development as it provides livelihood to a major portion of the population. As per the Economic survey report of Assam, 2014-15, the sector supports more than 70% population of the state by employing around 53% of the workforce. The cropping season is mainly divided into two periods: The period between March and June is called Zaid, and summer crops are grown. The farmers follow single and double cropping systems of farming practice in all three seasons. Among all crops, rice is the dominant crop grown across all districts, contributing to about 80% of the gross cropped area. The average annual rainfall is about 2000mm, which provides adequate standing water for rice growth (Talukdar et al., 2004). Pulses are other important crops grown in Assam during the Rabi period. However, certain other pulses are also grown in some other districts during the Kharif season. Black gram, green gram, linseed, lentil, peas, beans, etc., are farmed extensively in Assam. Crops such as jute, pea, potato, wheat, and vegetables are grown under different cropping techniques.

The study area of the current research lies within the Brahmaputra River extending from Majuli upstream to Dhubri downstream, as shown in Figure 3.1. For exploring the sediment characteristics of various sandbars within the river, soil samples were collected across 42 different locations. The decadal land-use land cover changes were also examined. Further, two different districts were selected wherein the existing cropping practices were analysed, and the potential of selective cropping approaches for agricultural economic benefit was studied. The study was based on sandbar areas in those districts: one is the Barpeta district, and the other is the Kamrup district in the Lower Brahmaputra Valley (LBV), described as the study site 1 and study site 2, respectively. A dominant agricultural sandbar was

considered for a detailed analysis of the LULC change and identification of the cropping pattern, and the current cropping pattern was analysed in the Barpeta district.

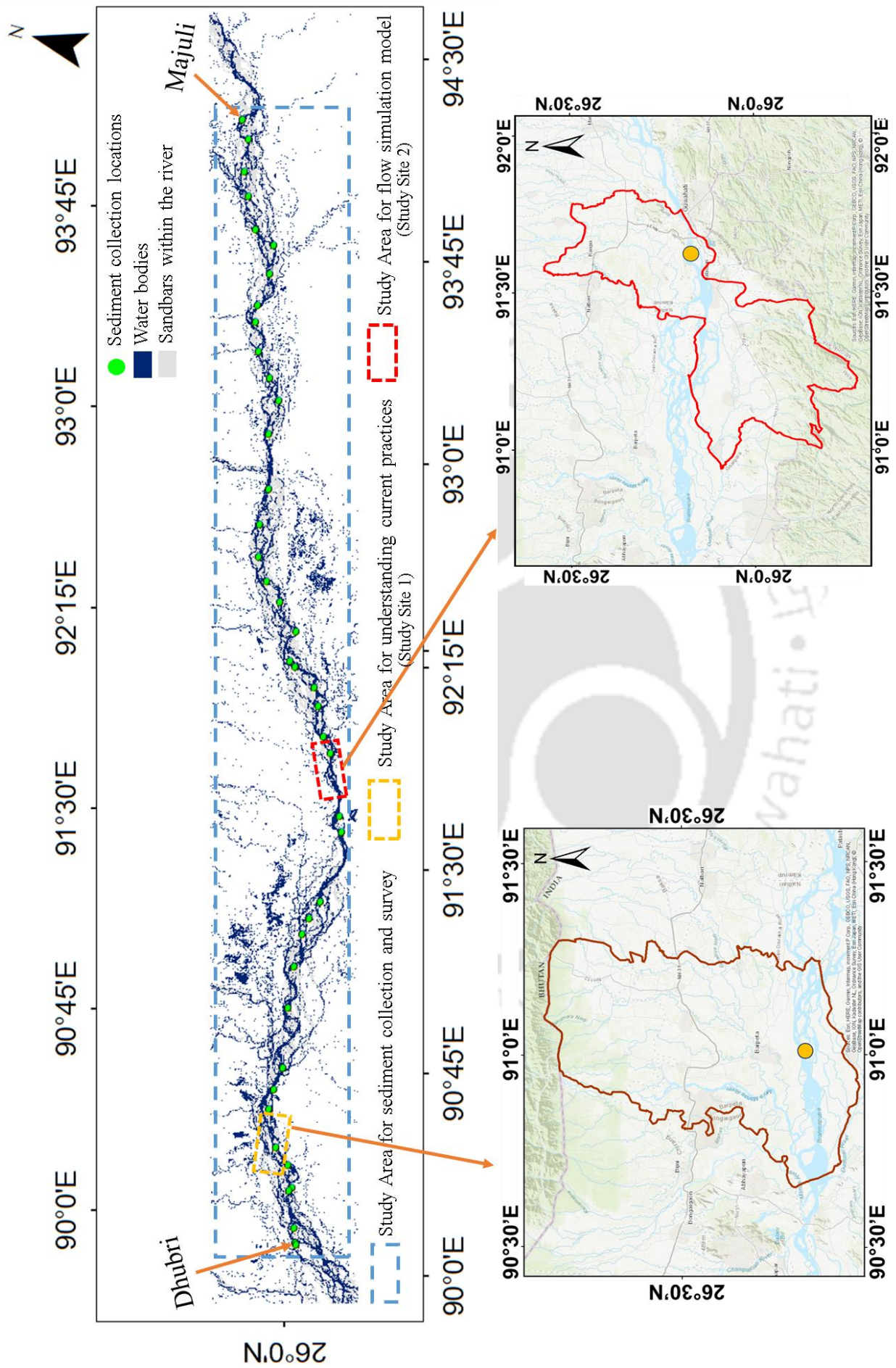

Figure 3.1: Study area showing the Brahmaputra River in Assam, India

Study site 1

For analysing the cropping pattern change during two different years, 2016 and 2019, an agricultural portion in the mid sandbars of the Brahmaputra River in the Barpeta district of Assam was considered. The district lies in the lower Brahmaputra zone between 26°45' to 26°49' North latitude and 90°45' to 90°15' East longitude. It has a total geographical area of 3,24,500 Hectares (Ha) and is one of the leading agricultural districts of Assam. The total gross cropped area of the district is 3,10,000 Hectares, and the net-cropped area is 1,76,900 Hectares. The soil in the district can be classified as alluvial, sandy, sandy loam, and forest soil. The district experiences tropical monsoon during two seasons; summer (March-May) and winter (June-September). The average annual rainfall ranges from 1400 mm to 4000 mm, and the average temperature varies from around 8°C to 30°C. The principal crops grown are Paddy, Mustard, Rapeseed, Wheat, Jute, Oilseeds, Fruits, Sesame, and Vegetables. The area was chosen to compare the existing cropping practices with cropping patterns derived from the optimization model. The data on the type of crops grown in the Barpeta district, their production, and their yield were collected from the Directorate of Economics and Statistics, Government of Assam. According to the socio-economic Survey Report (2002−2003) by the Directorate of Char Areas Development of Assam, a total of 3,60,927 Hectares of char land prevails within the Brahmaputra River, out of which 2,42,277 Hectares were cultivable lands. The district has total char land of about 36,655 Hectares. A total of 277 char villages exist within the river in the district. Market prices associated with the particular commodity for the current study were acquired from market surveys. The information on cultivation and production costs was obtained from various sources, research papers, reports, and interviews with farmers. The existing cropping pattern in the district dominates paddy as the major crop covering about 63% of the total cropped area, followed by oilseeds, vegetables, pulses, etc., each covering less than 10% of the total crop area. For the present study, a sandbar area of about 37,717 Ha within the District was considered, out of which water bodies covered about 6,748 Ha. Thus, the total available area (TA) was 30,969 Ha. Figure 3.2 shows study site 1.

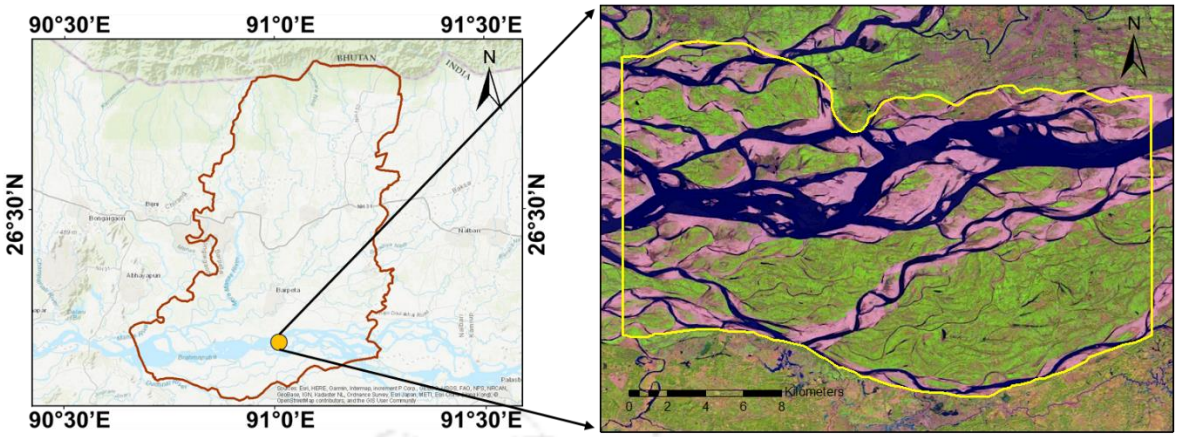

Figure 3.2: Study site 1- Agricultural portion in the mid sandbars of the Brahmaputra River in the Barpeta district, Assam

Study site 2

The site lies between 91°44'15.09" E, 26°11'41.06" N to 91°51'12.43" E, 26°14'24.51" N within the Brahmaputra River located near Pandughat in Kamrup district, Assam. The soil type found is primarily alluvial and comprises sandy, loamy, clayey, and laterite soil. Seasonal flooding brings alluvium, making the soil fertile for agricultural activities. The marginalized community has utilized the sandbar for livelihood opportunities and other income-generated activities. Figure 3.3 shows study site 2, which is an agricultural sandbar.

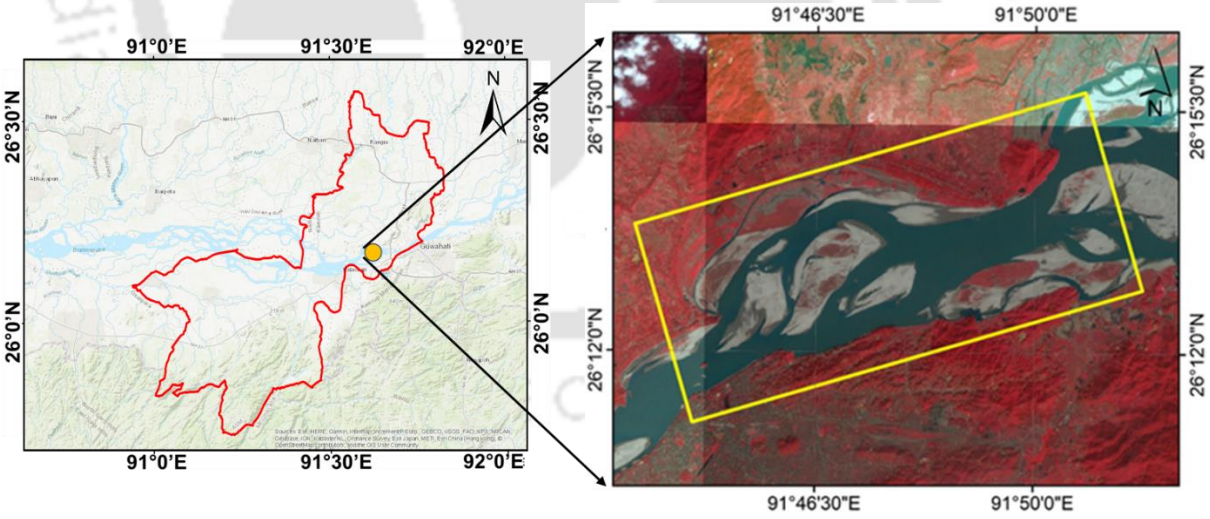

Figure 3.3: Study site 2- Agriculture dominated sandbar located in the Kamrup District, Assam

3.3 Field investigation, data acquisition, and questionnaire surveys

Understanding the changes in the cropping pattern and the socio-economic aspect of the dwellers residing and practicing sandbar cultivation is of prime importance. The present

work was initiated by carrying out a satellite-based study, followed by field investigations and questionnaire surveys that provided details about the type of crops cultivated, the pattern of cropping, age of farmers, duration, profit, production, etc. For the field verification of the above findings and for investigating other essential aspects of sandbar utilization, a field survey was conducted among the farmers residing and practicing cultivation in the sandbars. The detail of the crop types, yield, and cultivation cost was derived by referring to both primary and secondary data. Secondary data gives an idea about the characteristics of agricultural production. Sometimes these data may not be sufficient to fulfill the objectives of the study. Therefore, primary data was gathered to achieve the goals. The data were collected from various households of dwellers and farmers specifically practicing sandbar cultivation. For primary data, a questionnaire survey was conducted, and this information gathered has been presented in Tables 3.1 and 3.2. The primary information derived from the survey was about sowing and harvesting time of crop, types of crop cultivated, crop duration, sowing area, production, and profit obtained from the current agricultural practices prevailing within the riverine ecosystem. The cultivation cost comprises both fixed and variable costs. Fixed costs consist of land on lease or rental payments and variable costs include labor costs, raw materials costs, transportation costs, etc. In addition, the seasonal food demand and self-sufficiency information were also accounted from the farmers and implemented in the optimization framework.

To understand the traditional practices prevailing in the riverine sandbars, an unstructured in-depth interview of farmers representing different classes was conducted. The age of farmers and dwellers practicing agriculture varied between 18-70 years and were mostly illiterate. The age groups among the interviewed farmers were categorized into three farmer classes, i.e., Farmer class-I (age between 18-30 years), Farmer class-II (age between 30-60 years), and Farmer class-III (age >60 years). In addition to the questionnaire, personal interviews were also conducted. The responses received from them were in the local language (Assamese, Bengali), and that information was translated into English and incorporated into the questionnaire. The prime objective of the survey was to derive the socio-economic condition of the farmers, difficulties faced, knowledge gained, and risks involved in sandbar cropping. From the questionnaire surveys and interviews with the farmers, it was found that the farmers prefer sandbar cultivation based on the (1) size of the landholdings, (2) self-consumption and sufficiency, (3) market demand during different seasons. It was also found that new farmers or farmers with less sandbar cultivation

experience do not prefer taking a higher risk of damage and instead follow the cropping pattern similar to experienced farmers or as in previous years' pattern. However, it is to be noted that cropping practices vary across different locations in the sandbars. Figure 3.4, 3.5, 3.6, and 3.7 shows the crop cultivation, field preparation, personal interviews, and sample collection in sandbars within the Lower Brahmaputra Valley (LBV).

Source: Field survey photograph
Location: 26.2646^{0}N, 91.8465^0 E

Figure 3.4: Mustard plantation in a sandbar of Brahmaputra River, Assam

Source: Field survey photograph
Location: 26.6192^0 N, 92.5237^0 E

Figure 3.5: Field preparation before sowing of crops in a sandbar within the river

Source: Field survey photograph
Location: 26.6235^{0}N, 92.5235^0 E

Figure 3.6: Personal interview with farmers regarding current practices and problems faced

Source: sediment sample collection
Location: 26.6266^{0}N, 93.1452^0 E

Figure 3.7: Sediment sample collection from a sandbar in the Brahmaputra River

Table 3.1: Information derived from survey on crops grown/activities performed in the sandbars within the Brahmaputra River, Assam

Sl. No	Crops / activities	Farmer class I (>60 years)		Farmer class II (30-60 years)		Farmer class III (18-30 years)	
		Cultivation performed in sandbars	Duration (months)	Cultivation performed in sandbars	Duration (months)	Cultivation performed in sandbars	Duration (months)
1	Paddy	×	3-4	✓	3	✓	4
2	Maize	×	1.5-3	×	-	✓	4
3	Pea	×	1.5-2	✓	1.5-2	✓	1.5-2
4	Beans	×	1.5-2	×	-	✓	2-3
5	Turnip	✓	2	×	-	×	-
6	Brinjal	✓	1.5-2	×	-	✓	4
7	Bitter Gourd	✓	1.5-2	×	-	×	-
8	Pumpkin	✓	3	✓	3-4	×	-
9	Carrot	✓	3	✓	4	✓	4
10	Chilli	✓	2-3	×	-	✓	-
11	Potato	×	2-3	✓	2-3	✓	2
12	Ground Nut	×	-	×	-	✓	3-4
13	Mustard	×	1.5-3	✓	2	✓	2
14	Capsicum	×	1-2	×	-	✓	-
15	Cabbage	✓	2-3	✓	3	✓	2-3
16	Cauliflower	×	1.5-2.5	×	-	✓	2-3
17	Jute	×	-	×	-	✓	3-4
19	Potato	×	-	×	-	✓	2-2.5
20	Tomato	×	-	✓	6	✓	3
21	Black gram	✓	2-3	✓	2-3	✓	3-4
22	Dairy faming	×	-	✓	-	✓	-

✓ represents activities practiced at least once on the sandbars × represents activities not practiced at least once on the sandbars

Note: The cropping pattern of different class of farmers vary within the farmers practicing sandbar cultivation. From the questionnaire, it was also found that certain famers in the age group between 30-60 and 18-30 years prefer dairy farming practices due to low maintenance cost and less cost on feeding the cattles. The by-products of paddy and vegetables serves as the cattle feed. However, the initial investment for buying cattles were reasonably high that cannot be borne by certain class of farmers in class 3 categories even though they prefer cattle rearing practices in sandbars. The class 1 farmers were mostly illiterate and unwilling to shift from their traditional method of cultivation. In addition, they maintain a similar practice of cropping throughout year. The family sizes to such class of farmers was more than 5-6 members. However, they have a knowledge of cultivation in sandbars for more than 10 years, which was lacked by the class 3 farmers. Therefore, the net benefit and damage due to seasonal flooding varies accordingly among different farmers. It was also found from the survey that although some farmers do not cultivate certain crop types, however, they have the knowledge of duration taken from sowing to harvesting of the crops.

Table 3.2: Raw information acquired during the survey from different class of famers practicing sandbar cultivation

Crops	Sowing	Harvesting	Duration	Area (Bigha***)	Seeds/ Plantings	Production	Profit/Income (Rs/Ha)
Ahu Paddy	Jan/Feb	May/June	3-4 months	5	NI	160-200 Kg/Bigha	-
Ridge Gourd	Oct/Nov	Jan/Feb	3-4 months	1	CE	-	-
Brinjal	Oct/Nov	Jan/Feb	3-4 months	1	NC	500-600 Kg/Bigha	62,000-1,24,500
Cabbage	Oct/Nov	Jan/Feb	3 months	1	7000 nos.	-	1,24,500-1,86,500
Cauliflower	Oct/Nov	Jan/Feb	3 months	1	NC	535-600 Kg/Bigha	90,000-1,24,500
Chilli				1	2000-2500 nos.	300-400 Kg/Bigha	70,000-90,500
Dairy	dryland	-		10-20	-	(4-5 lts/cow)**	40/- per litre
Groundnut	Oct/Nov	Mar/Apr	4-5 months	-		-	-
Jute*	Jan/Feb	May/June	4-5 months	5	NI	180-200 Kg/Bigha	65,000-75,000
Maize	Oct/Nov	Mar/Apr	4-5 months			-	-
Potato	Oct/Nov	Mar/Apr	3-5 months	1		600-1000 Kg/Bigha	1,50,000-1,70,000
Pumpkin	Oct/Nov	Mar/Apr	4-5 months	1	NC	200 nos.	30-60/pc
Raddish	Oct/Nov	Jan/Feb	3-4 months	1	-	500-600 Kg/Bigha	50,000-90,000
Sesame	Oct/Nov	Jan/Feb	3-5	1	-	120-200 Kg/Bigha	30,000-38,000
Social Activities****	Dec-Jan	-	-			-	30,000-50,000*****
Tomato	Oct/Nov	Jan/Feb	3 months	1	NC	1100-1400 Kg/Bigha	2,24,000-3,50,000
Boro Paddy	Jan/Feb	Apr/May	3 months	1	-	800-1500 Kg/Bigha	62,800
Black gram	Oct/Nov	Jan/Feb	3 months	1	NC	80-200 kg/Bigha	25,000-50,000

* can survive in flooded conditions upto certain level and duration ** Milk production *** Unit of measurement of land in Assam (1 Bigha = 0.14 Hectare)
**** Social activities includes camping, picnics, eco camps, water sports, festivals and other recreational activities
***** Depends on the location and visit of tourists/local people

The information provided in the chart is based on the questionnaire survey performed among various class of farmers practicing sandbar activities. Moreover, the crops/activities listed are according to the structured questionnaires and personal interviews. Therefore, the cropping practices, profits, area under each activity/crops, sowing/harvesting time vary accordingly among the farmers and certain class of farmers may or may not cultivate all the crops/perform the activities simultaneously.

Approximate costs: (1) Tractor charge per Bigha = Rs. 1500-2000; (2) Fertilizer costs per Bigha (vegetables) = Rs.7000-8000; (3) Labour cost per Bigha (Vegetables) = Rs. 350-400. The costs vary seasonally and among different crop types.

CE=Choice experiment (i.e. cultivation practiced for the first time); NC = No count: NI = No Information

The secondary data includes the data collected from government and non-government sources. Various official reports, records, journals, and publications of agencies such as FAO, World Development Report, Asian Development bank, Census of India, Government of India economic survey, Department of Agriculture and Co-operation, Ministry of food and agriculture, Planning Commission, Directorate of Economic and Statistics, Govt. of Assam, Directorate of Agriculture, Assam, etc. formed the preliminary data source. The data on the type of crops grown in the districts, production, and yield were collected from the Directorate of Economics and Statistics, Government of Assam (https://des.assam.gov.in/information-services/agriculture). The selection of crops that survives at different depths has also been gathered from the questionnaire survey, and varieties of hybrid/deep water/flood-tolerant crops have been obtained from the Ministry of Agriculture and Farmers Welfare, Government of India (https://pib.gov.in/newsite/PrintRelease.aspx?relid=123999). The information on cropping seasons and crops grown has been obtained from the Department of Agriculture and Horticulture, Directorate of Agriculture, Government of Assam (https://diragri.assam.gov.in/portlets/crop). The sandbar/char area information was obtained from the Assam Human Development report 2014 (GoA, 2016). Therefore, the primary and secondary information was assimilated to formulate the optimization framework and develop the damage estimation model. For the model simulation, the streamflow data used was obtained from the Pandu gauging station.

3.4 Conclusions

The study area selected for the current research is the sandbars within the Brahmaputra River in Assam, India. The collection of field data as well as the emotions, understandings, and experiences of famers and dwellers practicing agriculture and farming activities, is challenging. The study envisaged the necessity to make people understand the need for such studies for their development and the socio-economic development of society. The satellite imageries over the areas of interest could provide vital information about the land-use land cover changes over time. Frequent field visits were made during different seasons, and soil samples were collected. The in-situ data were required to understand the cropping practices followed, crops grown, duration, and season of cropping in the riverine sandbars. Furthermore, the variation in water level in different seasons is a prerequisite for undergoing any agricultural activities. The sediment analysis for the type of soils and the

feasibility of such soils for crop growth and their mineral and nutrient content were analyzed during the research, explained in the subsequent chapters. The data gathered from the current cropping practices were used to validate the research findings derived through model studies. To develop a framework for suggesting optimal cropping patterns, the field observations and questionnaire responses were integrated to derive benefit along with the social-economic upliftment of the marginalized communities.

4

Mapping agricultural activities and their temporal variation

4.1 Introduction

The riverine ecosystem and its associated services play key roles in social and economic development. They are rich in biodiversity and serve a vital role in sustaining people's livelihoods and traditions. Agriculture is one of the most important sectors in boosting the country's economy. It plays a significant role in employment and food security, adding to the country's Gross Value Added (GVA). There is a need to boost this sector with innovative research and technologies. The real-time assessment of activities carried out within the riverine ecosystems is crucial, and the use of remote sensing (RS) and GIS (Geographic Information System) techniques can overcome these challenges. RS and GIS are imperative tools in monitoring several indicators such as crop growth and yield, estimating biophysical parameters, and surface changes in the vast landmasses at spatial and temporal scales. Remote sensing studies can classify landscapes on a greater scale and map the changes with varying technologies in various sectors (Ozesmi and Bauer, 2002). It is a valuable tool in capturing the seasonal behavior of vegetation in agricultural studies (Wardlow et al., 2007). The availability of long-term imageries and the metadata stored in the images provide needful information. These remotely sensed data provide realistic information on crop health and productivity, which is essential for agriculture planning and management (Karthikeyan et al., 2020). The data from the remote sensing image time series at different spatial resolutions provide vital information about the vegetation status. It helps to examine the seasonal variation in cropping and discriminate among other crops grown during different periods. High spatial resolution satellites like Landsat 7 and 8 provide accurate and detailed information about the changes and phenological characteristics in

agricultural studies. More detailed maps can be obtained through these higher-resolution satellites (Peña and Brenning, 2015; Zheng et al., 2015).

LULC changes are considered one of the essential measurements to evaluate differences across a wide range of spatiotemporal scales (Lambin, 1997). These changes are important elements in understanding the global environmental changes. The LULC information has been helpful in better assessment of the relationship among the forest covers, cropland, settlements, and wetlands within rivers. In large rivers like the Brahmaputra, thousands of hectares of agricultural land have been eroded over the years due to flooding and breaching of embankments, which has led to a shortage of agricultural mainland (Sarkar et al., 2012; Thakuriah and Saikia, 2018). However, sandbars formed within the rivers by aggradation and degradation have been productive for agricultural purposes and remain stable for a more extended period (Rahman and Rahman, 2012). These sandbars vary in shape and size and could be utilized for various activities. This study has been carried out to examine the LULC change in the sandbars formed within the Brahmaputra River from Majuli to Dhubri, Assam, across a distance of approximately 620 kilometers (km), on a decadal scale. The study aims to investigate the accessibility to sandbars, understand the existing cropping practices, and the potential for expanding these sandbars into cultivable land. High-resolution satellite images were derived from the google earth platform, and cropping patterns were analyzed.

4.2 Satellite datasets used

For the study, georeferenced satellite imageries of the Brahmaputra River were collected for the years 1976–80, 1993–95, 2003–04, 2008–11, and during the flood period of the year 2016-17. For the period of 1993–95 (IRS 1B, LISS I) and 2003–04 (IRS P6, LISS III), the imageries were procured from National Remote Sensing Centre (NRSC) Hyderabad. The United States Geological Survey (USGS) provided satellite images from 1976–80 (Landsat MSS) and 2008–11 (Resourcesat-1, LISS III). The layer stacking and mosaicking of these datasets were done using the ERDAS tool. The RISAT-1 images were procured to analyze the changes during the flood period of June-July 2016. Table 4.1 describes the specification of different satellite sensors.

Table 4.1: Satellite sensor specifications

Specifications	Landsat 1,2	IRS-1	IRS-P6	Resourcesat-1	Landsat 8	RISAT
Sensor	MSS	LISS I	LISS III	LISS III	OLI and TIRS	SAR
Band	4	4	4	4	11	1
Spatial Resolution (m)	80	72.5	23.5	23.5	30,15 (Panchromatic)	36
Swath (km)	185	148	141	141	185	10-225
Date of acquisition	1976-80	1993-95	2003-04	2008-11	2016,2019	2016-17

Monthly cloud-free images from Landsat 8 OLI (Operational Land Imager) and TIRS (Thermal Infrared Sensor) satellite for the agricultural portion during the years 2016 and 2019 for the Barpeta District were derived from USGS (United States Geological Survey) earth explorer. The path and row and the date of acquisition of those images are shown in Table 4.2. Temporal variations to determine cropping patterns over the years were monitored using the NDVI (Normalized Difference Vegetation Index) and NDWI (Normalized Difference Water Index) analysis. ArcGIS 10.4 tool was used for processing and analysing the satellite images.

Table 4.2: Monthly time series Landsat 8 data for the years 2016 and 2019

Year	Path and row	Date of Acquisition
2016	137, 42	17/01, 16/02, 19/03, 04/04, 06/05, 07/06, 27/09, 29/10, 14/11, 16/12
2019	137, 42	30/01, 24/02, 25/03, 22/04, 21/05,18/07, 19/08, 26/09, 18/10, 23/11, 17/12

4.3 Land-use and land cover (LULC) of the study area

Image classification provides useful information about the land-use and land cover of an area. It translates the raw image into meaningful and understandable information (Al-talib and Ahmed, 2013). Land cover information collected from satellite imageries is the spatial and spectral attributes derived from individual cover types. Two approaches are widely considered: (a) Supervised classification and (b) Unsupervised classification. Both the approaches have their assumptions based on the scene to be classified. In supervised

classification, information about the land cover types is needed before classification to define the signature of different land cover classes. Whereas no such information is required for unsupervised classification as it divides the scene into spectral clusters. The accuracy of the unsupervised approach is well evaluated for land-use/cover classification for urban and agricultural areas (Fukue et al., 1988).

In this study, the unsupervised classification approach was applied to develop the land cover map of the study area and highlight the changes in the area corresponding to different classes. Landsat, IRS, and Resourcesat satellite images were classified using Iso cluster unsupervised classification. This tool performs classification by combining the functionalities of the Iso cluster and Maximum likelihood classification on a series of input raster bands. One advantage of such an approach is that the signature file generated from this tool can be used by another classification tool. The pixels are clustered based on spectral distance and homogeneity. The imageries collected for the years 1976-80, 1993-95, 2003-04, 2008-11, and flood period of 2016-17 of the Brahmaputra River from Majuli to Dhubri were divided into 4 classes: Waterbody, Dry Sandbar, Cropland, and Vegetation. The classified land-use/cover maps for the corresponding years can be seen in Figures 4.1, 4.2, 4.3, 4.4 and 4.5.

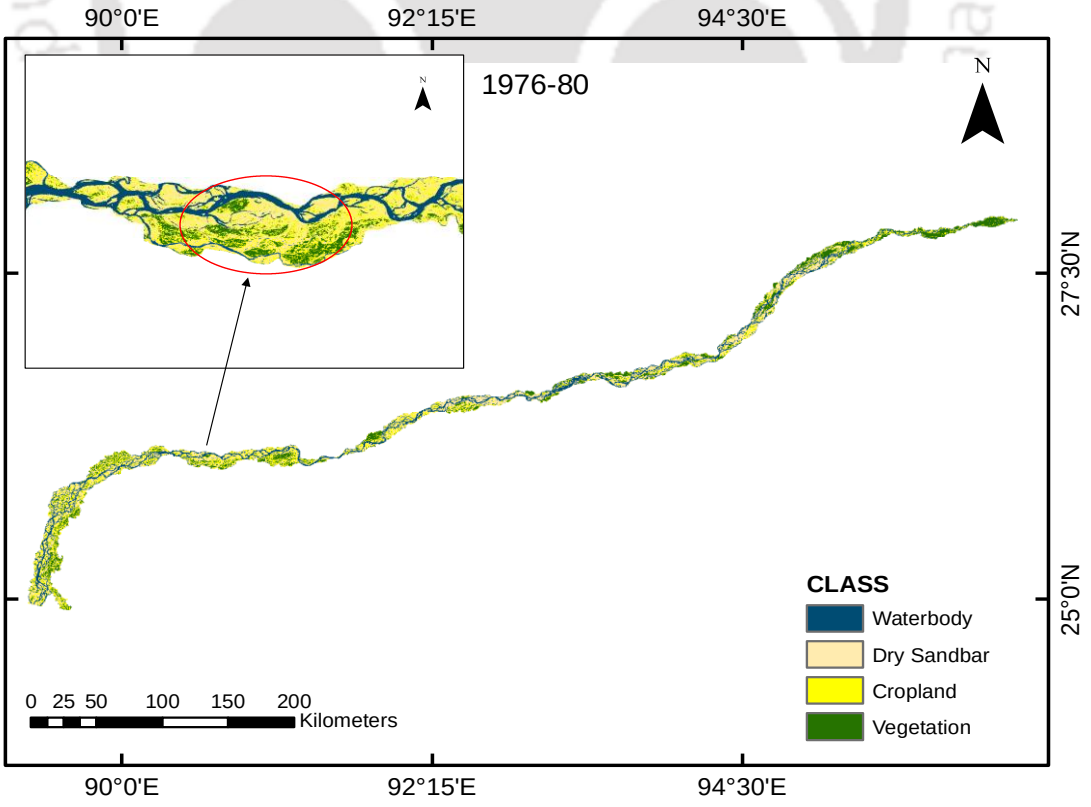

Figure 4.1: Land-use Land Cover (LULC) map of Brahmaputra River for the year 1976-80

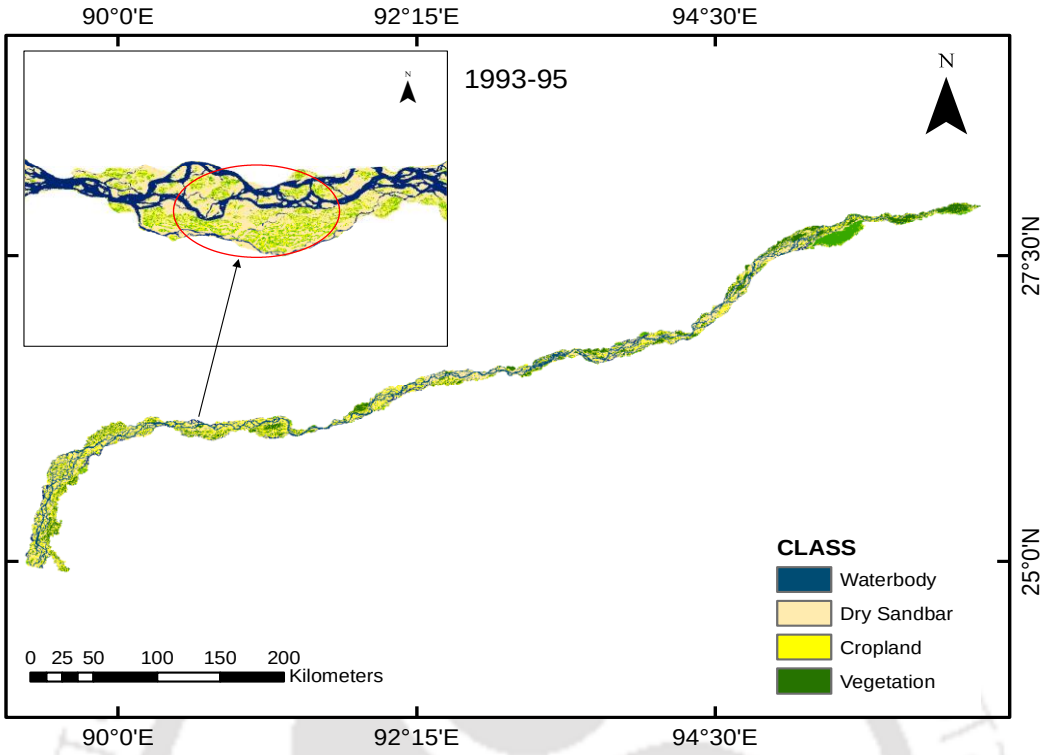

Figure 4.2: Land-use Land Cover (LULC) map of Brahmaputra River for the year 1993-95

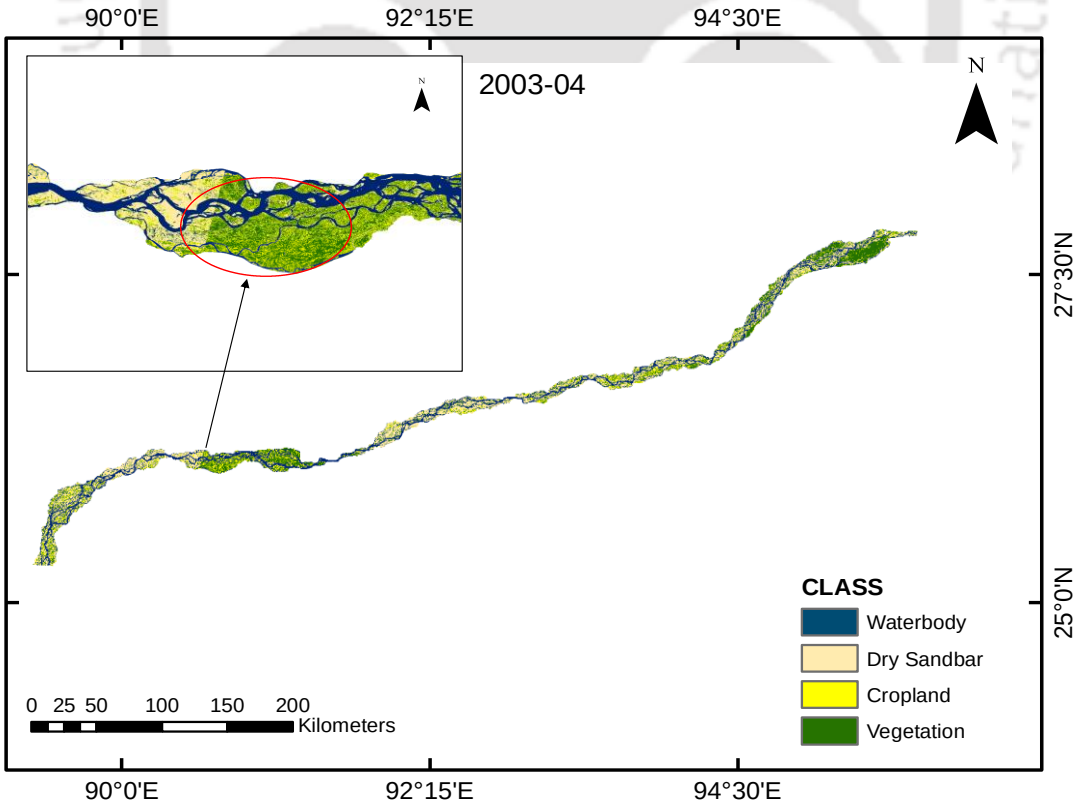

Figure 4.3: Land-use Land Cover (LULC) map of Brahmaputra River for the year 2003-04

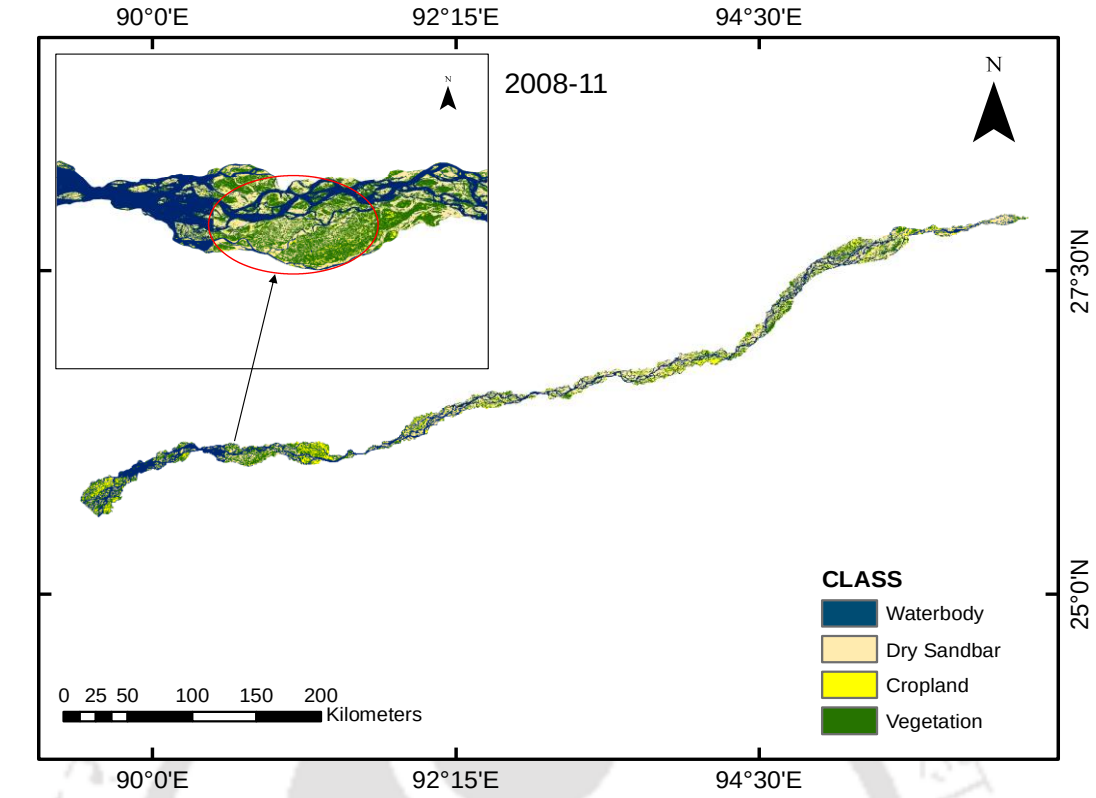

Figure 4.4: Land-use Land Cover (LULC) map of Brahmaputra River for the year 2008-11

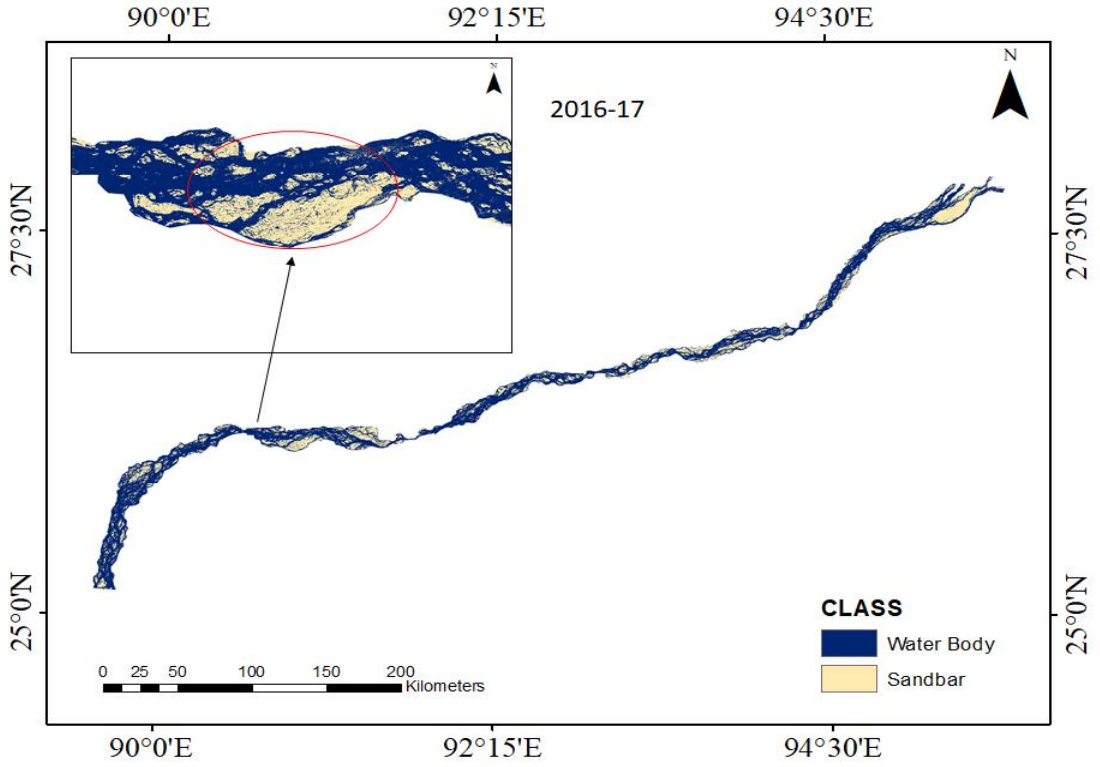

Figure 4.5: Land-use Land Cover (LULC) map of Brahmaputra River during the monsoon period for the year 2016-17

4.3.1 Sandbar dynamics and change detection

Sandbar utilization for farming and agricultural activities is a unique challenge within a riverine ecosystem. Large dynamic braided rivers like the Brahmaputra River undergoes flood every year during the monsoon period. The huge volume of water flow and sediment deposition leads to a change in the morphology of the river. Flooding can be beneficial to some extent, such as increasing fish production and recharging wetlands (Thorslund et al., 2017). However, once the floodwater recedes, the river provides numerous opportunities for various activities. The floodplains and sandbars of the river are inhabited by the poor community, who are dependent primarily on agriculture for their livelihood (Chakraborty, 2013). The formation of sandbars or their migration is because of the shifting sediment load carried by floods every year in the Brahmaputra River. Some sandbars disappear, and some persist for more than 3-4 years. Sarker et al. (2003) found that almost 68% of these sandbars are less than 6 years old, and sandbar areas increase due to the widening of the river. The change in the area of all the classes was studied using unsupervised classification, which will eventually help understand the changes in the land-use land cover in the sandbar portion. This classification aims to understand the pattern of changes in the sandbars from barren to vegetation to cropland. This will provide knowledge about the sandbars being utilized and an understanding of their dynamics. From the classification, it has been found that the percentage of dry sandbars remains more or less unchanged, occupying 25-30% of the riverine system. However, the cropland area can be seen decreasing from 25% to 11%, and vegetation cover increasing from 20% to 25% over the years. The sandbar dynamics and the change in the land cover area corresponding to different classes can be seen in Table 4.3 and Figure 4.6.

Table 4.3: Change in LULC area over the Brahmaputra River for various classes

Class/Year	1976-80		1993-95		2003-04		2008-11	
	Area (Ha)	% Area	Area (Ha)	% Area	Area (Ha)	% Area	Area (Ha)	% Area
Water Body	168837.5	22.6	184629.2	22.5	178767.8	25.8	229279.2	32.1
Dry Sandbar	235969.3	31.7	287162.5	35.0	233924.5	33.7	224248.5	31.4
Cropland	188079.4	25.2	140403.5	17.1	77889.2	11.2	81125.9	11.3
Vegetation	150947.2	20.2	206803.2	25.2	202086.2	29.1	177856.5	24.9
Total	743833.5		818998.4		692667.7		712510.2	

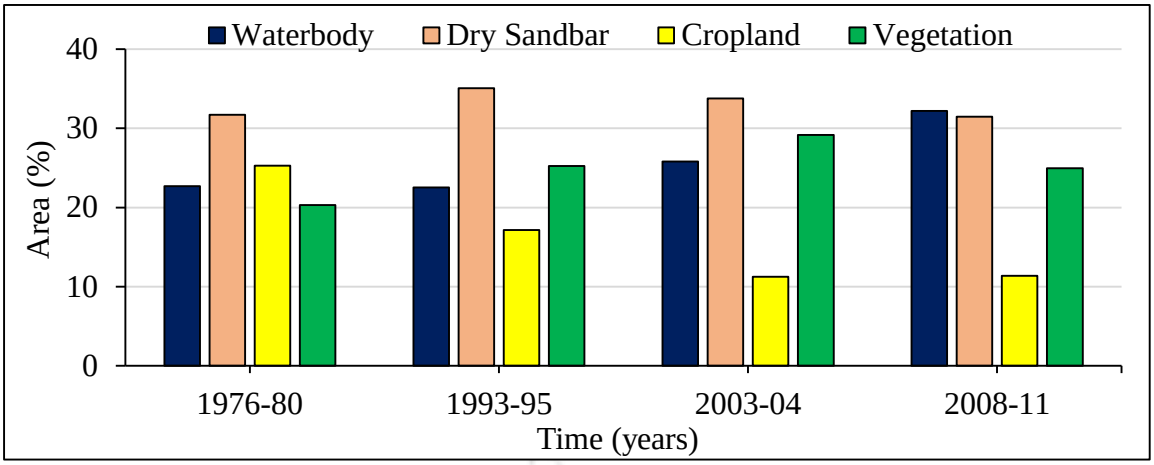

Figure 4.6: Bar Plot of percentage area under waterbody, Dry Sandbar, Cropland and Vegetation during 1976-80 to 2008-11. The dry sandbar has remained consistent over the years within the river. With the increase in vegetation cover, the cropland area has decreased.

4.3.2 Accuracy assessment

For evaluating the performance of the classification, an accuracy assessment was performed for the observed changes in the LULC for the years 1976-80, 1993-95, 2003-04, and 2008-11. A common way of measuring accuracy is by formulating the error/confusion matrix. Overall accuracy is considered an important measure for calculating the error, wherein it evaluates the percentage of correctly classified classes. Another important parameter called the kappa statistic, developed by Cohen (1960), has been widely used in estimating the chance agreement between the observed and predicted values and calculated as follows (Bishop et al., 1977):

$$\text{Estimated Kappa } (K) = \frac{N\sum_{i=1}^{r} - X_{ii} - \sum_{i=1}^{r}(x_{i+})(x_{+i})}{N^2 - \sum_{i=1}^{r}(x_{i+})(x_{+i})} \quad (4.1)$$

where, r represents the no. of rows in the matrix, N represents no. of observations, X_{ii} represents the no. of observations in the i^{th} row and i^{th} column (diagonal elements) and x_{i+} and x_{+i} represents marginal totals of row r and column i, respectively.

Information for assessing the classified images for the corresponding years was obtained from google earth and used as ground control points. The classification performed was also compared with the field survey conducted in October 2019 from Majuli to Dhubri, and assessment was done using overall accuracy and kappa statistics. To validate each class, a comparison between the simulated data and field survey was performed by calculating the producer's accuracy and the user's accuracy. Both the accuracies were implemented to check the correctness of individual classes. However, cropland and vegetation classes with a rrelatively poor user and producer accuracy were found (Table 4.4). This could be due to

difficulty in recognizing the actual crop grown and the vegetation cover in the sandbars during the classification process. To distinguish between the two classes, i.e., cropland and vegetation, a dominant agricultural sandbar in the lower Brahmaputra Valley of the Barpeta district was considered, and classification was performed. Table 4.5 shows that the overall accuracy and kappa value of all four classes were found satisfactory, i.e.,> 0.75.

Table 4.4: Producer's accuracy and user's accuracy for individual classes

Year	Waterbody		Dry Sandbar		Cropland		Vegetation	
	PA (%)	UA (%)	PA (%)	UA (%)	PA (%)	UA (%)	PA (%)	UA (%)
1976-80	99.42	91.74	68.2	91.72	26	19.11	91.1	55.45
1993-95	98.81	100	100	89.86	53.21	96.67	94.73	49.31
2003-04	100	96.05	54.17	73.24	33.87	41.17	66.67	47.37
2008-11	100	86.49	72.84	79.73	51.11	60.52	57.45	52.94

Table 4.5: Overall accuracy and kappa statistics

Year	Overall Accuracy	Kappa value
1976-80	77.50%	0.78
1993-95	85.16%	0.87
2003-04	64.10%	0.68
2008-11	72.99%	0.75

4.3.3 Cropping pattern analysis, change detection and cropland acreage estimation

Cropping pattern is defined as the spatial and sequential arrangement of crops in a given area at a temporal scale. It is a dynamic concept depending on the variations in rainfall, temperature, soil properties, and other factors. The morphology of the braided river system and the flood intensity changes almost every year, resulting in a varying extent of cropping. To understand the cropping pattern in the sandbars, monthly images were derived from Landsat 8 satellite, and the changes were analyzed for the two years, 2016 and 2019. The stretch of sandbar considered lies in the Lower Brahmaputra Valley (LBV), predominantly in the Barpeta district of Assam, India. Early summer rice, summer vegetables, summer pulse, and groundnut are farmed in this district from February to May, late winter rice from

August to November, pea-potato, potato-vegetables, and pulses-vegetables from December to February. The soil type in the region varies from sandy to sandy-loamy. These types of soil are suitable for producing a variety of crops (Kandali et al., 2009).

Two vegetation indices, NDVI and NDWI, were used to detect the changes in the LULC. Band 6 (SWIR-1), Band 5 (NIR), and Band 4 (Red) of the Landsat 8 satellite were used for calculating these indices. NDVI has been widely used in understanding the changes in vegetation cover (Malik et al., 2019). It is determined by using the near-infrared (NIR) and Red (R) bands (Rouse et al., 1973) and is expressed as:

$$NDVI = \frac{R_{NIR} - R_{Red}}{R_{NIR} + R_{Red}} \quad (4.2)$$

where, R_{NIR} and R_{Red} represent the reflectance of NIR and Red bands, respectively.

Another vegetation index, NDWI (Gao, 1996; McFEETERS, 1996) has been used to monitor the moisture conditions of vegetation cover in large areas (Chen et al., 2005) and is expressed as:

$$NDWI = \frac{R_{NIR} - R_{SWIR}}{R_{NIR} + R_{SWIR}} \quad (4.3)$$

where, R_{SWIR} and R_{NIR} represent the reflectance of Short wave infrared (SWIR) and Near Infrared (NIR) bands, respectively.

Both the indices range from -1 to +1. Higher NDVI values reflect the greenness or the vegetation cover, whereas lower values reflect the vegetation stress (Gu et al., 2008). NDWI, on the other hand, reflects the changes in water content in vegetation canopies. The values are negative on dead grass and positive on green vegetation (Gao, 1996). Figure 4.7 shows the relation between NDVI and NDWI with R^2= 0.7563 for the year 2016 and R^2=0.8684 for the year 2019, respectively.

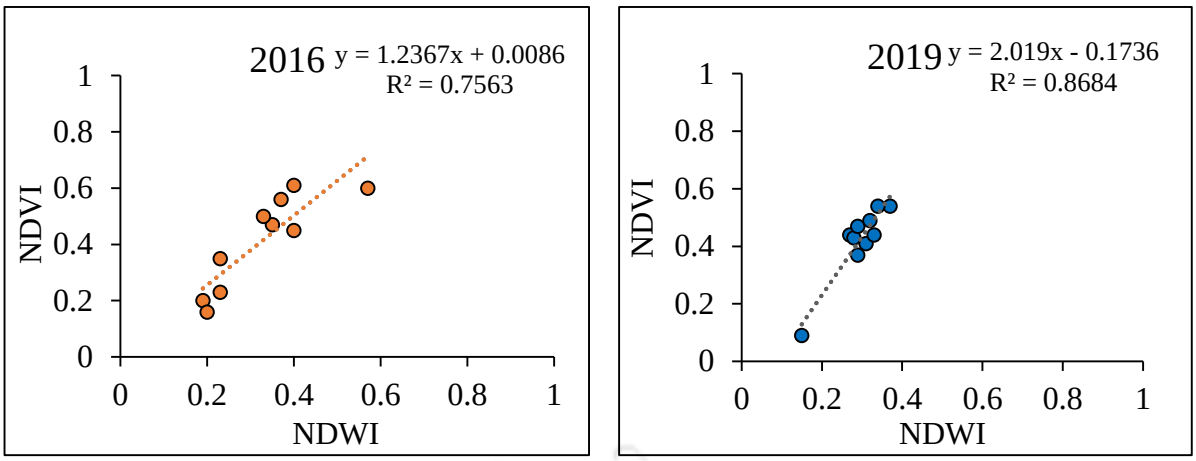

Figure 4.7: Relation between NDVI and NDWI for the years 2016 and 2019

Change detection is an efficient way of describing the variations observed in an agricultural field. In this study, the change detection in the agriculture sandbar was performed by analysing the monthly satellite imageries using an unsupervised classification approach for the years 2016 and 2019. The classes under consideration were waterbody, cropland, dry sandbars, and vegetation. After classification, the area under each land-use class was calculated. The increase or decrease in cropland area and the expansion/conversion of barren lands into agriculture/ vegetation were identified. To observe these changes, the cropland area during the year 2016 was overlaid on the cropland area in 2019. This was done during the pre-monsoon period (Jan-Apr) and the post-monsoon period (Sept-Dec). The difference in the areas of the corresponding class denotes the expansion of the cropland area in the sandbar. The area of land-use under different classes can be seen in Figure 4.8. The results show sandbars that were barren or uncultivated during the year 2016 were occupied with cropland in the year 2019 to some extent. This indicates the expansion of agricultural activities and the suitability of utilizing the sandbars within the river. The change and expansion of the cropland areas from 2016 to 2019 can be seen in Figure 4.9.

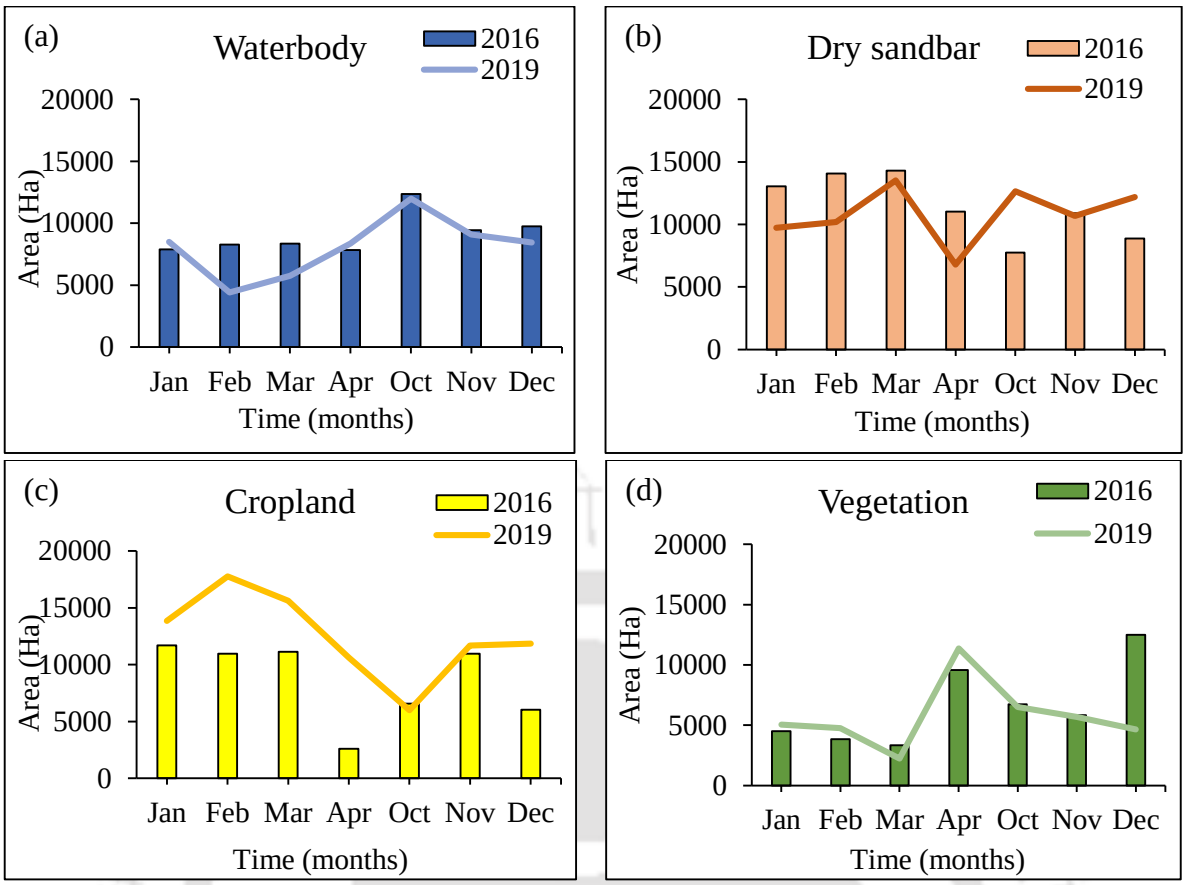

Figure 4.8: Interannual variation of area under different classes during the non-monsoon period of 2016 and 2019. The bar plots represent the change in the area during 2016, and the line plot represents the change during 2019. It is seen that the cropland area has significantly increased from 2016 to 2019 while the vegetation has remained consistent. The increased cropland indicates agricultural practice in the sandbars, resulting in decrease in the dry sandbars.

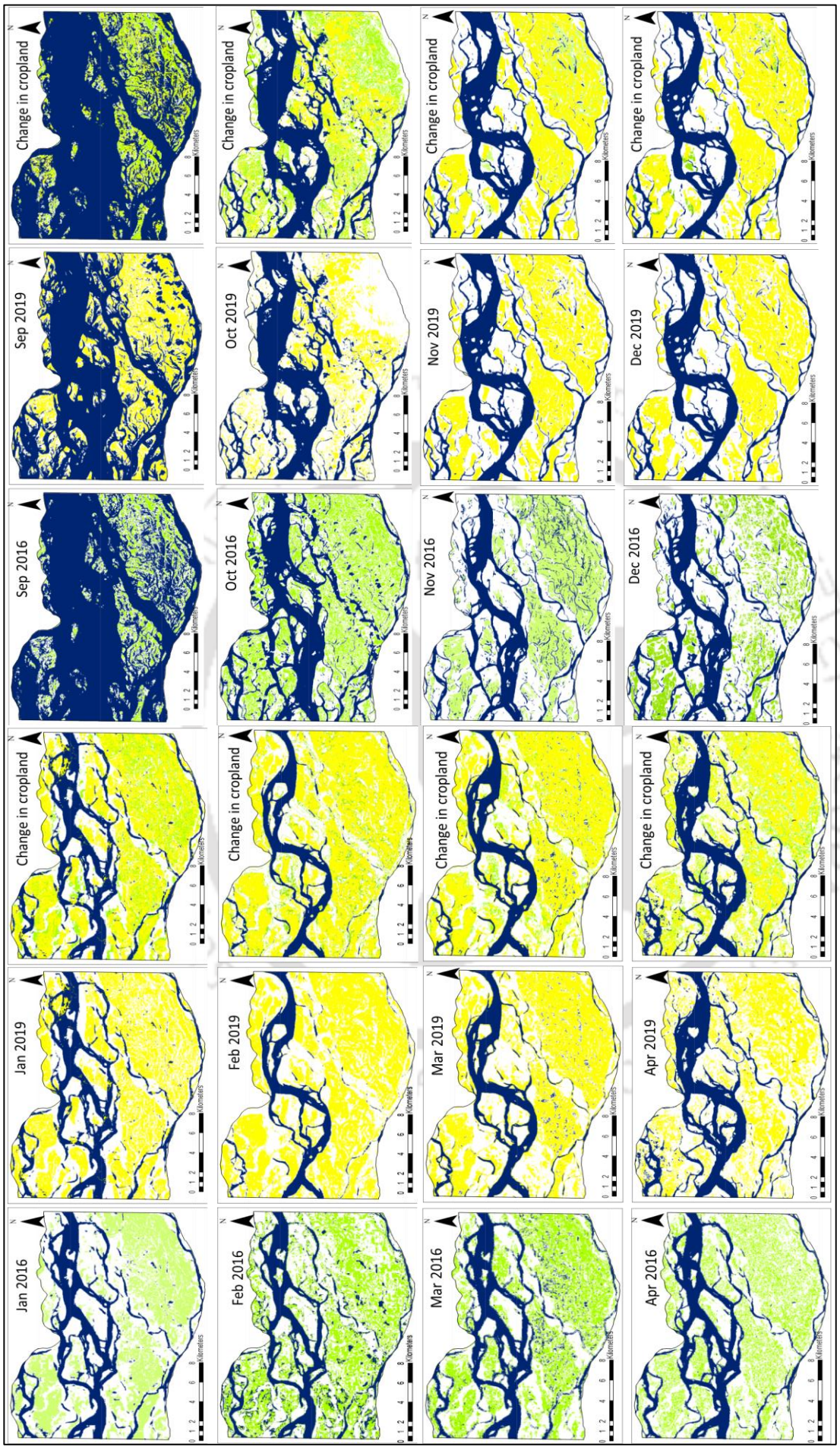

Figure 4.9: Cropland area changes from 2016 to 2019 during the non-monsoon period. The blue color represents waterbody, white color inside the study domain represents dry sandbar areas, green color represents cropland area in 2016 and yellow color represents the cropland areas in 2019. The increase in cropland areas can be seen during the months of Jan-Apr (pre-monsoon period) and Nov-Dec (post-monsoon period)

To further understand the current cropping practices within the sandbar in the district, two areas, A and B, were selected. High-resolution satellite data were obtained from the google earth platform for the selected regions. Although google earth images could distinguish between different crops grown, determining the type of crops grown in the sandbar was difficult. The images were extracted to ArcGIS 10.4 and projected to WGS 84 projection for analysis. To understand the actual type of crop being cultivated, a detailed field investigation is required. Figure 4.10 shows the change in the cropping pattern under different crop types in the sandbars in different periods. Table 4.6 summarizes the area covered by different crop types in two scenes for the years 2016 and 2019. Three crop types could be recognized in both the scenes, i.e., scene 2 (December) and scene 3 (March).

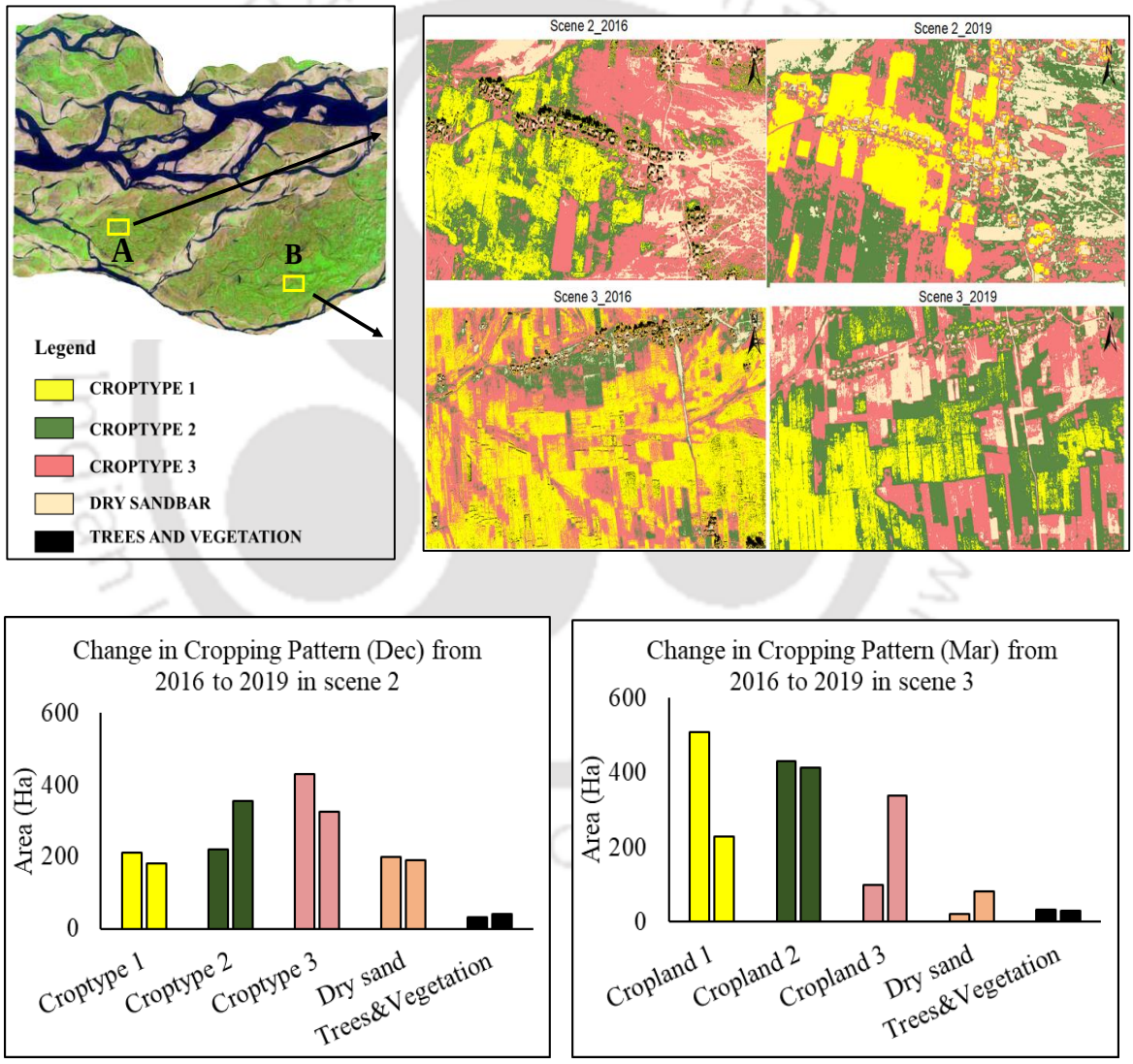

Figure 4.9: Change in cropping pattern under different crop types in the sandbars during different seasons

Table 4.6: Acreage estimation of different crop types in the regions A and B

	Scene 2_2016	Scene 2_2019	Scene 3_2016	Scene 3_2019
	Area(Ha)	Area(Ha)	Area(Ha)	Area(Ha)
Croptype 1	211.8	182.6	508.4	227.8
Croptype 2	220.7	355.2	431.2	412.9
Croptype 3	429.5	323.8	99.6	337.5
Dry sand	198.1	191.2	21.1	82.4
Trees andVegetation	31.7	39.20	32.01	31.2
Total	1092	1092	1092	1092

4.4 Results and Discussion

The initial classification work conducted on a decadal scale for the entire Brahmaputra River, across an average area of around 7,50,000 ha from Majuli to Dhubri, found that cropland area has been decreasing and vegetation cover has been increasing. To analyze the cropland area and vegetation cover changes, the study was conducted on a smaller area of approximately 37,117 Ha in the sandbar portion in the LBV.

4.4.1 LULC Change detection and acreage estimation

The LULC change and the area estimation of all four classes in this study were carried out using the Landsat 8 satellite imageries over an area of 37,117 ha. A finer resolution imagery was also analyzed to detect the type of crops grown over an area of approximately 1100 Ha. The analysis was carried out during two seasons, i.e., pre-monsoon (Jan-Apr) and Post monsoon (Oct-Dec). Table 4.7 depicts the change in area under different classes: waterbody, dry sandbar, cropland, and vegetation during the pre-monsoon and post-monsoon seasons in study site 1. During the pre-monsoon period in 2016, out of the total sandbar area of 37,717 Ha, about 35% of the sandbar was found to be dry sandbar, and about 28% were utilized for agriculture activities as cropland. While in the year 2019, about 27% of sandbars were dry sandbars, and the cropland area covered about 39% of the total area. This indicated a decrease in the dry sandbar areas by around 23% and an increase in the cropland area by around 36%. During the post-monsoon season, dry sandbar covered about 24% and 31% area, and cropland covered about 24% and 27% area in 2016 and 2019, respectively. This showed an increase in both cropland and dry sandbar areas, but the

percentage of increase in cropland area was less. The increase in dry sandbar areas was because of the massive amount of sediments carried and deposited during the high flow period during the monsoon season (May-Aug). Thus, from this analysis, it can be inferred that dry sandbars within the riverine ecosystem are being utilized for cropping and other agricultural activities, with an increase of around 24% of the cropland area during the period 2016 to 2019. To further investigate the crop types grown in the study area, two scenes were selected and analyzed, as discussed in section 4.3. In the case of scene 2, Croptype 3, which was dominant in 2016, was replaced by Croptype 2 in 2019. The area under Croptype 2 remained approximately equal in both years. However, no specific Croptype can be seen cultivated in the selected scenes on the sandbar during this analysis.

Table 4.7: Percentage change in area under different classes in 2016 and 2019

	pre-monsoon Area (Ha)			post-monsoon Area (Ha)		
	2016	2019	% Change	2016	2019	% Change
Water body	8080.42	6748.92	-16.48%	10509.87	9839.10	-6.38%
Dry Sandbar	13106.59	10054.38	-23.28%	9172.62	11838.69	29.06%
Cropland	10617.75	14464.48	36.22%	9087.84	9831.18	8.17%
Vegetation	5312.43	5849.43	10.10%	8347.02	5608.29	-32.81%

4.4.2 Vegetation indices and cropping pattern analysis

Understanding the vegetation status of the crops grown in the sandbars is essential for understanding the cropping pattern, productivity, and suitability of a variety of crops. The cropping pattern in the sandbars depends on the timing and intensity of the flood. Early monsoons with heavy floods may be unsuitable for agricultural activities in the sandbars. However, low-intensity floods may bring fresh sediments favouring agriculture. The study of cropping pattern change illustrates the proportion of area under different crops at a temporal scale. The spectral analysis provides information on different crop growth stages, i.e., sowing, plantation, harvesting, etc. These stages can be detected from the NDVI curve during different months. The spectral profile of NDVI is represented in Figure 4.11. It shows that the field preparation and sowing of seeds within the riverine sandbar starts in the month of March and reaches a peak during May-June. The crops grown have an average growth cycle from sowing to harvesting of around 110-130 days. These crops are probably summer crops like Ahu Rice, Black gram, and green gram. The period between July and

October is considered Kharif crops, which shows a peak, i.e., the harvest time during September. This interannual variation of NDVI values shows the practice of double cropping in the sandbars of the Brahmaputra River. The interpretation of NDVI values during different DOY (day of the year) corresponds to varying crop types grown in the sandbars.

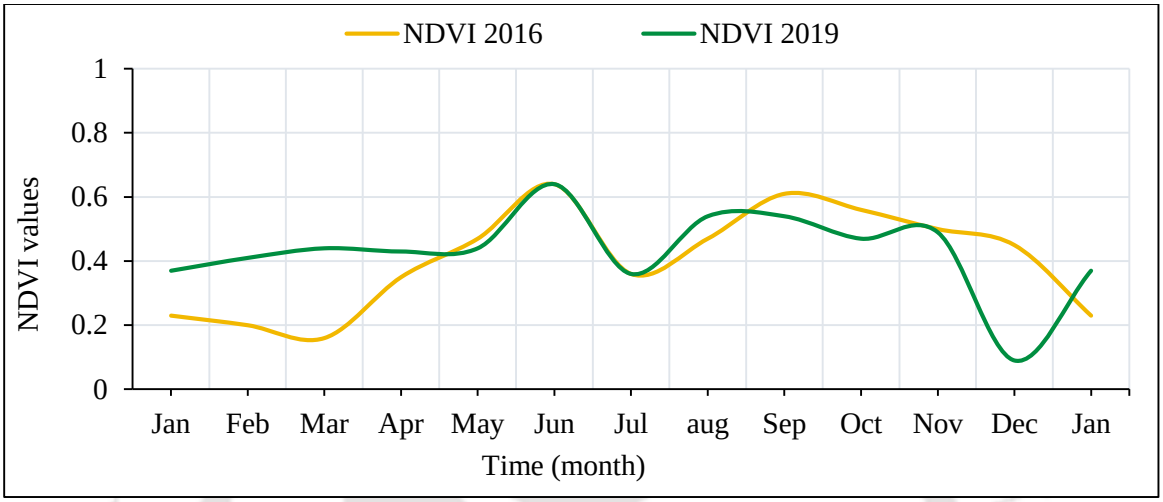

Figure 4.10: NDVI spectral profile for the years 2016 and 2019

4.5 Conclusions

In this study, an attempt has been made to understand the cropping practices, patterns, and suitability in River Brahmaputra's sandbars. Satellite images derived from Landsat 8 were helpful in determining the cropping pattern, and NDVI values recognized the stages of cropping very well. The sandbars developed within the river due to aggradation and degradation over the years, and those permanently existing in the river can be beneficial for various cropping and farming activities. The Brahmaputra River gives agriculture and aquaculture opportunities to communities that rely on it for their livelihood. This study revealed the scope and utilization of these sandbars in various agricultural activities. The dwellers have very well adopted sandbar cultivation in converting these barren lands into an income-generating source. However, no specific planning of crops can be seen cultivated in this study. With more than 30% of the dry sandbars prevalent over the entire river, an optimal cropping pattern with crop intensification techniques is suggested to increase productivity. It was found that the maximum land availability in sandbars of Brahmaputra River was from October to January and decreased gradually as the water level increased in the river. The data collection in the form of sediment sample collections from the sandbars, field visits, and questionnaire surveys among the farmers practicing sandbar

cultivation will provide necessary information about the suitability of crop growth, crop types, and the existing cropping pattern difficulties, and the scope of sandbar cropping practices. In addition, as the sandbars exists near the rivers, the streamflow varies and the water level fluctuates. The study of variations in the water level during different crop growth seasons could be achieved using flow simulation model. Figure 4.11 shows paddy cultivation near the riverbank of the Brahmaputra River in Assam.

Figure 4.11: Rice fields along Dikrong riverbank, a tributary of the Brahmaputra, in Assam (Rampini 2014).

5

Flow Simulation Model

5.1 Introduction

With the advancement in mathematical modelling techniques and computational facility, governing equations of two-dimensional (2D) unsteady flow can now be solved in its fully dynamic form, considering all significant forces that governs river hydraulics. The hydrodynamic (HD) model studies are a common and robust model for describing the behaviour of natural systems. They are helpful in the study of the complex simulation of river flows. Previous studies have shown the development of 2D models for understanding the braided and meandering configuration of the rivers. This makes it essential to understand the link between the morphological changes within the river and the ecosystem services it provides to the human population.

The Brahmaputra River exhibits complex morphological characteristics due to wider braided river width, high flow, and sediment variability with erodible banks (Karmaker et al., 2017). In addition, sandbars are highly dynamic and migrate over a short time. In the present objective, an attempt was made to study the water depth in the sandbar areas available during different seasons. The aim is (a) to develop a simulation model at a study reach wherein an agricultural sandbar is present within the Brahmaputra River; (b) to study the area available in the sandbar under different flow conditions to understand the scope of its utilization at different time scales. Therefore, a two-dimensional (2D) hydrodynamic model MIKE 21C, was set up with river bathymetry and simulated at different discharges. The response to different flow conditions was analyzed, and sandbar areas available at different cropping periods were determined.

5.2 Basic governing equations

MIKE 21C is a generalized mathematical modeling system for simulating the hydrodynamics of two-dimensional (2D) surface flow and sediment transport using a rectilinear or a curvilinear grid (DHI, M., 2011). It is based on an orthogonal grid that solves a set of elliptic partial differential equations. The orthogonal grids used makes the difference equations easier to solve, making the numerical scheme more accurate and improving the computational speed. Figure 5.1 shows the schematization of a river in a rectilinear and curvilinear grid. The following elliptical differential equations are solved to obtain the orthogonal curvilinear grid.

$$\frac{\partial}{\partial s}\left(g\frac{\partial x}{\partial s}\right)+\frac{\partial}{\partial n}\left(\frac{1}{g}\frac{\partial x}{\partial n}\right)=0 \tag{5.1}$$

$$\frac{\partial}{\partial s}\left(g\frac{\partial y}{\partial s}\right)+\frac{\partial}{\partial n}\left(\frac{1}{g}\frac{\partial y}{\partial n}\right)=0 \tag{5.2}$$

where, x, y = Cartesian coordinates; s, n = Curvilinear coordinates; g = Weight function

The hydrodynamic (HD) model simulates the flow and water level variations in rivers and estuaries. The simulations were carried out on the curvilinear grid generated over the entire area. This model solves the fully dynamic and vertically integrated Saint Venant Equation (continuity and momentum equation) in two directions. The equations solved in MIKE 21C are:

$$\frac{\partial p}{\partial t}+\frac{\partial}{\partial s}\left(\frac{p^2}{h}\right)+\frac{\partial}{\partial n}\left(\frac{pq}{h}\right)+2\frac{pq}{hR_n}+\frac{p^2-q^2}{hR_s}+gh\frac{\partial H}{\partial s}+\frac{g}{C^2}\frac{p\sqrt{p^2+q^2}}{h^2}=RHS \tag{5.3}$$

$$\frac{\partial q}{\partial t}+\frac{\partial}{\partial s}\left(\frac{pq}{h}\right)+\frac{\partial}{\partial n}\left(\frac{q^2}{h}\right)+2\frac{pq}{hR_s}+\frac{q^2-p^2}{hR_n}+gh\frac{\partial H}{\partial n}+\frac{g}{C^2}\frac{q\sqrt{p^2+q^2}}{h^2}=RHS \tag{5.4}$$

$$\frac{\partial H}{\partial t}+\frac{\partial p}{\partial s}+\frac{\partial q}{\partial n}-\frac{q}{C}+\frac{p}{R_n}=0 \tag{5.5}$$

where, s, n = coordinates in the curvilinear coordinate system; p, q = mass fluxes in the s and n direction, respectively; H, h = water level, water depth, respectively; g = gravitational

acceleration; C = Chezy roughness coefficient; R_s, R_n = radii of curvature of *s*- and *n*-lines, respectively, and RHS describing all of Reynold stresses

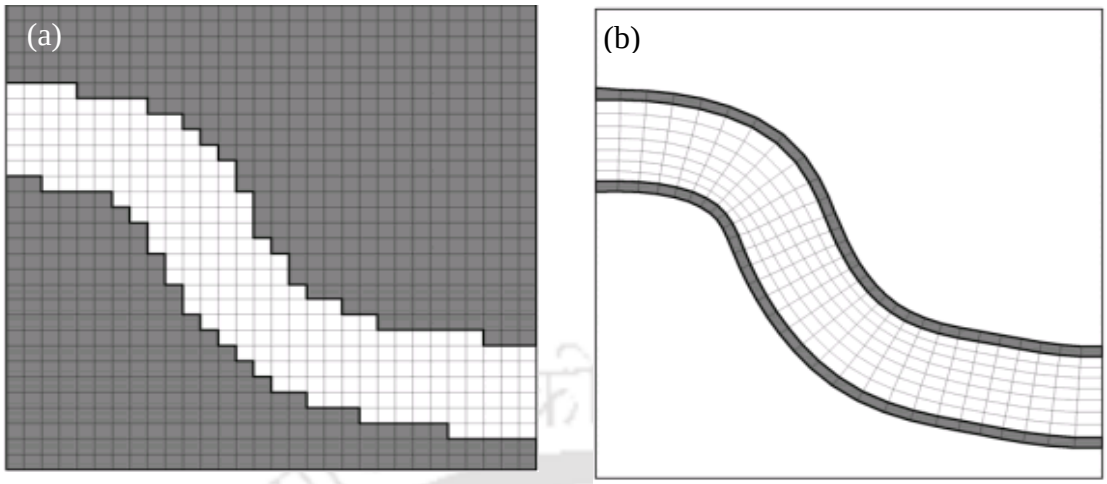

Figure 5.1: Schematization of a river in (a) rectilinear and (b) curvilinear grid

5.3 Model description and formulation

The curvilinear MIKE 21C model requires fewer computational points and hence smaller capacity than the rectilinear grid, thus providing better flow resolutions (Morianou et al., 2016). In application to river study, an accurate boundary resolution is required, and hence the curvilinear grid is favorable in such situations. An accurate prediction of flow depth and velocity is thus assured while using the curvilinear grid.

5.3.1 Computational grid and bathymetry

The study area considered is study site 2, as described in section 3.2. To evaluate the current scenario of the sandbar, a reconnaissance survey of the selected site was performed. A reach of around 11 km was chosen from Kuruwa to Umananda, lying between 91°44' to 91°51' East longitudes and 26°11' to 26°14' North latitudes in the Kamrup District, Assam. Before the simulation, a bathymetric survey was conducted using an Echo sounder, Flow meter, Global Positioning System (GPS), and Total Station (TS). The velocity was measured at different cross-sections in the river and was used to validate the model (Table ST1). To get an accurate image of the river morphology, the bathymetry of the river was taken at appropriate intervals of the cross-section over a strip of sufficient width. The water level readings were gathered at the start of each survey to construct a daily water surface profile during the survey period (Table 5.1). The flow velocity was measured with the help of Cup Type Current meter during the survey period. Figure 5.2 depicts the satellite imagery planform showing the agricultural activities performed in the sandbars and new dry

sandbars developed in the river reach. To include the bathymetry into the model and to compute the water depth and velocity, a computation grid of size 400×200 was generated, as shown in figure 5.3. The elevation points and their coordinates were incorporated into the MIKE 21C model for grid generation. The model incorporated the discharge parameters and their corresponding water level as the boundary conditions. Figure 5.4 and figure 5.5 represents the three-dimensional (3D) view of the generated bathymetry and the interpolated river bathymetry developed using a curvilinear grid generator.

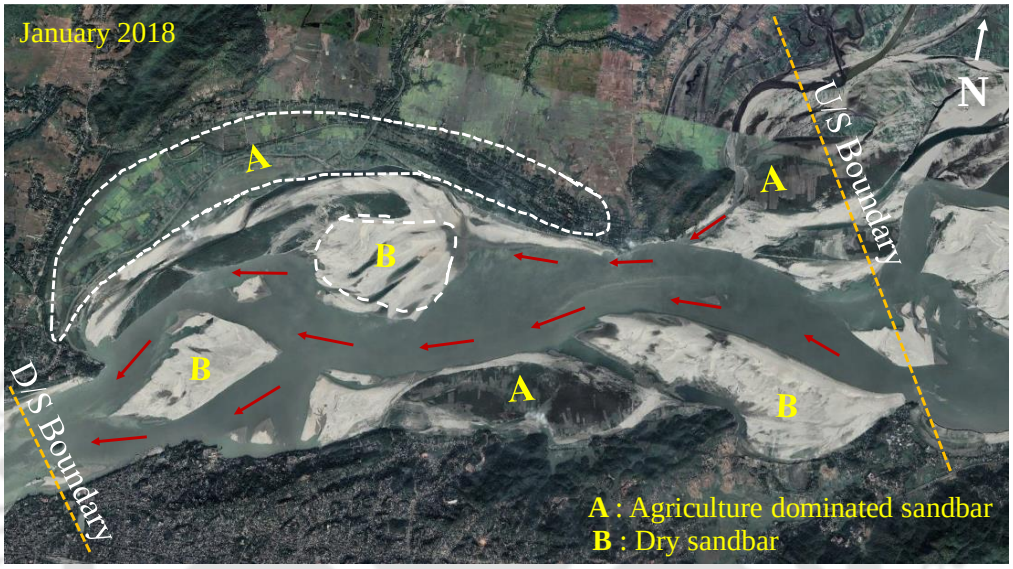

Figure 5.2: Satellite imagery planform showing the agricultural activities performed in the sandbars as well as new dry sandbars developed in the river reach.

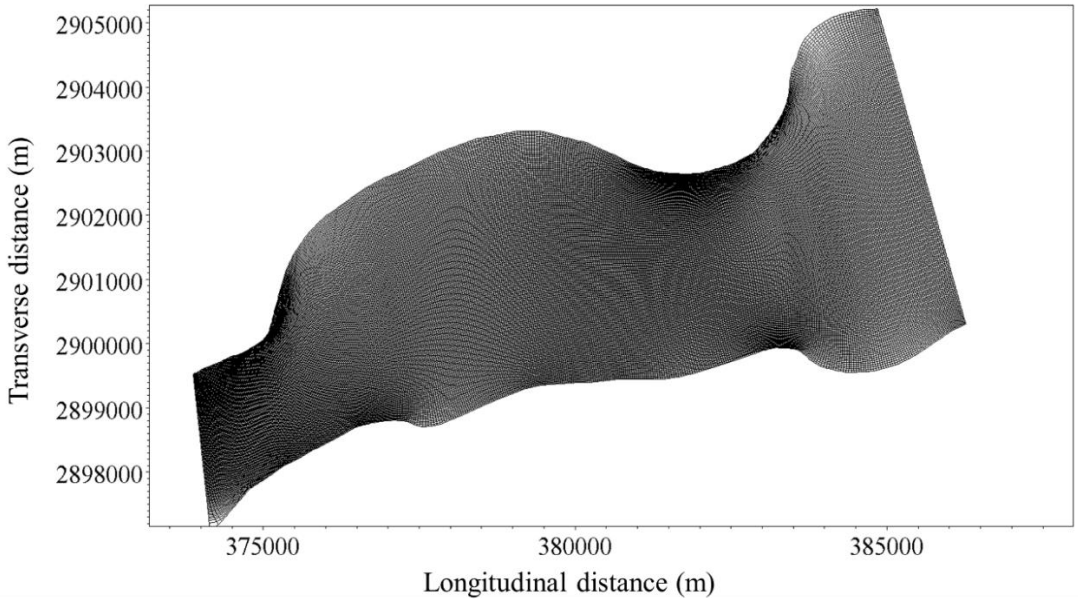

Figure 5.3: Computational grid of the study area

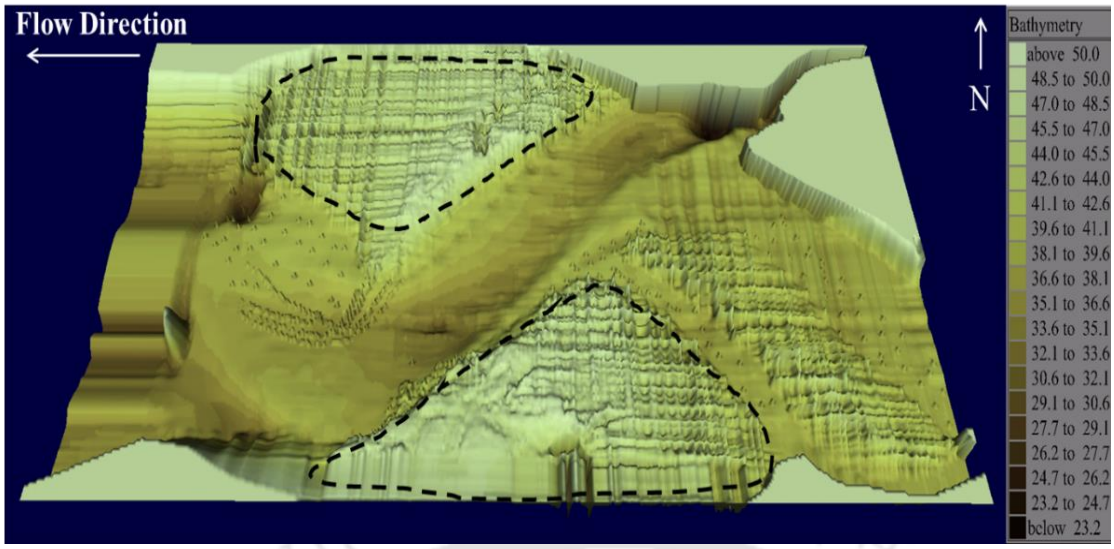

Figure 5.4: Three-dimensional (3D) view of bathymetry generated for the study area. The dashed lines represent the sandbar portion on the North and South side of the river

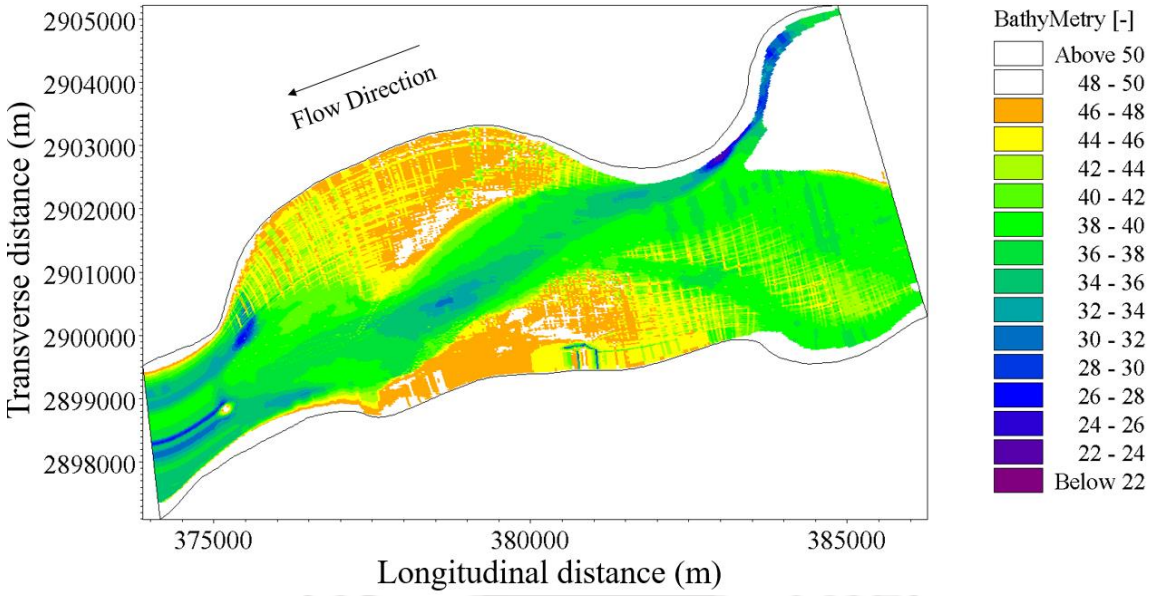

Figure 5.5: Interpolated River bathymetry developed using curvilinear grid generator

Table 5.1: Water level readings measured during the bathymetric survey

Date	Timings	Water level	Average water level (m)
09-01-2018	08:21 AM	41.41	41.52
	04:30 PM	41.64	
10-01-2018	08:38 AM	41.62	41.61
	04:22 PM	41.61	
11-01-2018	09:11 AM	41.6	41.6
	04:50 PM	41.61	
12-01-2018	08:33 AM	41.61	41.54
	04:42 PM	41.47	
18-01-2018	08:53 AM	40.99	40.99
	04:15 PM	40.99	
19-01-2018	09:27 AM	41.21	41.27
	04:02 PM	41.33	
20-01-2018	09:15 AM	41.07	41.04
	04:35 PM	41.02	
21-01-2018	08:51 AM	41.06	41.06
	04:12 PM	41.05	
22-01-2018	08:45 AM	42.41	42.39
	04:33 PM	42.38	

5.3.2 Initial and Boundary conditions

The model requires either a water level or a discharge at all open boundaries. The streamflow data and the corresponding initial water surface level were introduced as the input parameters to the model at upstream and downstream, respectively. The streamflow data were collected from the Brahmaputra Board, Ministry of Jal Sakti, Govt. of India at the Pandu gauging station from 1999 to 2015. Ten daily data were converted into a monthly scale using the simple averaging method. The maximum streamflow value corresponding to a season (Zaid, Kharif, Rabi) was used for the simulation process. The maximum streamflow value corresponding to a season was simulated in the model run, and water depth was calculated. In India, the cropping season varies seasonally. Moreover, the daily streamflow values generally do not undergo large fluctuations unless extreme events occur. Prediction of such disastrous extreme events is difficult. Farmers were also interested in land area availability at a monthly to seasonal scale depending on the crop types and duration of crop planting and farming.

The setting up of the MIKE 21C, in general, necessitates the following steps:

1. The computational grid is extended over the entire reach of the study area. The extent can vary from a few hundred meters to more than 100 km. The grid size depends on the channel width, depth, and flow direction. The coordinates and bed level are entered in an ASCII (American Standard Code for Information Interchange) format into the grid. Various interpolation and extrapolation processes are processed within it.
2. The boundary conditions at upstream and downstream are specified appropriately, and the simulation period is planned accordingly. Basically, a time series of discharge and water levels are specified upstream and downstream, respectively.
3. At last, the initial conditions favourable for the study area are defined and modified based on the need of the study. The model's output comprises the following parameters within a predefined time step throughout the simulation time.
   a) The 2D water depth map
   b) The 2D flow velocity map in both the x and y-direction
   c) Time series plot of water level, flow velocity, water depth, etc.

5.4 Model calibration and validation

The model was calibrated with the velocity measured at the downstream section of the River. The velocity was obtained by performing the survey using a cup-type current meter. The current meter measurement was taken at 0.8D and 0.2D at three locations, i.e., Upstream, Middle, and downstream sections. The average velocity at the downstream portion at 0.2D and 0.8D was found to be 0.545m/s and 0.432m/s, respectively. The simulated velocity resulting from the model study was found to agree with the measured velocity, as shown in Figure 5.6.

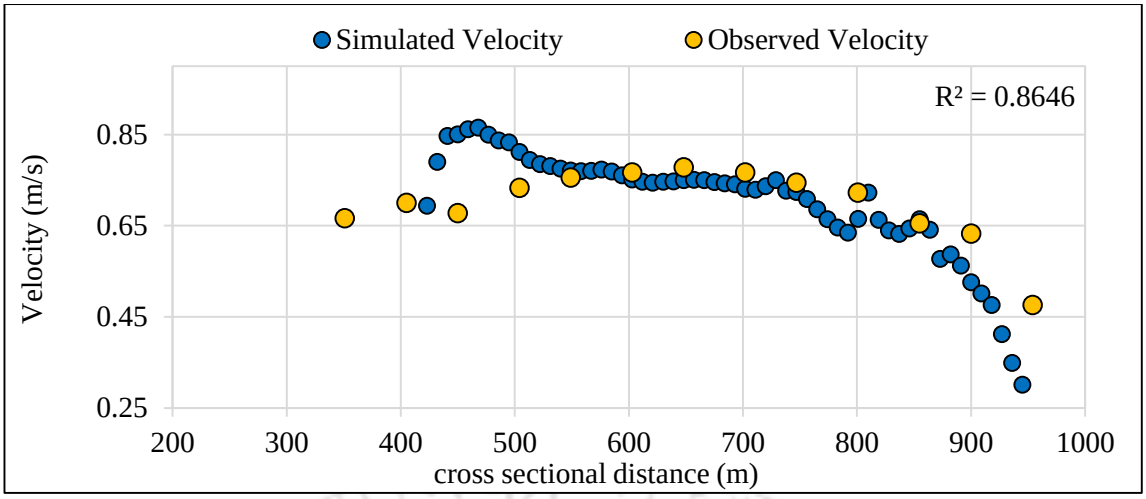

Figure 5.6: Comparison of observed velocity and simulated velocity across a river cross-section within the study reach.

5.5 Results and Discussion

The simulation results exhibit the water depth under varying streamflow along with current speed and velocity vectors across the study reach. Figure 5.7 represents the flood inundation and current speed and the velocity contours during low flow and high flow periods, respectively. The low and high flow corresponds to a discharge of approximately 2900 cumecs and 20000 cumecs, respectively, in this case. It was found that the velocity ranged between 0.1-0.4 m/sec in the sandbar portion while it ranged above 1.4m/sec in the river portion. It can also be seen that during the low flow period, there are large sandbars formed in the north and south side of the sandbars. These sandbars have been used for agricultural activities by the farmers and dwellers residing in the nearby areas to sustain their livelihood. Because these sandbars originate within rivers, they are susceptible to seasonal floods due to fluctuating water levels. Therefore, the objective of the mathematical model simulation was to determine the water depth corresponding to different discharges from the years 1999 to 2015. The water depth resulting from different simulation runs was processed in the GIS tool, and the total sandbar area available under the corresponding streamflow was calculated. As cropping pattern varies seasonally, the area available was also required on a seasonal basis. Thus, the maximum streamflow corresponding to a particular season was taken into consideration for area calculation. For the present work, the maximum depth considered for performing any sandbar cropping activities was taken as 0.9m. The area upto 0.9m was categorized into four water depth ranges. i.e., dryland area, area between 0-0.3m depth, between 0.3-0.6m depth, and between 0.6-0.9m depth. The categorization was based

on the crop survival and growth stages. However, any depth could be considered at different depth ranges based on the study area, regional crop selection, and other factors. Figure 5.8 depicts the sandbar area available in the dryland portion in all three seasons as box plots. The dryland portion of the sandbar remains non-inundated as water does not reach this portion of the sandbar under different flow simulations. Thus, the area fluctuates in each given season, and the portion of area available for dryland cropping can be determined. It was found that the area available during the Zaid period was more compared to Rabi and Kharif periods. The Kharif crops are usually sown at the beginning of the first rainfall during the advent of the southwest monsoon season. They are harvested at the end of the monsoon season, i.e., during September-October. However, during this period, the area availability was found to be less in the sandbar regions as most of these sandbars remain submerged. Furthermore, it was found during the questionnaire survey (Appendix) that certain classes of farmers do not prefer cultivation during this period as the risk of crop damage from floods. Nevertheless, another class of farmers cultivates a certain variety of crops such as Jute and Deepwater paddy in the waterlogged sandbars. Figure 5.9 shows the box plots of the area available under three different depth ranges for the Zaid, Kharif, and Rabi periods. It was found that during the Zaid and Rabi period, the area available remained almost similar varying between 40 Ha to 100 Ha. However, during the Kharif seasons, the area available was reduced, which varies between about 20 Ha to 60 Ha.

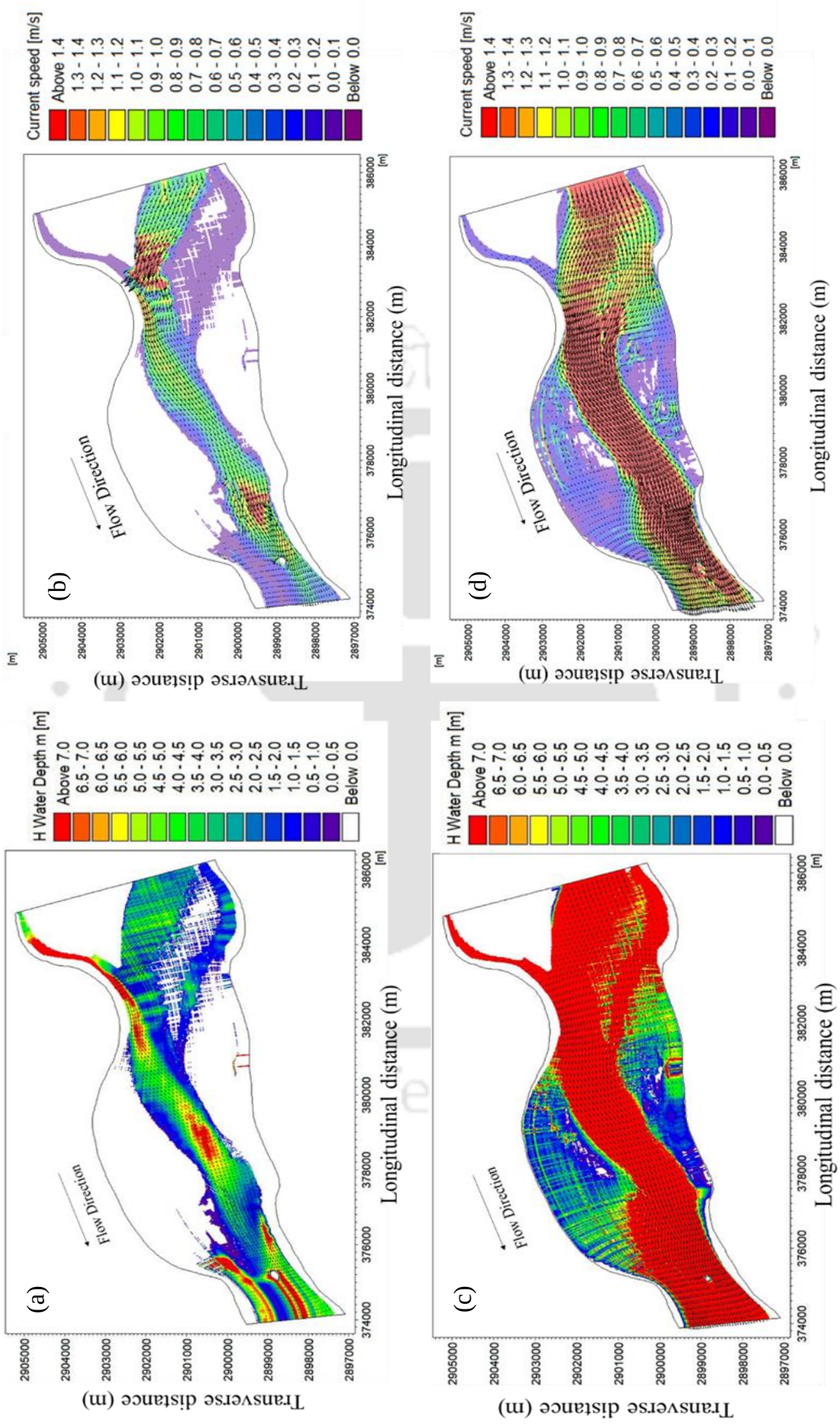

Figure 5.7: Sandbar area inundation under low flow and high flow conditions. Fig (a,b) represents the water depth and current speed under low flow conditions, and Fig (c,d) represents the water depth and current speed under high flow conditions. The white region within the flow domain represents the emerged sandbar unaffected by flood during low and high flow conditions. The X-axis and Y-axis represent the longitudinal and transverse distance in UTM (Universal Transverse Mercator) coordinate system.

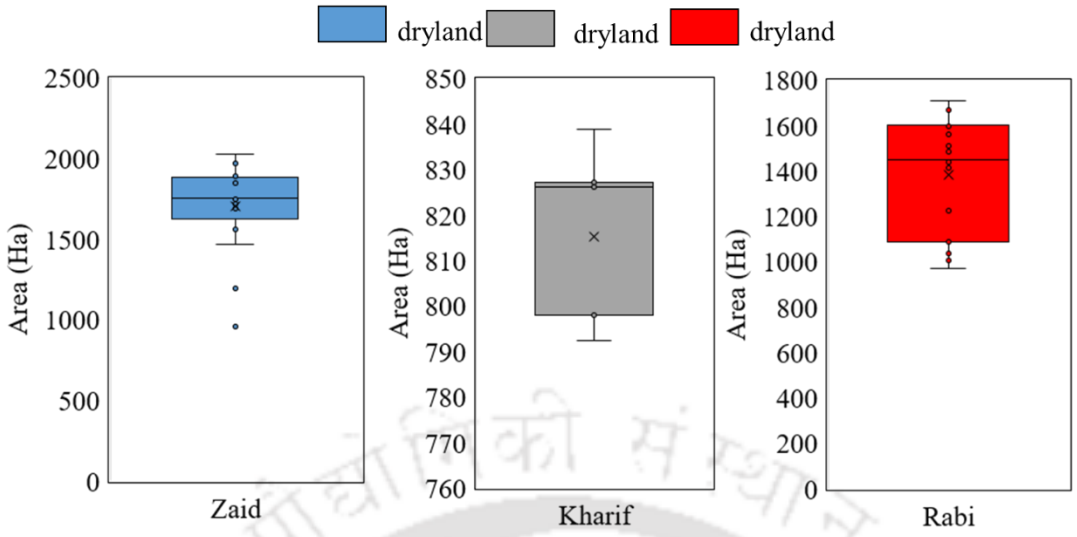

Figure 5.7: Box plot showing the dryland area available during the Zaid, Kharif, and Rabi period for the maximum streamflow values in the years 1999-2015.

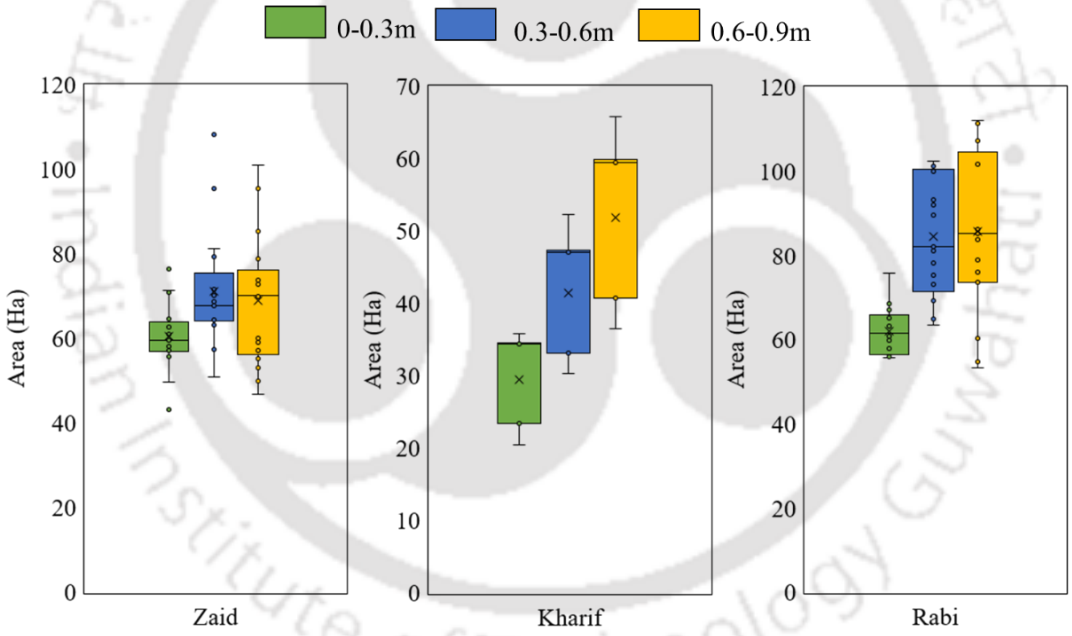

Figure 5.8: Box plot showing the area available at 0-0.3m, 0.3-0.6m, and 0.6-0.9m water depth during the Zaid, Kharif, and Rabi period for the maximum streamflow values in the years 1999-2015.

5.6 Conclusions

In India, unorganized agriculture is traditionally practiced in the sandbars of its large braided rivers like the Brahmaputra, as vast landmasses are available within the river. A more organized approach to utilizing these sandbars is necessary to obtain optimal benefits without disturbing the river ecology. This study can be regarded as the beginning of such an organized approach. In the present objective, a 2D mathematical model was simulated

to investigate the water depth under varying streamflow in a selected reach within the Brahmaputra River. A curvilinear grid was employed where the grid follows the bank line of the river. The dense curvilinear grid and bathymetry file derived from the field survey provided a good flow analysis near the boundaries and junction of the main channel and sandbar portions, thereby generating high simulation accuracy of the water flow. Regarding the calibration and validation, the simulation results were found to be in good agreement with the field measurements. After the successful validation process, the 2D maps of water depth and flow velocity were produced. By using the MIKE 21C simulation results, the dynamic behaviour and sandbar area available within the study reach could be specified.

The results of the study lead to the following observations:

1. The findings of the study revealed new insights into the flow dynamics of large braided rivers, as well as a broad range of potential applications in the areas of food production in barren yet fertile sandbars, income and asset generation, increased food consumption, improved nutrition, and alternative risk management strategies during lean periods.
2. From the simulated water depth, the sandbar area available during different seasons was determined for planning agricultural activities. The crops that survive under the selected depths could be considered. An optimal cropping pattern can be planned to generate income to the farmers and dwellers while supporting socio-economic upliftment.
3. The river also carries tremendous sediment and deposits it in the sandbars. These sediments may consist of alluvium and other minerals and nutrients, which could be favourable for cultivating crops. Therefore, analysing these sediment characteristics could significantly impact the suitability and favourability of crop growth in the riverine sandbars.

This study would be helpful for the researchers working in a similar environment and provide a vast scope in planning suitable activities according to the environmental flow conditions and river characteristics across different rivers around the world.

6

Sediment analysis to understand sandbar characteristics

6.1 Introduction

Sediments are an important component of rivers and play a significant role in the geomorphological, hydrological, and ecological functioning of river basins. It provides a substrate for organisms and fertile soils in floodplains, which are highly suitable for agriculture. Riverine sandbars are dry areas adjacent to rivers and are susceptible of being inundated by water from occasional or periodic flooding. Sediment yield studies are important for various soil and water conservation-planning processes such as changes in river morphology, riverbed siltation, reservoir sedimentation analysis, agricultural planning, etc. Sandbars are formed by sandy and alluvial deposits and constitute an important feature of the landscape. The floodplains and sandbars of the river are inhabited by the poor community, who are dependent primarily on agriculture for their livelihood (Chakraborty, 2013).

Large dynamic braided rivers like the Brahmaputra River undergoes flood every year during the monsoon period. The huge volume of water flow and sediment deposition leads to changes in the morphology of the river. However, once the floodwater recedes, the river provides numerous opportunities for various activities. The sandbars developed within the river due to aggradation and degradation can be beneficial for various cropping activities. The physicochemical properties of sediments reflect the composition of parent rock materials due to mechanical and chemical weathering phenomena. Investigating the

sediment quality has been a logical extension of studies related to sediment yields and dynamics, which has the potential to further understand the sediment behaviour in rivers (Webb, 1995). The shape and size are important physical properties of sediments. Therefore, for economical utilization of the sediments, it is necessary to identify the minerals present, and understand their characteristics and suitability for socio-economic utilization by supporting and enhancing livelihood opportunities.

6.2 Sediment characterization and analysis

Sediment characteristics such as particle size and sediment type vary across the bed in lateral and vertical directions due to changes in the morphologic and hydraulic parameters in the rivers (Lick 2008). To study the characteristics of sediments within the sandbars, a field survey was performed from Majuli upstream to Dhubri downstream. A total of 126 samples from 42 sandbar locations were collected and tested in the laboratory. Figure 6.1 shows the locations of sediment collected from sandbars across the Brahmaputra River, Assam. From each location, three samples were collected from topsoil (surface), subsoil (upto depth of 30 cm from the surface), and bottom soil (from 30-100 cm depth). The samples were categorized into newly formed sandbars, vegetated sandbars, cultivated sandbars, and others. In the present study, the vegetated sandbars are those sandbars where no present cropping has been observed. The cultivated sandbars were those where some agricultural activities were seen performed and the newly formed sandbars were fresh deposits of sediments after a recent flood event. The classification of these sandbars was based on the field surveys, visual investigations, and the author's knowledge.

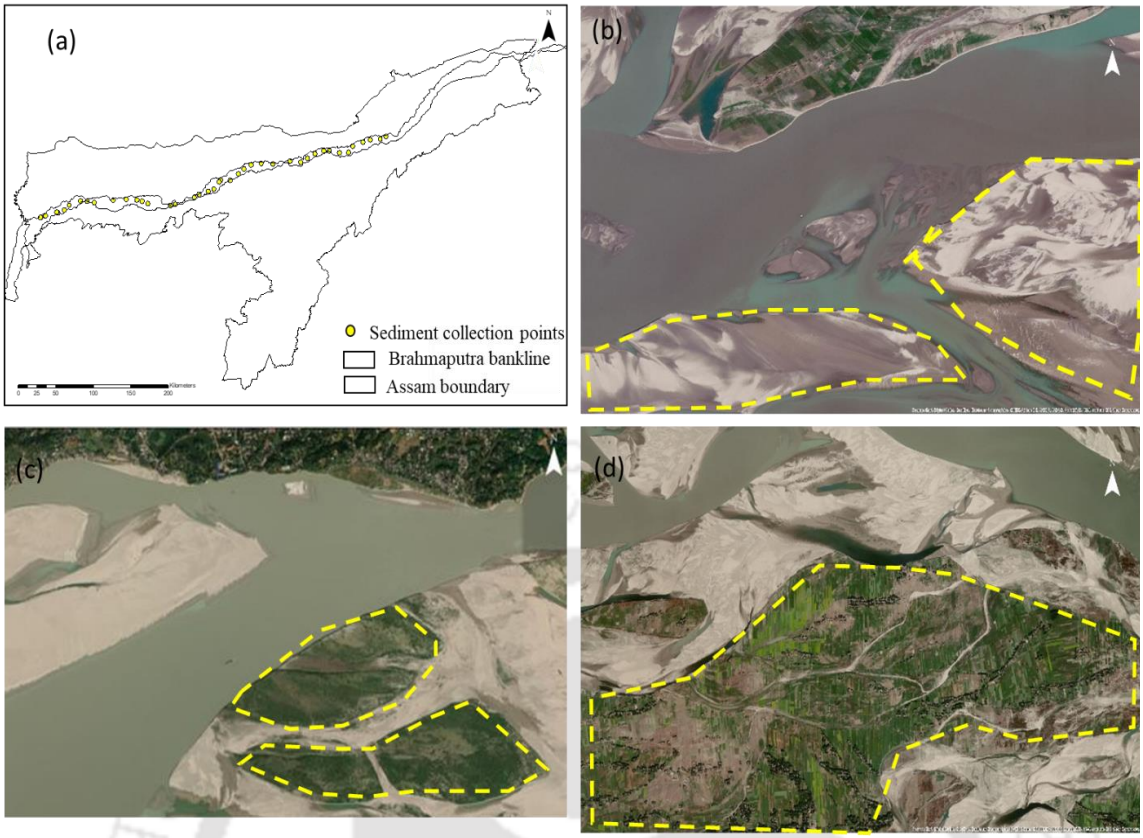

Figure 6.1: (a) Locations of sediment collected from sandbars across the Brahmaputra River, Assam. The figures (b), (c), (d) represent the newly formed sandbars, vegetated sandbars, and cultivated sandbars, respectively, describing seasonal agricultural practices within the river (marked as dashed yellow lines).

6.2.1 Particle size distribution

Particle size analysis (PSA) is a measurement of the size distribution of individual particles in soil samples. The major features of PSA are the dispersion of large soil aggregates into smaller fractions by chemical and mechanical means, thereby separating the particles based on different size limits. The soil particles span a large size range, varying from boulders (exceeding 300mm) to clays (<0.002 mm). As per the Indian Standard Soil Classification System, soils are grouped according to size and divided into coarse, medium, and fine subgroups, as shown in Table 6.1. The particle size analysis data is represented as a cumulative particle size distribution curve, wherein the percentage finer is plotted against the logarithm of effective particle diameter.

Table 6.1: Indian Standard Soil Classification System.

Very coarse soils	Boulder		> 300 mm
	Cobble		80-300 mm
Coarse soils	Gravel (G)	Coarse	20-80 mm
		Fine	4.75-20 mm
	Sand (S)	Coarse	2-4.75 mm
		Medium	0.425-2 mm
		Fine	0.075-0.425 mm
Fine soils	Silt (M)		0.002-0.075 mm
	Clay (C)		< 0.002 mm

Two methods are available for determining the distribution of grain sizes of soils: (a) sieve analysis and (b) hydrometer method. For grain sizes larger than 75-micron sieve, wet and dry sieving is applicable, and for soil sizes lesser than 75 microns, the pipette method and hydrometer method are suitable. For dry sieving (soil passing through 4.75 mm sieve and retained on 75 microns IS Sieve), the samples are oven-dried at 105ºC to 110ºC. The samples are weighed and sieves are arranged in a manner such that the sieve size opening of 4.75mm is placed at the top and sieve size opening of 75 microns is placed at the bottom i.e. in order of 4.75mm, 2.36mm, 1.18mm, 600 microns, 425 microns, 300 microns, 150 microns and 75 microns, respectively. The samples are rolled over the sieve and the amount retained on each sieve is weighed. The soil fractions retained on and passing 4.75mm shall be taken separately for analysis. The mass of the material retained on each sieve should be recorded. The retained particles are then transferred into the next corresponding sieve, and the process is repeated through all the sieves. The cumulative mass retained on each sieve is calculated based on the mass of the sample retained on the 4.75 mm sieve for further analysis.

For soil samples passing through a 75-micron IS sieve, the pipette method and hydrometer method are suitable. The amount of silt and clay is usually determined by sedimentation procedure and uses the principle of sedimentation called Stoke's law. In both the methods, the coarser fractions are measured by sieving, and the finer fractions are measured based on Stoke's law. The law states that the amount that a particle sinks depends on the density of the particle when suspended in a liquid. However, both methods are suitable if more than 10% of the weight of the sample passes through the 75-micron IS sieve. The hydrometer

method based on Stokes' law gives a relationship between the fall velocity, particle diameter, viscosity, and specific weight of the particle. The fall velocity (*v)* is determined as follows:

$$v = \frac{2}{9}\frac{G_s - G_f}{\eta}\left(\frac{D}{2}\right)^2 \quad (6.1)$$

where, *v* = Fall velocity (cm/s); G_s = Specific gravity of particle; G_f = Specific gravity of fluid; η = viscosity ((g/(cm*s)); *g* = 981 cm/s^2; *D* = particle diameter (cm)

The particle diameter (D) can be determined by,

$$D = k\sqrt{\frac{H_e}{t}} \quad (6.2)$$

where, K is a factor equal to

$$k = \sqrt{\frac{30\,\mu}{g(G_s - G_w)\rho_w}} \quad (6.3)$$

where, H_e = Effective depth in cm; *t* = Time in minutes; μ = Coefficient of viscosity of water in poise, 1Poise = kg/m sec; ρ_w = density of water (g/cc); G_w= specific gravity of water (g/cm^2)

Figure 6.2 shows the hydrometer instrument and experiment being conducted for soil grain size analysis. For performing the test with a hydrometer, instruments such as a glass measuring cylinder (1000 ml capacity), thermometer, chemical reagents, stirrer, glass rod and hydrometer were required. 50 gm of samples were taken and mixed with 100 ml of reagent. The reagent (sodium hexametaphosphate solution) was prepared in distilled water to make 1 liter of the solution. The hydrometer was then inserted into the solution, and the readings were taken at 0.5 minutes, 1 minute, 2 minutes, 4 minutes, 8 minutes, 15 minutes, 30 minutes, 60 minutes, 2 hours, 4 hours, 8 hours, 16 hours and 24 hours as specified in the IS: 2720 (Part 4) – 1985. The percentage finer (N) was calculated as:

$$N = \frac{G_s}{G_s - 1} \times \frac{R_c}{M_s} \times 100 \quad (6.4)$$

where, G_s = Specific gravity of particle; M_S = Mass of dry soil in gm; R_c= corrected hydrometer reading

The hydrometer readings were determined at different intervals, *t* as specified, and the effective depth, H_e can be obtained from the calibration curve based on the Table 6.2 using H_e=255.99-240×R_h. While inserting the hydrometer into the measuring cylinder, the meniscus rises, and readings could not be truly recorded; thus, a correction was needed. The readings were taken at the top and bottom of the meniscus, and the difference gave the meniscus correction (C_m), which is always positive. The addition of dispersing agent in soil suspension increases the density of the liquid, which necessitates a correction to the observed hydrometer readings. Hence, a dispersion agent correction (C_d) is required to get the corrected readings. A corrected hydrometer reading (R_c) was calculated before all the computations, as shown in equation 6.5. The distance from the lowest calibration mark on the stem to each of the major readings in the hydrometer (R_h) shall be measured and recorded.

$$R_c = \left((R_h + C_m \pm C_t - C_d) - 1\right) \times 1000 \qquad (6.5)$$

where, C_m = Meniscus correction; C_d = Dispersion agent correction; C_t = Temperature correction.

From the readings, a graph was plotted between the diameter of the particle (*D*) and the percentage finer (*N*) to classify the type of soil. The diameter of the particle (*D*) is plotted in log scale on X-axis and the percentage finer (*N*) on Y-axis. The distance, *H*, is the length from the neck of the bulb to the readings (R_h). The effective depth (H_e) corresponding to each major reading were calculated as shown in Table 6.3. Figure 6.3 shows the calibration curve obtained from the experiment.

Table 6.2: Calibration of Hydrometer

R_h	Neck	1.03	1.025	1.02	1.015	1.01	1.005	1	0.995
H	0	1.835	3.035	4.235	5.435	6.635	7.835	9.035	10.235
H_e	6.959	8.794	9.994	11.194	12.394	13.594	14.794	15.994	17.194

Table 6.3: Measurements of the Hydrometer used in the experiment

Height of bulb (*h*)	15.9 cm
Volume of Hydrometer (V_h)	60 cc (cubic centimetre)
Sectional area of cylinder (*A*)	30.3 cm^2
Effective Height (H_e)	$H_e = H + \frac{1}{2}(h - V_h/A)$

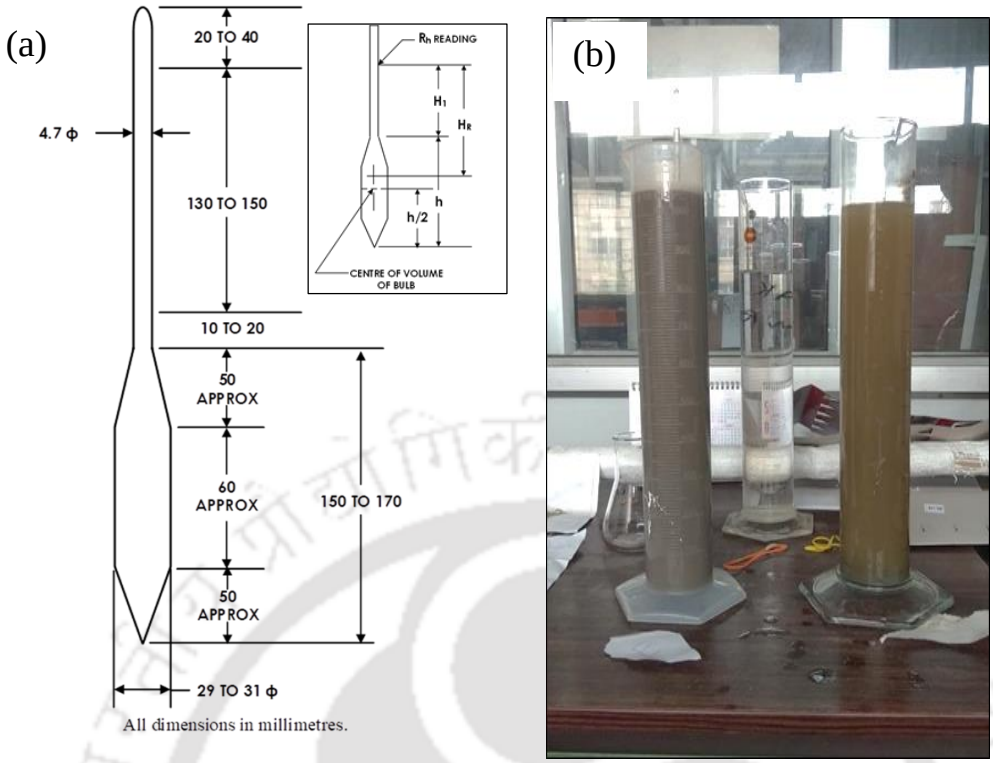

Figure 6.2: (a) Hydrometer (IS: 2720 (Part 4) – 1985) and (b) Hydrometer experiment for soil grain size distribution

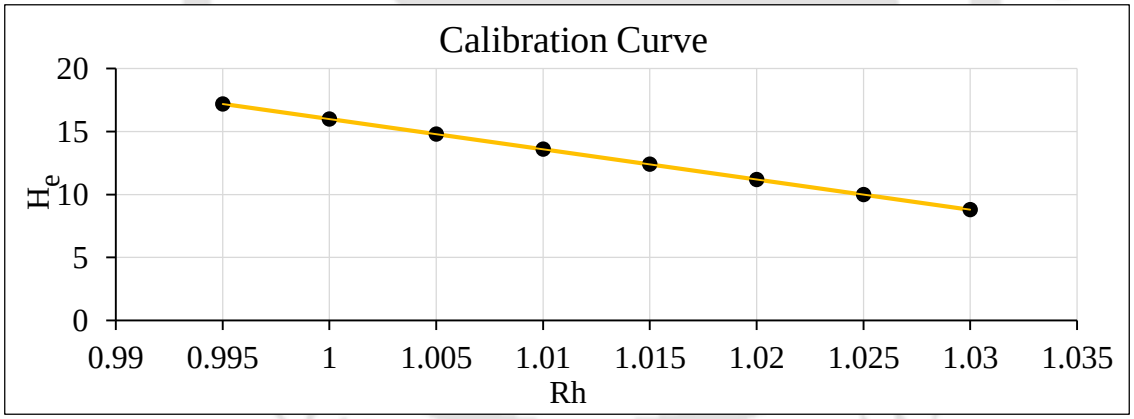

Figure 6.3: Calibration curve obtained from the experiment

6.2.2 X-Ray Diffraction (XRD) analysis

Identifying and characterizing minerals is necessary to extract important information about their composition, crystallinity, and structure. XRD is an analytical technique used for the identification and mineral characterization of sediments and determines the phase of a particular soil structure. It is helpful in identification of different minerals in a mixture. Each component of the mixture produces its characteristic pattern, which helps in identifying the various constituents by matching them with the reference patterns.

6.2.2.1 Principle of XRD

X-ray diffraction is based on the constructive interference of monochromatic X-rays and a crystalline sample. The X-rays are generated by a cathode ray tube, filtered to produce monochromatic radiation, and directed towards the sample. X-Rays lie in the range of 0.01 to 10nm and are shorter than UV ray's wavelength and larger than Gamma ray's wavelength. The rapid deceleration of fast-moving electrons produces the X-Rays as they impinge on the matter (Klug and Alexander, 1974). The rays in phase constructively interfere to form the intense beams (diffracted beams), and those out of phase have minimal significance with destructive interference. This system of constructive and destructive interference in crystals is called as X-Ray Diffraction. The principle and analysis of X-Ray diffraction is based on Bragg's law, which defines the scattering of waves from a crystalline structure.

$$n\lambda = 2d\ sin\Theta \qquad (6.6)$$

where, Θ = Angle between the beam and the plane; d = Interplanar spacing between equivalent atomic planes in the crystal (d-spacing); λ = Wavelength of the radiation; n is an integer representing the order of reflection.

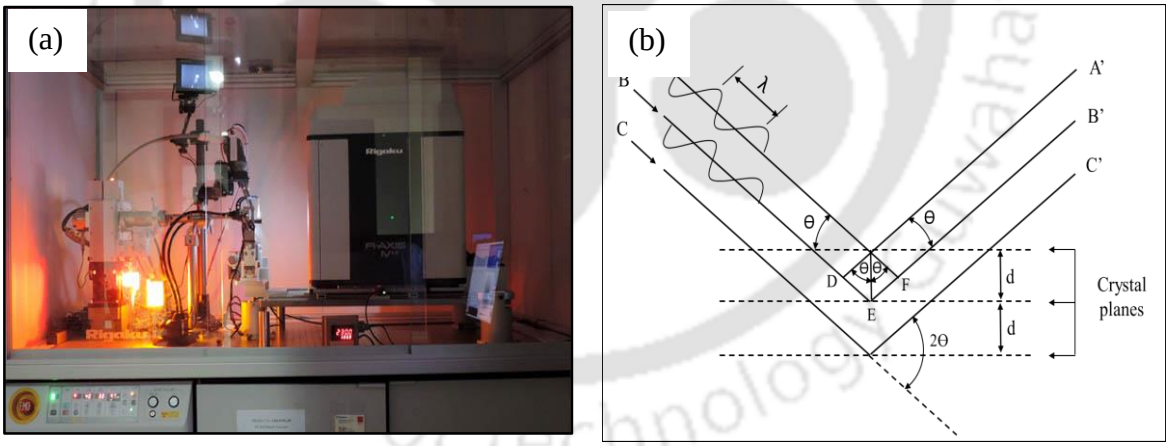

Figure 6.4: (a) Large Molecule Single Crystal X-ray Diffractometer (b) Schematic representation of XRD principle.

Figure 6.4 (a) shows the X-Ray Diffractometer. The analysis of the materials largely depends on forming the diffraction patterns. Each material has its unique diffraction beam, which defines and identifies the material by comparing the beams with standard database in Joint Committee on Powder Diffraction Standard (JCPDS) library. Figure 6.4 (b) expresses the diffraction condition, where for a given spacing 'd' as well as wavelength 'λ', the diffraction occurs at an angle between the incident beam and the set of planes. The

diffraction is based on the sample and the X-rays. The X-rays are generated through a cathode ray tube, producing radiation that is concentrated and focused on the sample. When the incident beam interacts with the sample, constructive interference is produced, satisfying the Bragg's law. However, in Bragg's equation, the 'd' spacing is of interest and can be determined by fixing the value of λ and measuring the corresponding angle where the peak of the X ray's intensity occur. These diffracted rays are then sensed, processed, and counted. The samples are then scanned through a range of 2Θ angles, and different directions of the lattice is obtained. The peaks obtained and the corresponding 'd' spacing values allow identification of the mineral when compared with standard reference patterns of the 'd' spacing.

6.2.2.1 Sample preparation and analysis

X-ray diffraction works are generally carried out on crystalline material and powdered samples. In a powdered sample, it is advisable to have samples with a smooth plane surface in the size of 0.002 mm to 0.005 mm. In our study, during the sample preparation, the samples were grinded to powdered form (Figure 6.5) and were oven dried at a temperature of 100°C. The XRD instrument used was the Micromax-007HF model of Central Instruments Facility, IIT Guwahati. It uses copper to generate the wavelength of 1.54184 Å. The X-ray detector used was R-AXIS IV++, which detects the diffracted rays. The sample was placed in the region of a small glass plate, pressed with a glass slide, and the sides were cleaned, so that excess powder was not present in the region. The sample was then placed in the sample holder inside the instrument and the 2Θ interval range was set from 3° - 90° with a step size of 0.02.

XRD Sample Preparation
Location: CIF Laboratory, IIT Guwahati

XRD Sample Preparation
Location: CIF Laboratory, IIT Guwahati

Figure 6.5: Sample preparation before the XRD test

6.2.3 Energy-Dispersive X-Ray Spectroscopy (EDS) analysis

Energy-dispersive X-ray spectroscopy, also known as EDS, EDX, or EDXS, is an analytical technique to map the distribution of elements present in sediment samples. Its study aided in understanding the minerals present in the soil samples. The quantitative analysis gives the concentration of elements present in the sample recorded by the intensity of its peaks. However, the qualitative analysis shows the peaks corresponding to each atomic structure of an element within its specified positions in the spectrum.

6.2.3.1 Principle of EDS

The main principle of spectroscopy is that each element has a unique atomic structure, which develops unique peaks on its electromagnetic emission spectrum when the X-ray source strikes the sample. A high-energy beam of electron or proton is focused into the sample to excite the emission of characteristic X-rays from the specimen. The atoms present in the sample are initially at the ground state. The incident beam excites the electron in the inner shell, making it unstable, and hence it gets ejected from the shell creating an electron-hole in that shell. An electron from the outer shell having higher energy fills the hole and releases energy when it jumps from a higher energy shell to a lower energy shell. This difference in energy is released in the form of X-rays and is measured using an energy dispersive spectrometer (EDS). EDS helps in estimating both the quantitative (relative abundance) and qualitative analysis (elements present) in the samples. The quantitative analysis gives the concentration of elements present in the sample recorded by the intensity of its peaks. However, the qualitative analysis gives the peaks corresponding to each atomic structure of an element within its specified positions in the spectrum. Figure 6.6 shows the principle of EDS and mineral detection using Field Emission Scanning Electron Microscopy (FESEM)

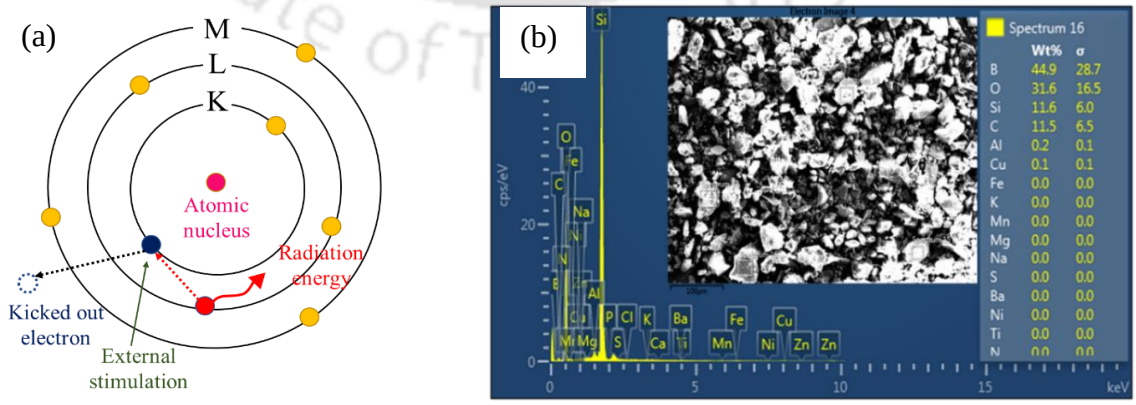

Figure 6.6: (a) Generation of X-rays in EDS (b) Detection of minerals in EDS Field Emission Scanning Electron Microscope (FESEM) with OXFORD EDS, Make: Zeiss, Model: Sigma

6.2.3.2 Sample preparation and analysis

The samples were oven-dried at a temperature of 105ºC – 110ºC for 24 hours and crushed into powdered form. The composition of samples was determined using the FESEM instrument having a high spatial resolution of up to 1 nanometer. The instrument gives the elemental information of a variety of samples at a magnification factor of 10X to 300,000X.

The spectrum generated in the spectrometer was displayed in a digitized form with X-axis representing the energy range in KeV (Kilo Electron Volt) and Y-axis representing the counts per second per electron volt (cps/eV). The concentration of elements present in the samples was characterized into three categories, as shown in Table 6.4. Major components: having >10% weight, Minor components: having 1-10% Weight, and Trace element: having < 1% weight (Hafner, 2006).

Table 6.4: Categorization of minerals in terms of percentage weight

Major Components	Minor Components	Trace Elements
More than 10 % weight	1-10 %weight	Less than 1% weight

6.3 Results and Discussion

6.3.1 Soil Physical characteristics and suitability

As per Indian Standard (IS) 1498:1970, boundary classification can occur between fine-grained soils as silty-sand (SM) and clayey-sand (SC). As per the United States Department of Agriculture (USDA) classification, soil with 30-40 % of silt is classified as sandy loam, and soil with 50% of silt is classified as silty loam. During the experimental analysis, it was found that the sediment collected from the vegetated sandbars contained around 45-50% of silt and clay, whereas the sediments collected from cultivated sandbars contained 30-40% of silt and clay. The gradation of the samples was calculated by finding the uniformity coefficient (C_u) and is the measure of particle size range given by the ratio of D_{60} and D_{10} particle sizes, while Cc measures the gradation of the soil particles.

$$C_u = {}^{D_{60}}/_{D_{10}} \tag{6.7}$$

where, D_{60} represents the size (diameter) of the particle below which 60% of particles are finer than this size and 40 % are coarser, i.e., these particles make up 60 % of the soil.

Similarly D_{10} represents the size of the particle for which 10% of particles are finer than this size.

$$C_c = {(D_{30})^2}\Big/{D_{60}.D_{10}} \quad (6.8)$$

where, D_{30} represents the size of the particle corresponding to 30% finer

Figure 6.7 shows a detailed analysis of the particle size distribution of the sediments collected across the sandbars of the Brahmaputra River. It can be understood that the soil in all three layers of vegetated and cultivated sandbars contains a significant amount of silt and clay particles. It was interesting to note that the distribution of silt or clay in the 'others' group varied in all three layers. This meant that silt and clay were found at the topsoil in some sandbars, while in others, it was found below the surface.

For the gradation of soil, the values of C_u has been established, wherein, C_u> 4 represents well-graded gravel and C_u> 6 represents well-graded sand. For uniformly poorly graded soil, the value of C_u equals 1. C_c describes the shape of the gradation curve wherein the soil to be well-graded must have the value of C_c within 1 and 3. Table 6.5 represents the soil gradation in the collected sandbar sediment samples. During the sediment analysis, it was found that the C_u values of the newly formed dry sandbars varied between 1.5-3, indicating poorly graded soil with higher sand content. However, for the vegetated and cultivated sandbars, the C_u values ranged between 3-15, which indicated well-graded soil. In addition, the C_c value was also greater than 1 in all three soil depths, i.e., topsoil, subsoil, and bottom soil. The sediment analysis showed that the sediment characteristics of the cultivated and vegetated sandbars were suitable for the growth of different crops in those sandbars. It was also observed that these sandbars had extensive grasslands known as *khaisa* or *oreatkin* grass, with deep roots used as fuel and construction of thatched houses in the chars. These grasslands also acted as grazing land for cattle, buffaloes, sheep, and goats.

Table 6.5: Gradation of soil collected from sandbars.

Location	Nature of Sandbar	C_u			C_c		
		Soil Depth (cm)					
		Top	0-30	30-100	Top	0-30	30-100
1	Newly Formed	1.5-3	1.5-4	1.5-3	0.9-1.5	0.9-1.3	0.9-1.6
2	Vegetated	3-7	2.3-4	2-15	1-1.2	1.2-1.3	0.6-1.3
3	Cultivated	3-4	0.7-1.2	2.5-4	0.9-1.2	3-3.4	1.1-1.2
4	Others	1-8	1.5-8	1.5-7	0.9-1.5	0.8-1.3	0.9-2

Location	Top soil (Surface)	Sub-soil (30 cm from surface)	Bottom soil (100 cm from surface)
1. (26.90768N, 94.15817E)	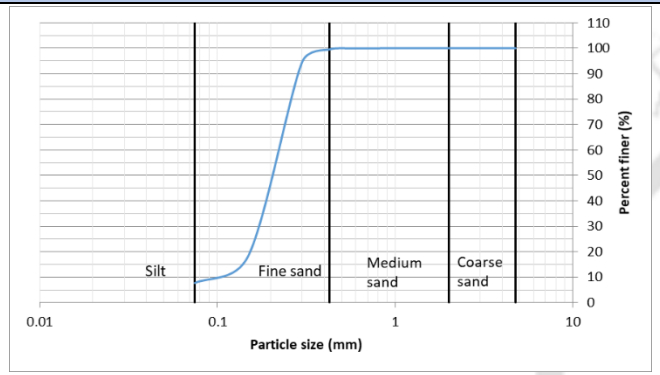	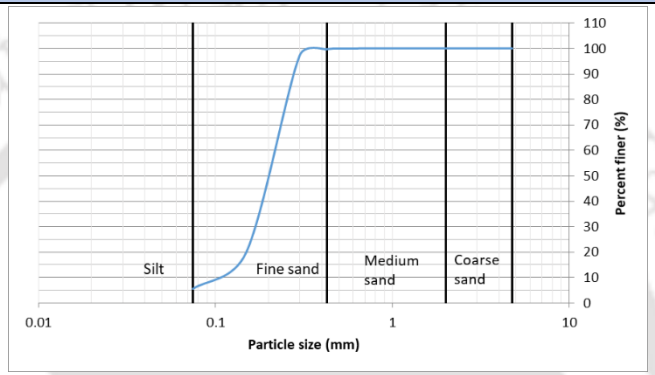	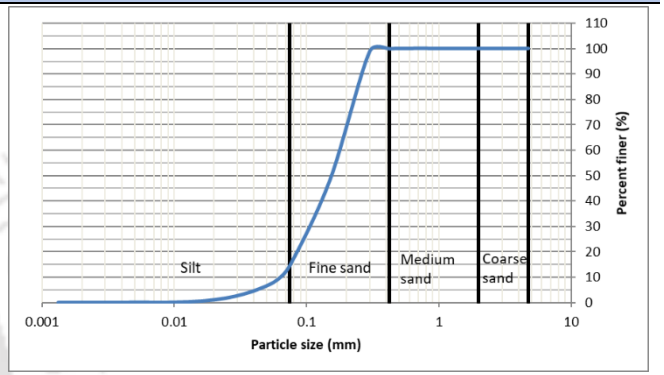
2. (26.87932N, 94.08992E)	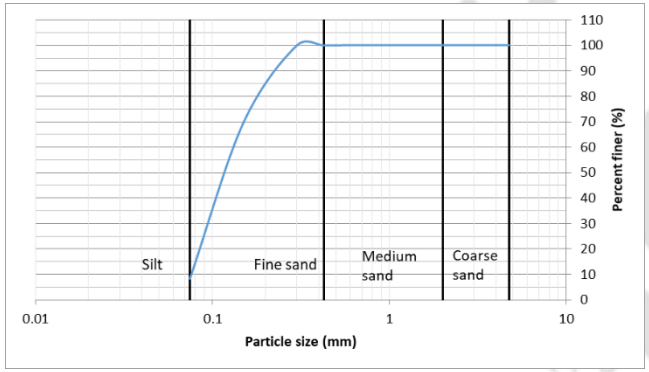	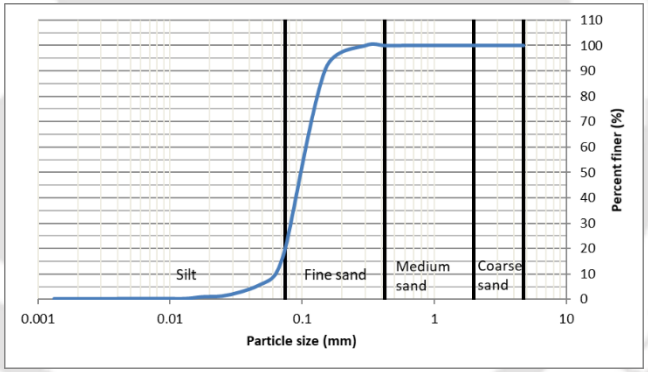	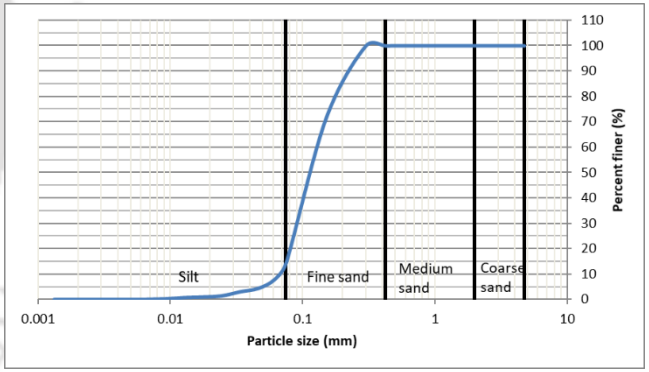

3.(26.87159N, 93.9688E)

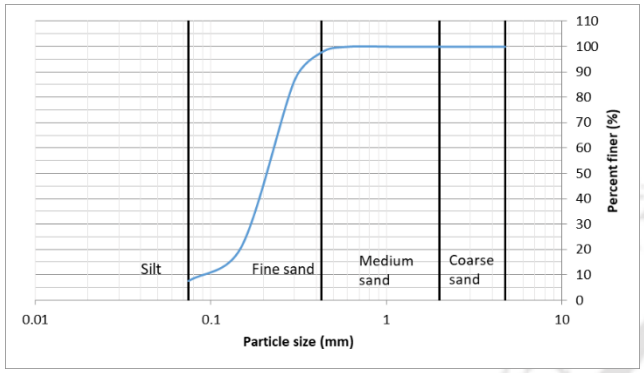

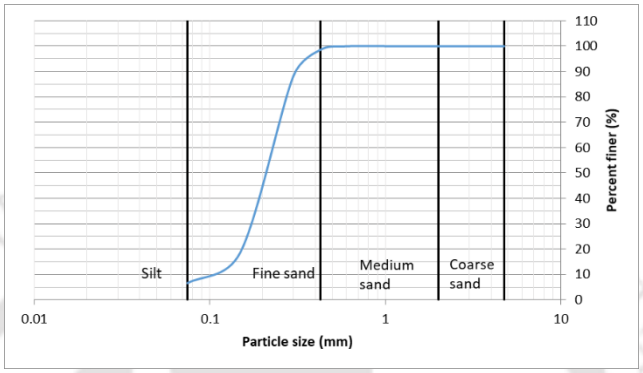

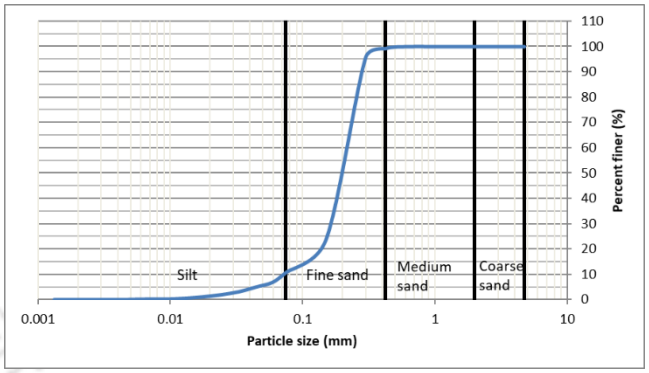

4.(26.84507N, 93.87987E)

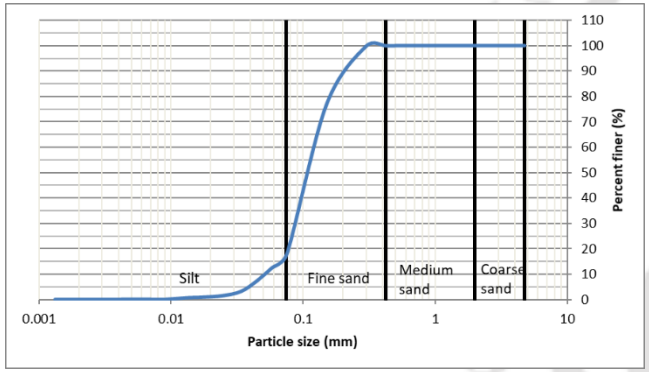

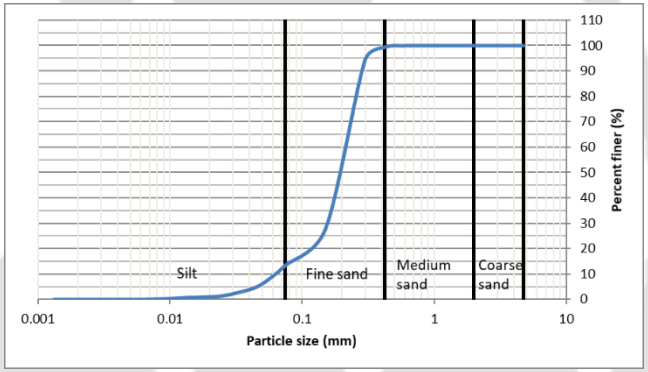

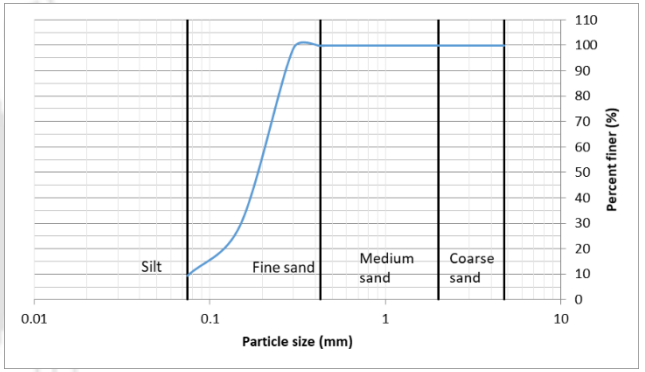

5.(26.8018N, 93.7600E)

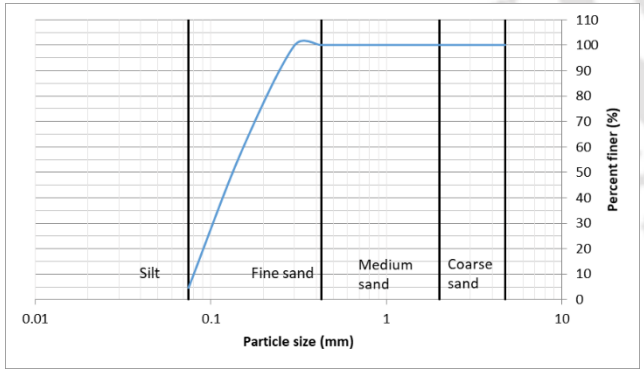

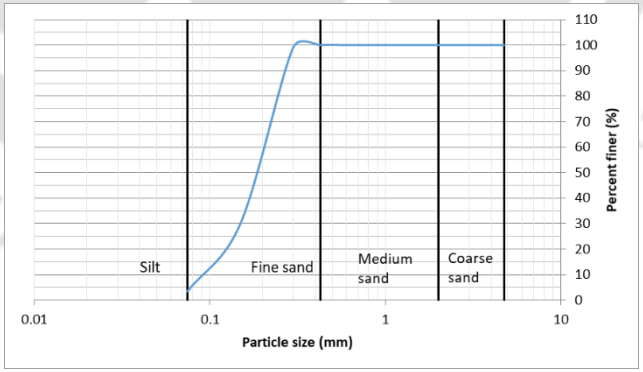

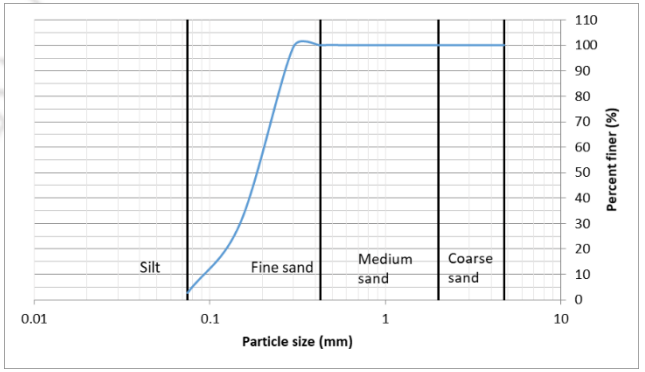

6.(26.73334N, 93.71042E)

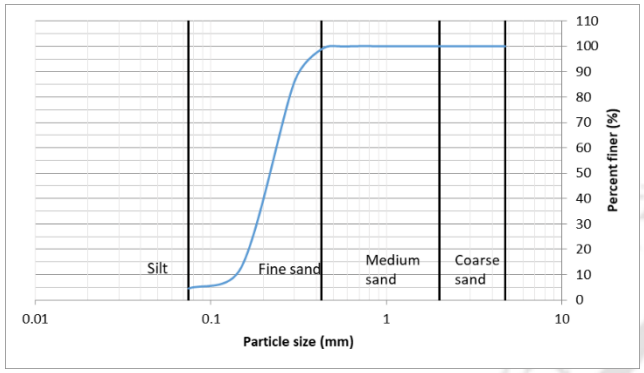

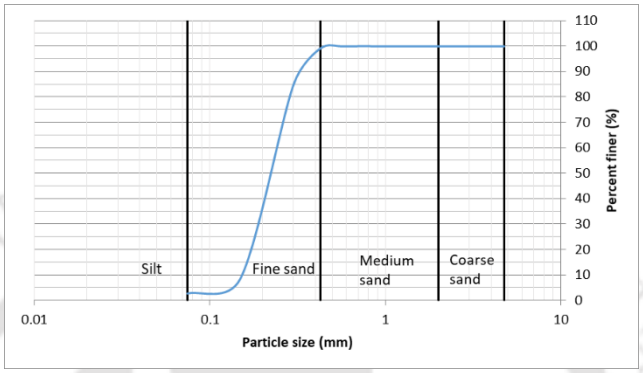

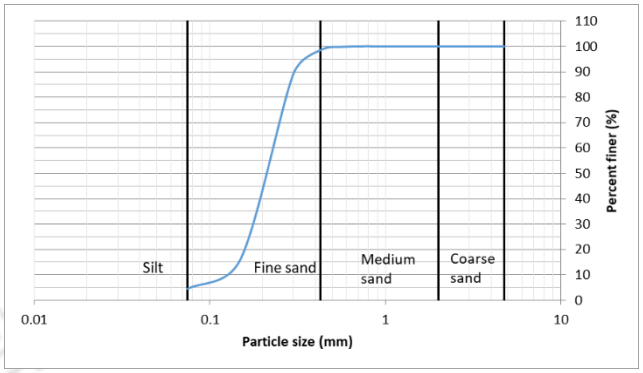

7.(26.72937N, 93.60203E)

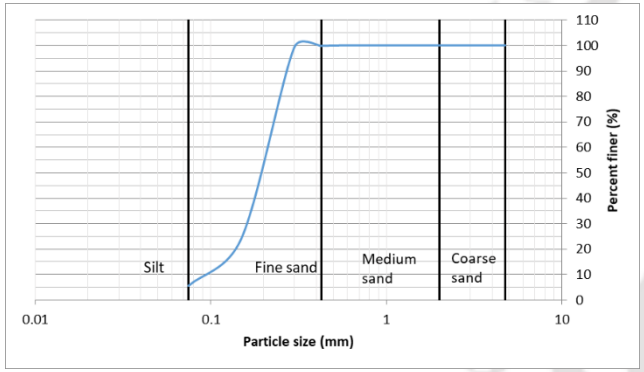

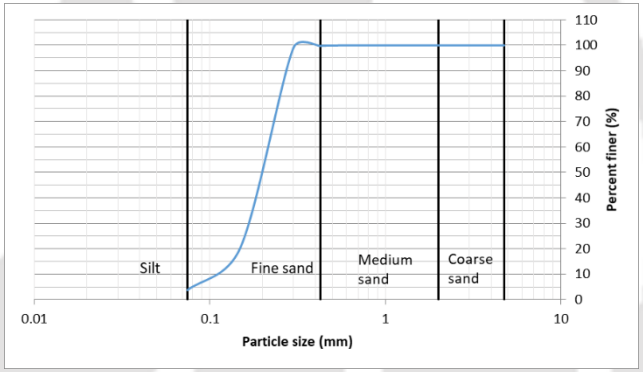

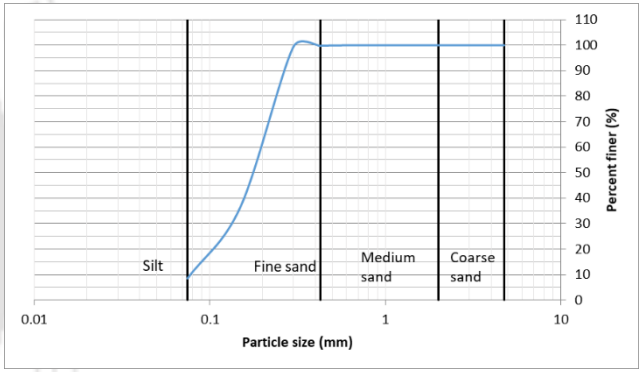

8.(26.75175N, 93.47914E)

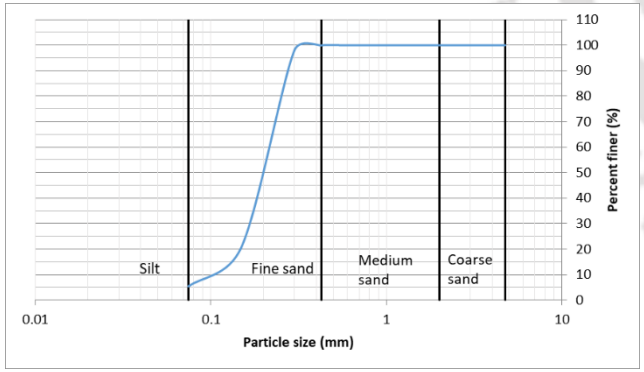

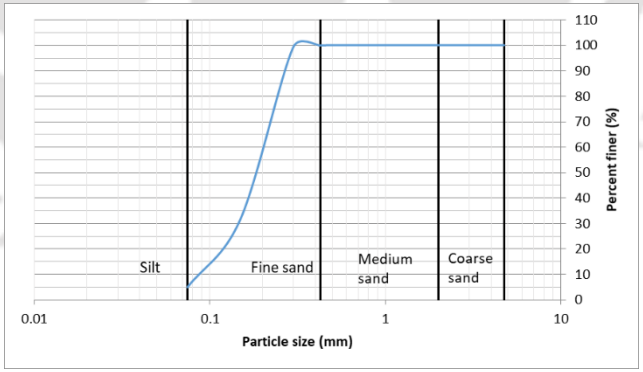

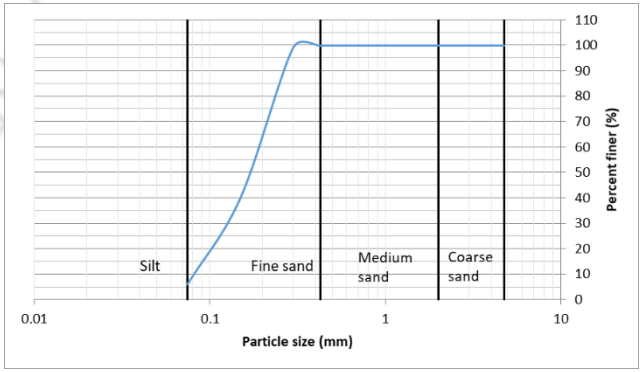

9.(26.7489N, 93.4125E)

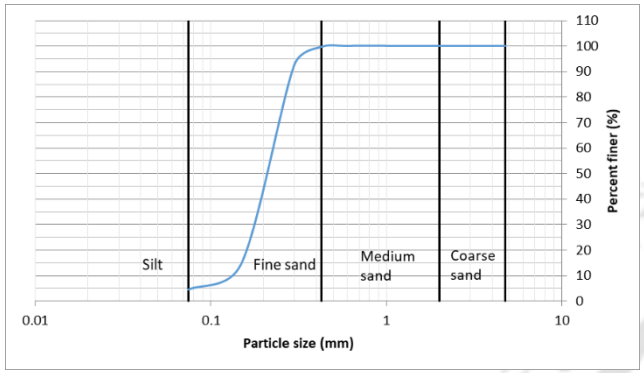

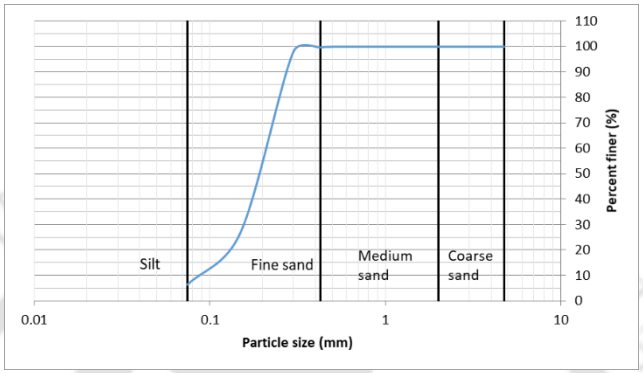

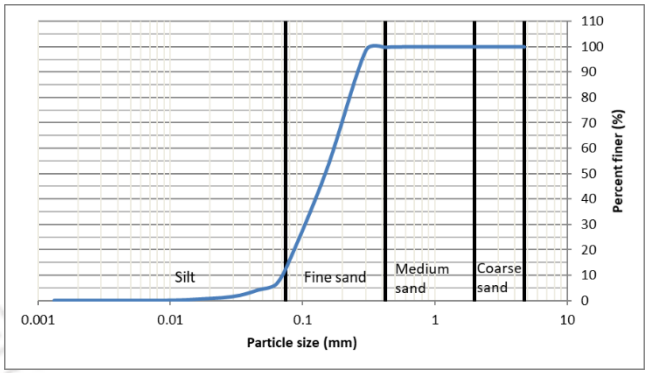

10.(26.7196N, 93.3080E)

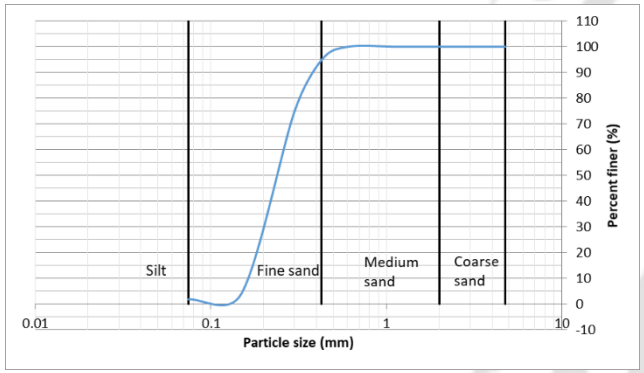

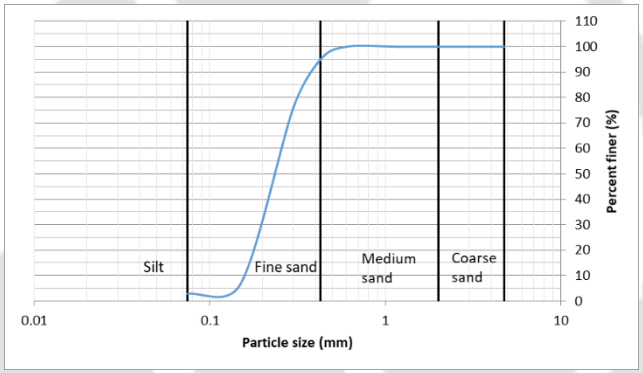

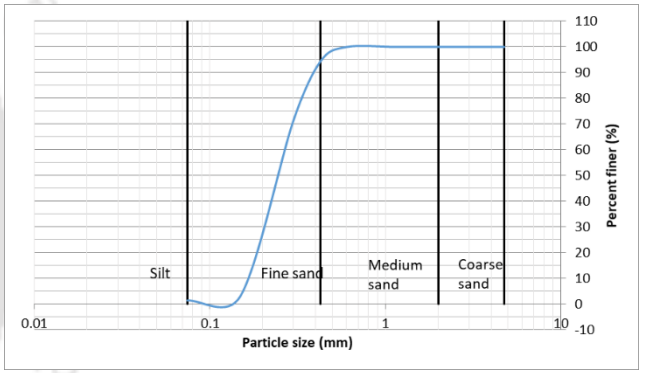

11.(26.6689N, 93.21642E)

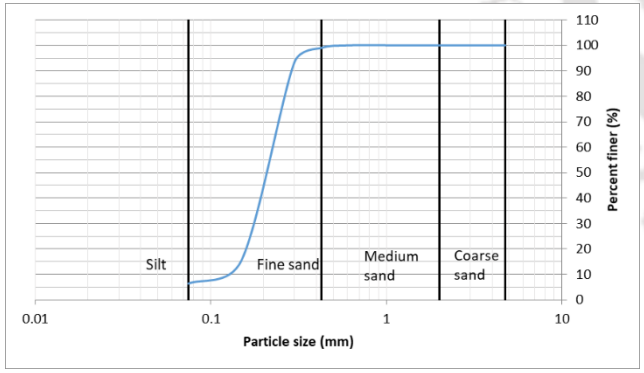

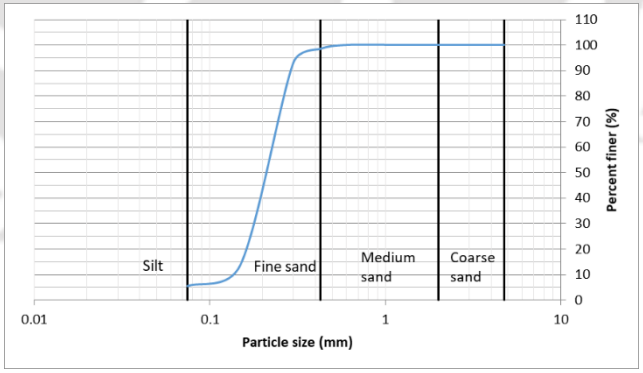

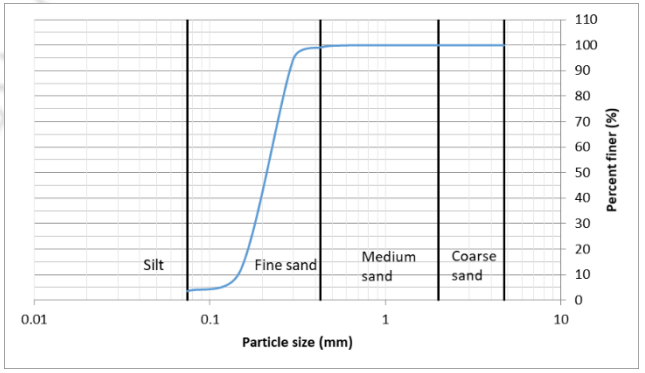

12.(26.6266N, 93.13526E)

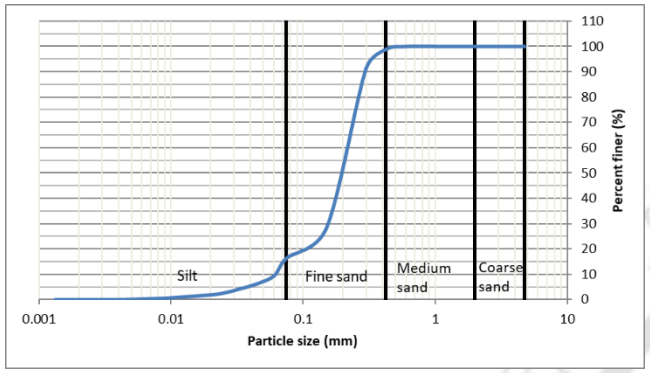

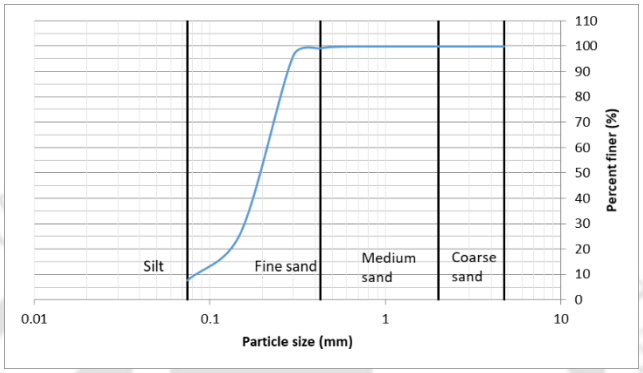

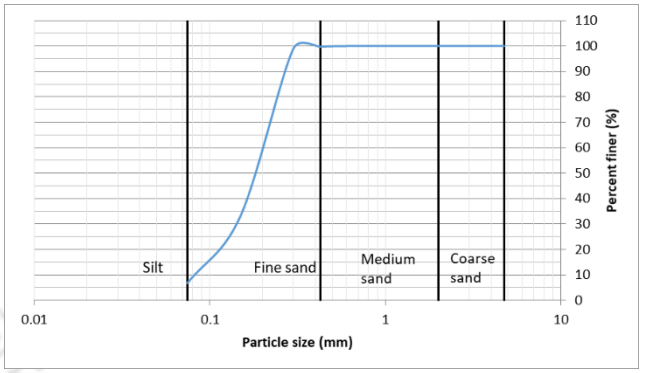

13.(26.6370N, 93.00835E)

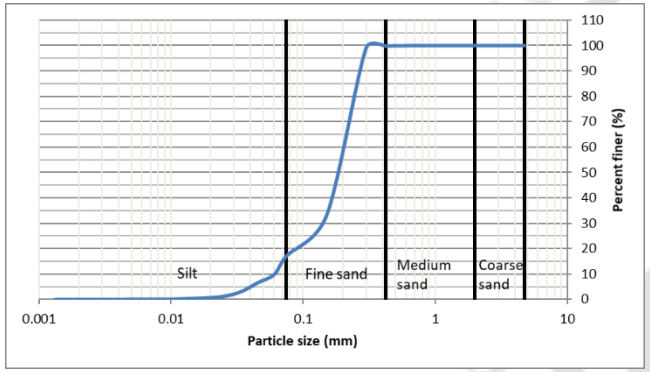

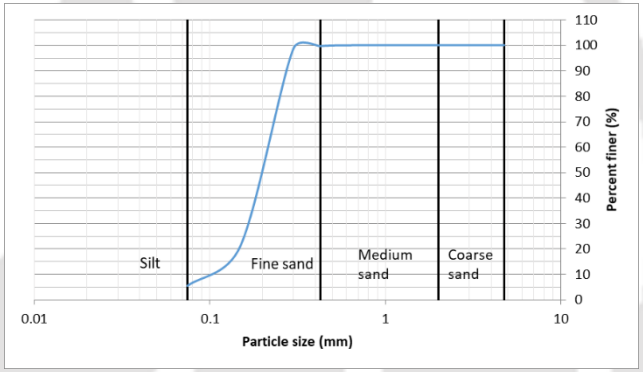

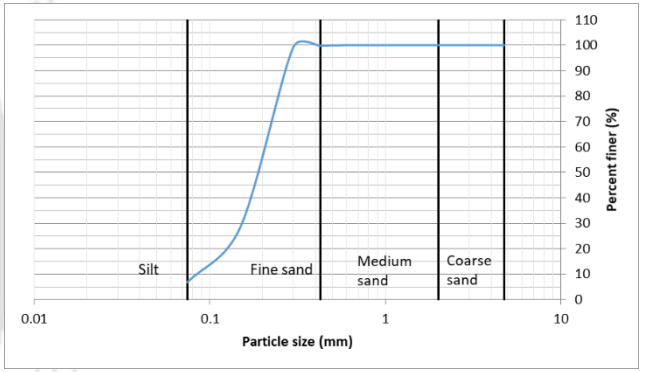

14.(26.6063N, 92.80293E)

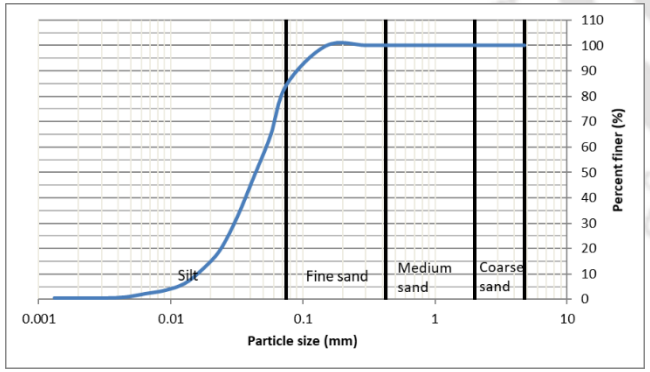

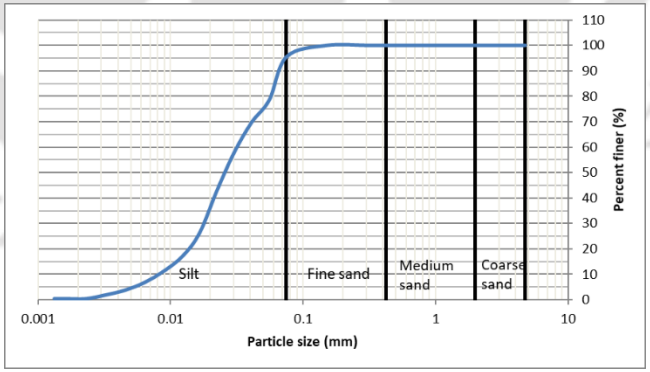

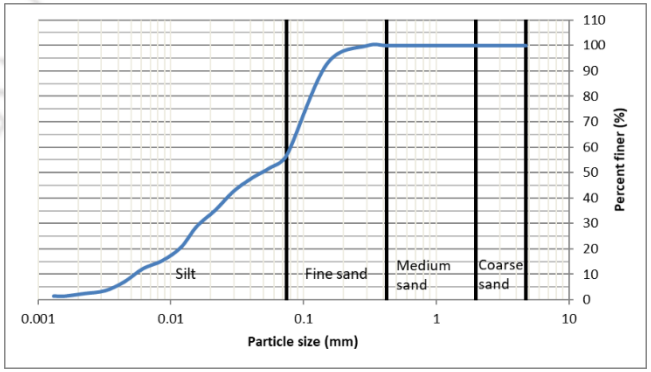

15.(26.6120N, 92.66261E)

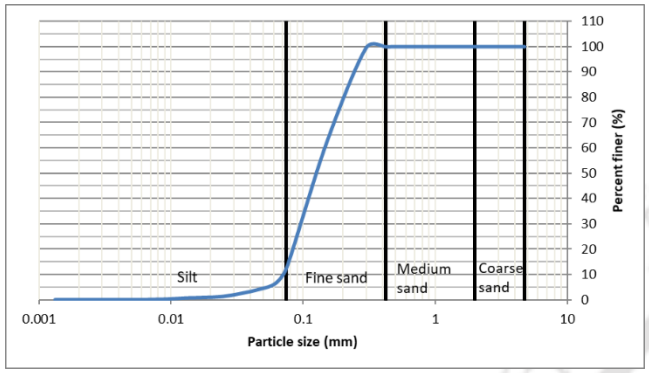

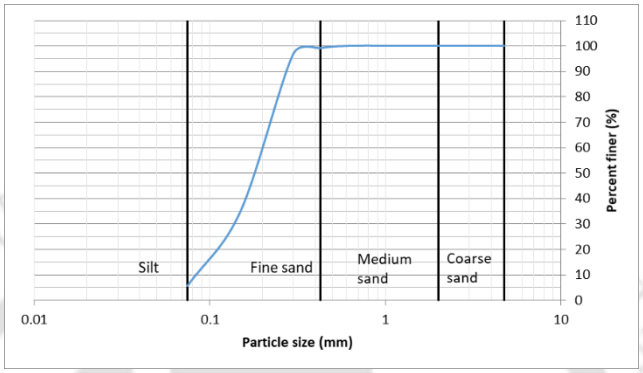

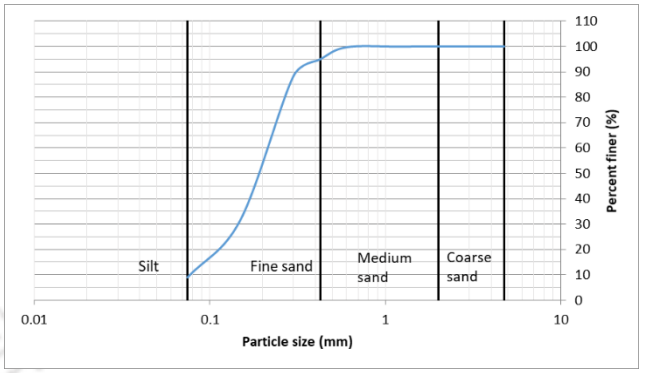

16.(26.5967N, 92.54186E)

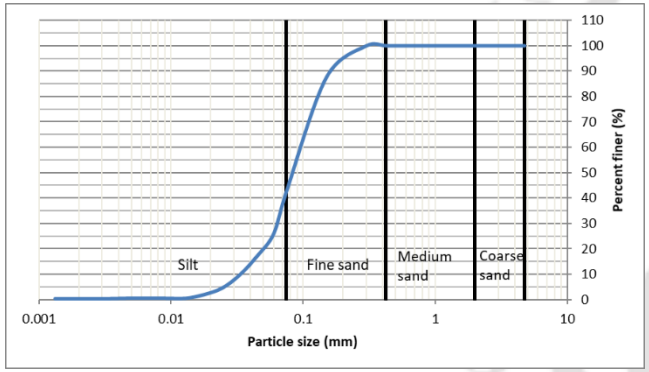

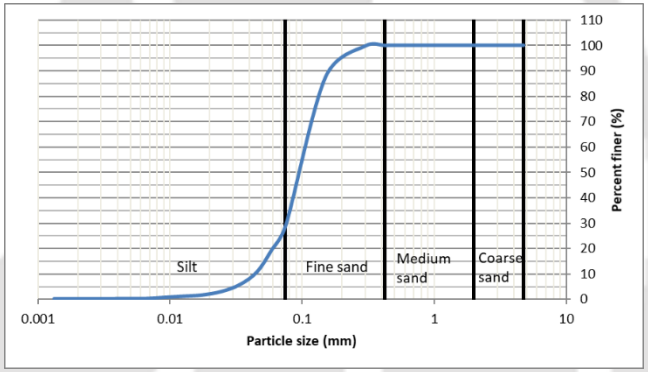

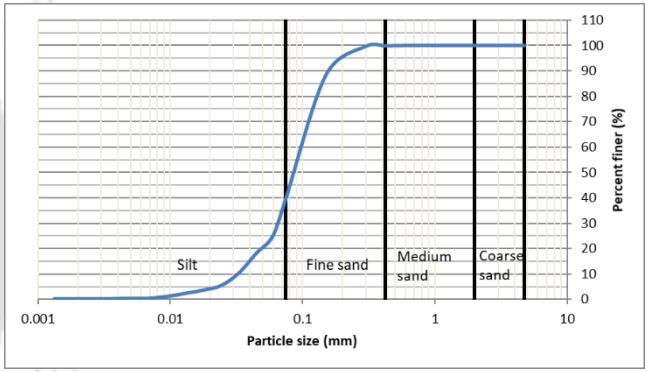

17.(26.5525N, 92.45606E)

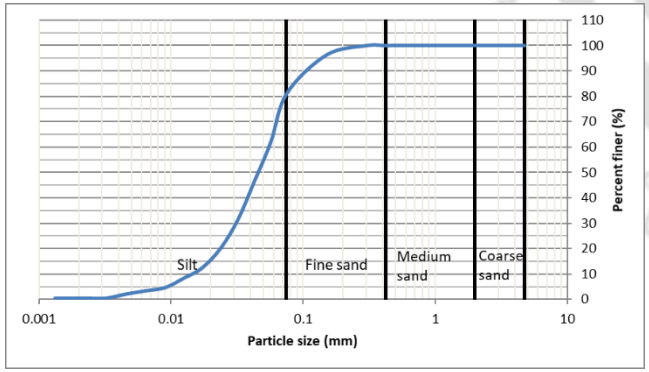

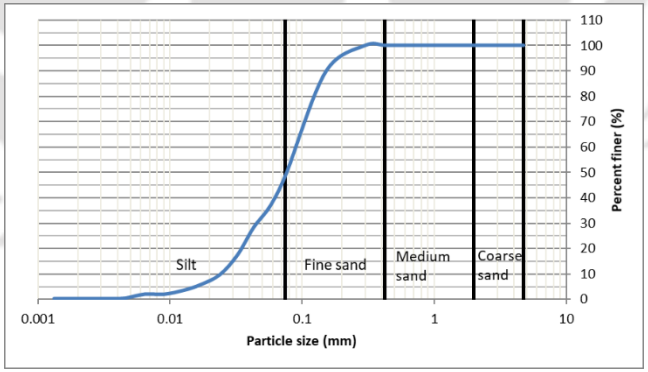

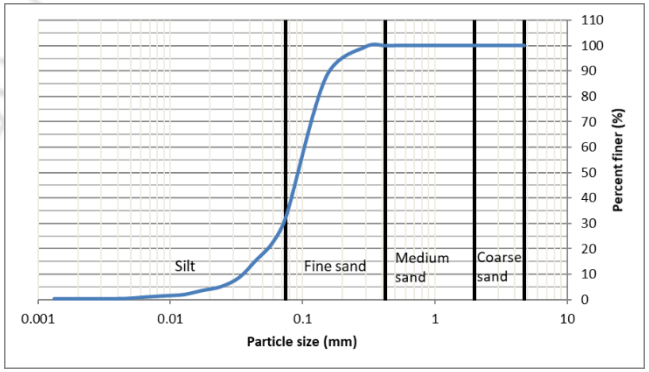

18.(26.4999N, 92.38974E)

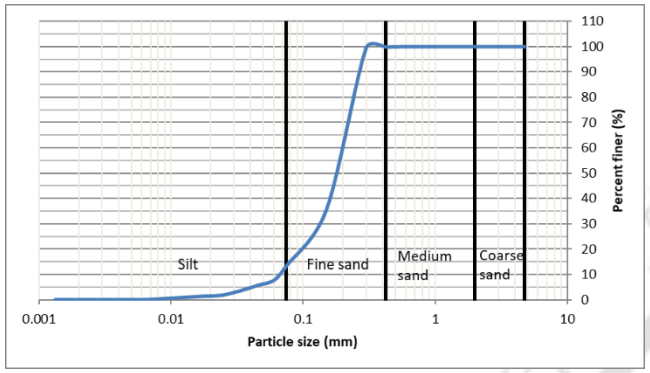

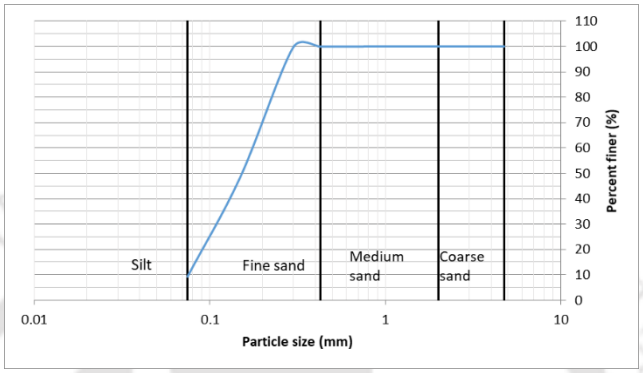

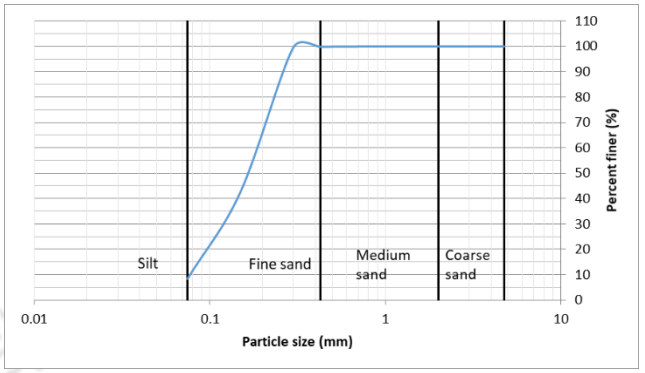

19.(26.4287N, 92.29034E)

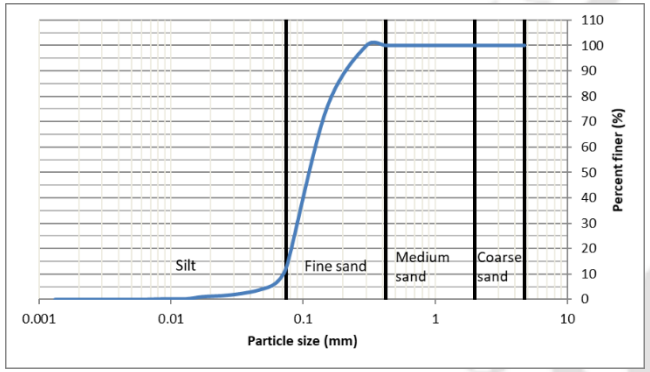

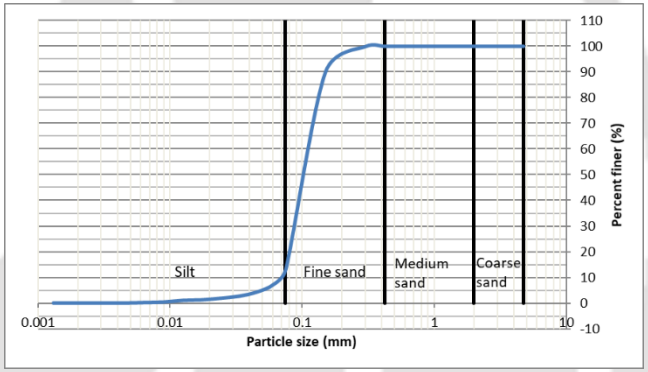

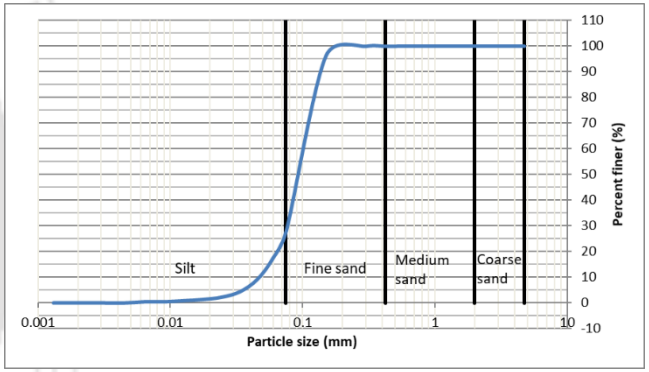

20.(26.4290N, 92.17612E)

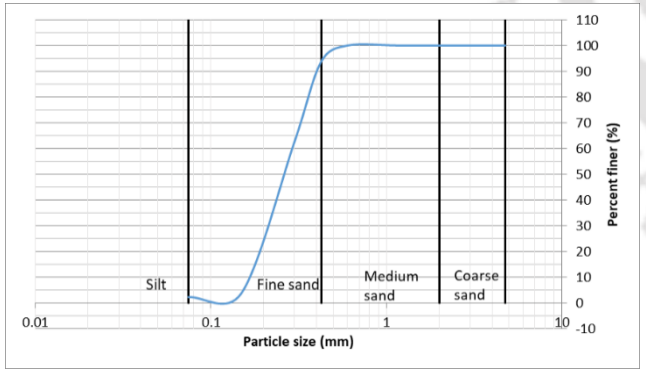

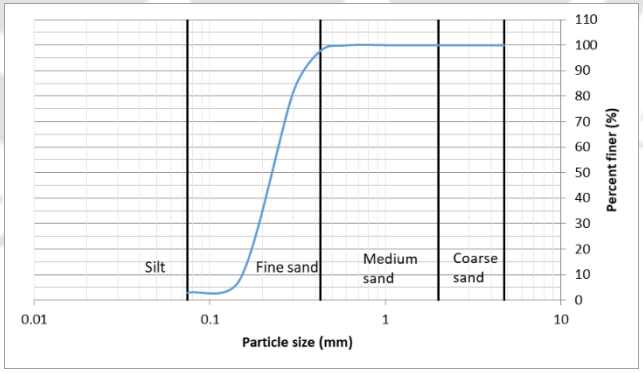

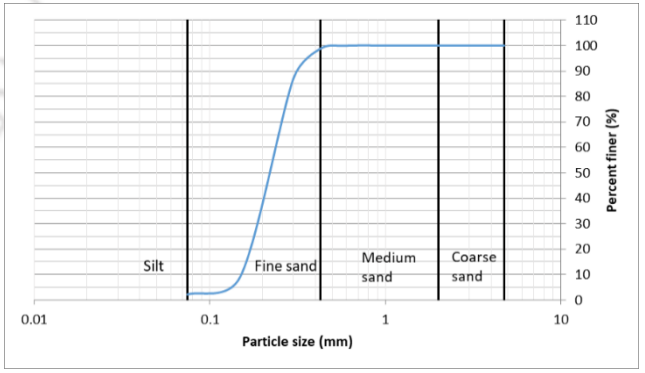

21.(26.4104N, 92.15871E)

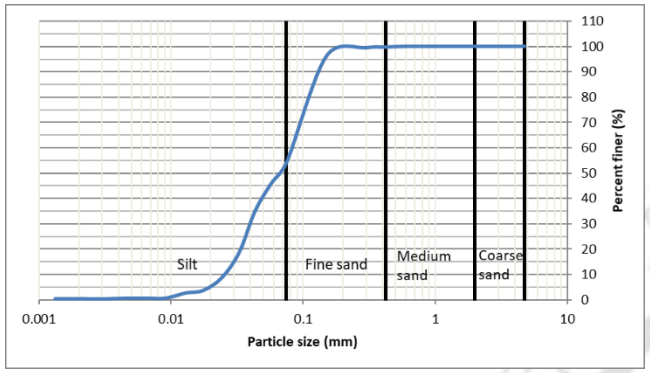

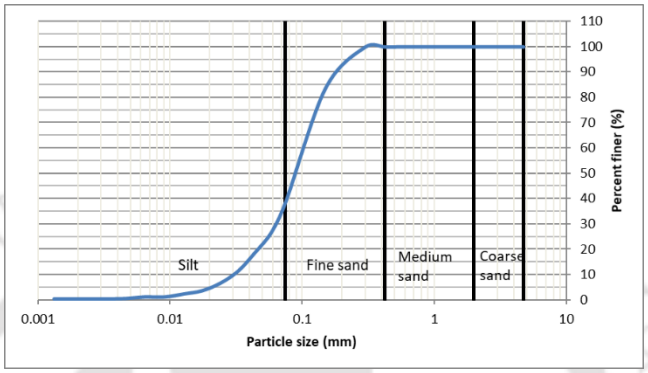

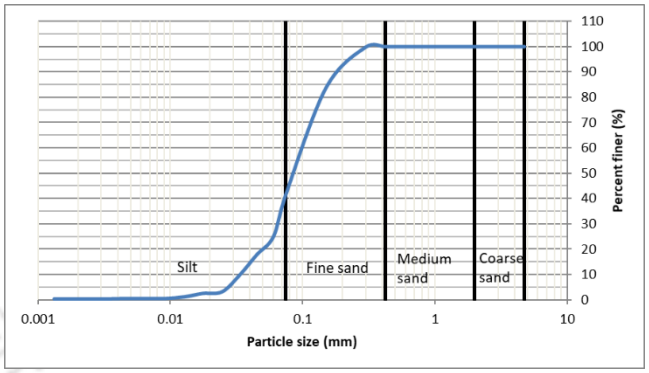

22.(26.3313N, 92.09475E)

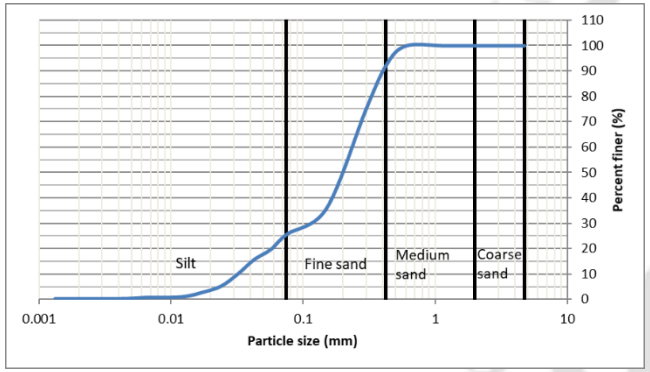

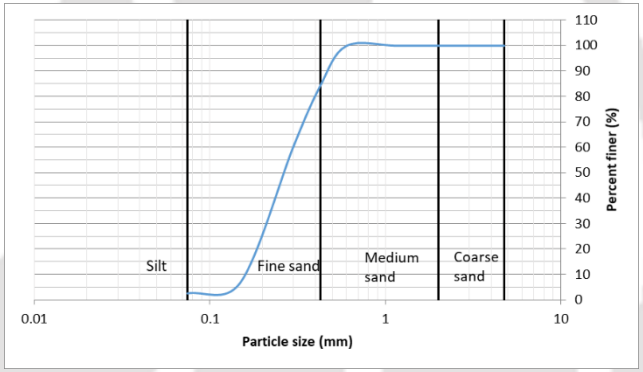

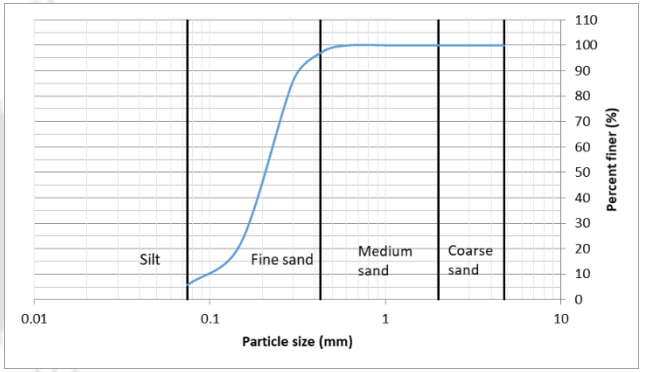

23.(26.3068N, 92.02809E)

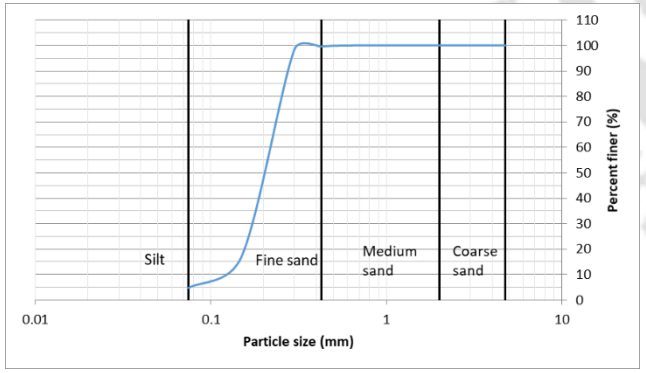

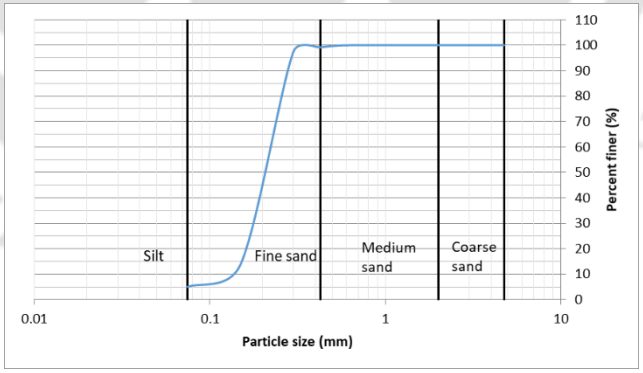

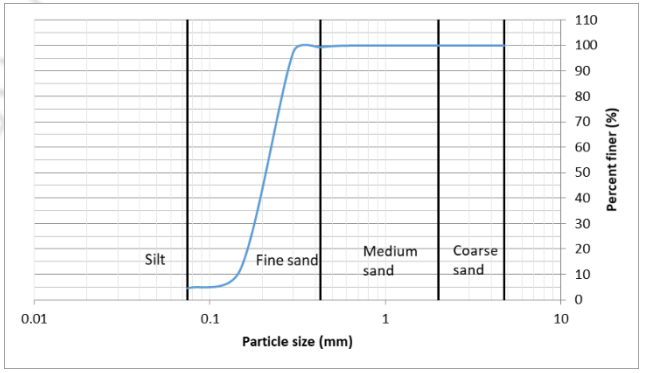

24.(26.2726N, 91.91728E)

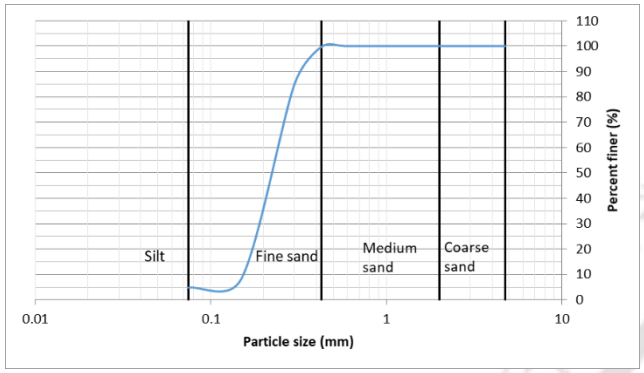

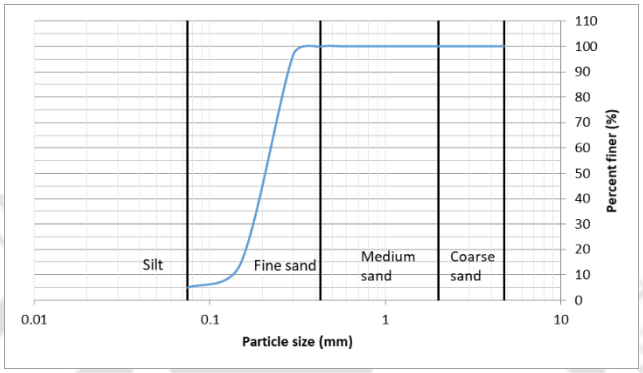

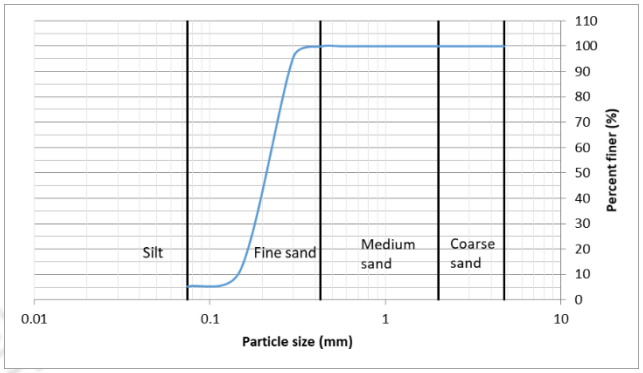

25.(26.2396N, 91.86164E)

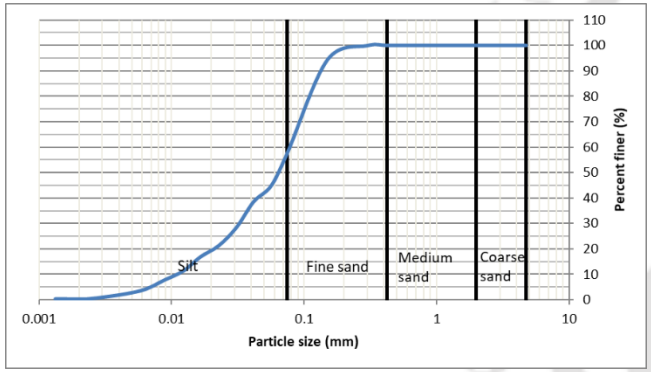

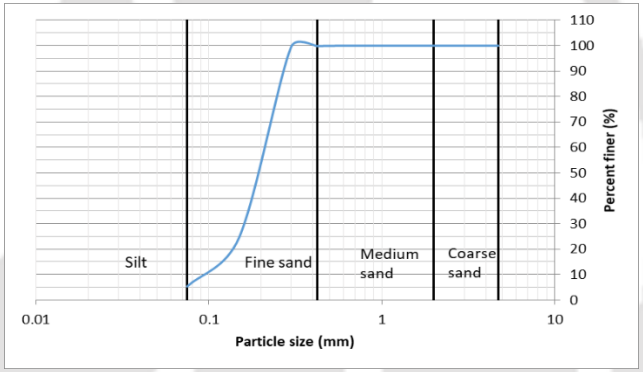

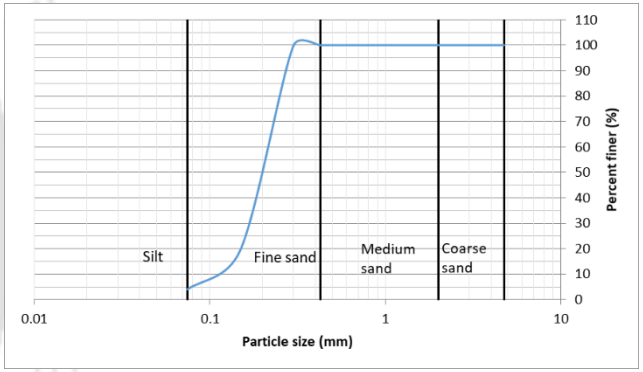

26.(26.1668N, 91.63483E)

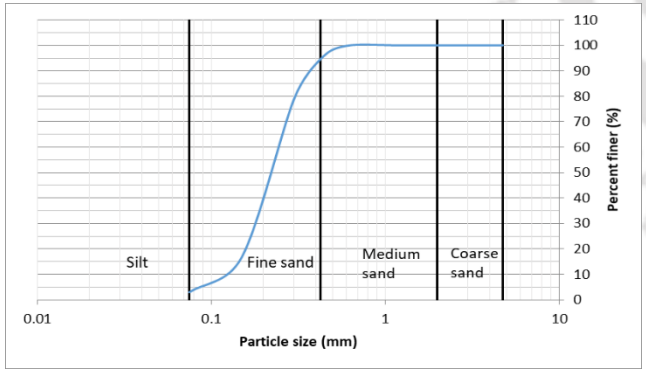

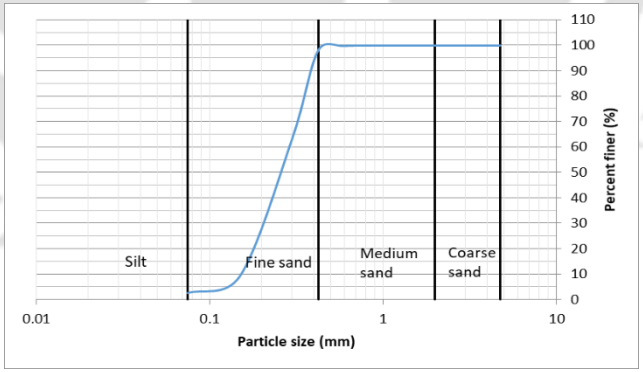

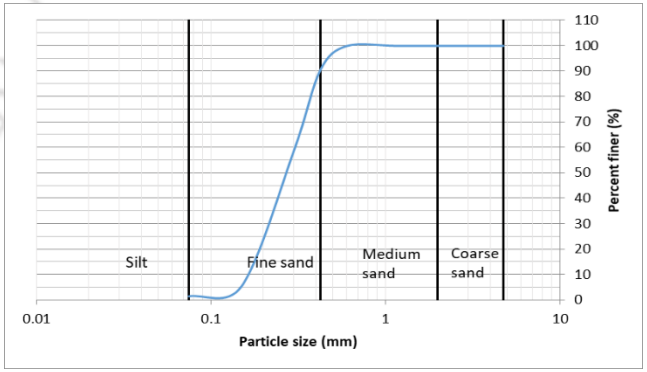

27.(26.15158N, 91.5768E)

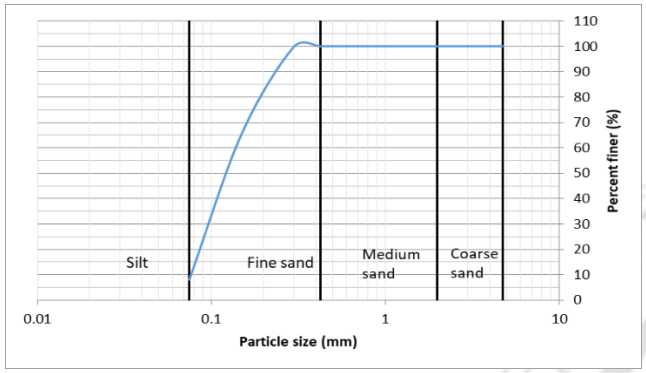

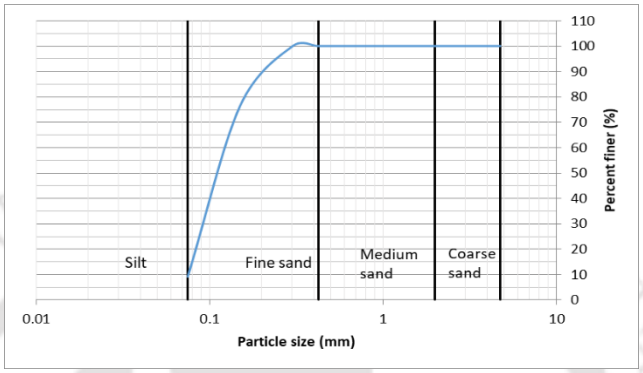

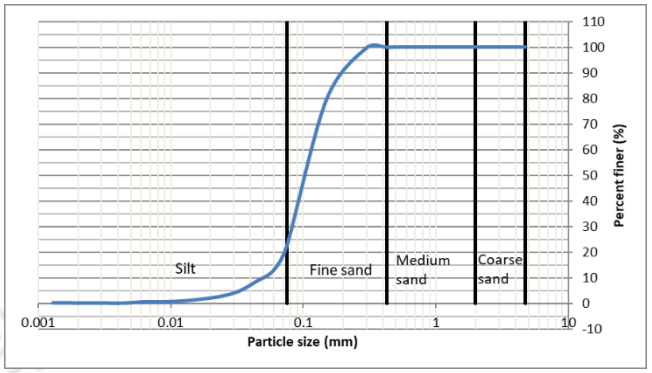

28.(26.175N, 91.304E)

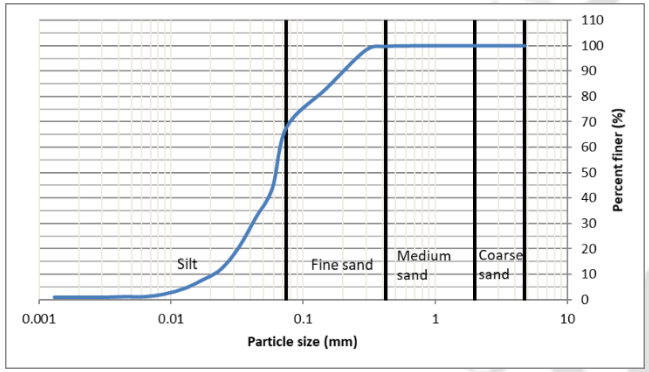

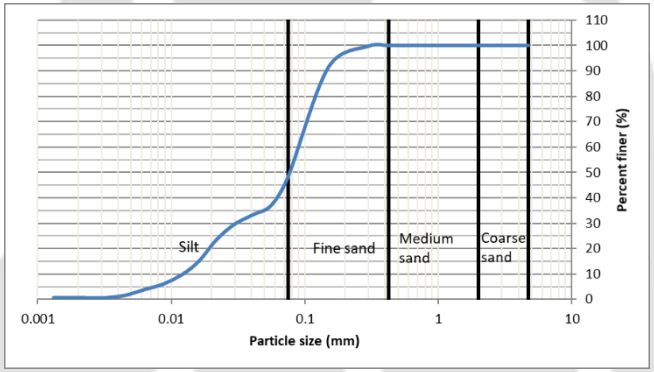

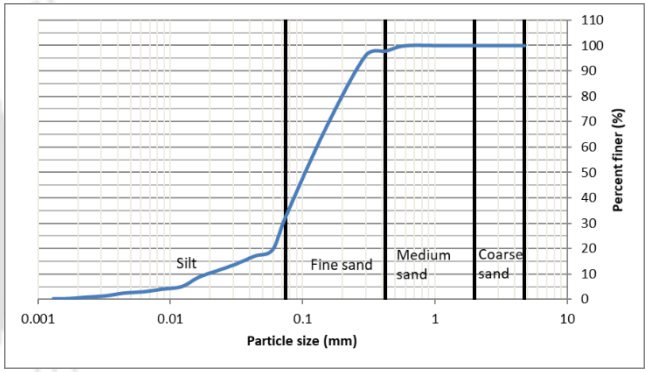

29.(26.1992N, 91.23551E)

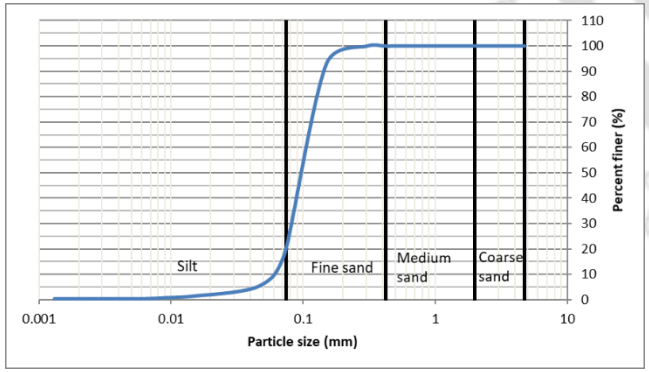

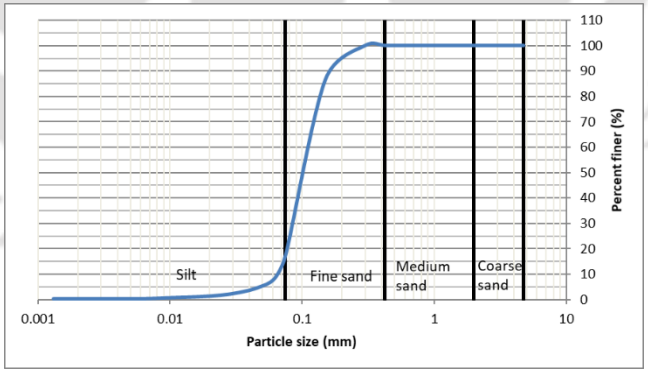

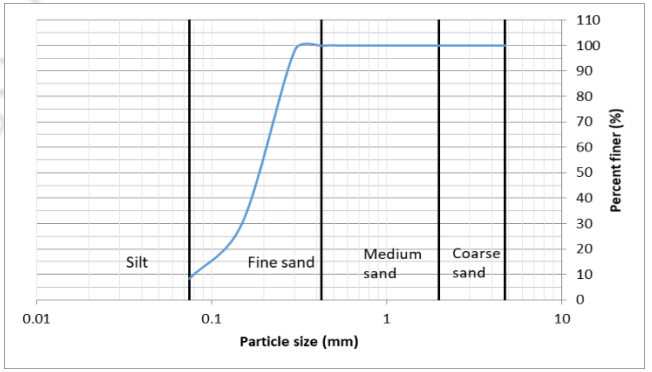

30.(26.2121N, 91.17158E)

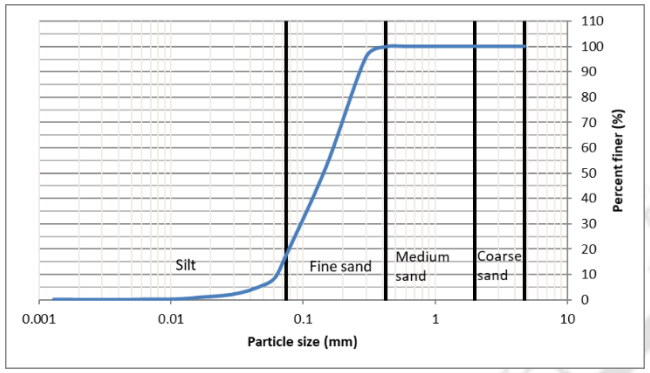

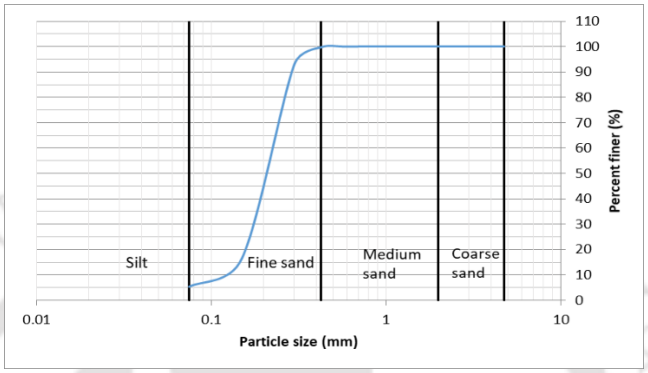

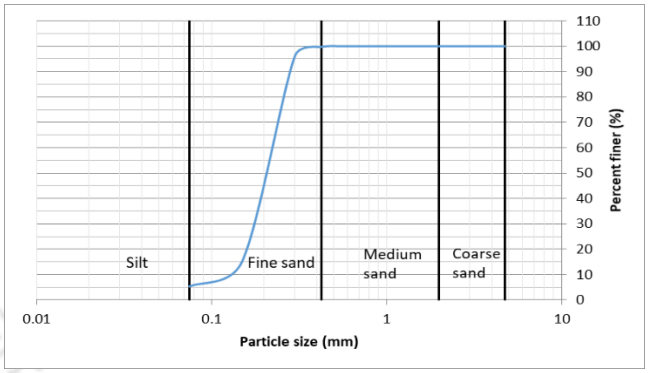

31.(26.2177N, 91.04398E)

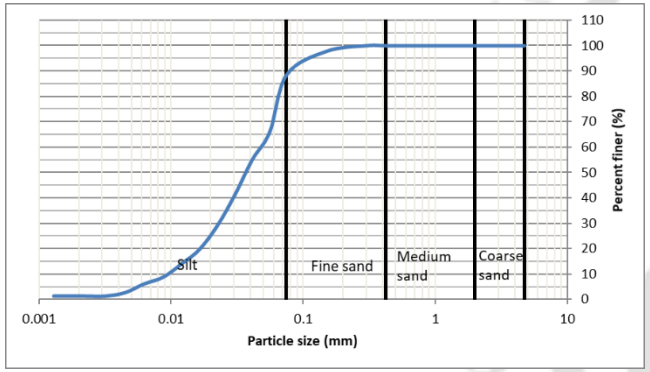

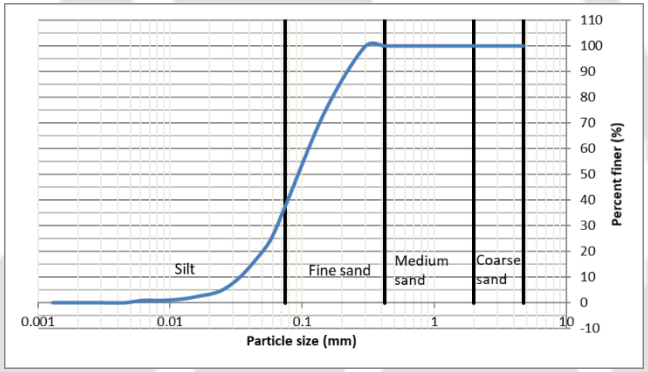

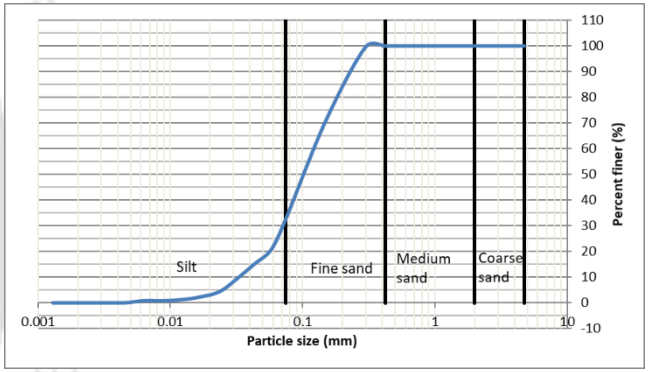

32.(26.20944N, 90.8864E)

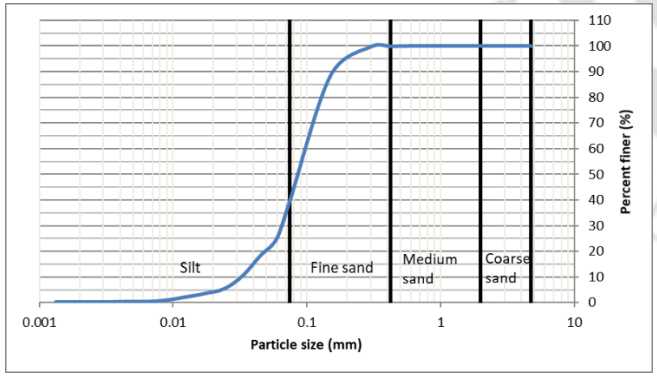

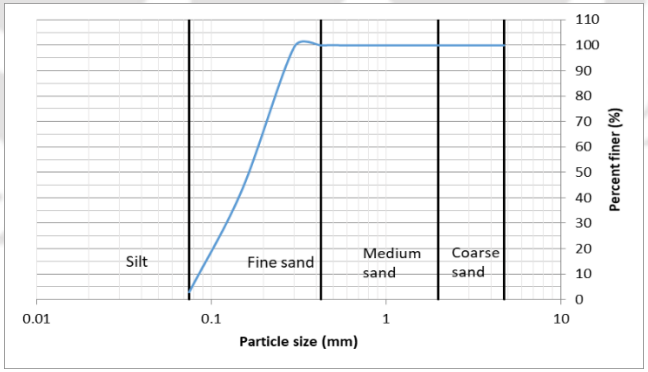

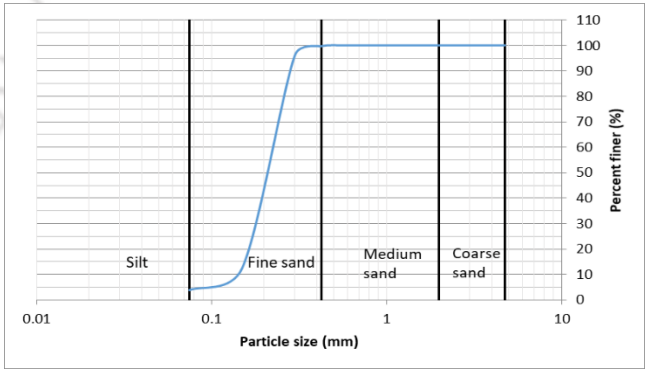

33.(26.18523N, 90.6597E)

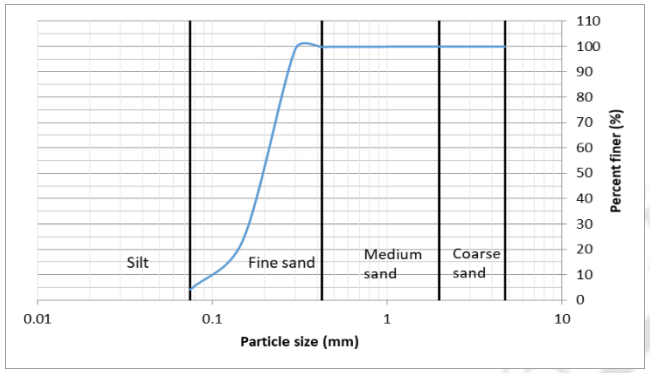

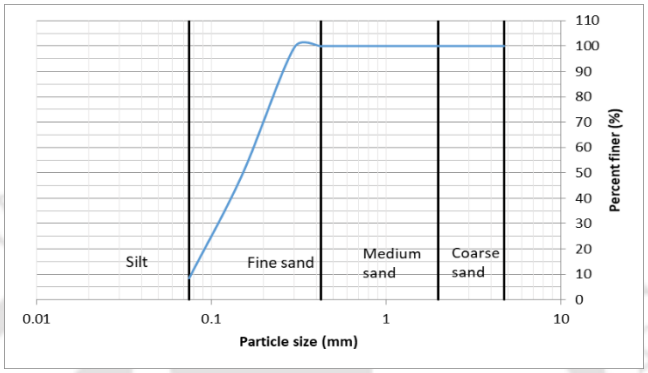

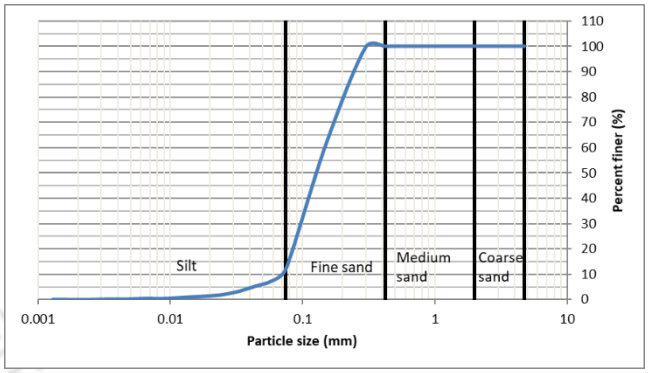

34.(26.1995N, 90.57506E)

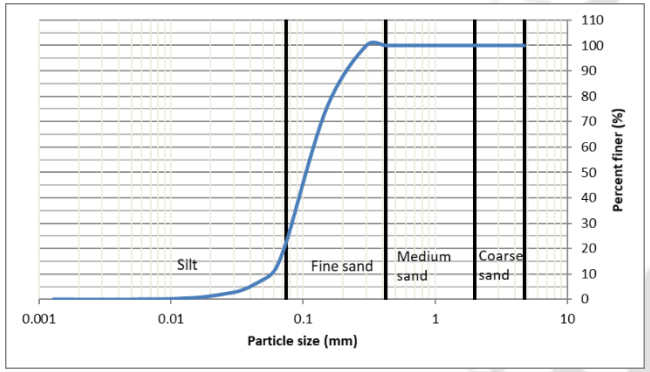

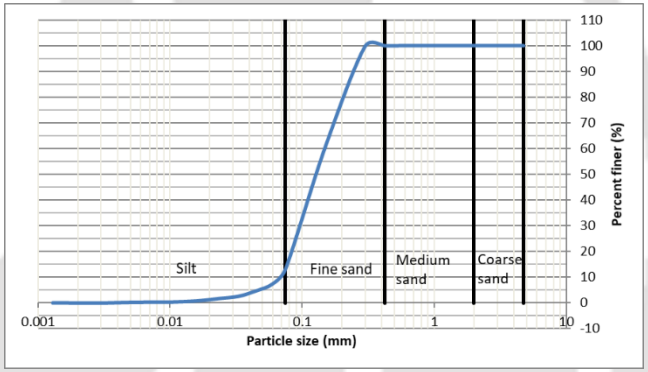

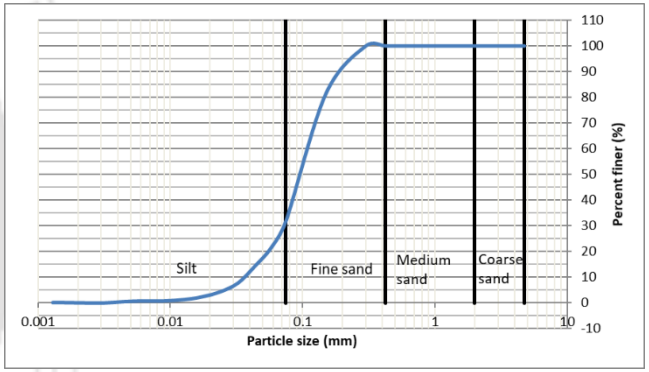

35.(26.2019N, 90.497E)

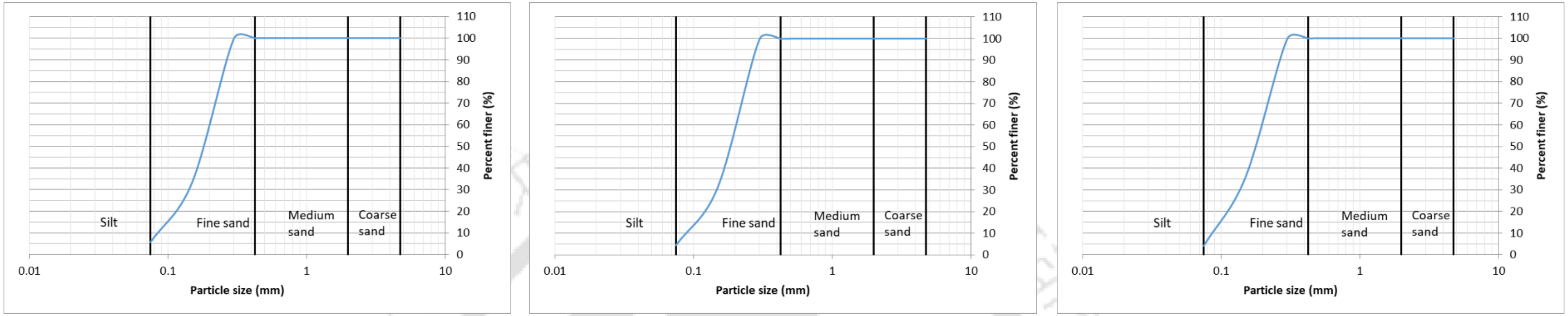

36.(26.15529N, 90.3602E)

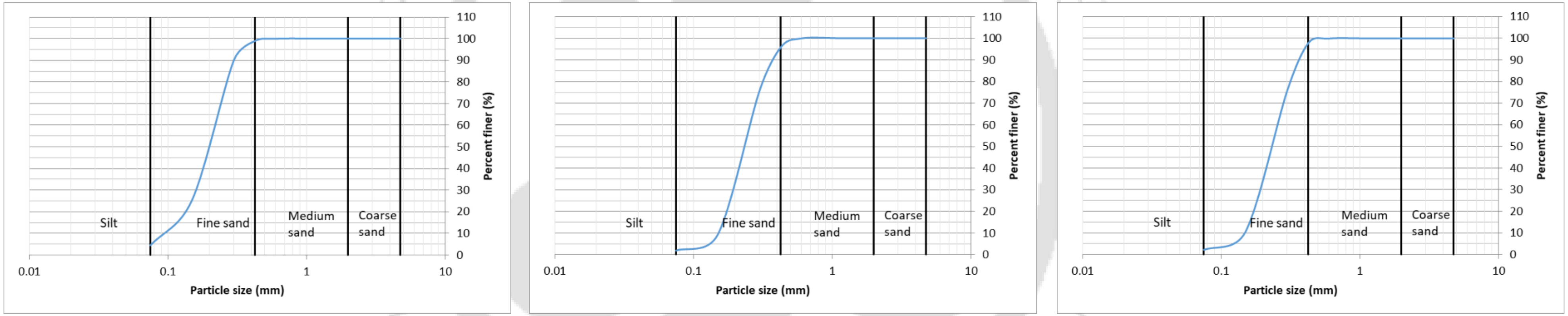

37.(26.102N, 90.3026E)

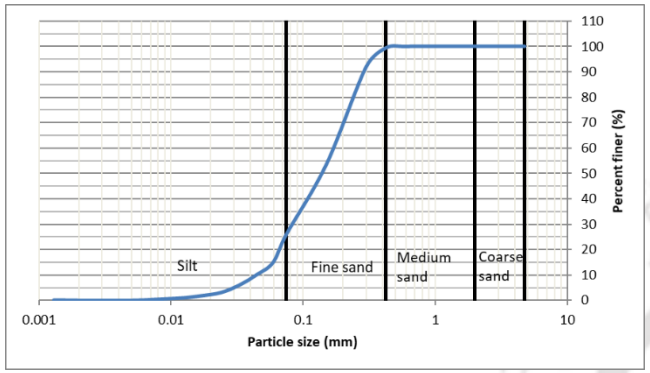

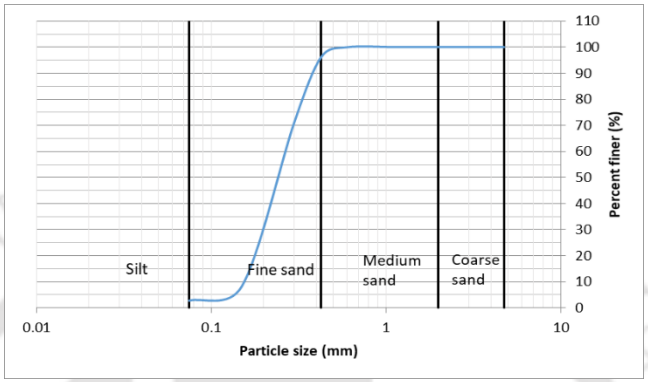

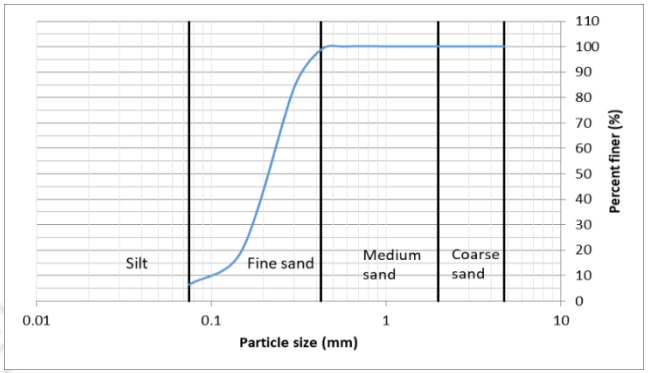

38.(26.073N2, 90.22382E)

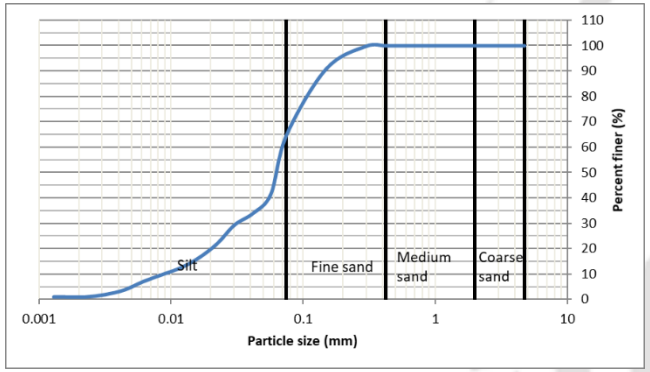

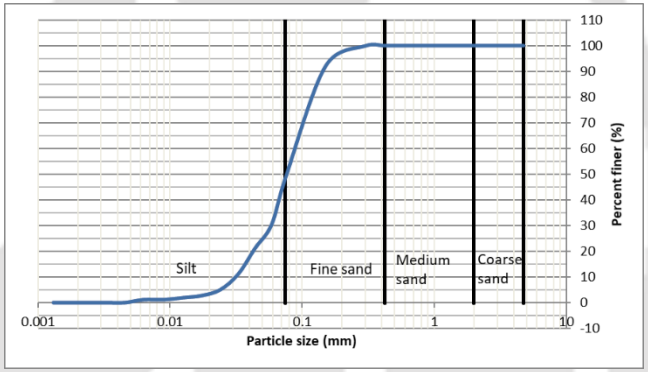

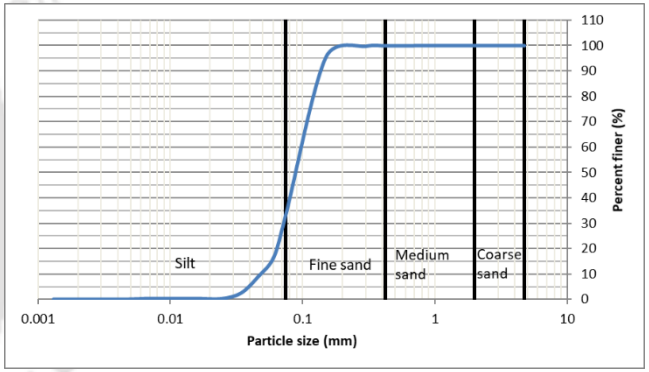

39.(26.0798N, 90.2104E)

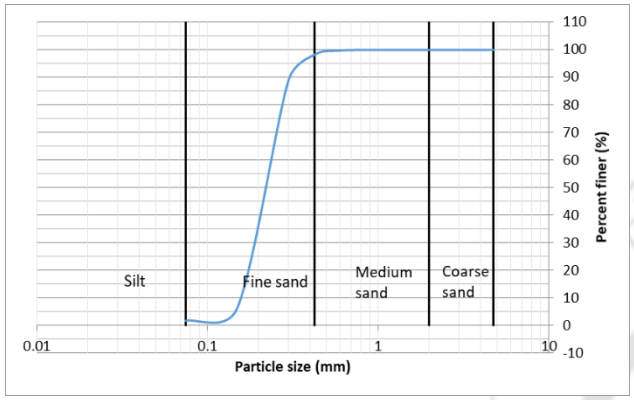

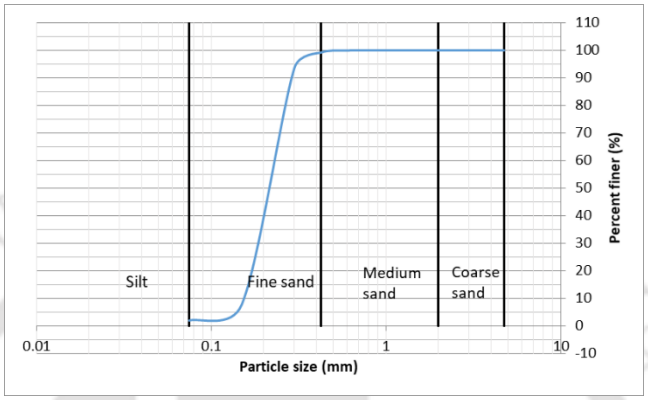

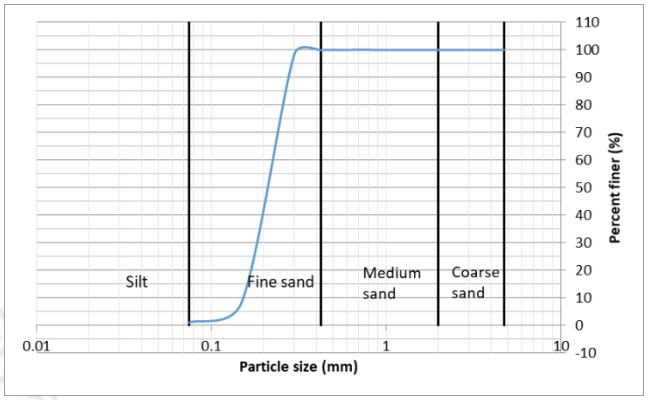

40.(26.039N, 90.0769E)

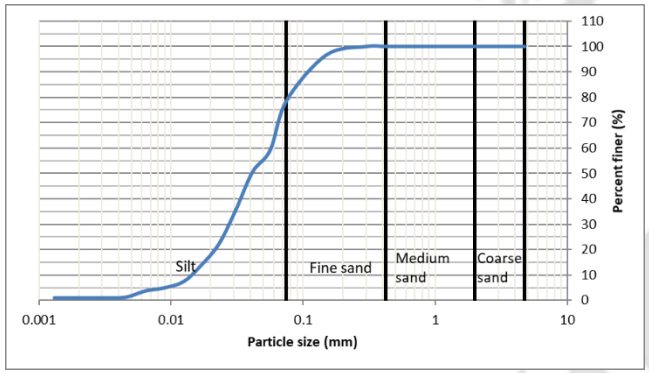

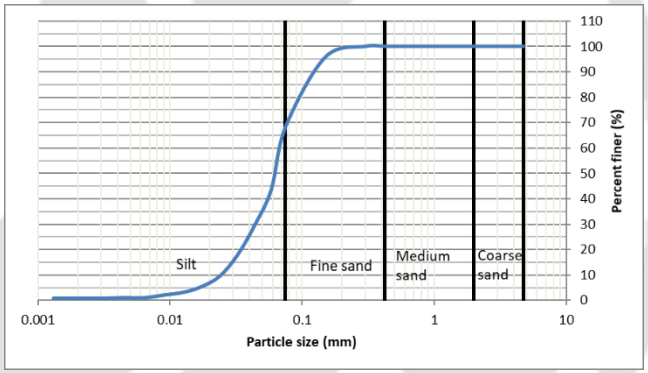

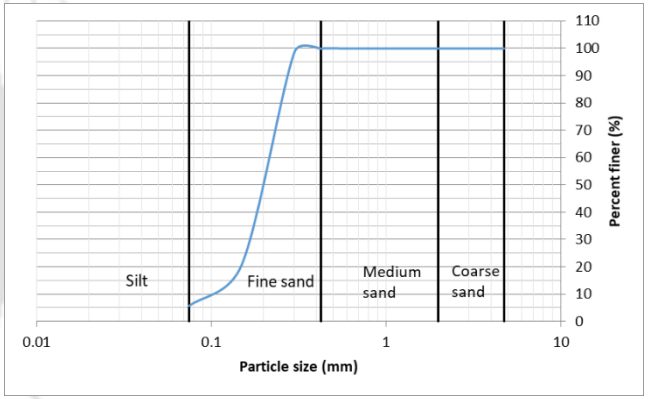

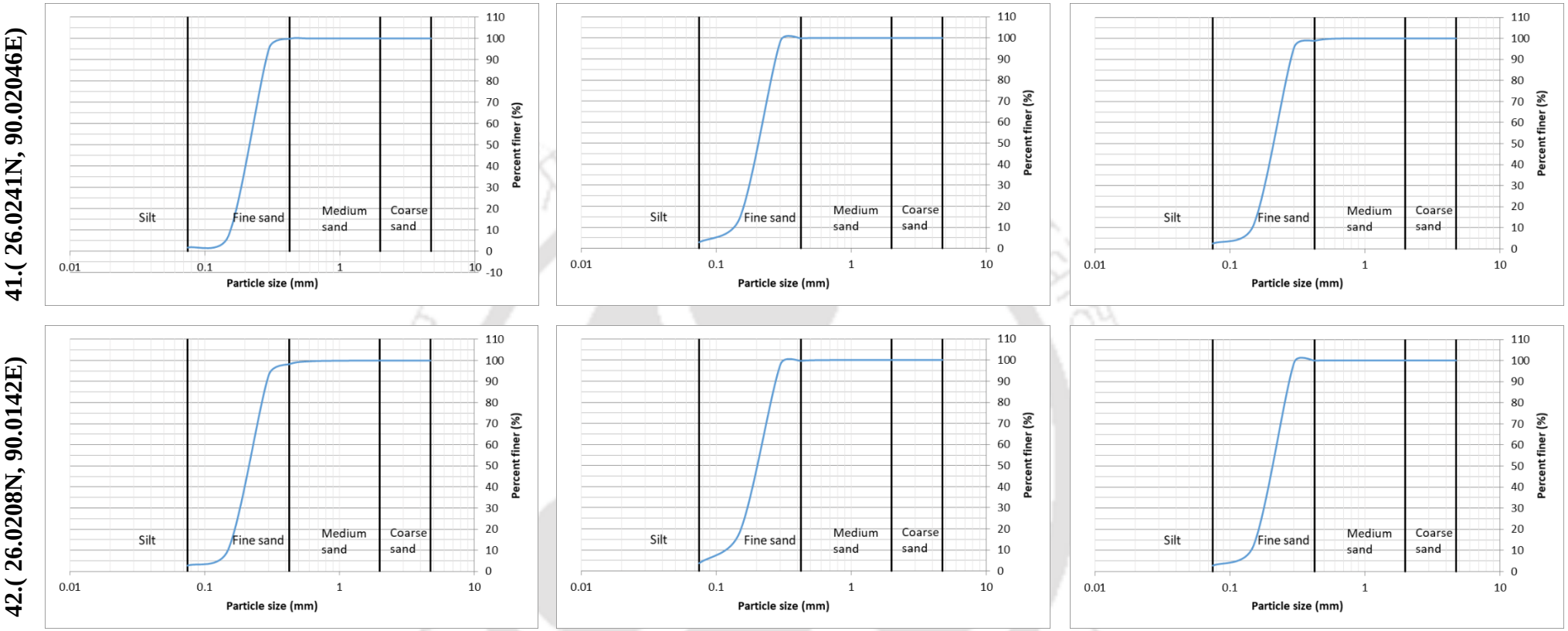

Figure 6.7: Analysis of the sediment samples collected from different sandbars within the Brahmaputra River

6.3.2 Mineral characterization and analysis

Studies pertaining to the deficiency and efficiency of mineral nutrient content in soils reveal crop responses to a particular nutrient. It depends on the soil type, environmental conditions, crop type, growth stages, and seasonality. In their study, Corey and Schulte (1973) found that the excessive amount of Boron hinders the uptake of other nutrients by the plants. Steinberg et al. (1955) found that concentration of Calcium (Ca), Magnesium (Mg), Nitrogen (N), Potassium (K), Copper (Cu), and Manganese (Mn) increased with the absence of Boron (B) in soil. Touchton and Boswell (1975) observed slight variations in Phosphorous (P), Potassium (K), Calcium (Ca), Magnesium (Mg), Sodium (Na), Zinc (Zn), Copper (Cu), Iron (Fe), Manganese (Mn) and Aluminium (Al) concentrations with location, and is not affected by the method or rate of Boron (B) application. Potassium (K) is a highly immobile nutrient that is limited and found in the form of Calcium (Ca), Aluminium (Al), and Iron (Fe) phosphates (Hirel et al., 2011). Patra et al. (2020), in their study, found the percentage of Total Nitrogen varied between 0.12-0.19 % in the upper (Top surface) and 0.13-0.25 % in the lower soil (30 cm depth) in betel vineyards site of coastal districts in Odisha. However, Inorganic Nitrogen was found to be in the range of 0.12-0.14 % and 0.09-0.15 % in the upper and lower soil, respectively.

To analyse the mineral concentration and identify the crystal structure of the samples, both EDX and XRD tests were performed on certain samples collected across the river. The samples consist of sediments collected from newly formed dry sandbars, vegetated sandbars and cultivated sandbars. The XRD analysis gives information about the mineral composition by phase identification by comparing it with the database of known structures (Ramasamy et al., 2009). The presence of minerals was recognized by observing the 2-theta values. From the XRD analysis in our sediment samples, we found Feldspar (F), Zircon (Z), Monazite (M), and Quartz (Q) as the key minerals, which were identified by comparing with Joint Committee on Powder Diffraction System (JCPDS) database. The findings of the study also matched with the study performed on the sandbars of Jamuna River in Bangladesh by Khalil et al. (2016). The peak of the samples observed at 2-theta values of 6.26, 8.8, 12.48, 20.82, 22.06, 26.6, 27.98, 29.8, 36.52, 39.2, 42.46, 50.08, 59.94, and 68.32 confirmed that the samples contain quartz, orthoclase, nitrogen oxide, phosphorous, sanidine, aluminum phosphate. Figure 6.8 shows the peak values of minerals present in the soil samples collected from various sandbars. It was found that the highest

peak was observed at the 2-theta value of 26.6, which represents the presence of Feldspar (F) and Zircon (Z) in higher amounts. Feldspar consists of Calcium (Ca), Sodium (Na), and Potassium (K), which are key nutrients required for plant growth. Na and K play a vital role in osmotic regulation in plants. Studies have shown the use of feldspar as K fertilizer in agricultural fields (Sanz Scovino and Rowell, 1988). Silicates are present in Zircon, which increases crop productivity and provides resistance to pathogens, insects, and pests (Meena et al., 2014). The other minerals found during the analysis were Monazite and Quartz. Monazite contains phosphate required for plant growth and is found in various fertilizers. Quartz is the most common crystalline form of silica (Silicon Dioxide). Silicon improves the defense against biotic constraints in the form of plant pathogens (fungi and bacteria) and animals (vertebrates and herbivores) (Luyckx et al., 2017). Although the XRD analysis provided relevant information about the compound type present in the sediment samples, EDX was performed to analyze the concentration of elements present in the samples.

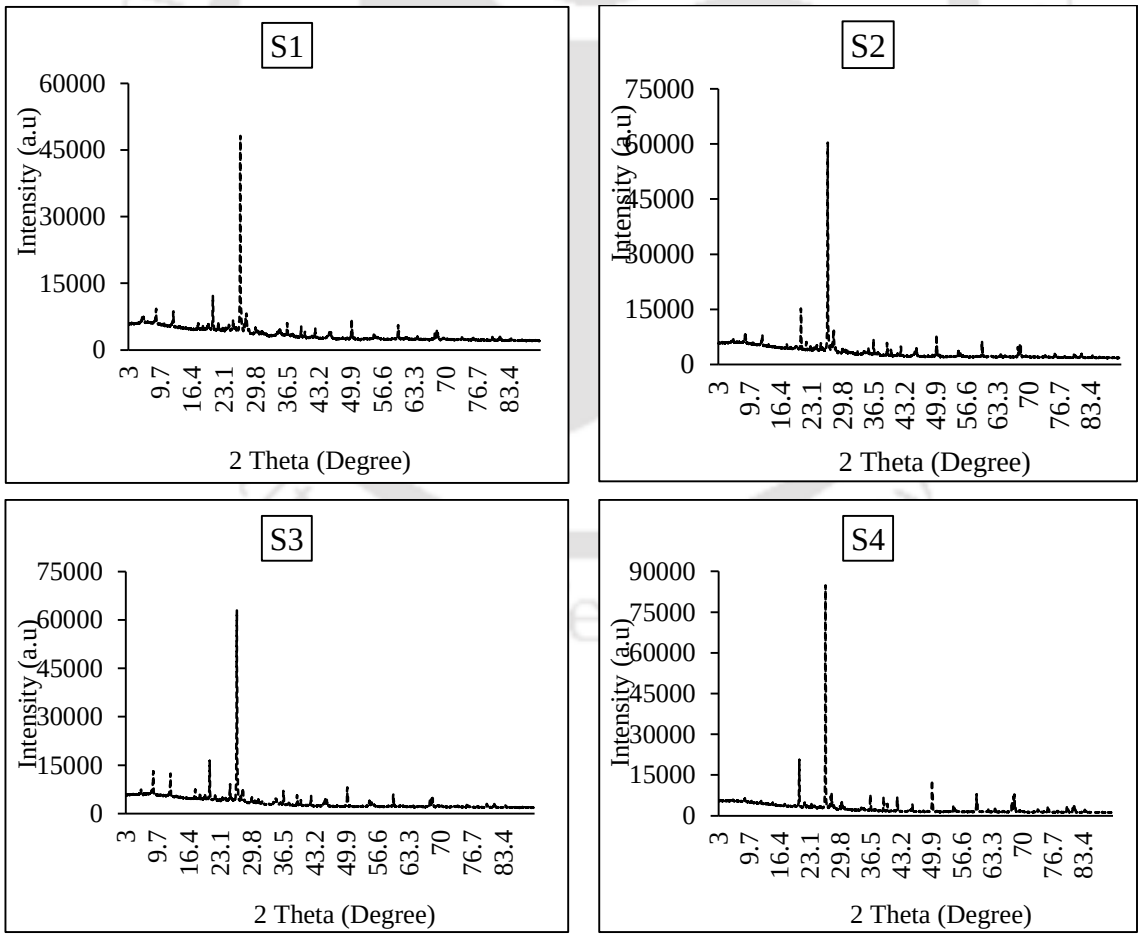

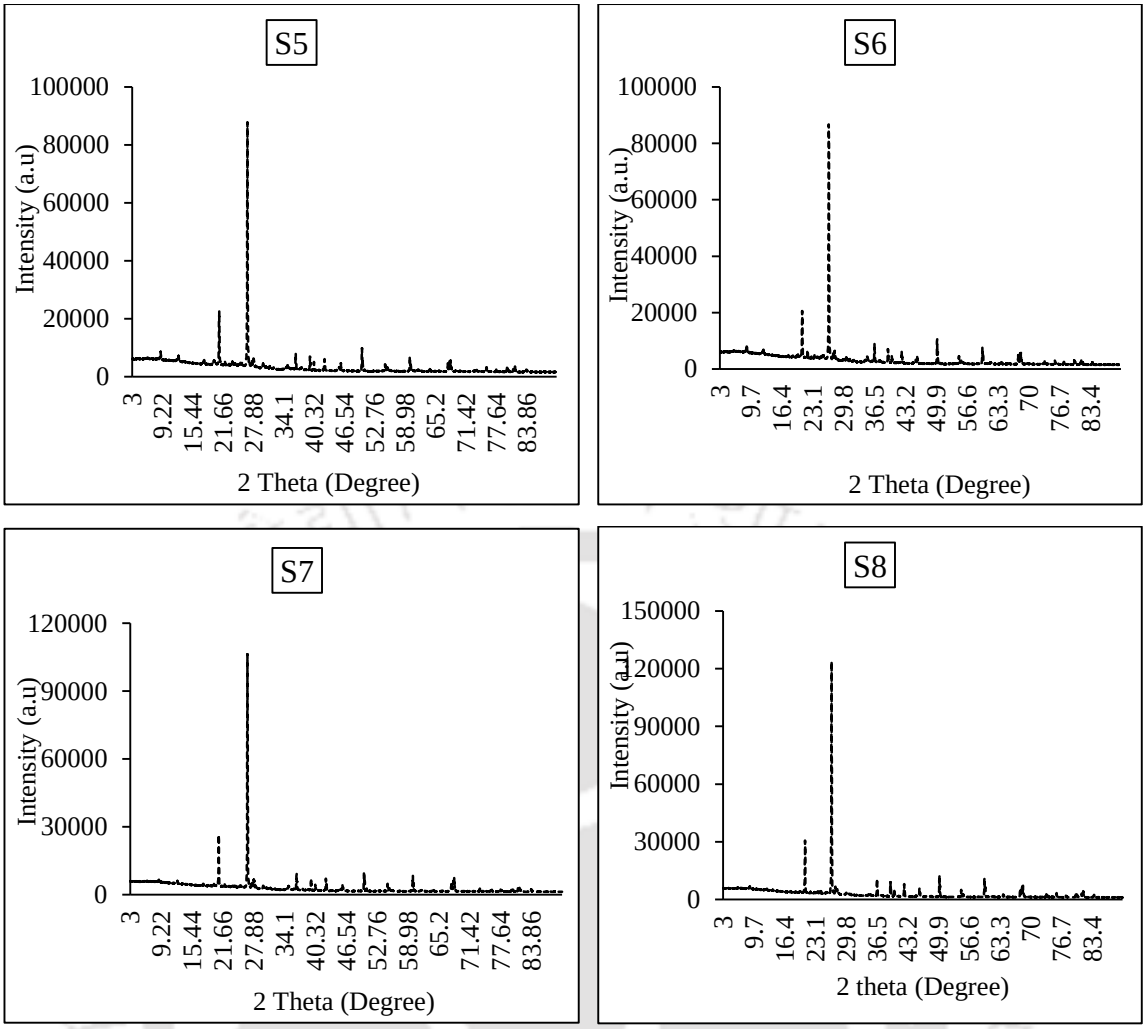

Figure 6.8: Results of XRD analysis representing the presence of minerals in the sandbar sediments.

The nutrients in soil play an important role in crop growth and survival. EDX analysis was performed to determine these nutrients in their elemental form and their distribution within the soil. It tells about the relative concentration of elements present in the sample as its weight percentage. Some soil nutrients like Nitrogen (N), Phosphorous (P), Potassium (K), Calcium (Ca), and Magnesium (Mg) are key components for plants and are collectively known as macronutrients. Micronutrients like Iron (Fe), Zinc (Zn), and Titanium (Ti) are required in small amounts for crop growth. Figure 6.9 represents the presence of different nutrients and their concentration in the selected sediment samples. It can be seen from figure 6.9 that Boron (B), Oxygen (O), Silicon (Si), and Carbon (C) have more than 10% weight and falls under the category of major components, as addressed by Hafner (2006). Aluminum (Al) and Iron (Fe) fall in the category of minor components with a weight % of less than 1, and potassium (K) and Nitrogen (N) fall under trace elements during the analysis. The results showed that the percentage of Boron (B) was sufficiently high (> 60%)

in all the samples, except for two samples. The absence of Boron in those samples significantly resulted in an increase in the percentage of other elements such as Silicon (Si), Aluminium (Al), Oxygen (O), and Carbon (C). Studies (Islam and Saha, 1969; Hernandez 2014) have shown that Silicon strongly influences micronutrients Boron (B) and Manganese (Mn) in soils. According to Islam and Saha (1969), Silicon (Si) application reduces the nitrogen (N), potassium (K), manganese, and iron (Fe) content of rice plants while increasing the Phosphorous (P), magnesium (Mg), calcium (Ca) and carbohydrate contents. Furthermore, Boron (B) concentration seems to have no or little effect on Aluminium (Al) and Sodium (Na). The percentage of Oxygen (O), Carbon (C), and Silicon (Si) were found to be more than 20% when compared with other elements (Fe, Mg, Al, Ti, Ca, Cu, K, and N) in the samples. The presence of certain minerals like Boron and Monazite indicated the use of fertilizers for crop growth. Feldspar contains macronutrient Potassium (K) and Calcium (Ca), which are vital for strengthening crops against diseases. The concentration of macronutrients, Nitrogen (N), and Potassium (K) were below 2% during our analysis, which concurs with the need to apply additional fertilizers for plant growth and physiological functioning. According to Gupta (1968), plants growing in sandy soils suffer Boron (B) deficiency. In addition, Nitrogen (N) deficiency restricts plant growth and causes yellowish color to leaves. According to Greger et al., (2018) it was found that Calcium (Ca) concentration increases with the presence of higher silicon (Si). Our results also corroborated with the results from the literature, showing an increase in Calcium (Ca) concentration in the samples of high Silicon (Si) concentration. Although the Iron (Fe) concentration was less than 5% in all the samples, the concentration was found slightly higher in the samples with high Silicon (Si) concentration.

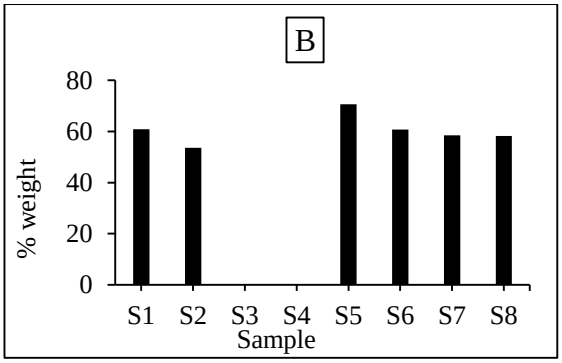

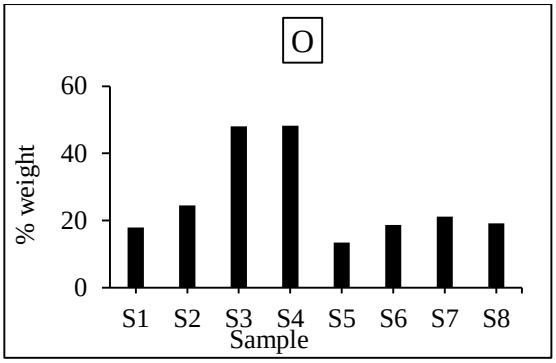

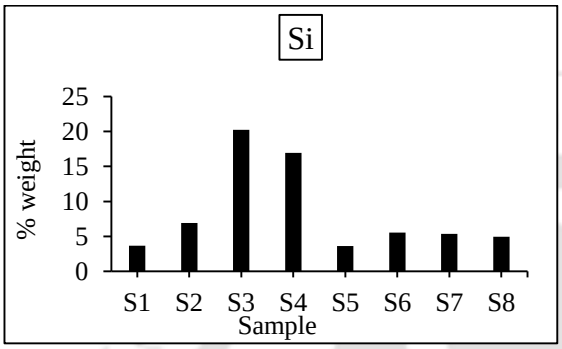

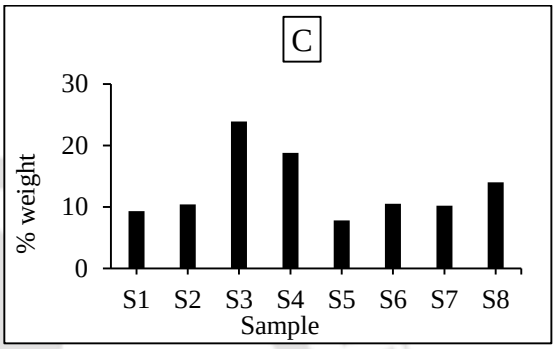

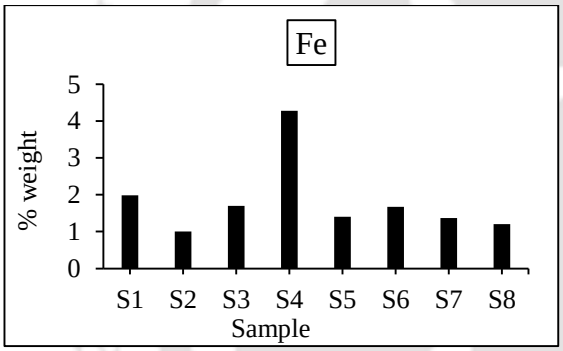

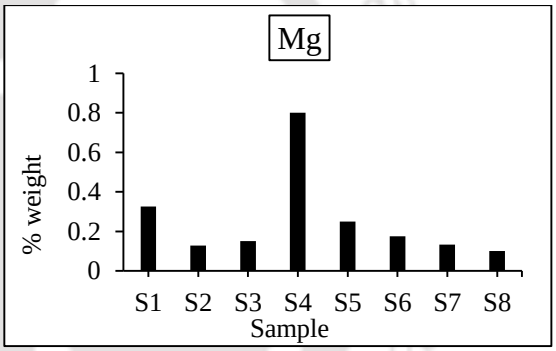

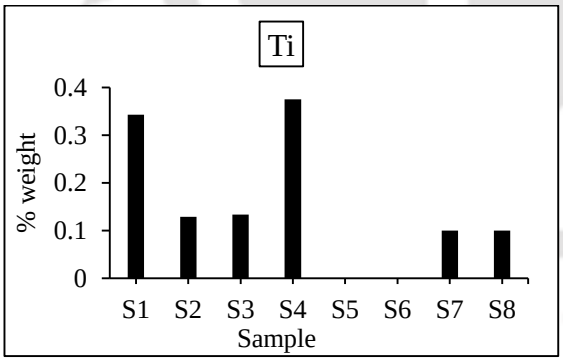

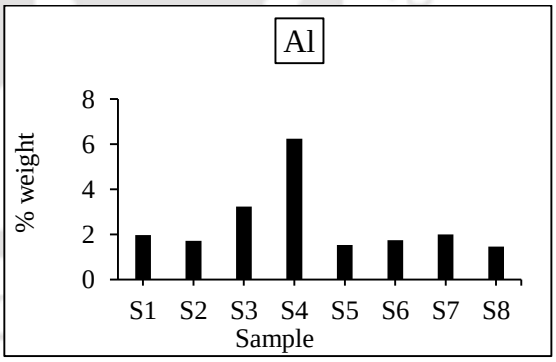

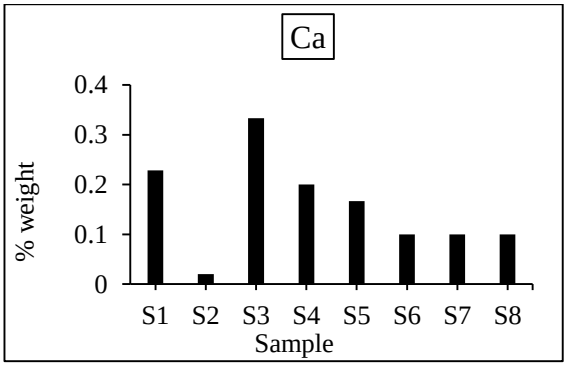

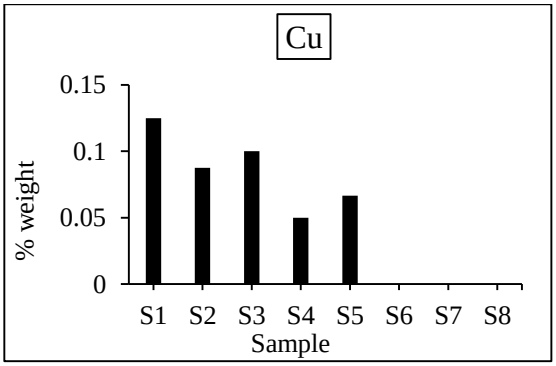

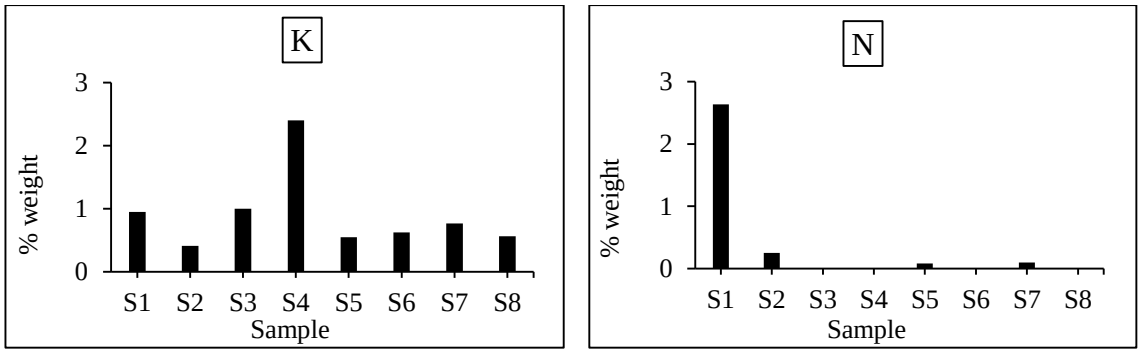

Figure 6.9: Percentage weight of elements present in the sediment samples

6.4 Conclusions

The sediment samples collected across different sandbars within the Brahmaputra River corroborated the soil types required for supporting plant growth and the presence of vital minerals. The study on nutrient analysis has shown the potential of sandbars for agricultural purposes with the presence of both macronutrients and micronutrients essential for plant growth. This preliminary analysis has also given a good insight into the soil characteristics of different sandbars. As suggested by various researchers, soil fertility, to some extent, is determined by its mineral composition. The presence of Feldspar and Quartz as primary mineral constituents plays a significant role in the overall dynamic of micronutrients, Potassium (K), and Calcium (Ca). Potassium (K) is considered a primary nutrient, and its presence in the samples indicated the application of fertilizers for crop growth and insect resistance. In our analysis, a significant concentration of Zircon was found. Its presence was believed to have been transported by water and deposited in the sandbars from upstream chemical processing industries. However, further investigation in this regard is necessary to confirm the actual source of Zircon. Often the supply of nutrients from soil is inadequate, and the use of fertilizers meets these deficiencies. The nutrients are present in different forms as dissolved, soil organic matter, minerals, and ions, together known as total nutrient content, of which only dissolved and ionic forms can be extracted. Phosphate is present in various fertilizers, and its presence is in the form of monazite. Silica, commonly known as Quartz, was also found in major quantities during our analysis. Literature has concluded that its presence is more in cultivated soil than that in non-cultivated soil. Its presence was also found in significant amounts in the sandy soils. Throughout the elemental analysis, the presence of Boron was found to be sufficiently high compared to other elements. This is because of the fertilizer, Borax, commonly used by the local farmers for

plant health and growth in the sandbars along with Urea and Potash. Nitrogen is required in amounts of 1-3% of the plant on a dry weight basis, after C, H, and O (Osman 2013), but maybe available in the range of 0.1 to 0.5% of total N content in soils. Its deficiency results in the yellowing of crops with stunted growth, and excess results in the delay of flowering and fruiting period. Phosphorous ranges between 0.1 and 0.5% of plant leaf dry weight than other macronutrients and stimulates seed growth, fruiting, and development. Calcium and Magnesium are intracellular regulators for plants that help maintain the uptake and production of food materials. Plants require other nutrients in fewer amounts to accomplish physiological functioning. Among all the nutrients, N, P, K are commonly deficient nutrients as they are removed from soil by the plants and are common in high rainfall areas. The nutrients also interact among themselves, inducing deficiencies, toxicities, or growth responses. Thus, from the sediment analysis, we can concur that the presence of nutrients in excess or deficit depends on crop type, crop growth stages, plant species, soil type, seasonality, etc., and is independent of the absolute concentration of a particular mineral. In addition, nutrient interaction plays a major role in the variation of nutrient concentrations and is complex in nature. It may suppress the biochemical reaction in one or enhance these reactions in others. Therefore, this analysis has shown the presence of nutrients and minerals in the samples, which are essential information derived before performing activities in the sandbars. From the sediment analysis, it can be inferred that the sandbars selected for study pose various characteristics. The cultivated sandbars contain less silt and clay as compared to vegetated sandbars and were well-graded, while the newly developed sandbars were poorly graded. Thus, the information on soil structure is vital for agricultural productivity, and this study is a preliminary step toward the utilization of sandbars for agricultural activities. It can be a boon to the agriculture revolution amidst urban expansions. Nevertheless, the proper utilization of such resources is complex. It needs to be dealt with optimally such that maximum benefits could be derived from the ecosystem, which could help in the socio-economic development of marginalized communities. In addition, the information on the behavior of hydrological parameters is vital for planning activities in a riverine environment. The use of seasonal forecasts could benefit the farmers; however, it depends on how well these parameters can be predicted and how much this information helps in the actual decision-making process.

7

Short-term streamflow forecasts and trend analysis for decision-making

7.1 Introduction

In the era of climate change, streamflow variability is one of the most influential contributors to the variation of food production, crop damage, and economic losses in agricultural systems. Hydroclimatic disturbances also adversely affect vegetation growth and crop yields (Sharma and Goyal, 2018). Predictions of water availability on a seasonal time scale are helpful for managers and planners, and flow forecasts are therefore essential for decision-making. Various researchers have performed flow-forecasting studies (Wilby et al., 2004; Tucci et al., 2008; Zhang et al., 2018). In the agricultural context, farmers are more likely to benefit from short-term decision-making forecasts. Previous studies (Svensson, 2016) have shown the importance of seasonal flow forecasts using flow analogues and their application on smaller scales and frequently changing meteorological influences in the UK. The essential premise behind utilizing analogues as a forecasting approach is that the hydro-climatic system can follow particular trajectories that repeat themselves. The phenomenon of hydrological variables such as streamflow is not easily predictable because streamflow characteristics are highly complex and of dynamic behavior with non-stationarity associated with it. The conventional methods, which are linear in form, may not fully capture this non-linearity. Data-driven techniques of Artificial intelligence (AI) for flow forecasting have received considerable attention in the past decades (Yaseen et al., 2015), which has motivated researchers to develop models for solving complex hydrological problems. The goal of data-driven modelling is to use

artificial intelligence (AI) techniques to extract documented data patterns from the past to forecast future streamflow data. It has proven to be a popular and effective forecasting tool, generating estimated streamflow data that accurately represent the actual streamflow data (Fathian et al., 2019). Several AI models have been established using Artificial Neural Networks (ANN) technique (Bai et al., 2016, Bahrami et al., 2016, Mutlu et al., 2008). However, no absolute AI model is appropriate for all modelling purposes (estimation, forecasting, classification, optimization, etc.) (Yaseen et al., 2015). From this perspective, it is evident that the certainty of the forecasted streamflow data can be effectively enhanced by the integration of two or more techniques to model and assimilate the data patterns (Fahimi et al., 2017). Incorporating forecasted data into optimization models could result in significant gains in efficiency.

In the agricultural environment, prudent cropping pattern selection and temporal modifications may be valuable for minimizing potential crop losses while maximizing economic returns and productivity, which can be achieved using optimization techniques. From various studies, it could be established that short-term streamflow prediction for agricultural crop planning within a riverine system is crucial for enhancing production and improving the socio-economic condition of marginalized communities. Furthermore, rising food consumption necessitates the expansion of agricultural lands. The approaches employed in the current study provide information on the seasonal area available under fluctuating streamflow and water level in rivers. The forecast study could help in decision-making and reduce the potential economic loss due to crop damage.

7.2 Flow forecasting methods

7.2.1 Historical Analogue (HA) and Persistence forecast (PF) method

The historical analogue refers to streamflow sequences in the historical record, and records similar to those that occurred recently may provide useful information about future flows. The persistent forecast method uses the flow anomaly of the most recent observed month to forecast for the next 1 or 3 months. The use of anomalies allows the forecast to follow the seasonal cycle rather than persisting a fixed flow value.

In this study, the monthly maximum streamflows were calculated from the 10-daily streamflows for the time series 1999-2015. A log transformation to the monthly streamflow data (q_t) were carried out, which makes the distribution of the flows more similar to a

normal distribution. As the streamflow has a seasonal cycle in both the monthly mean and standard deviation, standardized flow anomalies were used for the analysis. The mean (m_{mon}) and standard deviation (s_{mon}) were calculated for each month in a year and a series of standardized monthly anomalies (a_t) were calculated as:

$$a_t = \frac{q_t - m_{mon}}{s_{mon}} \tag{7.1}$$

where, *t* represents the serial number of the month during the start of the year and *mon* represents the month of the year.

Forecasts were made with the streamflow data for the latest and end months using the persistence of the previous month's flows and historical analogue forecasts. The persistence forecast method uses the standardized anomaly from the most recent month of the available streamflow observation and forecasts for the next 1-month, 3-month, or cropping season. Hence, the seasonal cycle of the flows is maintained in the forecast. In this study, the streamflow forecasts were made for three seasons: (i) Zaid (Jan/Feb-May/Jun), (ii) Kharif (Jun/Jul-Sep/Oct) (iii) Rabi period (Oct/Nov-Dec/Jan).

The historical analogue forecast is based on the assumption that the historical records of the streamflow that are similar to the recent past will provide valuable information for flows in the future. For this method, the monthly anomalies of the recent past were compared with the possible sequences of anomalies of the historical flows. For example, if the analogue was selected for the months July to October in the recent past, then the potential analogues were selected for the same sequence in the historical times series of flows. From this annual series of analogues, the number of potential analogues (N_{ana}) most similar to the recent past were selected based on the root mean square error (RMSE). The RMSE's were ranked from lowest to highest, with 1 being ranked the lowest value and increases to N_{ana} i.e., the number of analogues considered. The RMSE was calculated for each analogue as:

$$RMSE = \sqrt{\frac{1}{D_{ana}} \sum_{k=1}^{D_{ana}} (a_p(k) - a_r(k))^2} \tag{7.2}$$

where, $a_p(k)$ represents flow anomaly for each month k in the potential analogue of duration D_{ana}. $a_r(k)$ represents corresponding flow anomaly in the recent past, and k represents the month during the potential analogue duration.

The RMSE was assigned weights (w) for the selected number of analogue (N_{ana}) as:

$$w(b) = \frac{\frac{1}{RMSE(b)}}{\sum_{b=1}^{D_{ana}} \frac{1}{RMSE(b)}} \tag{7.3}$$

where, $b = 1 \ldots N_{ana}$ is the rank of the ordered RMSE's.

The historical analogue forecast anomalies, i.e., the weighted mean forecast anomalies $\left(a_f(m)\right)$ for each month in the forecast duration can be calculated as:

$$a_f(m) = \sum_{b=1}^{N_{ana}} w(b) a_{p,b}(D_{ana} + m) \tag{7.4}$$

where, $a_{p,b}$ represents the vector of the streamflow anomalies for the potential analogue with rank b. m represents the month in the forecast duration (D_f) which varies from m =1…D_f.

The forecasted anomalies were then converted back into streamflows by reversing equation 7.1. The anomalies were re-standardized before the conversion to obtain mean = 0 and standard deviation = 1. This was done by subtracting the hindcast anomalies from the mean and dividing them by standard deviation for the appropriate time of the year. The validation between the forecasts and hindcasts was done using the jack-knife validation method. Figure 7.1 presents the methodological framework of streamflow forecasting.

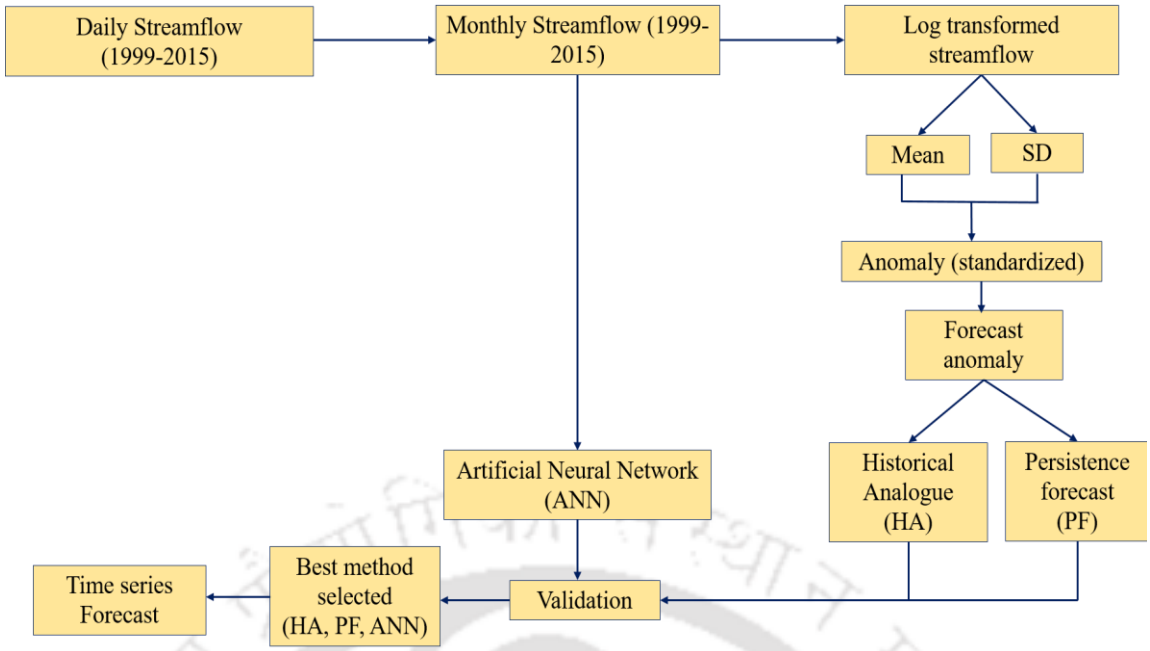

Figure 7.1: Methodological framework of the streamflow forecasting

Jack-knife validation refers to leave-one-out cross-validation. In the jack-knife test, one year was dropped from the total observations for the period of observations available. The flow anomalies from this missing year were forecasted from the remaining years in the record. This was followed for the total observations, and thus a hindcast was made for each year. After that, the flow anomalies from the observed record and the hindcast record were then compared, as shown in Figure 7.2. Out of all the cross-validations performed with different combinations of D_{ana} and N_{ana}, the best combination was selected for performing the seasonal forecasts. The correlation between the observed streamflow and the hindcast streamflow was performed to choose the best performance.

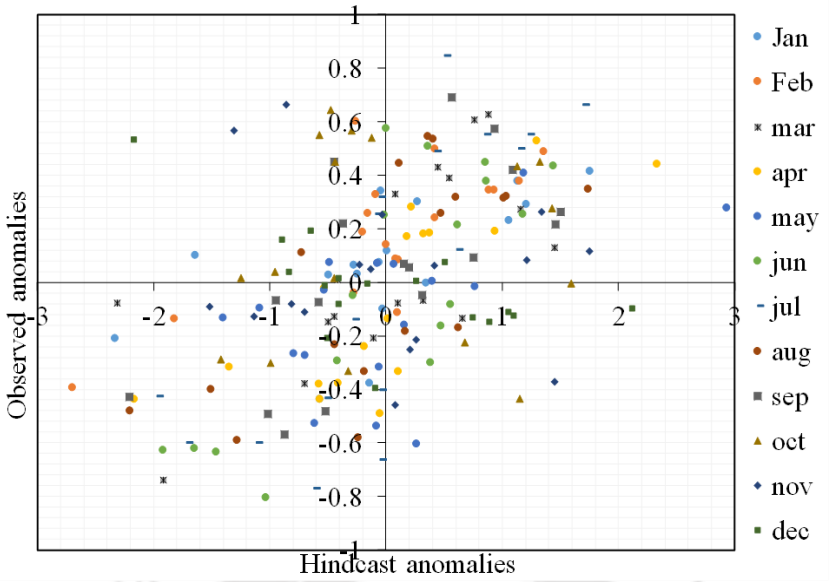

Figure 7.2: River streamflow anomalies with different combinations of D_{ana} and N_{ana}, between the observed and hindcast.

7.2.2 Artificial Neural Network (ANN) approach

Artificial Neural Networks (ANNs) are the most commonly applied approach among machine learning mechanisms (Grossberg, 1988). It contains interconnected components called neurons that transform a set of inputs into the desired output. Typically, ANNs are composed of three parts: (a) an input layer including a number of input nodes, (b) one or more hidden layers including the activation function, and (c) a number of output layer nodes. Each node typically applies a nonlinear transformation called an activation function to its net input to determine its output signal (Govindaraju, 2000). Figure 7.3 shows an example of a structure of ANN with one output layer.

Various epochs and neuron numbers were examined to determine the optimum input combination to the network. Through this process, extracted training and testing records with different proportions were used. The numbers of neurons used in the input, hidden, and output layers were 12, 6, and 3. Each node in the input layer (i = 1, 2, 3…, n) propagates the hidden layer's input patterns. Each hidden layer node (j = 1, 2, 3…, m) combines its weighted inputs to produce a net input to the neuron j and passes it to the activation function to compute its output. Weights were associated with each incoming input signal. In this study, three neurons in the output layer were used to train and test the model. Out of 17 years of observed monthly data from 1999-2015, 14 years of record were used for training and 3 years for testing. The monthly data were then aggregated into seasonal values. In

recent ANN architectures, the rectified linear unit (ReLU) was the most widely used activation function because it is computationally less expensive than tanh and sigmoid (Maas et al., 2013; Xu et al., 2015). Therefore, ReLU was used as the activation function for our model.

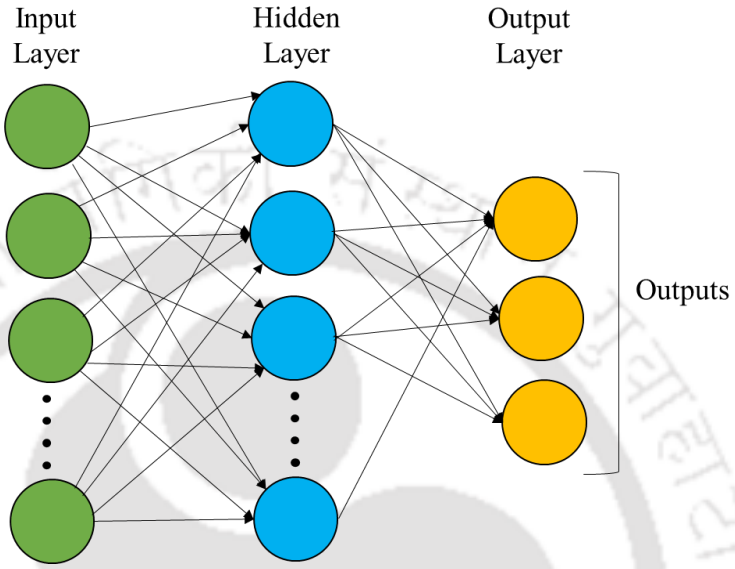

Figure 7.3: Example structure of an ANN with one output layer

7.3 Trend Analysis

Trend analysis is useful for understanding the dynamics and behaviour of hydrological and climatic variables such as streamflow, rainfall, temperature, etc. It provides valuable information for effective water resources planning and management over a long-term period. It gives an idea of whether a hydroclimatic time series observed values are rising or declining. The two approaches to identifying the changing patterns are the parametric and non-parametric approaches. However, non-parametric approaches are robust and have the advantages of data not being normally distributed but should be free from serial correlation (Yue and Wang. 2004). The non-parametric Mann-Kendall (MK) trend test was used for the trend analysis. Subsequently, Sen's slope test was applied to estimate the change in streamflow at monthly and annual time-scale.

7.3.1 Mann Kendall trend test

Among several approaches for detecting trends in various hydroclimatic variables, the Mann-Kendall (MK) trend test (Mann, 1945; Kendall, 1975) has been widely used. MK

test is a non-parametric test used to identify a trend in a series. It can also be used to determine whether a time series has a monotonic upward or downward trend. The null hypothesis (H_0) shows no trend in the series. The alternative hypothesis (H_a) indicates that the data follow a monotonic trend (i.e., negative, non-null, or positive trend). Under the null hypothesis, the data are independent and identically distributed. The MK test statistic (S) can be calculated as

$$S = \sum_{i=1}^{n-1} \sum_{j=i+1}^{n} sign\,(X_j - X_i), \qquad for\ all\ 1 \le i < j \le n. \tag{7.4}$$

where, X_j and X_i are sequential data in the series in the j^{th} and i^{th} observations; n represents the number of observations; *sign* represents the signum function that extracts the sign of a real number, which is calculated as:

$$sign(X_j - X_i) = \begin{cases} 1, & if\ (X_j - X_i) > 0 \\ 0, & if\ (X_j - X_i) = 0 \\ -1, & if\ (X_j - X_i) < 0 \end{cases} \tag{7.5}$$

The variance, S can be estimated as,

$$Var(S) = \frac{n(n-1)(2n+5) - \sum_{p=1}^{q} t_p(t_p-1)(2t_p+5)}{18} \tag{7.6}$$

where, n represents the length of the time series, t_p represents the tie values (same value occurring in the time series). In a two-tailed test for trend at the given significance level, the null hypothesis is rejected, if $|Z| > Z_{1-\alpha/2}$ and significant trend exists in the time series.

The standardized test statistic (Z) can be calculated as

$$Z = \begin{cases} \dfrac{S-1}{\sqrt{Var(S)}}, & when\ S > 0 \\ 0, & when\ S = 0 \\ \dfrac{S+1}{\sqrt{Var(S)}}, & when\ S < 0 \end{cases} \tag{7.7}$$

Z indicates the direction of the trend. The negative value of Z suggests a decreasing trend and vice versa. At the 1%, 5%, and 10% significance levels, the null hypothesis of no trend is rejected if the absolute value of Z is higher than 2.33, 1.96, and 1.65, respectively **(**Kuriqi 2020**)**. The significance of the change in monthly and annual streamflow was estimated using the MK test. In this study, the test was performed by considering a 10% significance level. Figure 7.4 presents the methodological framework of streamflow forecasting.

7.3.2 Sen's Slope estimator

The MK test does not quantify the trend magnitude. The robust Kendall slope (β) was used to assess the slope of the monotone trend (Sen, 1968). Sen's slope method was used to evaluate the annual and monthly streamflow changes for the time series. The test statistic is given as follows:

$$\beta = median\ \left(\frac{X_j - X_i}{j-i}\right) \quad for\ all\ i < j \tag{7.8}$$

A positive value of Sen's slope estimator indicates an upward trend, and a negative value indicates a downward trend. Despite the robustness of the MK test to the distributional aspects of data, the presence of a positive (negative) serial correlation in the time series increases (decreases) the probability of detecting trends when no trend exists actually. To counter this effect, a modified MK test was proposed by Hamed and Rao (1998), in which the variance was modified to take into account the autocorrelation of the time series.

$$Var^*(S) = Var(S).\left(\frac{n}{n_e^*}\right) = \left(\frac{n(n-1)(2n+5)}{18}\right)\left(\frac{n}{n_e^*}\right) \tag{7.9}$$

where, $\frac{n}{n_e^*}$ represents the correlation due to correlation in time series and is calculated as:

$$\frac{n}{n_e^*} = 1 + \left(\frac{2}{n(n-1)(n-2)}\right)\sum_{i=1}^{n-1}(n-f)(n-i-1)(n-i-2)\rho_e(i) \tag{7.10}$$

where, n represents the actual sample size and n_e^* represents the effective sample size required to account for the autocorrelation factor in the data; $\rho(i)$ represents the autocorrelation function of the ranks of observations and can be calculated as :

$$\rho\ \ (i) = 2\ sin\left(\frac{\pi}{6}\rho_e(i)\right) \tag{7.11}$$

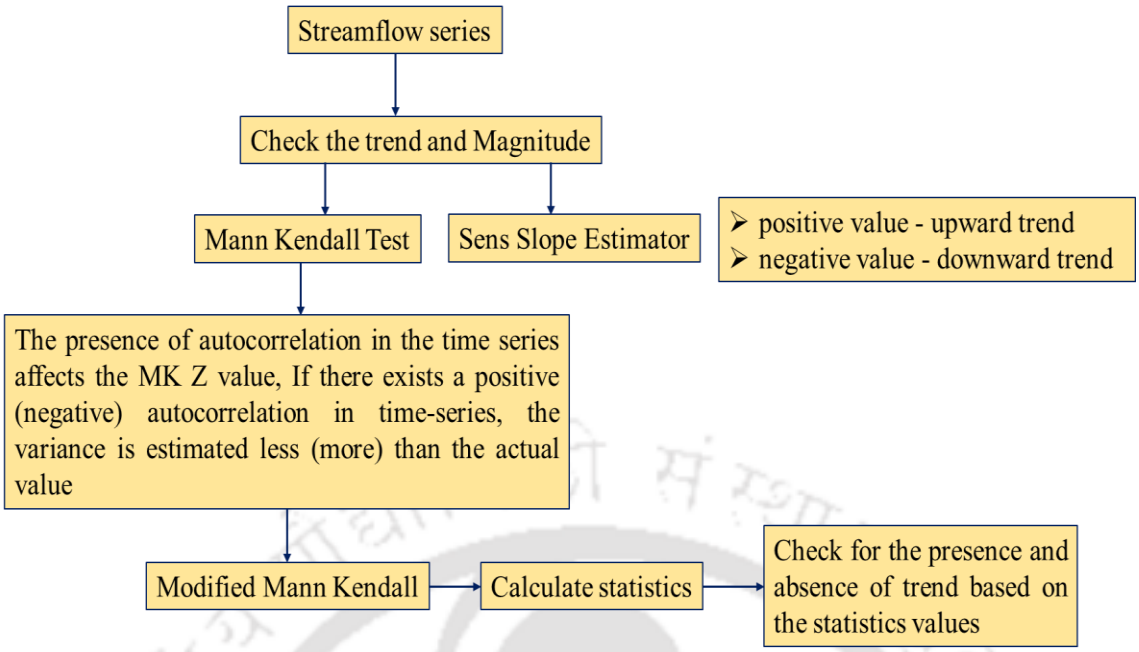

Figure 7.4: The methodological framework of the trend analysis of streamflow

7.4 Results and Discussion

For the analogue forecasts, different combinations of the number of potential analogues (N_{ana}) with different duration (D_{ana}) were performed based on the seasonal need of the forecasted observations. The performance of different combinations of D_{ana}, N_{ana} and D_f was assessed based on the correlation between the observed and hindcast anomalies, as shown in Table 7.1. Pearson correlation, r ≥0.5, significant at 10% significance level for a two-sided test was performed. The values of r ranging from 0.4 to 0.7 were considered moderately correlated (Dancey and Reidy, 2007). For a Pearson value, r ≥ 0.5, the performance of different numbers and duration of analogues were assessed by counting the total number of significant forecasts for the combinations. From our study, we found the best combination for $D_{ana} = 7$ and $N_{ana} = 5$ for the Rabi period and $D_{ana} = 4$ and $N_{ana} = 7$ for the Kharif period. For the Zaid period, the combination of $D_{ana} = 4$ and $N_{ana} = 5$ were found to be best. Therefore, considering these combinations as usable forecasts, the seasonal streamflow predictions were performed for the future period of this study in the Brahmaputra River.

Table 7.1: Significance test of various combinations based on Pearson's correlation

Sl. No	D_{ana}	N_{ana}	D_f	Significant forecast (%)	R ≥ 0.5 (%)
Comb-1	5	7	4	58	50
Comb-2	5	5	4	58	50
Comb-3	3	5	4	67	42
Comb-4	3	9	4	58	50
Comb-5	7	5	4	75*	67*
Comb-6	9	5	3	83	58
Comb-7	9	7	3	75	67
Comb-8	4	5	4	67**	42**
Comb-9	4	7	4	67***	42***
Comb-10	8	9	4	17	17

D_{ana}= 3 (Jul-Sep), 4 (Jul-Oct), 5 (May-Sep), 7 (Mar-Sep), 8 (Nov-Jun), 9(Jan-Sep)
D_f = 3 (Oct-Dec), 4 (Oct-Jan), 4 (Jul-Oct),
Best combination: * Rabi period, ** Zaid period, *** Kharif period

We found that the HA and PF method performed well in forecasting the streamflow during the Rabi, Kharif and Zaid periods, as shown in Figure 7.5. However, during the Kharif period, both methods could not capture the fluctuations in the flow of the recent past. It can be seen from Figure 7.6 that the streamflow values predicted through HA and PF were very high during the Kharif period. Therefore, to overcome the difficulties, the ANN model was applied in the study to handle the complexities accurately. The model's performance was evaluated using the mean square error (MSE). The comparison of the ANN predicted streamflow with the observed streamflow for the year 2013-2015 was good, with R^2= 0.9 (Figure 7.7). The model was then applied to predict the seasonal streamflow during the Kharif period for the period 2016-2021. The results highlight that the ANN approach effectively handled the complexities of forecasting the streamflow during the high flow period. Figure 7.6 represents the forecasted streamflow using the three methods: Historical analogue (HA), persistence forecast (PF), and artificial neural network (ANN).

On analysing the results obtained from the hydrodynamic model and categorizing the water depth corresponding to the forecasted streamflows, it was found that during the Zaid period, streamflows varied between 7818 and 15096 cumecs, and the cultivable area was found to be ~2254 ha, and ~1694 Ha, respectively. Similarly, for the Kharif and Rabi periods, the

streamflow varied between 20409 cumecs and 27104 cumecs and between 11764 cumecs and 15033 cumecs. The details of area available under 0-0.3m, 0.3-0.6m, 0.6-0.9m and dryland area for the forecasted years can be seen in Table 7.2.

Table 7.2: Area available under water depth of 0-0.3m, 0.3-0.6m, 0.6-0.9m and dryland area for the forecasted years

	Year	**2016**	**2017**	**2018**	**2019**	**2020**	**2021**
	Discharge (cumecs)	**12779**	**15096**	**7778**	**9494**	**7952**	**7818**
Zaid period	Dryland (Ha)	1688.69	1470.57	2139.23	1914.59	2120.2	2139.23
	0-0.3m (Ha)	76.53	59.56	33.27	55.64	33.69	33.27
	0.3-0.6m (Ha)	71.56	79.33	40.80	63.31	41.20	40.80
	0.6-0.9m (Ha)	72.83	84.15	41.62	52.87	42.17	41.62
	Discharge (cumecs)	**15033**	**14747**	**14616**	**13321**	**12564**	**11764**
Rabi period	Dryland (Ha)	1485.71	1549.34	1914.59	1197.71	1688.69	1721.48
	0-0.3m (Ha)	56.51	58.62	55.64	57.07	69.53	64.37
	0.3-0.6m (Ha)	78.36	87.08	63.29	108.29	71.56	68.65
	0.6-0.9m (Ha)	85.33	82.35	52.87	95.43	72.82	73.87
	Discharge (cumecs)	**27046**	**30920**	**23796**	**23656**	**21503**	**20409**
Kharif period	Dryland (Ha)	815.76	786.39	903.58	903.58	973.66	1055.07
	0-0.3m (Ha)	33.36	17.07	42.62	42.62	67.75	61.77
	0.3-0.6m (Ha)	42.73	27.03	78.82	78.82	101.41	102.84
	0.6-0.9m (Ha)	54.17	32.03	95.56	95.56	102	114.37

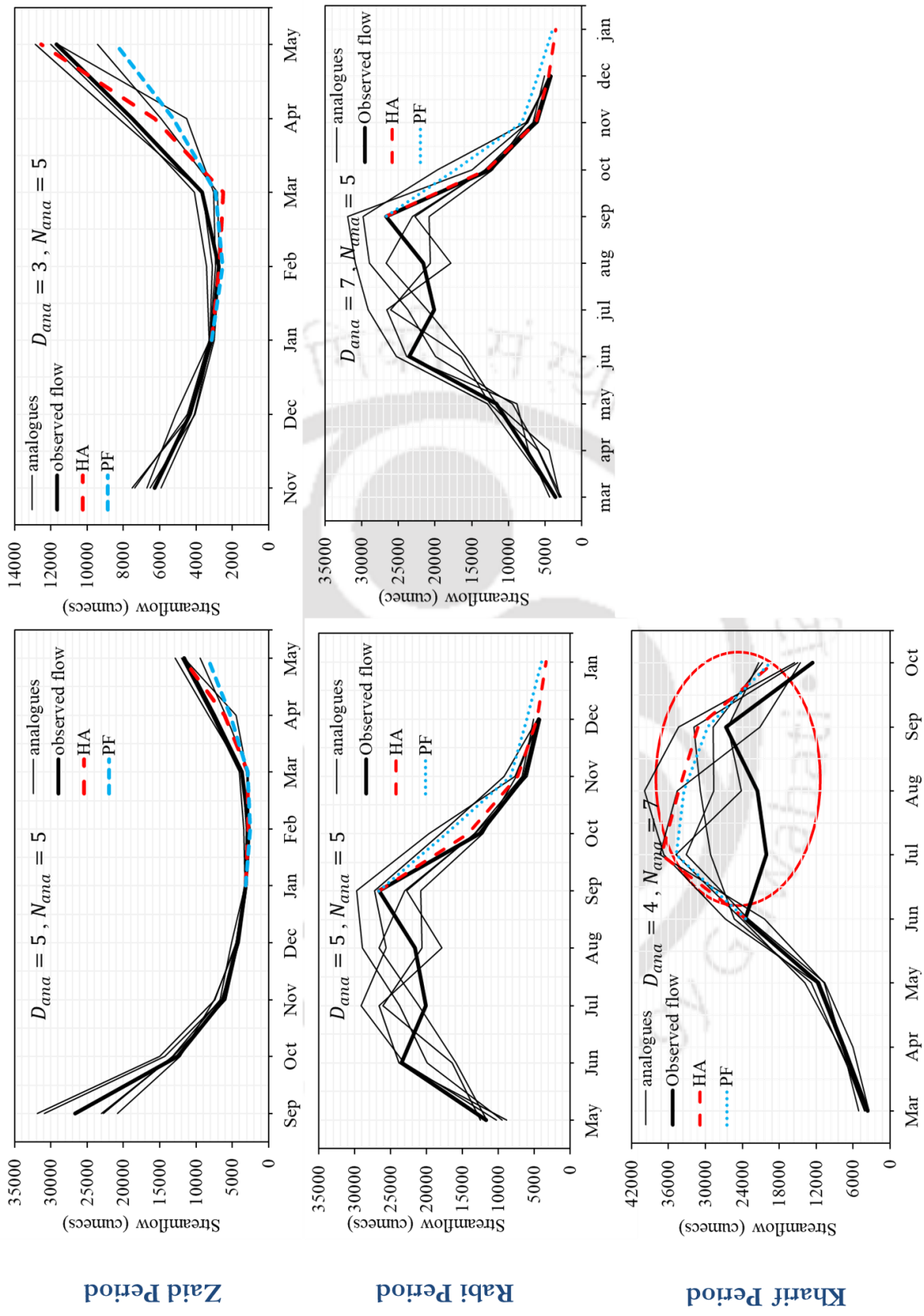

Figure 7.5: Seasonal streamflow forecasting using the Historical analogue (HA) and Persistence forecasts (PF) methods under different combinations of D_{ana} and N_{ana} for all three seasons Zaid, Rabi and Kharif.

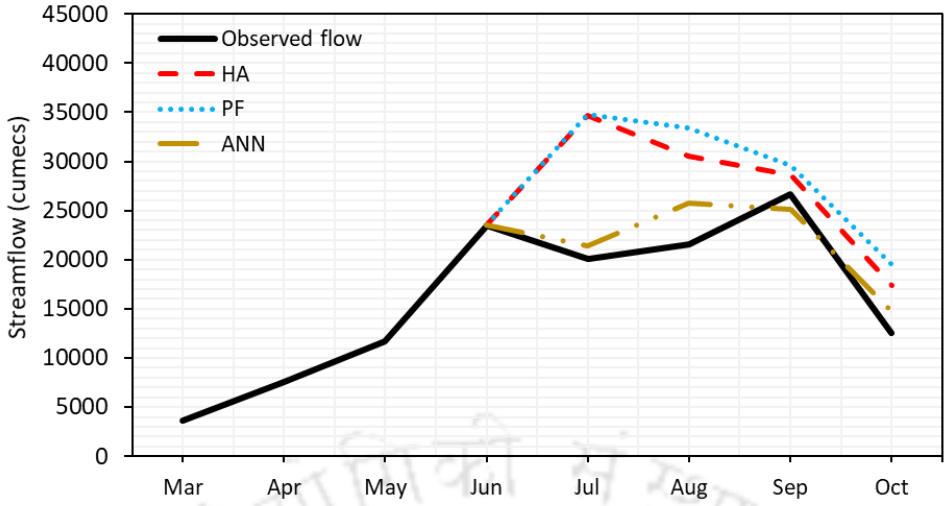

Figure 7.5: Streamflow forecasting for the Kharif period using ANN and comparison with historical analogue (HA) and persistence forecast (PF) methods.

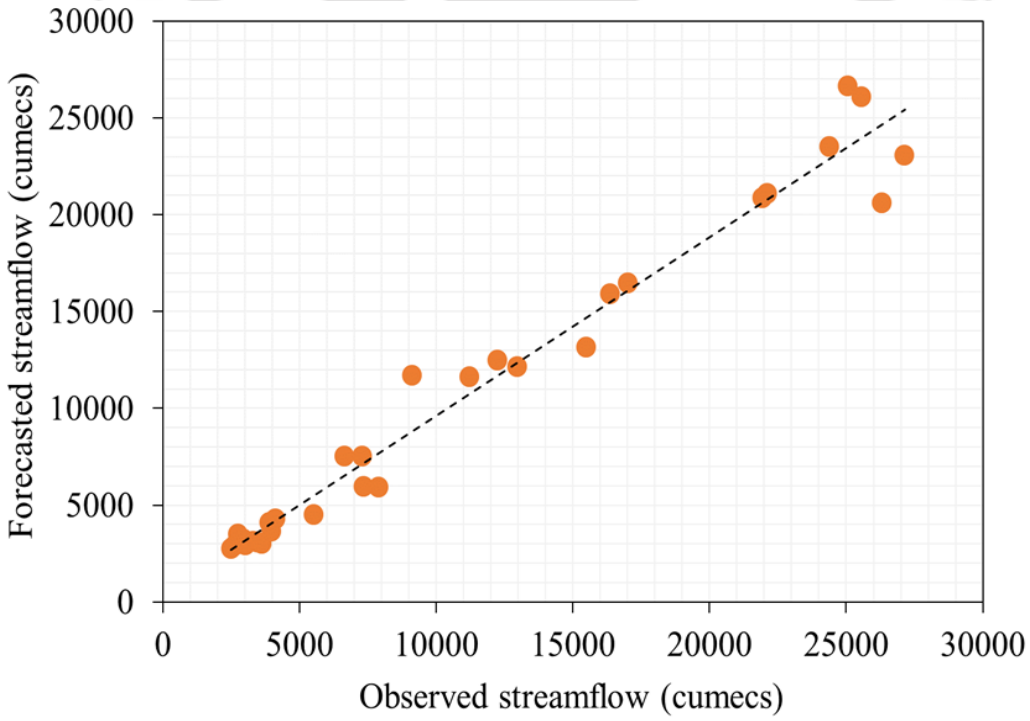

Figure 7.6: Plot of observed and forecasted streamflow using ANN for the period 2013-2015

The results obtained from the monthly streamflow trend analysis study have been presented in Table 7.3. From the study, a significant rise in streamflow during the month of December till February can be seen. This time period corresponds to the low flow in the river, which tends to show an increase in the streamflow. The streamflow for June - November has shown a downward trend though it is non-significant at a 5% significance level. This corresponds to the high flow period witnessed at the Pandu station in the Brahmaputra River. The highest rate of the significant increasing trend was observed in the month of February (+69.41 m^3/s/year). The highest rate of non-significant increasing and a decreasing trend was observed during the months of March (+100.35 m^3/s/year) and (September (-240.69 m^3/s/year), respectively. The trend observed for the annual time series of the observed data was found to be a non-significant increasing trend. Figure 7.8 shows the minimum and maximum streamflow trends observed during the study.

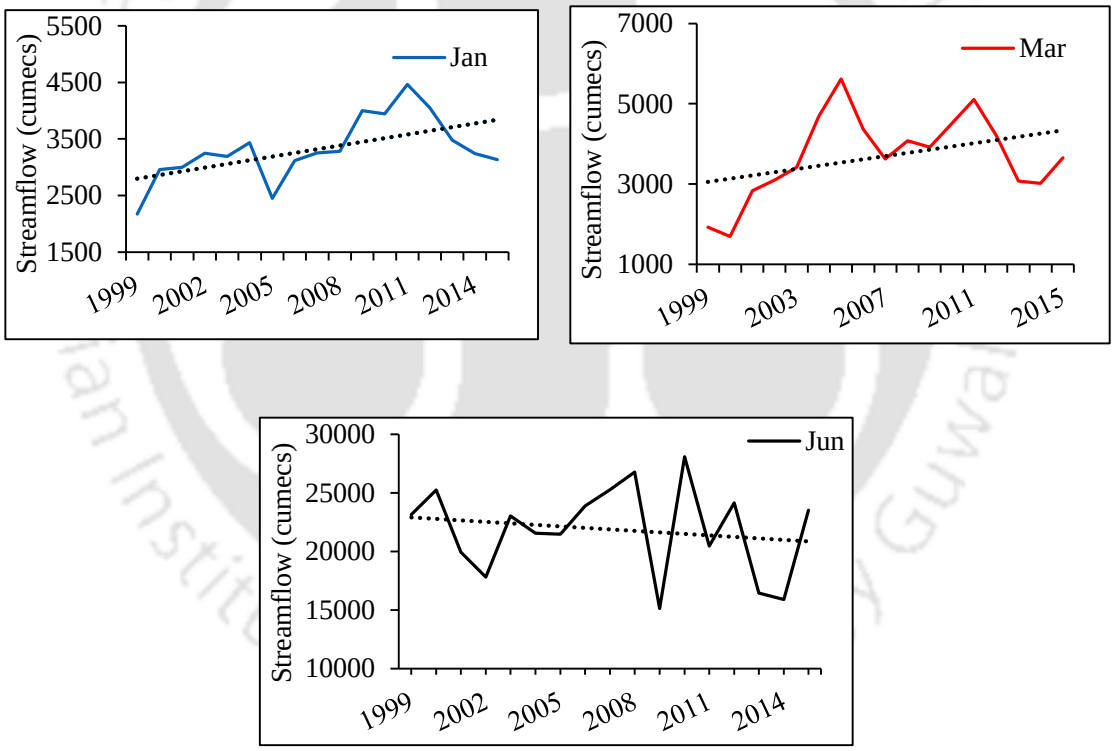

Figure 7.7: Trends in the minimum and maximum streamflow.

Table 7.3: Mann-Kendall test static (Z) and Sen's slope estimator (SS) for different months of streamflow time series

	Jan	Feb	Mar	Apr	May	Jun	Jul	Aug	Sep	Oct	Nov	Dec
Z statistic	3.48*	2.75*	0.882**	0.617**	1.27**	-0.25***	-0.62***	-0.37***	-0.71***	-1.27***	-0.78***	0.535*
p-Value	0.0119	0.005	0.201	0.536	0.201	0.836	0.536	0.71	0.483	0.201	0.433	0.592
SS	64.18	69.4	100.3	58.24	99.57	-78.54	-191.66	-161.46	-240.69	-188.81	-43.95	17.01

*Significant (positive trend) at 5% significance level, **non-significant (positive trend) at 5% significance level, ***non-significant (negative trend) at 5% significance level

7.5 Conclusions

The study demonstrated the usefulness of short-term flow forecasting in deriving optimal agricultural planning in a riverine ecosystem. GIS environment effectively assessed the land area availability of specified crops under different seasons and depth classes.

Following are the key conclusions derived from the study:

1. The seasonal forecasts were helpful in farmers' decision-making process as it predicted the expected streamflow in the near future. The HA and PF forecast methods contain the historical information of the recent past event and use that information to predict the short-term flow. Hence, the seasonal cycle is preserved in the forecast. ANN, being an AI-based technique, could train the model reasonably and provide good results for the high flows.
2. The results from the trend analysis indicate the importance of trend analysis for practicing cropping and farming activities in a riverine ecosystem. The trends in the streamflow could be beneficial before planning such activities, and forecasted streamflows could be incorporated in assessing the risk of agriculture practice and minimizing the damage.
3. The findings of the study showed that the knowledge of both forecasting and optimization together could deal with the near future events in the agricultural sector accurately, which in turn could help tackle the associated damages and provide a judgment of selective cropping in such a riverine environment. The model framework and solution methods could be applied to other regions with similar challenges.

8

Optimization model for land-use planning

8.1 Introduction

Increased urbanization has led to diminished land for agricultural activities. To meet the increasing demand for food, agricultural production needs to be increased. Over 113 million people in 53 countries are suffering from acute hunger because of conflict and food insecurity, climatic shock, and economic turmoil (FSIN 2020). Accordingly, many researchers have emphasized that water, energy, and food are under stress, and their demand will increase significantly in the upcoming decades (El-Gafy et al., 2017; Endo et al., 2015). According to an assessment by the United Nations Convention to Combat Desertification (UNCCD), urbanization would result in the loss of 1.5-3.3 million hectares of agricultural land between 2000 and 2030. The proportion of the global population living in cities is estimated to increase by around 2.5 billion in 2050, with built-in areas expanding towards fertile soils and farmland. The loss of these valuable croplands would result in a production loss, leading to a global food shortage. Therefore, agriculture needs to be displaced to other favorable locations and riverine sandbars could be considered as potential landmasses. These sandbars provide fertile land that supports agriculture and farming practices and provides livelihood opportunities to marginalized communities. Agriculture, a prime user of land and water resources, is essential for food production (Sadeghi et al., 2020), and its sustainability requires efficient management of these resources (Garg and Dadhich, 2014). The competition for these resources in different sectors drives the need to improve crop productivity for current and future demand. These demands can be achieved by either increasing the cultivation area or increasing the crop yield per area (Singh and Panda, 2012). In addition, the optimum usage of existing land

and water resources is essential to sustainably meet the increasing demands for food, water, and energy (Barik et al., 2017; Singh, 2012).

Optimization being an important tool for judicious crop planning, has been proposed by various researchers in studies of land allocation (Sethi et al., 2006), irrigation (Huang et al., 2012; Mahmoodi and Rafiee, 2020), water allocation (Raju and Kumar, 1999; Guo et al., 2014), and reservoir operation planning (Kumari and Mujumdar, 2017). The traditional approaches of optimization employed in optimal cropping patterns are linear programming (LP), nonlinear programming (NLP), and dynamic programming (DP). Evolutionary algorithms (EA) and multiobjective programming (MOP) have also been extensively applied to a different class of problems, such as deficit irrigation (Ganji et al., 2006), cropping patterns (Sarker and Ray, 2009; Zeng et al., 2010), water resource systems (Sulis and Sechi, 2013), irrigation planning (Anwar and Haq, 2013), and economic optimization (Groot et al., 2012). Linear Programming (LP) models require less computation time for computing global optimal solutions among all the models. These models can effectively solve the optimal decision-making process problems (Cai et al., 2018). Linear programming techniques have also been used extensively when both objective function and constraints are linear with easy formulations and application (Daghighi et al., 2017). At the same time, nonlinear programming problems need rigorous mathematical computations involving high computation time (Singh, 2012), and dynamic programming problems are unable to provide optimal global solutions (Ming et al., 2015). Multi-objective optimization approaches offer opportunities for land-use planning under different dimensions of sustainability. It involves finding all optimal land-use configurations under conflicting objectives with a certain set of constraints.

Crop planning involves several possible and valuable objectives, which may or may not conflict with each other. A choice of judicious cropping pattern and temporal adjustments therein may be a useful strategy to minimize the possible crop damages and maximize economic returns and productivity. Traditional Linear Programming (LP) has been widely used in decisions relating to crop area; however, in actual planning problems, certain goals and constraints, along with the coefficients, may not be precisely defined. This uncertain information in the crop planning system is inevitable and may not be tackled through traditional approaches. The decision problems contain uncertainties, which need to be addressed in an "approximately equal to" or "approximately satisfactory" way. Therefore, fuzzy objective functions and fuzzy constraints would be appropriate ways to address such

cases. For fuzzy programming, the uncertain parameters are considered fuzzy numbers, described by fuzzy membership functions (Wang et al., 2015). Various researchers have considered the fuzzy multiobjective linear programming (FMOLP) problems by defining the membership functions of objective functions and constraints, which deals with the fuzziness of the decision-makers (DM) aspirations (Regulwar and Gurav, 2012; Li et al., 2017). Due to accelerated urbanization, the agricultural mainland has been shrinking, which could lead to a serious food crisis in the near future. Therefore, we believe that a riverine environment, particularly sandbars, that emerge within the river because of the morphological processes, is fertile and provides adequate landmass for agricultural and farming activities. The uncertainties associated in the agricultural system could be handled through optimization approaches to planning optimal cropping patterns. This enables decision-makers to plan the cropping pattern ahead of time, decreasing crop losses and damage.

8.2 Study area

To develop the optimization framework and carry out the optimization process, two sandbars were considered in the districts of Barpeta and Kamrup. The details about the study area have been described in Section 3.2. Figure 8.1 and figure 8.2 shows the study sites selected for performing the optimal cropping pattern under different scenarios.

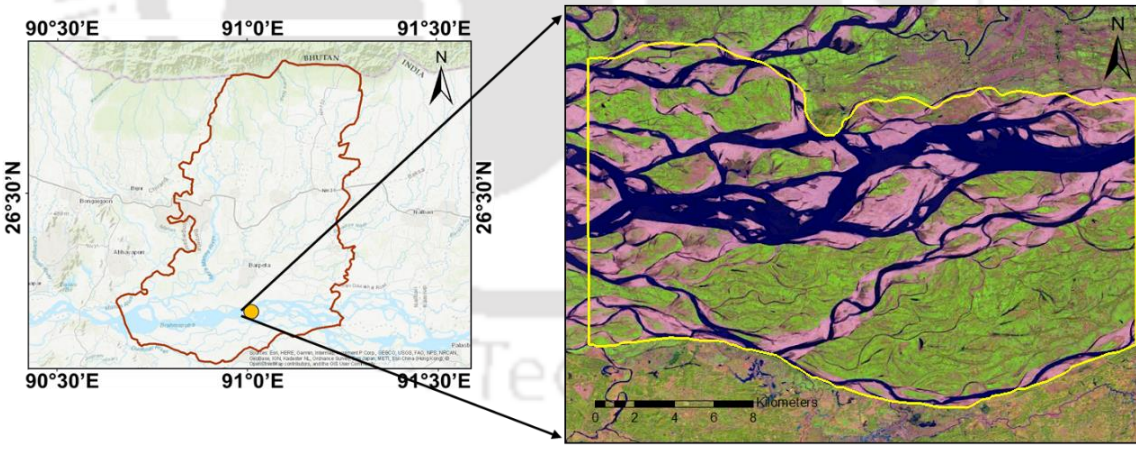

Figure 8.1: Study site-1: Sandbar developed in the Barpeta District, Assam

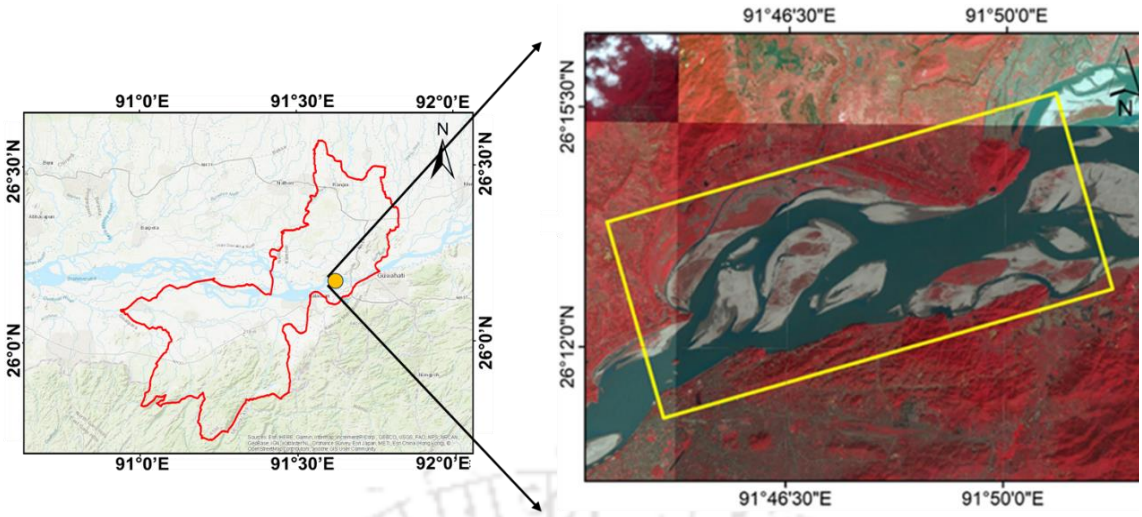

Figure 8.2: Study site-2: Sandbar developed in the Kamrup District, Assam

8.3 Model formulation

In the agriculture sector, the farmers allocate multiple resources such as land and water to meet the targets for cultivating a variety of crops under different periods. Their primary objective being maximizing net benefit and increasing crop production to sustain livelihood. Therefore, they plan to cultivate the crops according to their food demand, seasonality, and self-sufficiency. Before using an optimization problem in solving complex activities, the primary task is formulating the problem. The process begins by identifying the decision variables and then developing the objective function with certain constraints. The final task entailed setting some variable bounds to the problem. Linear programming models can very well handle these problems in optimal decision-making. Therefore, a constrained LP model was developed under a set of constraints and objective functions. However, in actual panning practice, several factors and parameters, such as market prices, crop yield, food demand, and cost of cultivation are fraught with uncertainties that could not be expressed as deterministic values. Therefore, these uncertainties were addressed by further developing a fuzzy linear programming model to address the multiple objectives under the fuzzy environment.

Three aspects of optimal cropping patterns were considered. The first aspect compares the existing cropping pattern in the Barpeta district with the optimal cropping pattern derived from the linear programming model. The second aspect involves developing a constrained linear programming problem to determine the optimal cropping pattern by considering the fluctuating water level in the riverine sandbar of the Kamrup district with the objective of

maximizing the economic benefit. The third aspect deals with determining the optimal cropping pattern to maximize crop production and net economic benefit under fluctuating water levels with consideration of the uncertainties existing in the crop planning system.

8.3.1 Complexities in determining land availability

The riverine ecosystem is under continuous change, and so is the land-use pattern. Availability of agricultural land mass within a river depends on the flow pattern, seasonality, location, and other anthropogenic factors like the bridge, river training works, etc. Also, the suitability of the soil depends on the particle size and nutrient richness. Therefore, determining an optimal cropping pattern, that too by considering various other sandbar-dependent economic activities inclusively, is a highly challenging task. The emergence and submergence of sandbars are of concern for practicing any agricultural activities. With the increase in water level, the cultivable area decreases, demanding selective crop cultivation during different seasons. Some varieties of crops can resist high water levels, and some cannot. Determining the optimal cropping pattern is, therefore, more complex in sandbars. Thus, considering these complexities, the optimization problem was formulated. The selection of crops during different seasons was based on their suitability and seasonal variability. Rice being the most preferable and suitable crop for cultivating in all three seasons, the maximum area was allocated to paddy cultivation. Maibangsa et al. (2015) evaluated the growth and yield of different crops in the Brahmaputra sandbars. They found that vegetables such as knolkhol, potato, lentil, garlic, and brinjal gave higher yield as compared to tomato, pumpkin, carrot, beans, etc. In a study conducted by Hossain et al. (2013) in the floodplains of Bangladesh, the researchers found that farmers cultivate different local varieties of rice, namely Boro rice in the dry season and Amon rice in the wet season. In their study, Robinson et al. (2016) found that seasonal variability in vegetation also affects livestock movements. Sandy loam soils were considered favourable for crops like Gram, Tur, peas, etc. and loamy and silty soils were favourable for Linseed, vegetables, Jute, etc. Depending on these conditions and considering the input received from indigenous sand bar cultivators, the limiting values for land availability for different crops in different seasons were determined, and land availability constraints were set accordingly in the model. The practice of cropping during different seasons along with the duration and favourable soil type, has been presented in Table 8.1.

Table 8.1: Crop calendar of major crops grown in the Barpeta district (https://barpeta.assam.gov.in/)

Crops	Type	Jan	Feb	Mar	Apr	May	Jun	Jul	Aug	Sep	Oct	Nov	Dec
Rice (Boro)	Early Kharif												
Rice (Ahu)	Summer												
Rice (Sali)	Kharif												
Rice(Bao)													
Wheat	Rabi												
Black gram	Summer												
	Kharif												
Green gram	Summer												
	Kharif												
Lentil	Rabi												
Rape-Mustard	Rabi												
Potato													
Jute	Kharif												
Vegetables													

8.3.2 Estimation of model inputs

(a) Constrained Linear Programming (LP)

The crop activity calendar was divided into three seasons: (i) Rabi (Oct-Jan), (ii) Zaid (Jan-May), (iii) Kharif (May-Oct). The objective function and the constraints formulated for the purpose are presented below:

Objective Function: A key objective in selecting the optimal combination of activities was to maximize the profit.

$$Maximize\ Z = \Sigma_{j=1}^{n}\Sigma_{i=1}^{m}\{(Y_{ij}.MP_{ij}) - CC_{ij}\}X_{ij} \quad (8.1)$$

where, Z= net annual benefit (Rs), Y_{ij}= Yield from i^{th} activity during j^{th} season (Kg/Ha), MP_{ij} = market price of i^{th} activity during j^{th} season (Rs/Kg), CC_{ij} = cost of cultivation or production for i^{th} activity during j^{th} season (Rs/Ha), X_{ij} = Area under i^{th} activity during j^{th} season (Ha), i= activity index, j= season index (1, 2, 3), m = Total activities, n = Total seasons.

The maximization of the objective function was subjected to the following constraints.

(a) Land Area constraint: The land area allocated to activities during different seasons in a year should be less than or equal to the total area available in all seasons.

$$\Sigma_{j=1}^{n}\Sigma_{i=1}^{m}X_{ij} \leq TA_j\ ; \qquad \forall\ i,j \quad (8.2)$$

where, TA_j = Total available area during j^{th} season,

(b) Food demand constraint: The production from various activities during different seasons should be greater than or equal to total demand or food requirements. The demand for food depends on the population, market reach, and export potential. Thus, it varies during different seasons and according to the need.

$$\left(Y_{ij}.X_{ij}\right) \geq Dij\ ; \qquad \forall\ i,j \qquad (8.3)$$

where, D_{ij} = Demand of i^{th} activity during j^{th} season

(c) Overlapping constraint: This constraint is applicable where the land area of one activity is overlapped during corresponding seasons. Practically, this means if an activity considers two seasons during its entire growth period, then the land area remains confined to the activity of the first season only and cannot be utilized in the next season.

$$X_{ij(1)} - X_{ij(2)} - X_{ij(3)} = 0 \qquad \forall\ i,j \qquad (8.4)$$

(d) Crop Area constraints: Assigning minimum and maximum land area depending upon the existing area.

$$\mu_{ij}^{min} EA_{ij} \leq X_{ij} \leq \mu_{ij}^{max} EA_{ij} \qquad \forall\ i,j \qquad (8.5)$$

where, μ_{ij}^{min} = Fraction to which existing area can be decreased, μ_{ij}^{max} = Fraction to which existing area can be increased, EA_{ij} = Existing area (Ha)

(e) Non-negativity constraints

$$Xi \geq 0 \qquad (8.6)$$

While formulating the problem, crop yield, cost of cultivation/ cost of production, and the market price of commodities were considered. The crop yield was calculated by dividing the production by the cultivated area. The data were collected from various primary and secondary sources, as discussed in Section 3.3, and have been used in the optimization framework. The information on the cost of cultivation/production for various activities has been provided in Table ST3 (Appendix).

(b) Constrained Linear Programming (LP) considering the water depth scenarios

In riverine environments, the water level fluctuation affects the cropping pattern. Therefore, the cropping pattern should be planned such that the crops are not affected entirely, and land areas are not left barren. The primary objective of this framework was to optimize the cropping pattern without compromising the constraints such as land area, food demand, and production. While developing the model, the land allocation during different seasons

was taken as the decision variable dependent on the streamflow parameter. The streamflow values were simulated through the hydrodynamic model, determining the water depth, as discussed in Chapter 5. The water depth was then categorized into different classes, and the area under each category was calculated.

In the agriculture sector, the farmers allocate multiple resources, such as land and water to meet the targets for cultivating a variety of crops under different periods. The primary objective being maximizing net benefit and increasing crop production to sustain livelihood. Therefore, they plan to cultivate the crops according to their food demand, seasonality, and self-sufficiency.

The generalized mathematical expression of the optimization model can be defined as follows:

Objective 1: Maximization of agricultural economic benefit

$$Max\ f_1 = \Sigma_{j=1}^{J}\Sigma_{i=1}^{I}\left\{\left(\left(Y_{ij}.MP_{ij}\right) - CC_{ij}\right)X_{ij}\right\} \quad (8.7)$$

Objective 2: Maximization of crop production

$$Max\ f_2 = \Sigma_{j=1}^{J}\Sigma_{i=1}^{I}\{Y_{ij}.X_{ij}\} \quad (8.8)$$

where, i= activity/crop type, j= seasons, Y_{ij}= yield from i^{th} activity during j^{th} season (Kg/Ha), MP_{ij} = Market price of ith activity during j^{th} season (Rs/Kg), CC_{ij} = Cost of cultivation or Production for i^{th} activity during j^{th} season (Rs/Ha), X_{ij} = Area under i^{th} activity during j^{th} season (Ha), the decision variable, I = Total activities, J = Total season. f_1 and f_2 are the objective functions.

The above objective functions were subjected to the following constraints.

Constraint 1: Sowing Area constraint. The sowing area allocated to different crops/activities should be less than or equal to the total cultivable area (TA) available in different seasons.

$$\Sigma_{j=1}^{J}\Sigma_{i=1}^{I}X_{ij} \leq TA_j\ ; \quad \forall\ i,j\ , \quad i = 1,2,3\ldots I; \quad j = 1,2,3 \quad (8.9)$$

Constraint 2: Food demand constraint. During different seasons, the production from various crops/activities should not be less than the food demand (D).

$$\left(Y_{ij}.X_{ij}\right) \geq Dij\ ; \quad \forall\ i,j, \quad i = 1,2,3 \ldots I; \quad j = 1,2,3 \tag{8.10}$$

Constraint 3: Area under defined water depth scale constraint. This constraint was developed based on the fluctuations in the land area due to changing water depth under different streamflow. As the water level fluctuates in different months and seasons, the area under *p*, *q*, *r*, and *dryland* changes.

$$\begin{aligned}
\Sigma_{j=1}^{J}\Sigma_{i=1}^{I}X_{ij}^{p} \leq TA_j^{p}; \forall\ i,j, \quad i = 1,2,3 \ldots I; \quad j = 1,2,3; \\
\Sigma_{j=1}^{J}\Sigma_{i=1}^{I}X_{ij}^{q} \leq TA_j^{q}; \forall\ i,j, \quad i = 1,2,3 \ldots I; \quad j = 1,2,3; \\
\Sigma_{j=1}^{J}\Sigma_{i=1}^{I}X_{ij}^{r} \leq TA_j^{r}; \forall\ i,j, \quad i = 1,2,3 \ldots I; \quad j = 1,2,3; \\
\Sigma_{j=1}^{J}\Sigma_{i=1}^{I}X_{ij}^{dry} \leq TA_j^{dryland}; \forall\ i,j, \quad i = 1,2,3 \ldots I; \quad j = 1,2,3;
\end{aligned} \tag{8.11}$$

Constraint 4: Overlapping constraint: This constraint would be applicable where the land area of one activity gets overlapped during corresponding seasons. Practically, this means if an activity/crop takes two seasons during its entire growth period, then the land area would be allotted to the crop cultivated in the first season and cannot be utilized during the next seasons.

$$X_{ij(1)} - X_{ij(2)} - X_{ij(3)} = 0 \qquad \forall\ i,j \tag{8.12}$$

Constraint 5: Allowable area constraints. This constraint assigns minimum and maximum land area to the crops/activities during different seasons.

$$X_{ij} \leq\ X_{ij\,max}\ ;\ X_{ij} \geq\ X_{ij\,min} \tag{8.13}$$

*Constraint 6: Non-Negativity constr*aints

$$Xi \geq 0; TA_j \geq 0; Dij \geq 0; \quad i = 1,2,3..I; j = 1,2,3 \ldots J \tag{8.14}$$

(c) Inexact multiobjective Fuzzy Linear Programming (IMOFLP)

The constrained LP approach can effectively address the agricultural cropping pattern problems and associated constraints. However, uncertainties such as market prices, crop yield, food demand, cost of cultivation, etc., may exist in the system. This could affect the decision-making process in many real-world situations. Therefore, such uncertainties expressed as interval numbers, fuzzy objectives, and constraints can be solved using the IMOFLP approach. The IMOFLP approach is an integration of inexact linear programming (ILP), multiobjective linear programming (MOLP), and fuzzy programming (FP) (Li et al., 2017), defined as:

$$Max\ f^{\pm} \cong C^{\pm}X^{\pm}$$
$$s.t.\ A^{\pm}X^{\pm} \lessapprox / \gtrapprox b^{\pm} \quad (8.15)$$
$$X^{\pm} \geq 0$$

where, symbols ± denotes interval numbers and + and – represent upper and lower bounds, respectively. ≅ represents the fuzziness associated with the objectives and constraints.

The membership functions for fuzzy objectives can be defined as follows:

For maximizing objectives,

$$\mu_l(f_L) = \begin{cases} 0, & C_lX \leq L_l \\ \frac{C_lX - L_l}{U_l - L_l}, & L_l < C_lX < U_l \\ 1, & C_lX \geq U_l \end{cases} \quad (8.16)$$

For minimizing objectives,

$$\mu_k(f_K) = \begin{cases} 1, & C_kX \leq L_k \\ \frac{U_k - C_kX}{U_k - L_k}, & L_k < C_kX < U_k \\ 0, & C_kX \geq U_k \end{cases} \quad (8.17)$$

where, μ_l and $\mu_k$is the membership function of the L^{th} and K^{th} objective function, respectively. L and U are the lower limits and upper limits for the fuzzy goal. C is the coefficient of the objective function.

The membership functions for constraints are as follows:

$$\mu_i(X_i) = \begin{cases} 1, & A_iX \leq b_i \\ \frac{b_i + d_i - A_iX}{d_i}, & b_i < A_iX < b_i + d_i \\ 0, & A_iX \geq b_i + d_i \end{cases} \quad (8.18)$$

$$\mu_j(X_j) = \begin{cases} 1, & A_jX \geq b_i \\ \frac{A_jX - (b_j - d_j)}{d_j}, & b_j - d_j < A_jX < b_j \\ 0, & A_jX \leq b_j - d_j \end{cases} \quad (8.19)$$

where, the subscripts "i" and "j" are for constraints with $\leq$ and $\geq$ symbol. $\mu_i(X_i)$ and $\mu_j(X_j)$ are the membership functions of the fuzzy constraints. d_i and d_j are the maximum allowable deviation from b_i and b_j, respectively. Figure 8.3 illustrates the membership function for the objective function and the constraints in the IMOFLP approach.

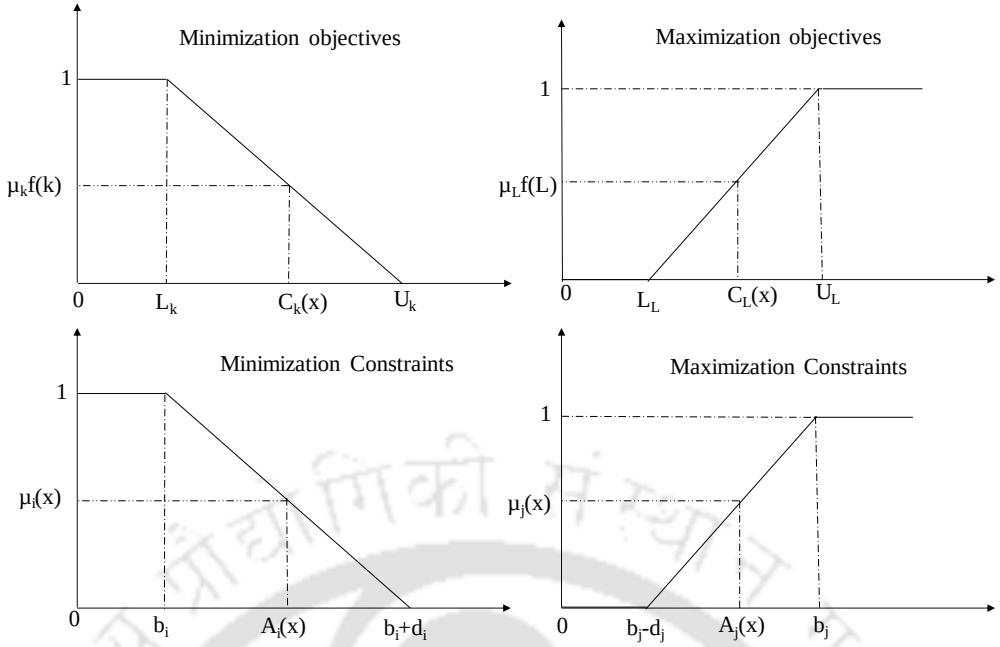

Figure 8.3: Fuzzy membership functions for objective functions and constraints

Therefore, the IMOFLP model can be formulated as:

$$Max\ f_k^{\pm}(X^{\pm}) = C_k^{\pm}X^{\pm} \cong f^{*\pm} \quad (8.20)$$

$$s.t.\ A_i^{\pm}X^{\pm} \cong b_i^{\pm}$$

$$A_j^{\pm}X^{\pm} \cong b_j^{\pm}$$

$$X^{\pm} \geq 0$$

According to the membership functions of the fuzzy objectives and fuzzy constraints, a fuzzy operator (λ) was introduced, which defines the overall satisfaction level of the system. The λ varies over a scale of 0 to 1, with 0 indicating no satisfaction and 1 indicating complete satisfaction. f^* denotes the fuzzy goals of the objective functions. The objective function for maximization of λ for the IMOFLP model was defined (Zimmermann, 1978) and expressed as follows:

$$Max\ \lambda^{\pm}$$

$$f_k^{\pm}(X^{\pm}) \geq C_k^{\pm}X^{\pm} \cong L_l^{\pm} + \lambda^{\pm}(U_l - L_l)$$

$$A_i^{\pm}X^{\pm} \leq (b_i^{\pm} + d_i) - \lambda^{\pm} d_i$$

$$A_j^{\pm}X^{\pm} \leq (b_j^{\pm} - d_j) + \lambda^{\pm} d_j \quad (8.21)$$

$$X^{\pm} \geq 0$$

$$0 \leq \lambda^{\pm} \leq 1$$

As suggested by Wu and Huang (2007), a single value of $\lambda^{\pm}$ may not function consistently for all objective functions; therefore, two separate operators ${\lambda_1}^{\pm}$ and ${\lambda_2}^{\pm}$ were introduced. ${\lambda_1}^{\pm}$ was assigned to ≤ constraints and ${\lambda_2}^{\pm}$ was assigned to ≥ constraints. Therefore, the equation was transformed as follows.

$$
\begin{aligned}
&Max\ \omega_1 {\lambda_1}^{\pm} + \omega_2 {\lambda_2}^{\pm} \\
&{f_k}^{\pm}(X^{\pm}) \geq {C_k}^{\pm} X^{\pm} \cong {L_l}^{\pm} + {\lambda_2}^{\pm} (U_l - L_l) \\
&A_i{}^{\pm} X^{\pm} \leq (b_i{}^{\pm} + d_i) - {\lambda_1}^{\pm} d_i \\
&A_j{}^{\pm} X^{\pm} \geq (b_j{}^{\pm} - d_j) + {\lambda_2}^{\pm} d_j \\
&X^{\pm} \geq 0 \\
&0 \leq {\lambda_1}^{\pm},\ {\lambda_2}^{\pm} \leq 1
\end{aligned}
\qquad (8.22)
$$

Where, ω_1 and ω_2 are the weight coefficients. The above equation was then transformed into two sub-models and solved accordingly.

8.3.3 Selective cropping approach

Determining an optimal cropping pattern by considering various other sandbar-dependent economic activities inclusively is a highly challenging task in a riverine ecosystem. The availability of agricultural land depends on the flow pattern, streamflow magnitude, seasonality, location, and other anthropogenic factors like bridges, river training works, etc. The emergence and submergence of sandbars are of concern for practicing any agricultural activities. With the increase (decrease) in water level, the cultivable area decreases (increases), demanding selective crop cultivation. The information on agricultural farming systems and seasonal variation of crop growth and yield concerning different flooding depths can be found in the literature (Oladosu et al., 2020). For the present work, the selection of crops was such that they could survive up to a certain water level and be normal or submergence tolerant varieties. The details of some of the flood resistance and submergence tolerant varieties of crops can be found in Appendix (Table ST4). For the present study, the water depth calculated was categorized into different stages, i.e., water levels varying between 0-0.3m (p-stage), 0.3-0.6m (q-stage), 0.6 to 0.9m (r-stage), and in the dryland region as shown in Figure 8.4. The maximum water depth under no damage scenario for crop planning was considered 0.9m and termed as optimal depth ($d_{optimal}$). When the water level is at a 0.9m, all crops cultivated in areas ranging from 0-0.9m depth do not suffer any damage. This is because the crop planning is such that submergence

tolerant varieties of crops are also grown in this cropping approach. As the water level rises or lowers, the crops will be affected likewise. At optimal depth, the crops and activities planned in the dryland area also do not suffer damage, i.e., this condition can be considered an optimal condition for cultivating different crops at the defined water depth scales. However, the area under each depth scale changes, and correspondingly, the cropping pattern also changes under seasonal fluctuations. Although a depth of 0.9m has been selected for the present study, any depths could be considered depending on the need, location, crop varieties, etc.

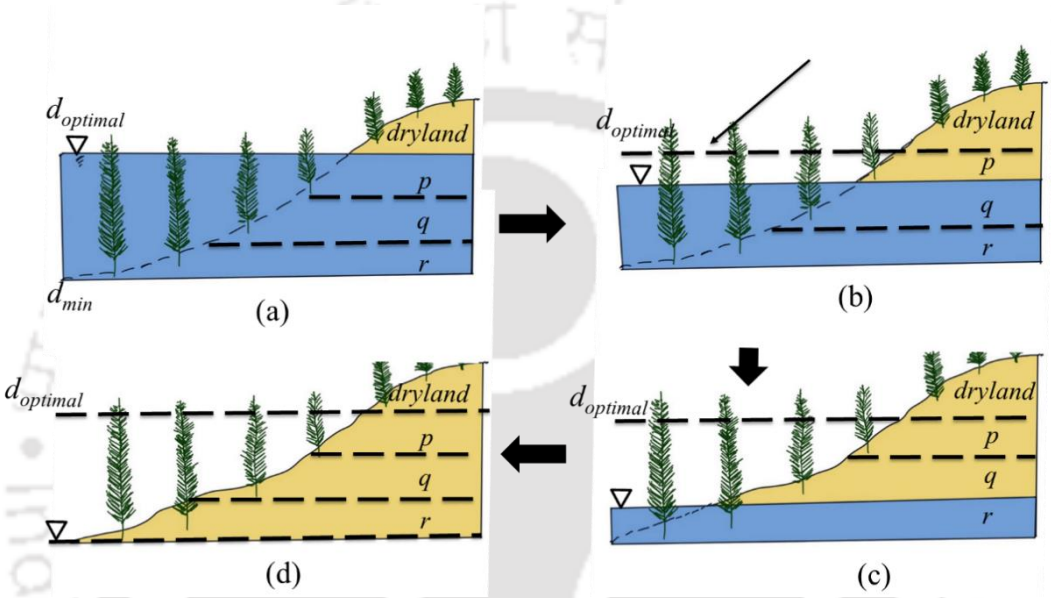

Figure 8.4: A schematic illustration of different stages of water level variability and area available in riverine sandbars. Crops incur damage as the water level rises/falls between optimal depth ($d_{optimal}$) and minimum depth (d_{min}) at various phases, resulting in economic loss.

8.4 Crop type and crop information

In India, the cropping season is mainly divided into Kharif (July-October) and Rabi (October-January). The crops grown between February/March till May/June are called Zaid crops. Crops like rice, wheat, barley, maize, oilseeds, jute, vegetables, potato, tuber crops, fibers, etc., are abundantly grown. In addition, cropping activities are conducted all year round in the state of Assam. A different class of farmers practices sandbar cultivation, and the type of crops grown and pattern of cropping varies among them. It was obtained from the survey that certain class of farmers do not prefer cultivation throughout the year and keeps the land fallow to regain the soil nutrients for increased productivity for the next season. In Assam, rice being the dominant food consumed by most people, a significant share of the land is occupied for paddy cultivation. However, with the increase in scientific

developments towards agriculture, various flood-tolerant and submergence tolerant varieties of crops, including paddy, maize, wheat, jute, etc., are available. Table 8.2 shows the practice of cropping during different seasons along with the duration and favourable soil type.

Table 8.2: Agriculture activities carried in Barpeta District along with favorable soil type and crop duration required.

Group	Crops/Activities	Season	Crop Duration	Favorable Soil type
Rice (63%)*	Autumn Rice (Ahu)	Mar-Jun	110-120	silty clayey
	Winter Rice (Sali)	Jun-Nov	140-160	silty clayey
	Summer Rice (Boro)	Nov-May	160-180	silty clayey
Pulses (4%)	Gram	Aug-Nov	60-80	sandy loam
	Tur (Arhar)	Apr-Sep	60-85	sandy loam
	Mug (Green Gram)	Feb-may	65-80	sandy loam
	Masur	Oct-Apr	60-80	sandy loam
	Black Gram	Aug-Dec; Feb-Apr	65-85	sandy loam
	Peas	Sep-Dec	100-120	sandy loam
Fibers (3%)	Jute	Mar-Sep	160-180	loam-sandy loam
	Mesta	May-Sep	145-160	loam-clayey loam
Cereals (5%)	Wheat	Jan-May ; Nov-Apr	110-125	loam-clayey loam
	Maize	Jan-May ; Sep-Jan	110-150	sandy-sandy loam
Oilseeds (10%)	Sesame	Jul-Oct	90-120	sandy loam
	Mustard	Oct-Feb	90-120	sandy
	Linseed	Oct-Feb	130-135	loamy
Others (15%)	Potato	Oct-Jan	80-120	sandy loam- loam
	Dairy	Pre and Post monsoon	-	sandy/loamy/silty
	Vegetables	Oct-Jan	80-110	sandy-loamy

Note: The numbers in the brackets indicates the percentage share of crops cultivated in the district.

8.5 Results and Discussion

8.5.1 Optimal cropping pattern and area allocation under constrained Linear Programming (LP) approach

The review of existing agricultural practices showed that the entire agricultural area was not utilized throughout the year. The cultivated area for different crops grouped under different seasons was found to be about 66% in season-1 (Oct-Jan), about 20% in season-2 (Jan-May), and about 14% in season-3 (May-Oct). This pattern has been practiced and perhaps has evolved based on the experience of several decades. It is worth mentioning that the necessity of various crops to be grown depends on their local needs, communication, storage opportunity, export potential, transport, and market facility. As most of these facilities are not prevalent, demand depends mainly on the local need and market facilities. Being primarily governed by these two factors, the sandbar cultivators have been cultivating various types of crops based on their experience. However, such speculated demands are always associated with some amount of uncertainty and, according to them, vary within 10 to 20%. In addition, to maintain the existing biodiversity, it is not advisable to go for mono-cropping with the cultivation of a lone highly profitable crop. In the absence of detailed information about sociocultural practices, demand, storage, communication facilities, etc., it was decided to allow a maximum of 20% variation from this existing cropping pattern while determining the optimal pattern for maximum benefit. Therefore, the optimization model was formulated by setting the upper and lower limit of different crops in different seasons accordingly. After detailed studies on the demand side and the creation of various facilities mentioned above, it may be possible to relax this demand constraint in the future.

The existing cropping pattern generated a net income of 1.3 Billion rupees annually. The optimal cropping pattern derived from the model displayed a significant variation from the existing pattern. The model recommended a 3% reduction of area under Autumn Rice, a 5% reduction under Winter Rice, and a 3% increase under Summer rice. The area under fibers and cereals increased by 1% and 2%, respectively. Potato and vegetable area increased to 6% and 13% of the cultivable area from 4% and 9%, respectively. As a result, the optimal cropping pattern highlighted a significant reduction of the overall rice area by 8% during different seasons and an increase in fibers, cereals, and vegetables by 7% annually. The area under Pulses, which includes Gram, Arhar, Green gram, Masur, and

Black gram, remains equivalent at 5% of the cultivable area. It is a general tendency of farmers to exercise traditional approaches to farming, and they are being influenced by their fellow mates to grow a similar variety of crops and patterns of cropping without variations. However, our model suggested a diverse cropping pattern which would incur a net benefit of 1.5 Billion rupees. Figure 8.5 shows the comparison of areas under existing and optimal patterns suggested by the model. The increase in the net benefit from various activities and crop types is shown in Figure 8.6. The highest net benefit was obtained from the cultivation of vegetables, followed by Winter Rice, Summer Rice, and potato. This implies that the cultivation of these crops can be beneficial for the farmers as the initial capital invested is lower, with better market reach. Another observation noticed during the questionnaire survey was that during the winter season, when the water level recedes in the Brahmaputra River, the local communities organize Eco camps and various festivals in the sandbars for the tourists which serves as an additional source of income generation.

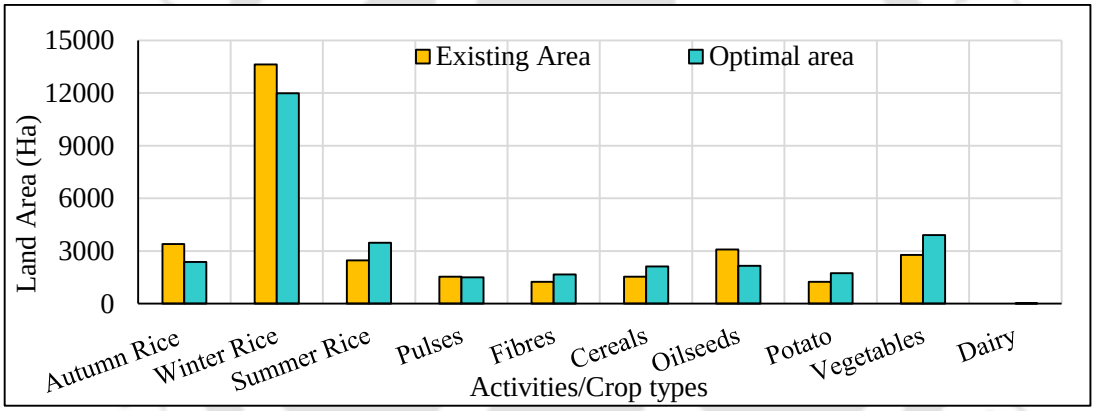

Figure 8.5: Comparison of area under existing pattern and optimal pattern suggested by the model. The percentage of rice in all three seasons has seen a considerable reduction, while the area under fibers, vegetables, and cereals has increased.

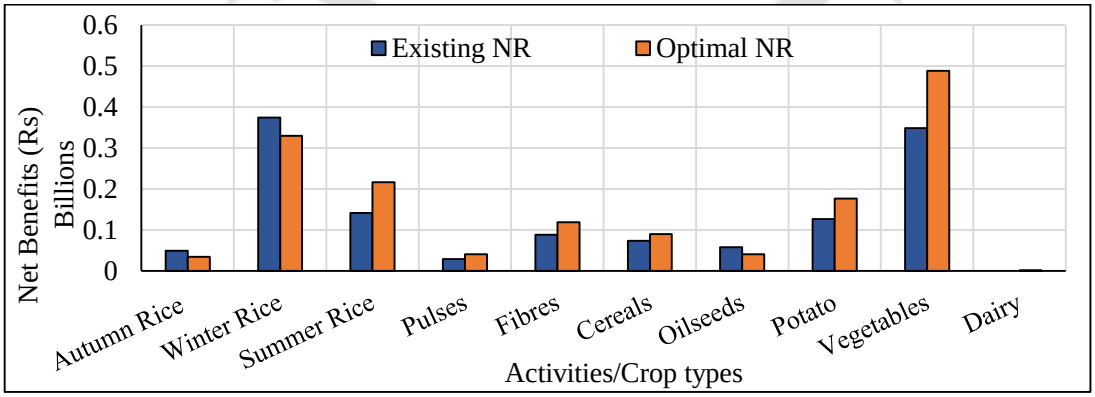

Figure 8.6: Bar plot of net benefits of individual activities obtained from the optimization model shows an overall increase in almost all activities/cropping except for autumn rice, summer rice, and oilseeds. The practice of dairy farming has added an extra benefit, which was not seen in the existing pattern.

8.5.2 Optimal cropping pattern and benefit maximization under different water depth scenarios

Before using an optimization problem to solve complex activities, the primary task is to formulate the optimization problem. The process begins by identifying the decision variables and framing the objective function with some constraints. The final task is associated with setting some variable bounds to the problem. To maximize benefit, optimization allots the land area based on the constraints as defined. This approach was applied for planning 12 crop types (i.e. (paddy (ahu, boro, sali, bao, deep water), maize, jute, pulses, wheat, oilseeds, potato, vegetables) and one dairy farming (livestock grazing) practice. It was found from the study that the benefit obtained from all three seasons varies according to the demand, production, area availability, seasonality, crop yield, and the total number of crops grown. The total cultivable area available in the Zaid, Kharif, and Rabi periods during the optimal cropping pattern was found to be about 1924 Ha, 862 Ha, and 1621 Ha, respectively. The optimization model was initially run without the allowable area constraints, and it was observed that the total area was diverted towards the activity/crop type that provided maximum benefit. However, such cropping practices were not encouraged as they affected the overall balance of the agricultural system. Also, it was obtained from the questionnaire survey performed among the farmers that although a single crop can be cultivated for the total area to attain maximum benefit, the farmers do not prefer such practices due to market price fluctuations, variable demand, flood risk and climate factors. Therefore, the model was further run by assigning the lower and upper crop area limits and demand constraints. In this scenario, it was seen that the maximum area was allotted to vegetables during the Rabi and Zaid period and Potato during the Kharif period (Figure 7.7). From the farmer's perspective, it was found that they do not prefer paddy cultivation in the sandbars due to the unpredictability of water level and the need for a huge workforce. Therefore, they favour vegetable cultivation in a pattern that does not damage the crop during minor flooding with water depths ranging between 0.3-0.6m. Figure S1 (Appendix) shows the pattern of vegetable cultivation in the sandbars during seasonal flooding to minimize the risk of damage.

The optimization model was applied to obtain the net benefit under two scenarios. The first scenario was without considering the depth-wise area available, and the second scenario was by considering the available depth-wise area. Table ST2 shows the area available in

all three seasons for the years 1999-2015. For the first scenario, during the Zaid period, when the total cultivable area available was considered only for the dryland area, the net benefit obtained was ~108.1 million rupees. While considering the second scenario, wherein the area available was in accordance with the water depth defined at various stages, the benefit obtained was ~130.25 million rupees. This shows an additional net benefit of ~20.6 % that could be achieved when the farmers' barren areas were utilized in the optimal cropping pattern. Similar observations were also found for the Rabi and Kharif periods with increased benefits of ~ 35.17% and ~18.4%, respectively. The optimization model found that vegetable cultivation generated the maximum benefit of about 75% of the total cultivable area during the Zaid period, followed by dairy farming practices. The area allocated towards dairy farming was nearly 3%, and it generated a net benefit of around 19.6%. For paddy cultivation, it was found upon interviewing that some classes of farmers cultivate paddy in smaller areas and use its products and by-products as fodder for the livestock community. Our model witnessed an allocation of around 0.5% of the total area available towards ahu and boro paddy cultivation during the Zaid period. Among paddy cultivation, the maximum allocation of the land area was found to be about 9% for sali paddy during the Rabi period, about 6% for deep-water (DW) paddy in the Rabi period, and about 3% for Bao paddy during the Kharif period. The water level gradually rises during the Kharif period, and certain sandbar areas are submerged. This restricts the growth of crops like gram, maize, oilseeds, and dairy farming activities, thereby allocating maximum area towards vegetable and potato cultivation. The percentage share of benefit was about 41% under vegetable crops and potato during this period. Due to the wide range and type of vegetables and their demand throughout the year, expanding areas under potato and vegetable cropping is desirable. However, it is to be noted that although the areas under defined depth ranges were less, it provided additional benefits to the farmers. During the Rabi period, it was found that a maximum net benefit of about 59% and about 21% was obtained solely from vegetable cropping and dairy farming practice, respectively. The area allocation under dairy farming was about 3%, with around 21 % of the total benefit. Based on the results obtained from our analysis, it was found that allocating maximum land area does not necessarily return maximum net benefits. The parameters associated with benefit maximization play a significant role in governing the outcomes from the model. The net benefits determined by the model under the optimal cropping pattern were found to be around 130.25 million rupees during the Zaid period, around 52.85 million rupees during

the Kharif period, and around 98.59 million rupees during the Rabi period. Figure 8.7 shows the optimal area allocation and net benefit under different activities.

Under the Constrained LP approach, the individual LP models for both the objectives, i.e., net benefit (NB) and crop production (CP), were solved under a set of constraints that gave the optimal cropping pattern. The coefficients of the objectives functions and constraints were crisp in nature, and the vagueness of the system was not considered. Table 3 shows the crisp optimal results pertaining to forecasted streamflow for 2016, 2017, 2018, 2019, 2020, and 2021 for the Zaid period. Vegetable cropping and dairy farming were preferable during the period, and the maximum area was allotted to both. The maximum net benefit and crop production were found to be Rs. 1.35×10^8 and 12.9×10^6 Kg, respectively. It was found that the maximum cultivable area was available during 2018 due to the low streamflow predicted by the forecasting models during that particular year. However, it is noteworthy that during the period 2018, less area was allotted to crops other than vegetables and dairy farming, although the cultivable area was maximum. To tackle the vagueness associated with the problems and consider the uncertainties associated with the parameters, fuzzy objective functions and constraints with interval parameters were introduced into the optimization framework.

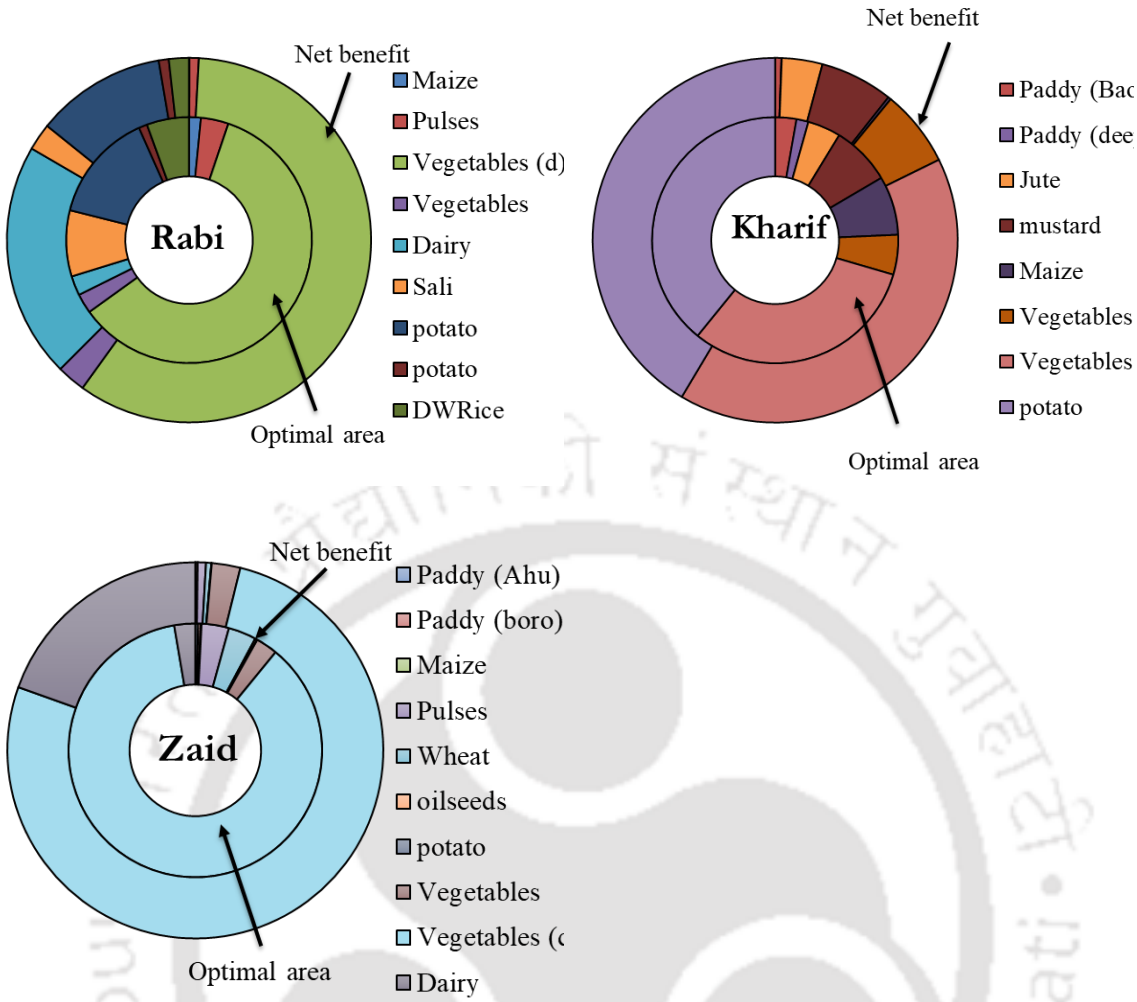

Figure 8.7: Optimal allocation of different crops/activities and their net benefits for the (a) Rabi (b) Kharif and (c) Zaid season. The inner pie represents the optimal area allocation (Ha) of different activities/crops and the outer pie represents the corresponding net benefits (in Rupees). DW represents Deep Water.

8.5.3 Optimal cropping pattern and economic benefit maximization considering the uncertainties

Linear programming (LP) models such as the constrained LP model, can effectively address the optimal cropping pattern along with the associated land and socio-economic constraints. However, in many real-world situations, uncertainties exist in the system components that could affect the decision-making processes. Moreover, uncertainties in the riverine ecosystem are unavoidable and are frequent depending on various climatic and hydrological factors. Uncertainties could also exist due to human-induced impreciseness and fuzziness and fluctuations in seasonal market prices and food demands.

To maximize crop production and net agricultural benefit simultaneously under uncertain conditions, the IMOFLP approach was used. The optimal cropping pattern was determined at different levels of satisfaction (λ). Two separate operators, λ_1 and λ_2, were introduced to tackle the problem, as specific λ values may not function accurately for objectives and constraints. Different scenarios were generated to derive a compromise solution and solution pertaining to the level of satisfaction of the decision-maker (DM). Weight coefficients ω_1 and ω_2 were incorporated to tackle the system behavior under these scenarios discussed as Scenario 1 (S1): Assigning full weightage, i.e.1 to ω_2 and 0 to ω1 ($\omega_2 > \omega_1$); Scenario 2 (S2): Assigning different weights between 0.25 to 0.75; Scenario 3 (S3): Assigning full weightage i.e.1 to ω_1 and 0 to ω_2 ($\omega_1 > \omega_2$). The weights ω_1 and ω_2 can be assigned by the decision-maker based on their experience or as per the requirements but $\sum_{k=1}^{N} \omega_k = 1$ and $\omega_k \geq 0$. The results from the two deterministic sub-models developed have been presented in Figure 8.8.

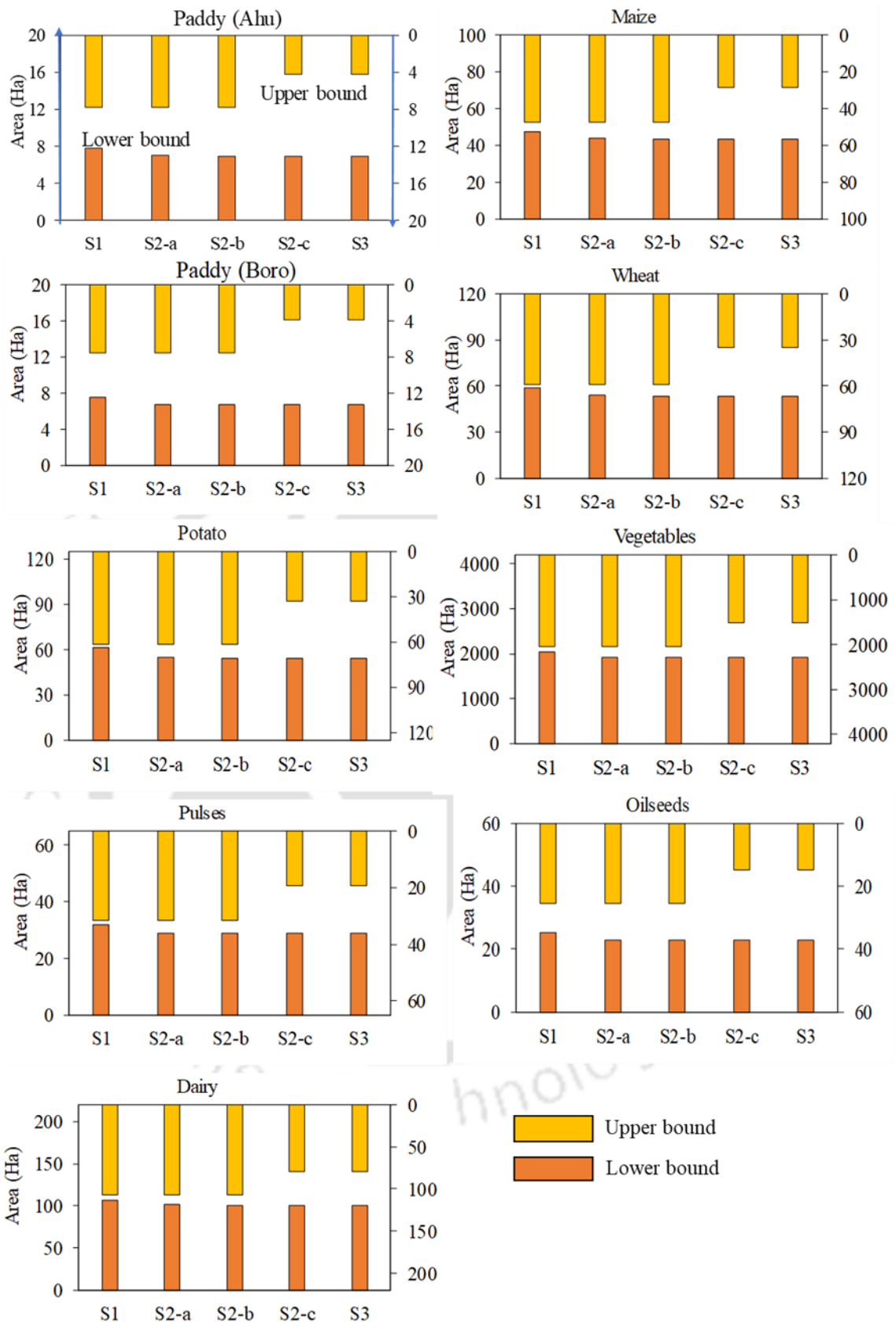

Figure 8.8: Optimal crop area allocation under different scenarios during the Zaid period (Primary axis denotes the Lower bound and Secondary axis denotes the Upper bound)

Figure 8.9 shows the optimal crop planning under different scenarios for maximizing benefit and crop production during the Zaid period. From the scenario analysis, it was found that the weight coefficients greatly influence the optimal cropping pattern. Five weight coefficients were taken into consideration (i.e. ω = 0, 0.25, 0.5, 0.75 and 1). The analysis found that the maximum net benefit and production were obtained when ω_2 varied between 0.5 and 1 and decreased when ω_1 gradually increased from 0.5 to 1. For Scenario S1, when ω_1=0 and ω_2=1, the net benefit varies between Rs. [1.27, 3.13] $\times 10^{8,}$ and the crop production was between [16.4, 20.8] $\times 10^6$ Kg. Under scenario (S2-a), i.e., ω_1=0.25 and ω_2=0.75, the net benefit and crop production slightly decreased and was found to be in the range of Rs. [1.20, 3.13] $\times 10^8$ and [15.5, 20.8] $\times 10^6$ Kg, respectively. For scenario S2-b, when ω_1= ω_2=0.5, the net benefit and crop production varied between Rs. [1.19, 3.13] $\times 10^8$ and [15.4, 20.8] $\times 10^6$ Kg, respectively. For Scenario S2-c, i.e., ω_1=0.75 and ω_2=0.25, the net benefit and crop production ranged between Rs. [1.19, 2.31] $\times 10^8$ and [15.3, 15.3] $\times 10^6$ Kg. Similar results were found under scenario S3 (ω_1=1 and ω_2=0). For scenarios S2-c and S3, when $\omega_1 > \omega_2$, the net benefit and crop production reduced drastically. This is because of higher weight being assigned towards the $\leq$ constraints. The level of satisfaction, λ, was found to vary in the range of [0.19, 0.84] under different scenarios.

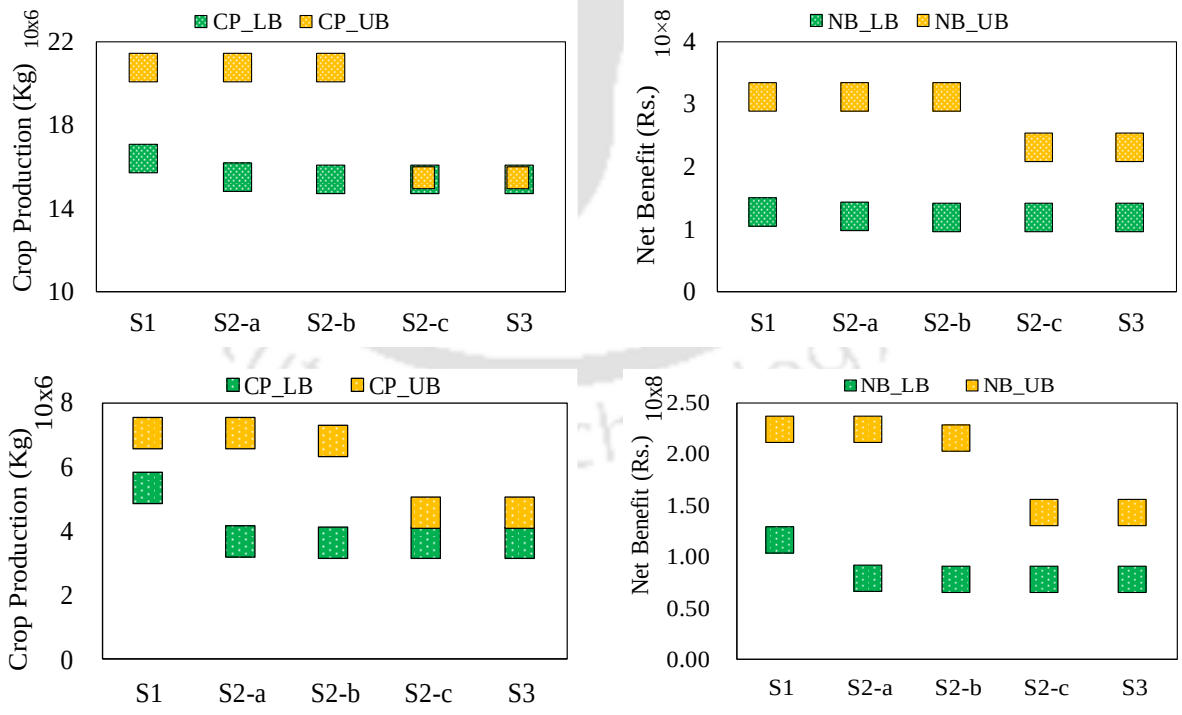

Note: CP: Crop Production; NB: Net Benefit; LB: Lower Bound; UB: Upper Bound

Figure 8.9: Maximization of net agricultural economic benefit and crop production during the Zaid period under different scenarios.

The comparison chart of optimal cropping patterns under the constrained LP approach and the IMOFLP approach has been provided in Figure 8.10 for the Zaid and Rabi periods. Under the constrained LP approach, the minimum and maximum total cultivable areas were 1696.61 and 2254.9 Ha, respectively, for the forecasted period from 2016 to 2021. The net benefit and crop production for the maximum cultivable area were found to be Rs. 1.92×10^8 and 18.3×10^6 Kg, respectively. The constrained LP approach provided a deterministic value with one possibility of outcomes, whereas the IMOFLP approach provided stable decision alternatives. The IMOFLP approach provided a range for the DM in attaining solutions at different levels of satisfaction. The fuzzy programming approach handled the uncertainties in agricultural management in the form of inconsistency in market price, cost of cultivation, crop yield, food demand fluctuations, etc.,. In addition, providing certain relaxations in the form of intervals could generate higher benefits and productivity. These findings would help understand the farmers' income and maximize productivity under uncertainties.

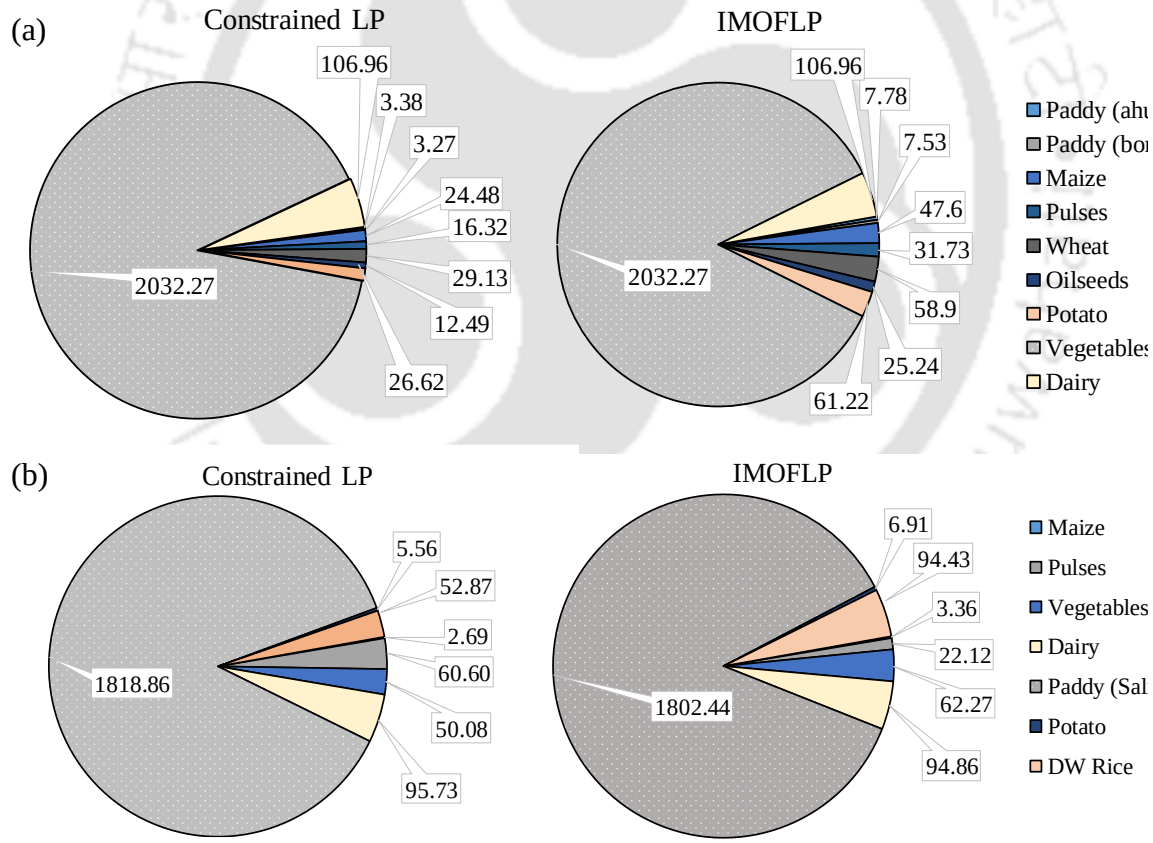

Figure 8.10: Comparison of optimal cropping pattern results using constrained LP and IMOFLP approach for the maximum cultivable area available during the (a) Zaid and (b) Rabi period.

8.6 Conclusions

The key conclusions derived from the results of the optimization approaches are described as follows:

1) By comparing the net economic benefits derived from the optimal cropping pattern and the existing cropping pattern in the Barpeta district, it was found that the optimal cropping pattern increased the net annual return by 0.22 Billion Rupees from the existing return of 1.32 Billion Rupees. The study suggested varying the crop types and allotting more areas in non-cropping activities such as dairy farming (poultry, milk, pig, and cattle rearing) could be beneficial.
2) The LP model suggested a decrease in the overall rice area by 8% and an increase in the area covered under fibers, cereals, and vegetable crops by 7% annually within the riverine areas. This recommended a shift in the agricultural pattern from traditional rice cropping to nutrition-based cropping.
3) In large rivers like the Brahmaputra, the extent of flooding is enormous, with the high volume of water flowing through it. However, post-monsoon, the river carries alluvium-rich sediments suitable for various agricultural activities. Thus, it is suggested that during the Kharif season, the pattern of cropping in the sandbars should be such that harvesting is completed before May (Pre-monsoon), and paddy to be sown during the month of September when there is little water favourable for rice cultivation.
4) Rice has been the principal crop grown at approximately more than 60% of the cultivable area and across various Assam districts. However, untimely rainfall and flood greatly affect the paddy seeds sown within the river system. Summer rice (Boro) can withstand high water levels and can be seen as a replacement for Autumn and Winter rice from the study. Alternate cropping patterns with jute and other cash crops should be grown alongside that can resist high water levels.
5) After harvesting, the agricultural leftovers and residues like the straw from Paddy, wheat, and rapeseed, tops and leaves from potato act as feedstock for cattle and pigs. On the other hand, animal dung can be used as manure for crops.
6) Both the constrained LP approach and the IMOFLP approach provided an in-depth understanding of the optimal cropping patterns within a complex riverine

environment. The results derived from the analysis considered the outcomes from both crisp and interval-based solutions. In many real-world situations, uncertainties exist in the system components that could affect the decision-making processes. Moreover, uncertainties in the riverine ecosystem are unavoidable and frequent depending on various climatic and hydrological factors and human-induced impreciseness and fuzziness. Therefore, such vagueness was very well handled by the optimization framework, and the solutions derived could provide room for the DM at different levels of satisfaction.

7) With the increase in water level in rivers and streams, the cultivable area decreases, demanding selective crop planning. Therefore, determining optimal cropping patterns is more complex in sandbars with the risk of crop damage. A damage estimation model has been developed in the study to assess crop damages due to water level fluctuations.

9

Damage estimation for determining agricultural economic loss

9.1 Introduction

Fluvial floods are a natural component of the hydrological cycle with a range of consequences including economic, social, ecological, and environmental damage (Pistrika 2010). To reduce and prevent significant economic flood losses, reliable tools are required to estimate potential river inundation effects. Until the recent past, either the flood damage evaluation was neglected or oversimplified approaches were taken into account as the expected loss was relatively insignificant to damage to urban areas (Merz et al., 2010). It is now widely considered an important aspect of determining their impact on agriculture decision-making. Various damage estimation models have been developed worldwide to evaluate flood damages, such as the SCADE (Silsoe College Agricultural Drainage Evaluation) Model, Rhine Atlas model (International Commission for the Protection of the Rhine (ICPR) model), FLODSIM (flood damage simulation) model, etc. (Brémond and Grelot, 2013). Few well-known loss estimation models available in the literature are; FDAP (Flood Damage Analysis Package), ANUFLOOD (Australian National University Flood-loss Adjustment and Abatement Computer Package), and ESTDAM (Flood Hazard Research Centre (FHRC)). However, these models do not provide the mechanism for integrating the actual flood event based on the physical characteristics of a flooded area (Dutta et al., 2003). In addition, a review conducted by Brémond and Grelot (2013) on flood damage to agriculture revealed that expert knowledge and farmers' perception must

be taken into account in damage estimation. As the flood events are occasional, the data extracted through surveys and site visits and interaction with farmers would be beneficial to construct damage functions that characterize the direct effect of floodwater on different types of exposed elements.

It was observed that limited studies had been reported on determining the damage to crops due to the effect of stochastic streamflow parameter, crop area variability, seasonality, and intensity of flooding. In practice, the farmers in the developing countries are benefitted by selling the seasonally harvested products, and the profit gained is utilized in procuring seeds, ploughing the fields, and labour wages. Moreover, optimization techniques concerning the economic loss due to the submergence of agricultural land in riverine sandbars and floodplains are of prime importance for optimal cropping patterns.

9.2 Model formulation

In the study, complexities in cropping were incorporated based on the observed streamflow and the cropping pattern subject to survivability under different water depths. Our primary objective was to see if an optimal cropping pattern was planned based on the average streamflow value and if the same pattern is implemented over the years, what could be the extent of crop damage the farmers may experience due to flow variation. While formulating the damage estimation model, the damage to crops was addressed at different levels/stages of water depth. The slope of the sandbar area is gradual as the distance increases from the river toward the dryland areas. Thus, the crops suffer damage with a gradual rise in water level and also suffer damage when the water level reduces from the defined depth stages (*p*, *q*, *r*, and *o*). Therefore, an optimal depth was considered as a threshold water level (maximum depth at which crops survive), above and below which the crops suffer damage. The objective was to determine the losses based on the seasonal variation in streamflow, starting from time, *t* to time, *t+k*. *"t =1"* represents the first year, i.e., 1999 in this case and *t+k* represents the year lagged by k^{th} year and *k* can take any value depending on the availability of flow data. We have considered up to 2015 in this study Thus, the net benefits obtained in the next time period would vary from those derived from the optimal cropping pattern. Figure 9.1 shows the framework of damage estimation to evaluate the economic loss and determine the actual benefit obtained.

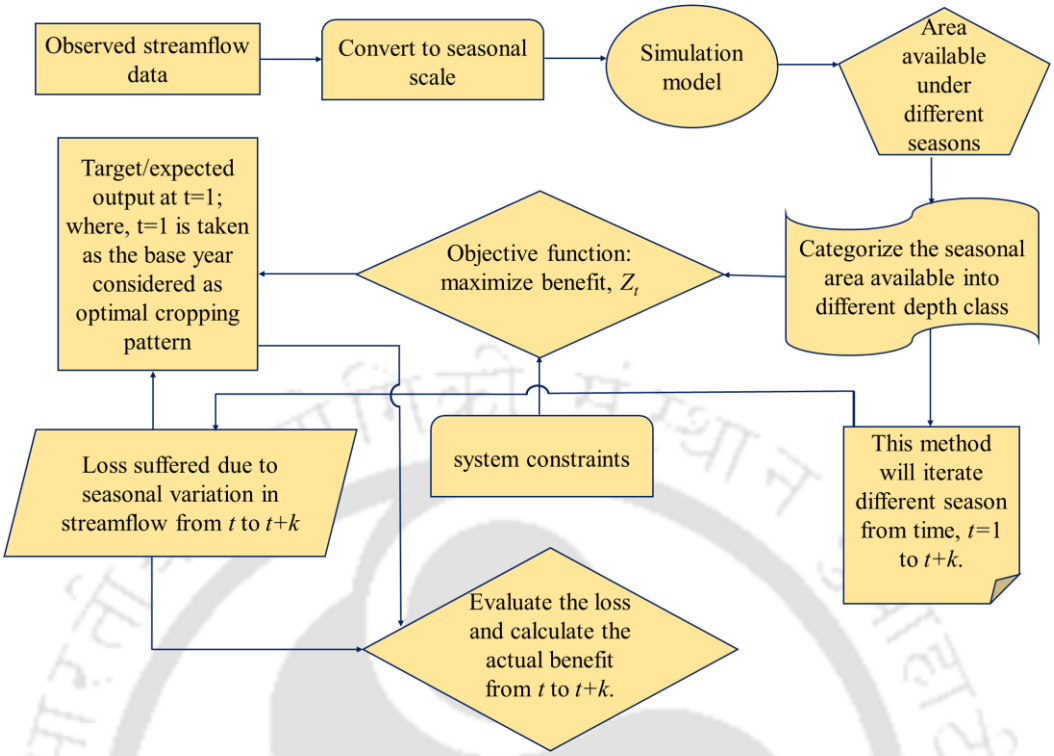

Figure 9.1: Framework for the proposed optimization model coupled with a damage estimation model

As stated, the study aimed to determine the actual economic benefit derived from an agricultural planning process within a riverine ecosystem; streamflow and water level fluctuations play a significant role. Therefore, the expected benefit from farmer's perspective or farmer's experiences from previous seasonal cropping patterns may vary in the future based on the hydro climatological fluctuations. For the present study, the complexities in formulating the model lie in determining the loss under the increased/decreased water level for the defined depth scales. Therefore, we have considered different depth stages at which the crops could potentially suffer damage due to fluctuations. When the water level varies between 0-0.3 m from the optimal depth, crops suffer damage in the *p* stage; when the water level varies between 0.3-0.6 m, crops suffer damage in the *q* stage. Further, when the water level varies between 0.6-0.9 m and at a level above the optimal depth, the crops suffer damage in the *r* stage and *o* stage, respectively.

To better comprehend the damages suffered due to streamflow variability, two cases have been considered i.e. Case A and Case B, wherein we have performed the analysis in reference to an optimal depth. As stated previously, the optimal depth is such that when the water level rises above this depth, all crops grown and activities performed in the total

cultivable area suffer a certain amount of loss. Similarly, when the water level recedes below this depth, the cropland areas in the *p*, *q*, and *r* stages suffer complete or partial damage, while crops grown or farming activities in dryland areas (stage *o*) do not suffer any damage. The actual economic benefit varies from the benefit obtained from the optimal cropping pattern. Therefore, the losses determined were in accordance to benefit from such practice. Likewise, to understand the damage estimation model, the underlying processes have been explained through mathematical equations (9.1-9.11). A schematic diagram of losses suffered at different depths under streamflow variations has been illustrated in Figure 9.2.

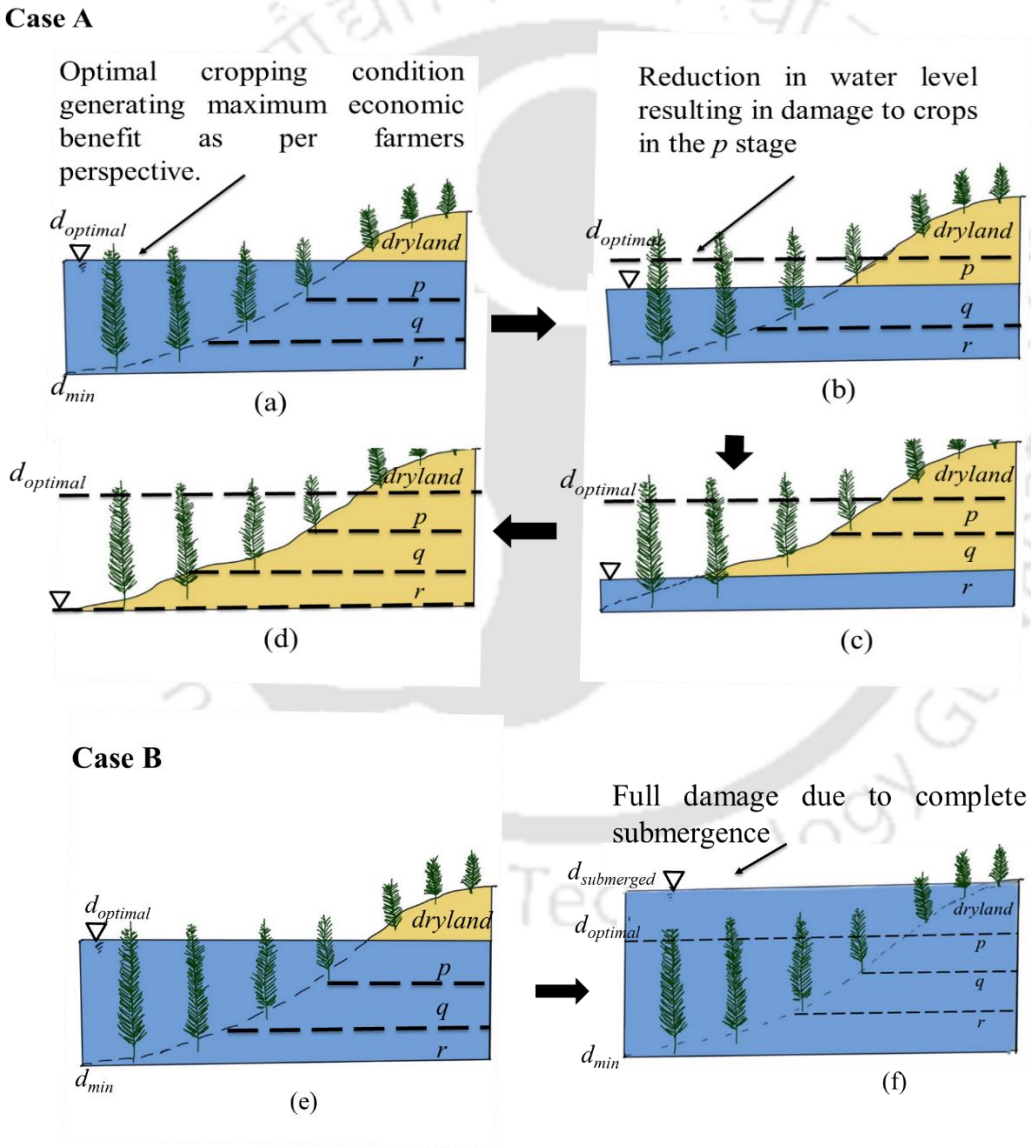

Figure 9.2: A schematic illustration of the process of damage suffered at different stages of water level variability and area available at different time scales. *p,q,r* varies between optimal depth to minimum depth (Case A), and o varies between optimal and submerged depths (case B). The optimal cropping pattern with maximum benefit is represented in figure a. For case A, as the water level decreases, the subsequent losses at

the defined depth stages are shown in figures b,c, and d. For case B, the rise in water level damages the cropping and farming activities in the dryland areas, as shown in figures e and f.

Case A: Crops suffer damage when water depth varies between the minimum depth (d_{min}) and optimal depth ($d_{optimal}$).

In this case, water above or below the optimal depth will lead to damage to crops. "d_{min}" corresponds to the condition when the water has not reached any landmass under the depth level considered.

When, $d_{\min} < d \le d_{optimal}$

$$Loss_{t+k} = DC.Z_t|_{p,q,r}$$

$$=\{(a(DF)^2 + 1 - a(DF)).Z_t|_p + (a(DF)^2 + 1 - a(DF)).Z_t|_q + (a(DF)^2 + 1 - a(DF)).Z_t|_r\} \quad (9.1)$$

$$DF|_{p,q,r} = \left|\frac{A_{d(t+k)}}{A_{a(t)}}\right| \quad (9.2)$$

$$DC = \{a(DF)^2 + 1 - a(DF)\} \quad ;0 \le a \le 1 \quad (9.3)$$

where, Loss $_{t+k}$ describes the potential economic loss due to changing streamflow for the k^{th} year. DC is the damage coefficient and is dependent on the damage factor (DF) which provides a relationship between the actual area available at the k^{th} time and the area at time t at the particular depth stages. The difference between them is termed as the damaging area. The DF is the ratio between the damaging area (A_d) and the available area (A_a). The absolute value of the ratio is taken since the damaging area in the subsequent years would be more or less than the available area of the year considered as the optimal cropping pattern. In both situations, this would lead to significant damage to the crops and result in substantial damage due to excess water leading to flood-like conditions and a deficit of water leading to drought-like conditions. The notations p, q, r represent the different water depth stages as discussed. a is a constant between 0 and 1 and represents the shape of the quadratic equation. A value of 0.5 has been considered in the present study.

Again,

$$DF_{p,q,r_{|t+k}} = \begin{Bmatrix} 0, & if\ A_{d(p,q,r)} < 0 \\ 1, & if\ A_{d(p,q,r)} = A_{a(p,q,r)|t} \\ otherwise, & if\ 0 \le A_{d(p,q,r)} \le A_{a(p,q,r)|t} \end{Bmatrix}; \forall p,q,r;t \quad (9.4)$$

Feasibility conditions;

$$0 \leq DF_p \leq 1; \quad DF_q = 0; \quad DF_r = 0 \qquad 9.5 \text{ (i)}$$

$$0 \leq DF_q \leq 1; \quad DF_p = 1; \quad DF_r = 0 \qquad 9.5 \text{ (ii)}$$

$$0 \leq DF_r \leq 1; \quad DF_p = 1; \quad DF_q = 1 \qquad 9.5 \text{ (iii)}$$

Here, d = water depth (m); A_d = Damage area (Ha); A_a = Available area (Ha) under p, q, r, o ; DF = Damage factor; DC = Damage coefficient; t = time period during which average streamflow was considered; p, q, r, o = water depth stages.

Three possibilities of determining the DF exists, i.e., when the water level is at the optimal depth ($d_{optimal}$), water level at the minimum depth (d_{min}), and water level varying between the minimum depth (d_{min}) and optimal depth ($d_{optimal}$). The feasibility conditions at various stages are such that when water level varies in a particular depth stage, the value of DF varies in the other stages. The condition determines the multiple stages of crop damage that could occur in agricultural fields in sandbars. In the worst-case scenario, the crops grown in all three stages suffer complete damage when the water level is below the r stage.

Case B: Crops suffer damage in dryland areas where water depth varies between the optimal depth ($d_{optimal}$) and submerged depth ($d_{submerged}$).

All crops considered in Case A suffer maximum damage, and those in case B suffer partial damage based on water level fluctuation in this stage. Water above the optimal depth will cause damage to crops and farming activities in the dryland region.

When, $d_{optimal} < d \leq d_{submerged}$

$$Loss_{t+k} = DC.Z_t|_o \qquad (9.6)$$

$$= \left(a(DF)^2 + 1 - a(DF)\right).Z_t|_o$$

where,

$$DF_o = \left|\frac{A_{d(t+k)}}{A_{a(t)}}\right| \qquad (9.7)$$

$$DC = \{a(DF)^2 + 1 - a(DF)\} \qquad (9.8)$$

Again;

$$DF_{o|_{t+k}} = \begin{Bmatrix} 0, & andif\ A_{d(o)} < 0 \\ 1, & andif\ A_{d(o)} = A_{a(o)|t} \\ otherwise, & andif\ 0 \le A_{d(o)} \le A_{a(o)|t} \end{Bmatrix};\ \forall v; t \quad (9.9)$$

Feasibility conditions;

$$0 \le DF_o \le 1; \quad DF_p = 1,\ DF_q = 1, \quad DF_r = 1 \quad (9.10)$$

The crops suffer damage due to water level fluctuation, which has been illustrated in the actual case scenarios. For Case A, Equation 9.1 describes the potential economic loss to be determined for the next period ($t+k$). The damage factor varies in the stages *p*, *q*, and *r*, subject to water level fluctuations at the corresponding stages. Equation 9.2 takes care of these damages and provides the DF value at these stages. Equation 9.3 gives the value of the damage coefficient when DF varies from 0 (no damage) to 1 (full damage). It is a quadratic form of loss estimation model taken from Nguyen et al. (2017). Equation 9.4 states three possibilities for determining the damage. Equation 9.5 is the condition that captures various stages of crop damage that could potentially happen in an agricultural field and is termed feasibility conditions. Similarly, for Case B, Equations 9.6 to 9.11 describe the process of loss estimation in the dryland areas.

To determine the potential benefit, Z_{t+k}, the computed economic losses were subtracted from the expected benefit, Z_t and the optimization problem was reformulated as described in Equation 9.11.

$$Z_{t+k} = Z_{opt} - \left\{Loss_{|d_{min}<d\le d_{optimal}} + Loss_{|d_{optimal}<d\le d_{submerged}}\right\}$$

$$\begin{aligned} = Z_{opt} - \{\sum_{j=1}^{J}\sum_{i=1}^{I}\{((Y_{ij}.MP_{ij}) - CC_{ij})A_{ij}\} \\ - \{\left(a(DF)^2 + 1 - a(DF)\right).Z_t|_p + \left(a(DF)^2 + 1 - a(DF)\right).Z_t|_q \\ + \left(a(DF)^2 + 1 - a(DF)\right).Z_t|_r \\ + \left(a(DF)^2 + 1 - a(DF)\right).Z_t|_o\}\} \end{aligned} \quad (9.11)$$

9.3 Results and Discussion

9.3.1 Loss estimation concerning crop damage under fluctuating water depth

The damage estimation model coupled with the optimization model was significant in determining the difference between the expected and actual benefits. Considering the optimal cropping pattern for all three seasons, the damage model generated a substantial variation from the maximum benefit in the subsequent periods while considering the crop damages suffered at different depths. The water level fluctuates in the river due to seasonal streamflow variability; the area under the defined depth stages is therefore affected. To better understand, we illustrated the process by considering damage suffered at different stages of water depth, as shown in Figure 9.2. When the water level fluctuates between 0-0.3m in the *p* stage about the optimal depth, the area under that level is affected, incurring damage to the crops. As the water level further decreases and is in the range of 0.3-0.6m, the crops under the *p* stage suffer complete damage and partial damage under the *q* stage. With the further decrease in water level in the range of 0.6-0.9m from the optimal depth, the crops grown in the *p* and *q* stages suffer complete damage, and crops grown in the *r* stage suffer partial damage. Similarly, for case B, when the water level rises above the optimal depth, the crops suffer partial damage up to the submerged depth ($d_{submerged}$), above which the total area under cultivation is damaged due to flooding conditions.

The variations in the streamflow resulted in the agricultural economic loss during the three seasons, which could be comprehended from Figure 9.3 (a-c). During the Zaid period, the maximum loss obtained from the model was estimated to be around 45.1 million Rupees, accounting for about 34.5% loss in 2010 compared with the expected benefit. That means a loss of around Rs. 37,000 per hectare was suffered during that period. For case A, during the Zaid period, the damage to crops resulted in about 3% loss in the depth range of 0.3-0.6m. The losses accounted for the crops damaged at the area under the water level range of 0-0.3m, and 0.6-0.9m was less than about 1%. For case B, the damage corresponds to a loss of about 31.1% in the dryland area in 2010; the maximum loss witnessed during this period. Similarly, the maximum losses seen during the Rabi and Kharif periods were about 24.4% in 2012 and about 14.4% in 2013, respectively.

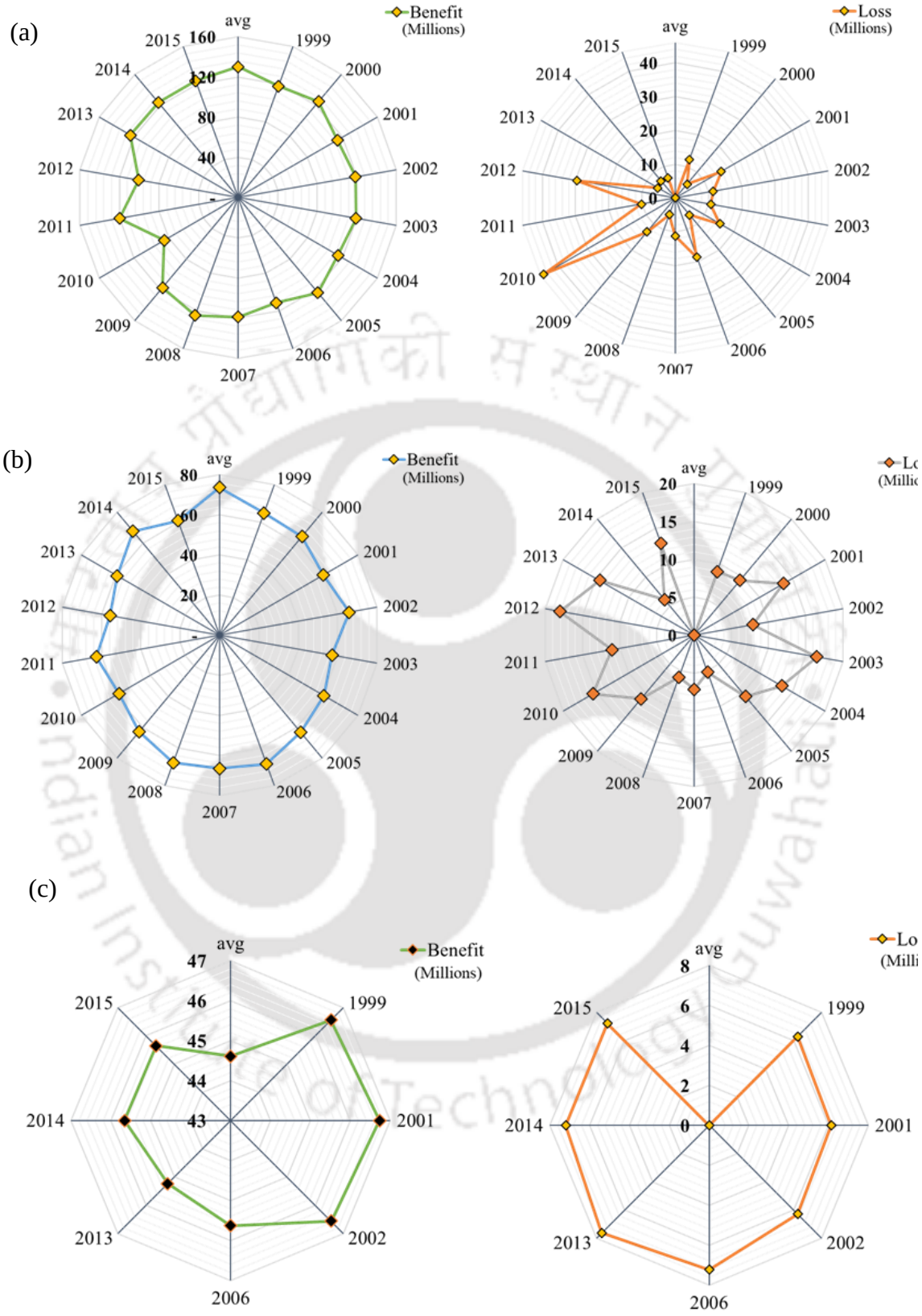

Figure 9.3: Plots showing the loss and actual benefit during different years under varying streamflow. (a) Zaid (b) Kharif (c) Rabi. The term "avg" represents the year of optimal cropping pattern where the net agricultural benefit obtained was maximum with no loss.

Figure 9.4 (a-c) represents the stage-wise loss suffered due to streamflow variation during the Zaid, Rabi, and Kharif periods. For the Zaid and Rabi period, the maximum loss of about 31.1% and 20% were suffered in the dryland area, and for the Kharif period, a maximum loss of about 6.8% was suffered in the depth range of 0-0.3m. For the Zaid period, the loss percentage at 0-0.3m, 0.3-0.6m, 0.6-0.9m and dryland area were found to vary in the range of 0.05%-0.64%, 2.15%-2.76%, 0.49%-0.77% and 0.62%-31.1%, respectively. Similarly, for the Rabi period, the variation of economic loss at 0-0.3m, 0.3-0.6m, 0.6-0.9m and dryland area were found to be in the range 0.01%-0.57%, 2.94%-3.5%, 0.87%-1.25% and 2.67%-20.1%, respectively. During the Kharif period, the riverine ecosystem experiences flooding with high flow in the river. Therefore, years in which streamflow was observed to be ≤ 30000 cumecs are considered while planning any agricultural activities. The rise in the water level limits the growth of certain crops in the defined depth scales, and thus the net profit reduces. The flood that inundated agricultural areas during the period 2012 in the study region mostly affected the crops, which can be seen in Figure 9.5.

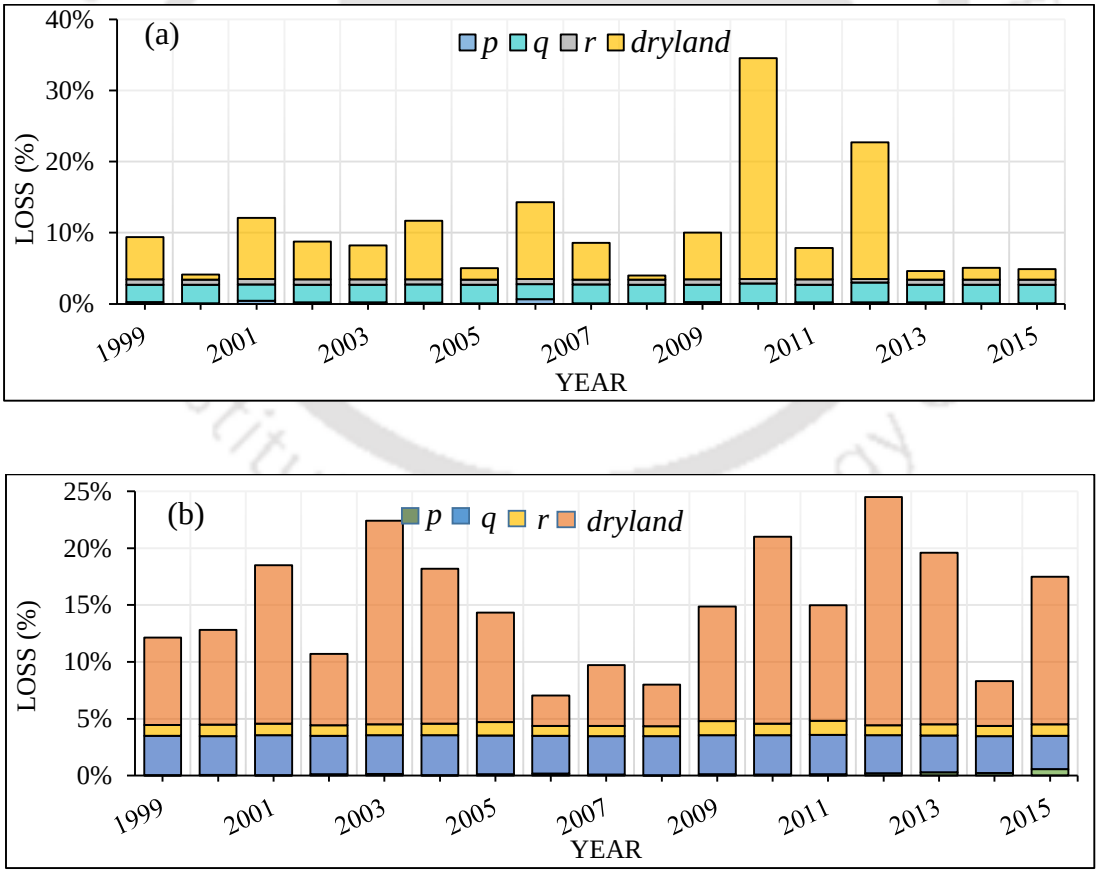

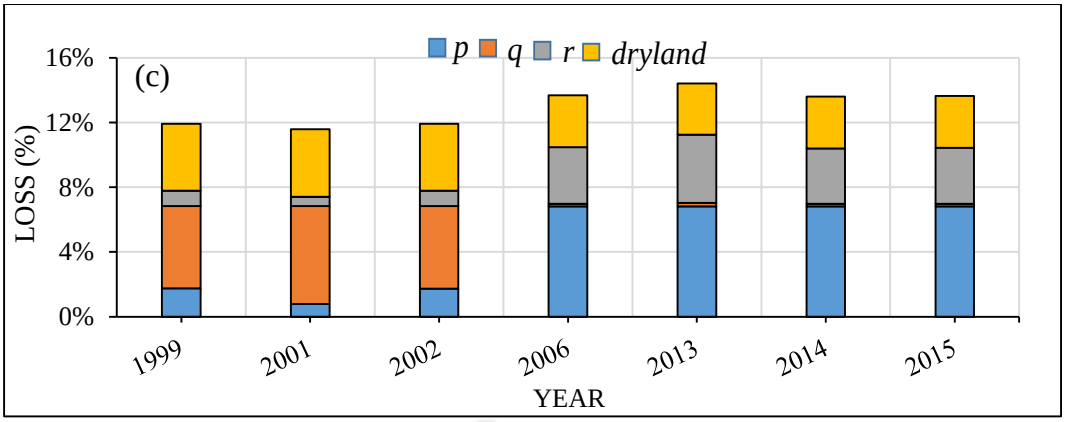

Figure 9.4: Plots showing the percentage economic loss under each depth class i.e. *p*,*q*,*r* and *dryland* stages for (a) Zaid (b) Rabi (c) Kharif period.

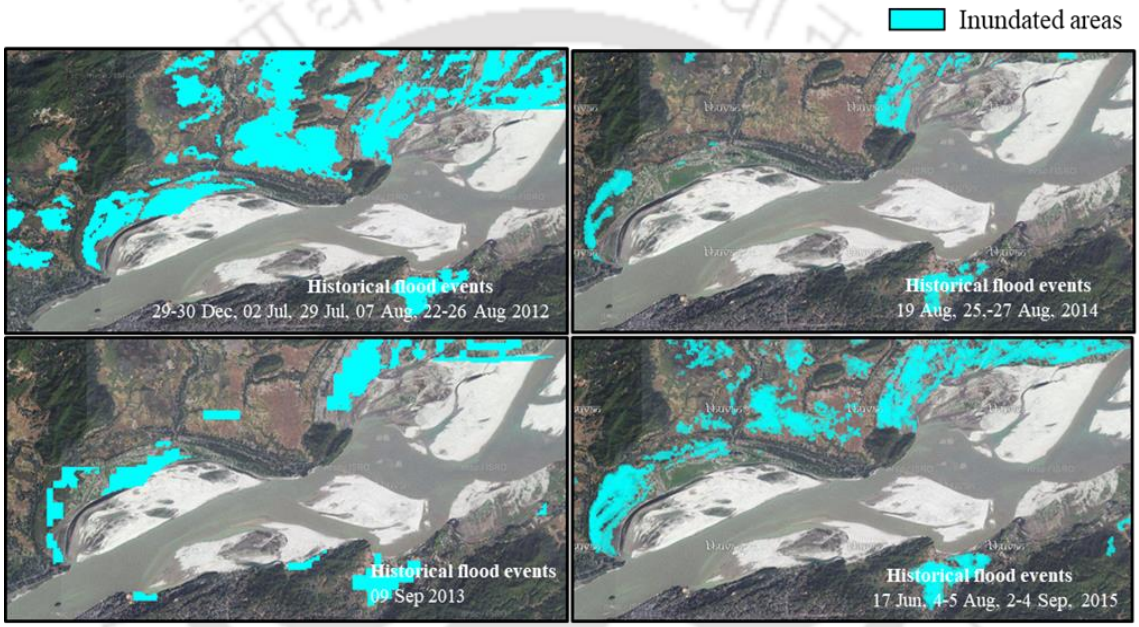

Figure 9.5: Satellite images showing the inundated areas for the historical flood events over the study region obtained from https://bhuvan-app1.nrsc.gov.in/bhuvandisaster/. The imageries show that flood events during 2012 showed maximum inundation resulting in damage to crops.

9.3.2 Profit reliability under flooding conditions

The economic evaluation of flood damage to crops is necessary for decision-making. Downton and Pielke (2005) evaluated the complications in accounting for the damage costs into three categories; (a) direct and indirect costs analysis; (b) damage variability under spatial and temporal extent, and; (c) damage due to intangible losses such as human health and physiological effects. Therefore, estimating the potential damage to crops provide essential information for assessing support needed for the short term and insurance and policy development in a long time. Our study focused on the losses incurred due to damage to crops and livestock under streamflow variability and the farmers' reliability to such cropping practices. The study recommended that selecting crop types under seasonal

flooding conditions is essential to maximize the net economic benefit. Therefore, the reliability of such cropping practices is dependent primarily on the farmers' choice. The present work witnessed a significant variation in damage in a particular depth class and near-constant damage at another depth class during the same period. Similar variations at different depth ranges were also seen for other seasons. Due to poor socio-economic conditions, farmers' independent potential to adapt to such losses is uncertain and inadequate. Crop insurance lessens the monetary risk and is an essential agricultural risk management tool to protect farmers from natural disasters and climate change (Fahad, 2018).

Agricultural losses are due to uncertain hydroclimatic parameters and inconsistent market prices. Crop insurance could be the better way to avoid these risks. Therefore, the model outputs estimate losses in all three seasons that would help in the process of decision-making by the farmers. The selection of crop types based on the market for the produce from a particular season is essential for adopting the crop insurance policy. This directly reflects their willingness to pay if the demand is high. On the contrary, the distance from the river negatively relates to farmers' desire to crop insurance, as the farmlands close to the river have a high risk of damage and loss. It was also found that few farmers have still not recovered from the losses suffered in the past. Therefore, crop insurances are advisable for such a class of farmers, encouraging them to cultivate on the sandbars. Farmers practicing livestock farming have mixed opinions on insurance as they are not much benefitted from crop production.

9.4 Conclusions

The study presents an overall understanding of the agricultural practices and the derived benefits and associated losses in riverine sandbars through a conceptual framework. The approach of integrating an agricultural damage estimation model with an optimization framework can help policymakers plan crop planting structures more efficiently thereby increasing food supply and improving socio-economic status. Cases A and B depicted the seasonal losses suffered at different water levels under varying streamflow. From the farmers' perspective, it was found that only the dryland sandbar areas were considered for optimal cropping patterns previously. However, with our approach of optimal agricultural planning at different water depths, additional net benefits have been achieved. From the crop damage point of view, our model estimated losses varying under uncertain streamflow

behaviour. Although it is challenging to understand farmers' behaviour in cropping practices, this study has incorporated farmers' opinions, experiences, difficulties faced, behaviour, and various socio-economic and cultural factors while formulating the problem locally. In addition, farmers' behaviour on abandoning production or continuing amidst floods could not be found in studies. Our model takes into account the stage-wise variations in water level and the expected damage could be determined. Some crops like Jute suffers damage if a required water depth is not maintained, which indicates that not only floods cause crop damage but drought-like conditions could also lead to damage. The study compared modelled results (seasonal profit) to actual agricultural profit records gathered throughout the survey and concluded that agricultural optimization approaches could provide avenues for guaranteeing food security. Promoting investments in agricultural infrastructure and extension services appear to be key drivers for improving food security. The study highlighted the need of crop insurance facilities to assess and manage risks that could provide financial support to famers, cover crop loss and damage arising from such events. By making marginalised communities living in riverine areas aware of the potential extent of damage and the necessity of insurance policies, the study aims to improve their socioeconomic conditions. In addition, the conventional practice of cultivating in limited areas could be further expanded through selective cropping approaches to enhancing food production. The advantages of the model are its simplicity in terms of applicability and tuning it with few parameters. Thus, calibrating the model for new locations would be easier for generalized framework and easy to apply to other regions globally, as many large rivers around the year develop sandbars seasonally. The formulated approach can assist the scientific community and decision-makers in attaining socio-economic benefits and food demand to feed the ever-increasing population. With the practice of sandbar cropping and farming in riverine environments, farmers and dwellers need to understand risk and have risk management skills to better anticipate problems and reduce consequences.

10

Agriculture risk assessment and adaptation measures

10.1 Introduction

Rivers and floodplains are important components of a country's socio-economic and cultural development. Riverine floodplains across the world have been used for agriculture because of its natural fertility. For instance, the lower reaches of the Tigris River in Iraq, the Rhine and Danube Rivers flowing through Germany, the River Yangtze in China and the Rivers Ganga and Brahmaputra in India and Bangladesh (Verhoeven and Setter, 2010). However, the danger of natural hazards due to the extreme probability of occurrence of events cannot be avoided. While dealing with flood issues, the term risk is a frequently encountered concept characterized by its complexity and ambiguity (Hazaa et al., 2021). In general, risk can be expressed as a product of probability and the consequence of a certain event (Bouma et al. 2005). Flood risk can be conceptualized into one-dimensional and multi-dimensional concepts. The former refers to the probability that the annual maximum flow with a return period occurs during *n* years (Solin and Skubincan, 2013). Conversely, it can be represented as the probability that the specified maximum flow value is not exceeded in any year. For the latter, in addition to the probable occurrence of flood, it also considers the negative consequences of the flooding. As per the Department of Environment, Food and Rural Affairs (DEFRA), “Flood risk is a combination of the likelihood or frequency of occurrence of a defined threat and the magnitude of its consequences”. In absolute terms, the determination of risk denotes the area under the damage-probability curve, which represents the total average annual damage (Zeleňáková et al. 2020).

Risk assessment and analysis are gaining attention in flood protection and risks, which allows for assessing the cost-effective mitigation measures and optimizing investments (Apel et al. 2009). Several approaches to flood risk assessment have been developed worldwide (Nascimento et al., 2006; Meyer and Messner, 2005). In general, these approaches are based on the principle of the loss curve method, which expresses the magnitude of damage to the financial cost depending on the hydraulic parameters such as water depth, flow velocity, duration, etc. In addition, assessments involve the damage amount expressed by relating the damage to property to its size or the percent of damage from the maximum possible damage to the property (Zeleňáková et al. 2020). Mathematical models give us an understanding of the extent of such parameters that could be investigated in risk assessments. The two-dimensional models are efficient in simulating the complex spatial conditions in irregular-shaped areas and along floodplains or in places of obstacles such as bridges, dams, etc. Flood damages can be categorized into direct and indirect damage, as illustrated in Figure 10.1. Floods cannot be eliminated entirely, but flood risk can be reduced. The common tool for evaluating the flood risk is flood frequency analysis (FFA), which constitutes the basis of disaster preparation and mitigation measures. FFA analysis is needed for floodplain management, development, and planning, in addition to flood insurance studies (Chen et al., 2010). The magnitude of an event is a concern in situations like floods and drought. Maximum flows are related to flood risk and repose strategies, whereas low flows analysis is relevant in understanding the hydrological drought, irrigation, agriculture, and managing ecosystems and natural resources.

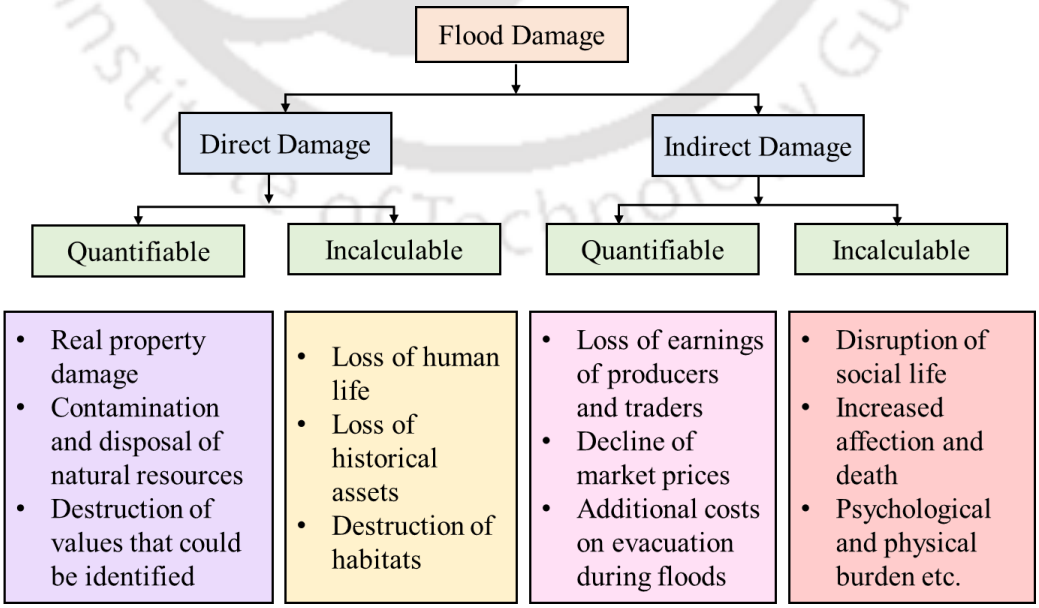

Figure 10.1: Categorization of flood damage (Zeleňáková, M. et al., 2020)

The consequences of flood damage could take multiple forms, such as property damage, personal injuries, environmental contamination, agriculture, and farm-based activities, etc. In this chapter, the assessment of agricultural damages caused due to water level fluctuations and streamflow variations over the years within a riverine ecosystem has been studied. It proposes a risk assessment approach for helping the decision-making process at a local level, addressing risks that affect agricultural areas near rivers, particularly the sandbars.

10.2 Statistical approaches for flow frequency analysis (FFA)

The objective of frequency analysis of hydrologic data is to relate the magnitude of extreme events to their frequency of occurrences through probability distributions. The selection of frequency distribution is essential for flood analysis as inappropriate distribution choices can lead to significant errors (Rahman et al., 2013). Various probability distributions, such as Log-Normal (LN), Gamma, Generalized Extreme Value (GEV), Gumbel, Weibull, etc., for fitting the hydrologic data have been used over the past years (Zhang et al., 2021).

10.2.1 Fitting the distribution

In statistical FFA methods, extreme discharge observations are fitted to a statistical distribution, which is then extrapolated to estimate quantiles such as 100 or 500-year discharge. A key component of FFA is choosing a frequency distribution that fits the data collection, as the wrong distribution choice might result in considerable inaccuracy. Smakhtin (2001) mentioned that different forms of Weibull, Gumbel, Pearson Type III, and Log-Normal distributions are the most frequently referred distribution functions in the literature for low flows. Five candidate distributions, namely the Log-Normal distribution, Gumbel Max distribution, Weibull 3P (three-parameter) distribution, GEV distribution, and Log Pearson 3P distribution, were selected, and the best-fitted distribution was selected among them using the goodness of fit tests. The formulas of the distributions are given in Figure S2 (appendix).

10.2.2 Parameter estimation and distribution selection

To check the fitting of probability distributions, the most commonly used tests of goodness of fit, namely Anderson-Darling (AD), Chi-Square (CS), and Kolmogorov-Smirnov (KS)

tests were applied to the data series. The test statistics of each test were computed and tested at (α = 0.05) level of significance.

1) Anderson-Darling (AD) test

The Anderson-Darling procedure is a general test to compare the fit of an observed cumulative distribution function to an expected cumulative distribution function. This test gives more weight to the tails than the Kolmogorov-Smirnov test. The Anderson-Darling statistic (A^2) is defined as:

$$A^2 = -n - \frac{1}{n}\sum_{i=1}^{n}(2i-1).[lnF(X_i) + ln(1 - F(X_{n-i+1}))] \quad (10.1)$$

H_0: The data follow the specified distribution.

H_A: The data do not follow the specified distribution.

The hypothesis regarding the distributional form is rejected at the chosen significance level (α), if the test statistic, A^2, is greater than the critical value obtained from a table.

2) Chi-Square (CS) test

The Chi-Squared test is used to determine if a sample comes from a population with a specific distribution. This test is applied to binned data, so the value of the test statistic depends on how the data is binned. The Chi-Squared statistic is defined as

$$\chi^2 = \sum_{i=1}^{k} \frac{(O_i - E_i)^2}{E_i} \quad (10.2)$$

where O_i is the observed frequency for bin i, and E_i is the expected frequency for bin i calculated by

$$E_i = F(x_2) - F(x_1) \quad (10.3)$$

where, F is the CDF of the probability distribution being tested, and x_1, x_2 are the limits for bin i.

H_0: The data follow the specified distribution.

H_A: The data do not follow the specified distribution.

The hypothesis regarding the distributional form is rejected at the chosen significance level (α), if the test statistic is greater than the critical value.

3) Kolmogorov-Smirnov (KS) test

This test decides if a sample comes from a hypothesized continuous distribution. It is based on the empirical cumulative distribution function (ECDF). Assume that we have a random sample x_1, ..., x_n from some continuous distribution with CDF *F(x)*. The empirical CDF is denoted by

$$F_n(x) = \frac{1}{n}.[Number\ of\ observations\ \leq x] \tag{10.4}$$

The Kolmogorov-Smirnov statistic (D) for a given CDF is based on the largest vertical difference between *F(x)* and $F_n(x)$. It is defined as

$$D_n = \sup_x |F_n(x) - F(x)| \tag{10.5}$$

where, sup_x is the supremum of the set of distances. Supremum is also referred to as the least upper bound.

The statistic measures the distance between two samples' ECDF or between the EDCF and the CDF of the reference distribution.

H_0: The data follow the specified distribution.

H_A: The data do not follow the specified distribution.

The hypothesis regarding the distributional form is rejected at the chosen significance level (α) if the test statistic, D, is greater than the critical value obtained from a table.

Based on the statistic, the distributions were ranked from best to worst and the lowest score among the three tests are assigned the best distribution for the given data series.

10.3 Risk assessment

Risk management measures the aim to reduce the negative effects of floods as well as droughts. Flood risk is a combination of potential damage and the probability of flooding. The frequency of floods varies seasonally, and losses in agricultural areas also have a clear seasonal pattern (Forster et al., 2008). During dry seasons, the return period of nonstationary low-flow series and risk analysis might help manage water resources. The critical considerations in managing water resources include the concept of return period

and its associated risk of occurrences causing damage to life, property, household, and agriculture. Fig 10.2 shows the flowchart of risk assessment developed for the study.

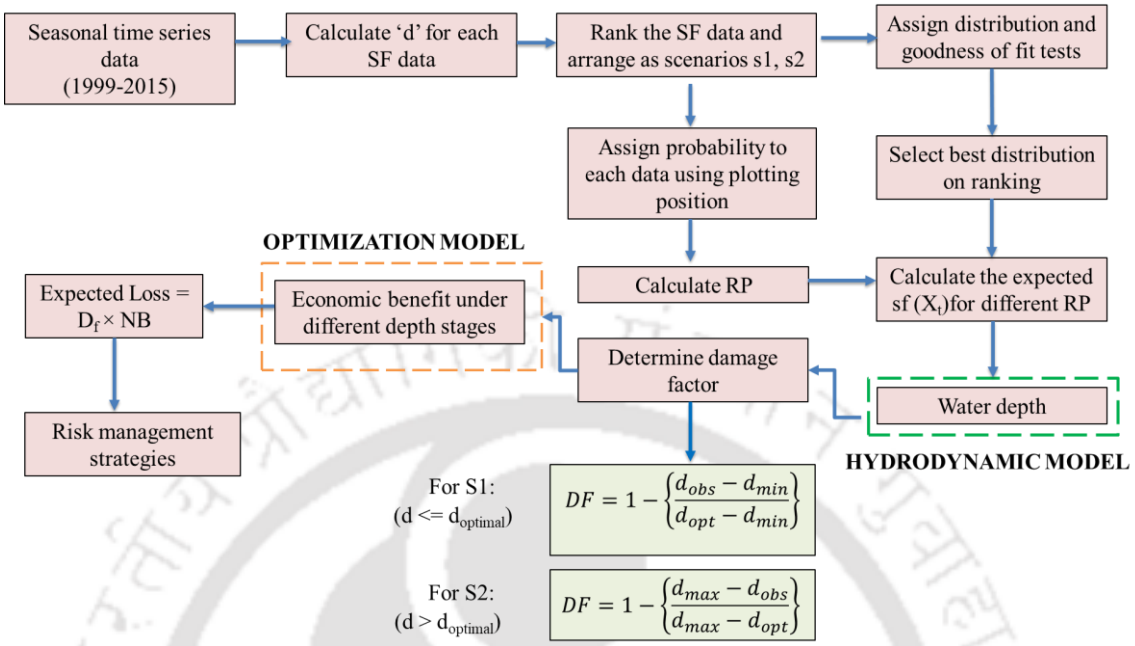

Figure 10.2: Flowchart of determining potential economic loss and risk assessment

10.3.1 Discharge-Frequency relationship

To determine the extent of flooding or non-flooding along the study region, the MIKE 21C hydrodynamic model was used. The seasonal streamflow data were fed into the model, and the corresponding water depth was derived as the output during the numerical simulation process. As discussed in Chapter 5, the study considered a water depth of 0.9m as the optimal depth, above and below which the crops suffer certain damage. Therefore, for each season, the discharge corresponding to a depth above and below the optimal depth was divided into two scenarios. In scenario-1 (S1), the discharge was considered for depths below the optimal depth, and for scenario-2 (S2), the discharge was considered for depths above the optimal depth. Therefore, for scenario S1, the streamflow was arranged in ascending order starting from the lowest flow observed in that season (rank 1) to the streamflow corresponding to the optimal depth (last rank). For scenario S2, the streamflow was ranked in the order of highest streamflow observed in that particular season to a streamflow value corresponding to just above optimal depth. In this work, we define the severity of low flow when the streamflow is lower, corresponding to depths below the optimal depth. It is to be noted that during the Kharif period, the water depth in the study

region was substantially high. Hence, the scenarios were not taken into account for this period.

Once the data series have been identified and ranked, the plotting position technique was used to estimate the probability of events. It refers to the probability value assigned to each data to be plotted. The probability P = $(m - b) / (n + 1 - 2b)$ was assigned to the ranked values, where *m* denotes the order and *n* denotes the sample size. Numerous methods could be found for determining plotting positions. As per Chow (2010), most plotting positions are empirical formulas and have a parameter, b, which varies accordingly. For normally distributed data, b=3/8 was found to be unbiased, while for extreme value distribution, b=0.44 was found to be the best. For LP-Type III distribution, the parameter b depends on the value of skewness coefficient (C_s); b>3/8, when data is positively skewed, and b<3/8, when the data is negatively skewed. Thereafter, a plot of magnitude vs. probability has been plotted to fit the distribution graphically. Alternatively, the best-fitted distribution obtained from the goodness of fit test is plotted against the plotting position.

10.3.2 Loss-Discharge-Depth relationship

The economic benefits obtained for each season under different depth scenarios were known from the developed optimization framework as discussed in Chapter 8. Alongside, the depth under fluctuant streamflow for different seasons was derived from the hydrodynamic model. From the varying depth, a damage factor was calculated for both the scenarios (S1 and S2), as shown below:

For S1 scenario,

$$DF = 1 - \left\{\frac{d_{obs} - d_{min}}{d_{opt} - d_{min}}\right\} \quad (10.6)$$

For S2 scenario,

$$DF = 1 - \left\{\frac{d_{max} - d_{obs}}{d_{max} - d_{opt}}\right\} \quad (10.7)$$

where, DF= damage factor; d_{obs}= observed water depth (m); d_{min}= minimum water depth (m); d_{max}= maximum water depth (m); d_{opt}= optimal water depth (m).

Using equations 10.6 and 10.7, the damage factor was assigned to each data. The potential economic loss for scenarios S1 and S2 was calculated by multiplying the expected benefits with the damage factor. Thus, the average potential losses were also calculated as:

$$L = \sum_i 0.5 \cdot (f_{i-1} - f_i) \cdot [L(f_{i-1}) + L(f_i)] \quad (10.8)$$

where, L is the economic loss as a function of flood frequency f; i is the index of the frequencies considered.

10.4 Results and Discussion

10.4.1 Analysis of fitted distributions

The five selected distributions were used to fit the streamflow datasets for Rabi and Zaid seasons, as shown in Figure 10.3. The goodness of fit test was used to estimate the parameters of these distributions and the estimated parameter values are shown in Table 10.1. For the Rabi period, the Log Pearson Type 3 (LP-III) and Generalized Extreme Value (GEV) distributions were found to best fit for Scenarios S1 and S2, respectively. For the Zaid period, for both scenarios, the Generalized Extreme Value (GEV) distribution was found to best fit the given data series (Figure 10.4 and 10.5). While performing the statistical analysis of fitted data for different distributions individually, it was found that different tests behaved differently. For scenario S1 during the Rabi period, the Weibull 3P distribution performed best with the K-S test, while for the A-D and Chi-Squared tests, the GEV distribution performed best. For Scenario S2, the GEV distribution was found to be the best for both K-S and A-D tests, while the LP-III distribution was found best using the Chi-Squared test. For scenario S1 during the Zaid period, the performance of three different distributions was found to vary contrarily. According to the K-S test, the Gumbel Max distribution was found to be the best fit distribution. In contrast, the GEV and LP-III distributions were the best distributions while performing the A-D and Chi-Squared tests, respectively. Therefore, based on the rank of the distributions from the three goodness of fit tests, the best distribution was selected.

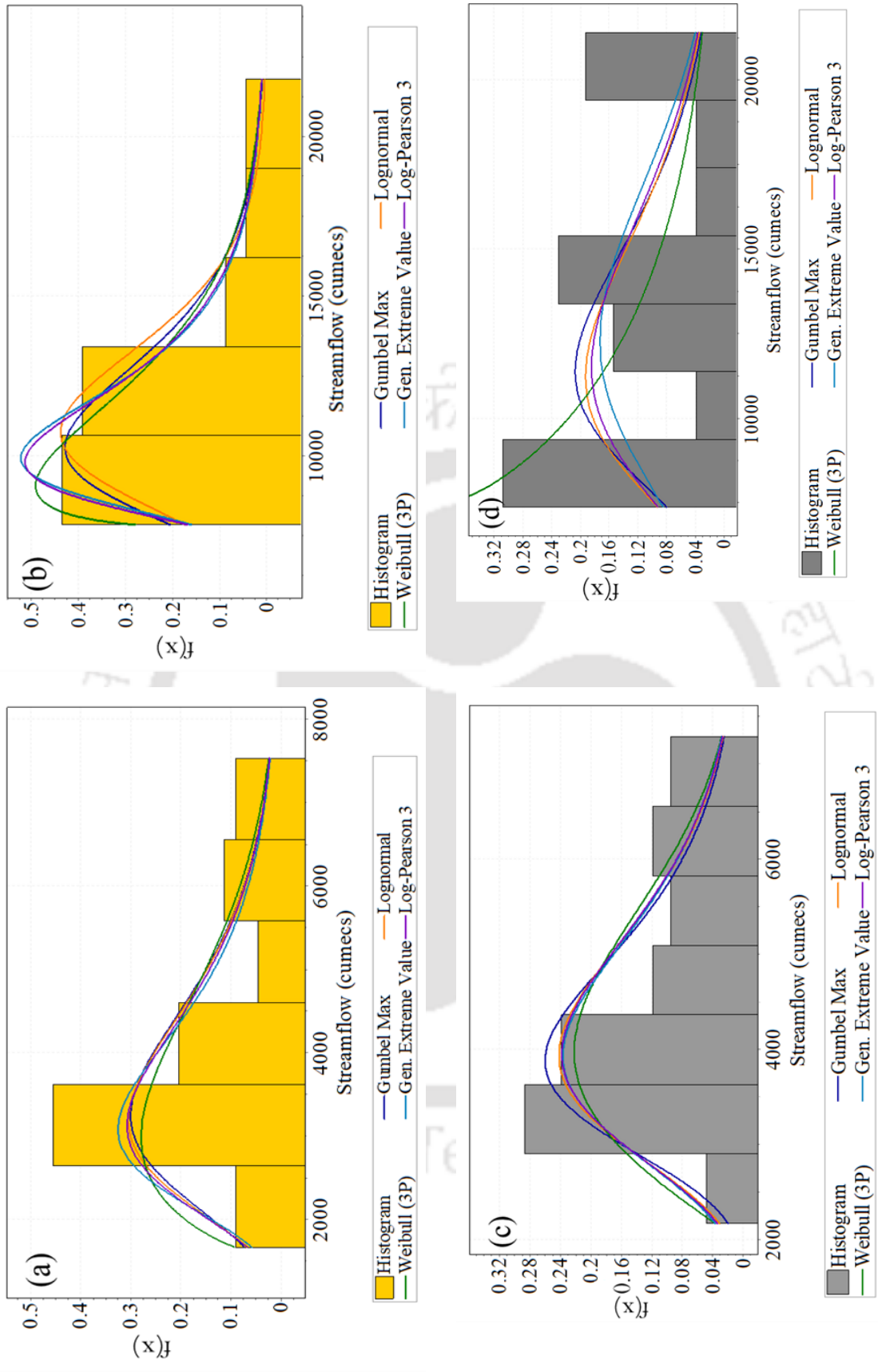

Figure 10.3: The fitting histograms of the five distributions. (a) Zaid period for scenario S1; (b) Zaid period for scenario S2; (c) Rabi period for scenario S1; (d) Rabi period for scenario S2.

Table 10.1: (a) Goodness of fit tests for scenario S1 for the Rabi period

Distributions	**parameters**						**K-S**		**A-D**		**Chi squared**			
	k	sigma	mu	alpha	gamma	beta	statistic	Rank	statistic	Rank	statistic	p-value	Rank	Sum
GEV	-0.0491	1138.2	3869.3				0.087	2	0.38	1	0.84	0.97	1	4
Gumbel max		1034.5	3876.4				0.1	5	0.487	4	0.67	0.66	5	14
LP3				2587	23.48	-0.0058	0.09	3	0.4	2	0.85	0.973	2	7
Weibull 3P				2	1964.9	2831.3	0.085	1	0.41	5	0.97	0.965	4	10
LN		0.293	8.36				0.095	4	0.411	3	0.853	0.97	3	10

Table 10.1 (b) : Goodness of fit tests for scenario S2 for the Rabi period

Distributions	**parameters**						**K-S**		**A-D**		**Chi squared**			
	k	sigma	mu	alpha	gamma	beta	statistic	Rank	statistic	Rank	statistic	p-value	Rank	Sum
GEV	-0.161	4320.9	11537				0.138	1	0.591	1	3.03	0.38	4	6
Gumbel max	3554.5	11379					0.152	4	1.01	4	2.32	0.313	3	11
LP3				125.02	13.41	-0.0316	0.131	2	0.691	2	1.65	0.436	1	5
Weibull 3P				0.961	7386	5692.5	0.22	5	5.1(reject)	5	NA		5	15
LN		0.346	9.45				0.132	3	0.781	3	1.89	0.38	2	8

Table 10.2: (a) Goodness of fit tests for scenario S1 for the Zaid period

Distributions	**parameters**						**K-S**		**A-D**		**Chi squared**			
	k	sigma	mu	alpha	gamma	beta	statistic	Rank	statistic	Rank	statistic	p-value	Rank	Sum
GEV	0.0951	1109	3178.9				0.122	3	0.579	1	1.11	0.892	2	6
Gumbel max		1197.7	3241.7				0.118	1	0.677	4	2.9	0.411	5	10
LP3				376.7	0.846	0.0192	0.123	4	0.615	2	0.523	0.913	1	7
Weibull 3P				1.6	1542.9	2662.5	0.142	5	0.736	5	2.51	0.641	3	13
LN		0.374	8.21				0.118	2	0.661	3	2.56	0.633	4	9

Table 10.2 (b) : Goodness of fit tests for scenario S2 for the Zaid period

Distributions	**parameters**						**K-S**		**A-D**		**Chi squared**			
	k	sigma	mu	alpha	gamma	beta	statistic	Rank	statistic	Rank	statistic	p-value	Rank	Sum
GEV	0.138	1983.5	10184				0.121	3	0.268	1	0.03	0.85	1	5
Gumbel max		2395.4	10259				0.114	1	0.34	3	1.26	0.73	5	9
LP3				5.35	8.78	0.101	0.123	4	0.291	2	0.341	0.56	3	9
Weibull 3P				1.28	7752.7	4187.7	0.148	5	0.421	5	0.267	0.87	2	12
LN		0.231	9.33				0.117	2	0.363	4	1.14	0.765	4	10

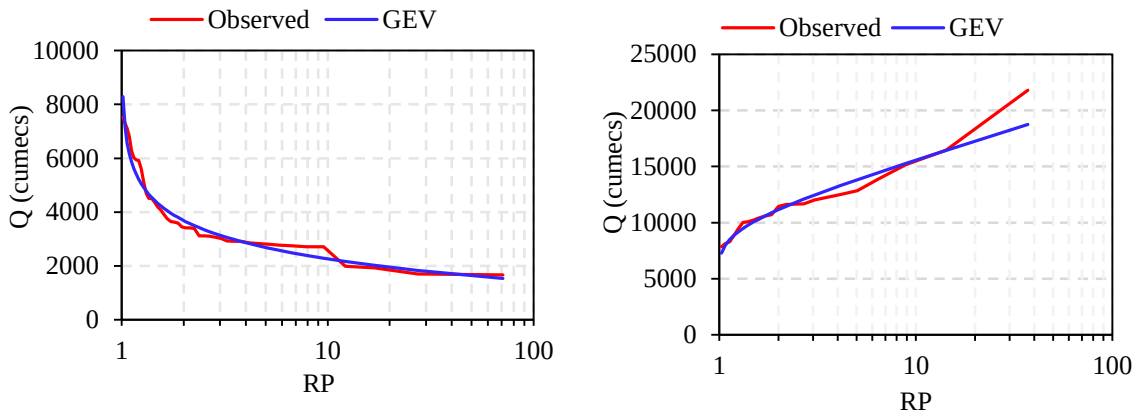

Figure 10.4:(a) GEV distribution, and (b) GEV distribution fitting with observed streamflow for S1 and S2, respectively, for the Zaid period

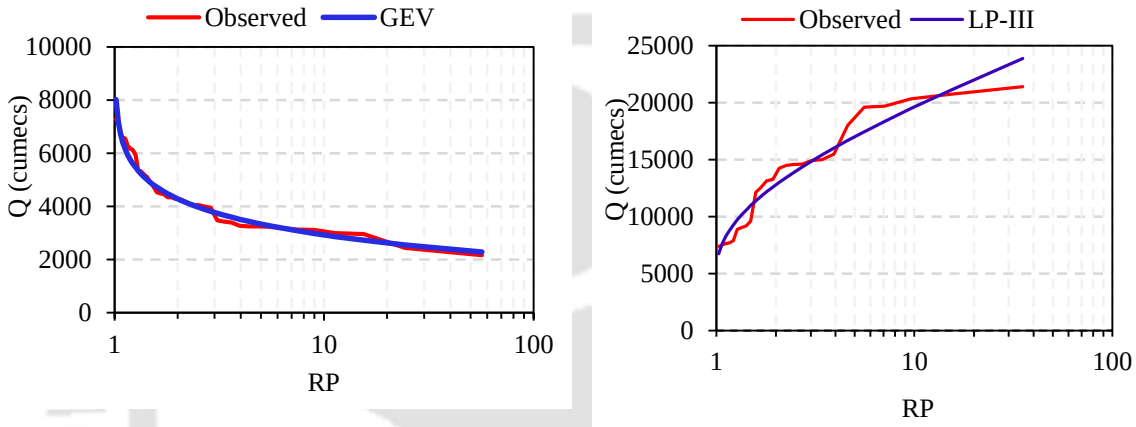

Figure 10.5: (c) GEV distribution, and (d) LP-III distribution fitting with observed streamflow for S1 and S2, respectively, for the Rabi period.

10.4.2 Agriculture risk assessment

Flood risk assessment involves a reduction in the probability of flooding and its potential adverse consequences on the environment, human health, cultural heritage, and socio-economic activities. In the context of this study, risk assessment was limited to the agriculture sector, wherein activities such as farming, cropping, fishing etc., are performed within the riverine sandbars. Promoting sustainable risk management measures and opportunities to work with natural processes are some strategies to benefit from flood risk management. The economic evaluation of flood damage to crops is necessary for decision-making. A widespread loss makes financial recovery particularly difficult and challenging (Barnett et al., 2008).

The study was conducted by observing the streamflow for the period 1999-2015 during the Rabi and Zaid seasons. It evaluated the loss corresponding to different streamflow under

fluctuant water depths. The magnitude of streamflow obtained using the best-fitted distribution during different periods varies. This could lead to drought-like conditions or flood situations, depending on the type of crops grown, weather, seasons, distance from the water bodies, etc. As discussed, Scenario S1 corresponds to a depth below the optimal depth. The basis of such consideration is that certain crops (e.g., Jute, Boro Paddy, and other submergence varieties) could suffer damage if a certain water depth is not maintained during its growth stage. Once the crops were cultivated and the expected water level does not reach the crop fields, it would incur damage resulting in potential economic loss to the farmers. The losses were determined by assigning a damage factor to each depth that changes below the optimal depth. From the cumulative loss-discharge curve (Figure 10.6 (a)), it can be seen that the loss suffered was sufficiently high when the discharge was low and decreased as the water level reaches near optimum for the scenario, S1. When the water level is at the optimal depth, there is no loss to the crops. As the water level diminishes from the optimal depth (0.9m in this case), or in other way, when the water level has not reached the particular depth stage, the loss increases at that stage (say under the *p*-stage). The slope change in the loss discharge curve is because the flood depth and related losses do not grow linearly with discharge. This is because different crops provide different benefits (discussed in Chapter 8), and cumulative assessment of loss results in a non-linear variation. For scenario S2, as the depth increases beyond the optimal depth, the crops grown in the dryland areas suffer damage. The extent of damage depends on the area of inundation and crops grown in the region. The Loss-Damage-Depth plots (Figure 10.6(b)) show the relationship between the potential economic loss and the changing water depth. Similarly, the damage assessment for both scenarios could be found during the Rabi period (Figure 10.7). However, the extent of risk within a riverine ecosystem varies depending on the streamflow variability.

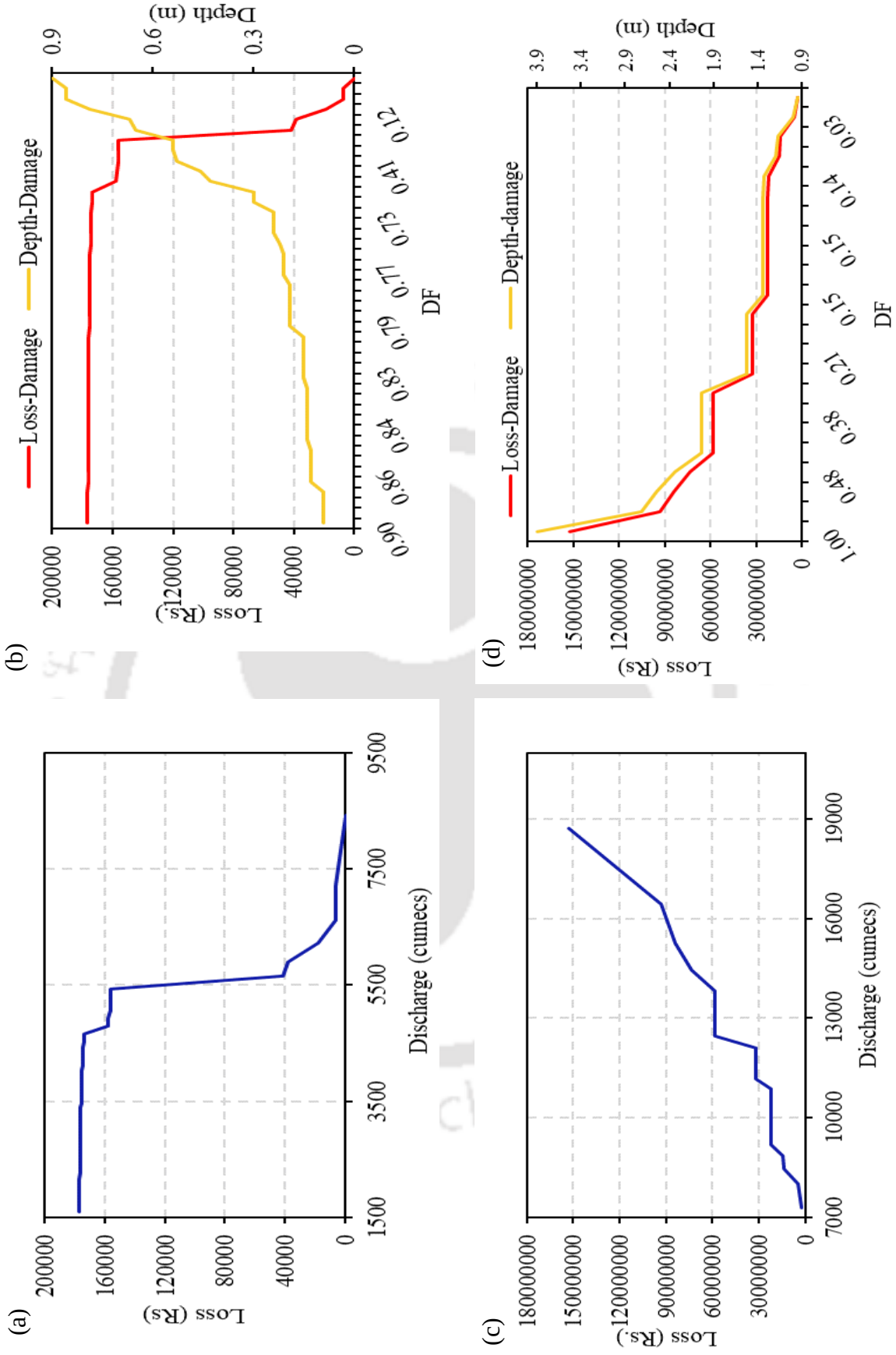

Figure 10.6 Plots showing the relationship between the cumulative (a) Loss-discharge (b) Loss-depth, for scenario S1, and cumulative (c) Loss discharge, (d) Loss-depth, for scenario S2, for the Zaid period

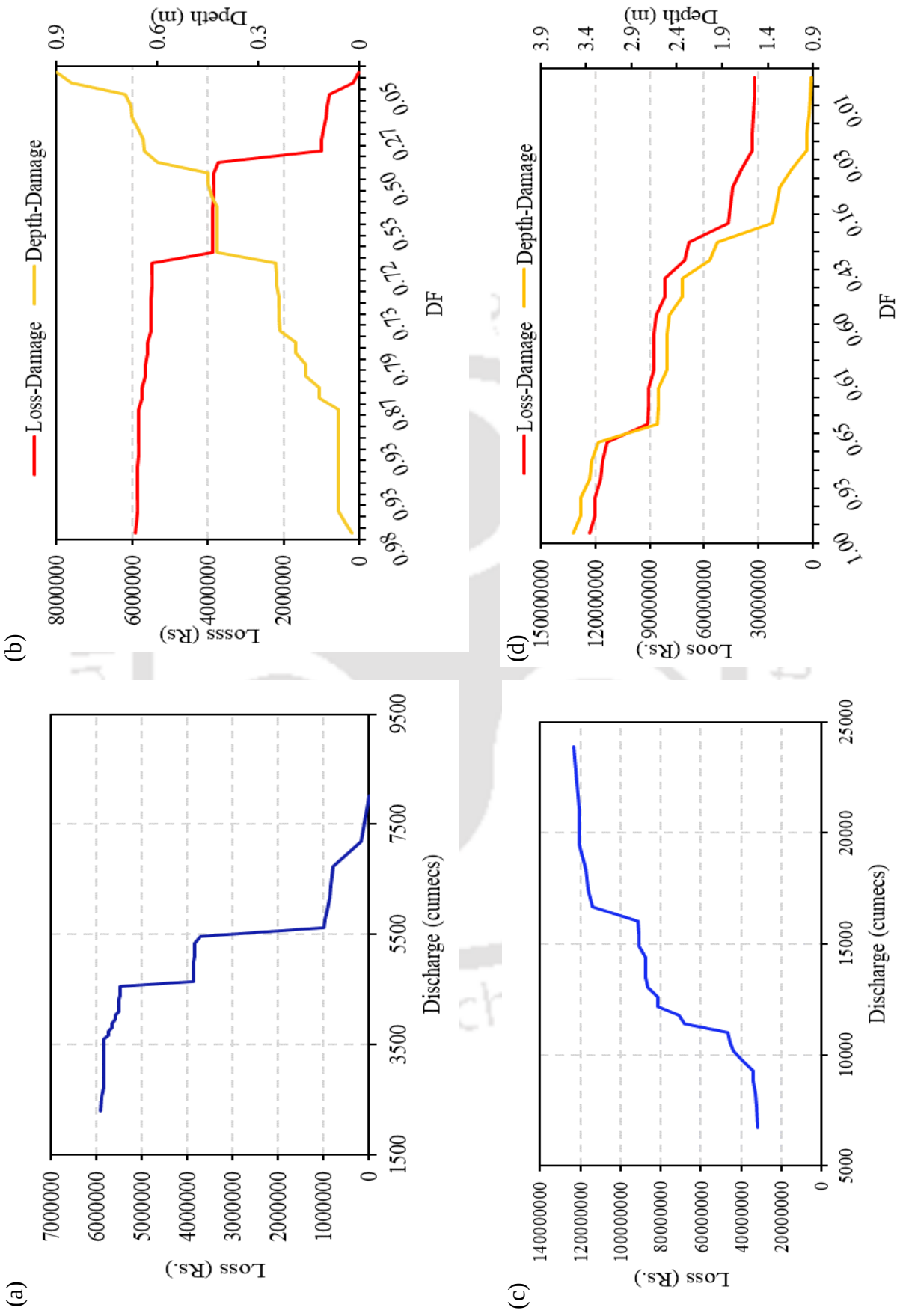

Figure 10.7 Plots showing the relationship between the cumulative (a) Loss-discharge (b) Loss-depth, for scenario S1, and cumulative (c) Loss discharge, (d) Loss-depth, for scenario S2, for the Rabi period

10.4.3 Adaptation strategies and decision making

The flood phenomenon can be viewed as an environmental risk. Riverine inhabitants are most vulnerable to risks and suffer significant agricultural losses due to the absence of risk mitigation strategies. The risk of flood, drought, and extreme events to communities depends on the probability of a flood occurring and the consequences of events. Recognizing the adverse effects of flood events in the agriculture sector, policymakers and researchers have devoted themselves to reducing the adverse effect of flood disasters on agriculture. Subsequently, empirical studies have been conducted to identify farm households' adaptation strategies to flood events (Alhassan, 2020). Risks may be reduced by a combination of adaptation and mitigation measures. While adaptation refers to actions to reduce flooding impacts, mitigation, on the other hand, refers to modifying the source to reduce the probability of flooding. The direct impact on food security comes from damage to standing food crops, stored grains, and livestock, while the indirect effects include low purchasing power, compromised health, and lack of modern facilities. Both low and high water levels could lead to risk in agriculture, leading to drought-like situations and high flood conditions, respectively. Crop insurance could be considered an essential agricultural risk mitigation tool to protect farmers from natural disasters and agricultural sustainability. It is a non-structural measure for flood management, and it can assist in the ex-ante management of flood risks by reducing the financial risks from flooding (Surminski and Oramas-Dorta, 2014). However, the willingness to pay for insurance depends on various factors such as the size of land, type of crops, location of cropping, distance from the water body, age, market reach, demand, etc. From the questionnaire surveys conducted over various households within the sandbars, it could be understood that the farmers who were risk averse were more likely to obtain insurance and were willing to pay for flood insurance for their crops. On the other hand, farmers practicing poultry and farming activities were hesitant to opt for insurance as such activities did not involve risk resulting from water level fluctuations in the sandbars.

10.5 Conclusions

The study's findings implied that most farmers residing within the riverine environment perceived high risk and also confront erosions, which worsened during the monsoon season due to the braided nature of the Brahmaputra River. However, the low and high water levels

could simultaneously lead to the problem of drought and flood in the riverine agricultural environment. The consecutive dry and wet days could affect the cropping pattern in different seasons. The potential losses were estimated within the study region by combining the depth-frequency and loss-discharge relationships. The study reflected two risk assessment scenarios in a riverine sandbar wherein scenario S1 considered the potential economic losses pertaining to depths below a certain threshold, while the second scenario, S2, assessed the potential losses relating to depths above the defined threshold during two cropping seasons. It was observed that the loss varied differently under different depth stages, which did not vary linearly. It could be established that significant losses could be incurred if the water level does not reach the desired depths. The results showed that various factors influenced farmers' flood insurance purchasing decisions. Farmers' group was significantly and positively associated with farmers' decision to purchase flood insurance. Small land-holding farmers with low income were interested in purchasing insurance schemes; however, the major concern for sustaining agriculture was the seed cost, fertilizer cost, cold storage facilities, and transport services. Households with large family members were less likely to pay for flood insurance premiums than households with small family members, which was found consistent with the findings of Wairimu et al. (2016). Agriculture and farming activities in riverine ecosystem is a dynamic process due to hydrological and morphological changes within the rivers. The adaptation measures such as using drought and flood resistant varieties of crops, optimal cropping pattern, crop diversification, shifting of planting periods, willingness to pay for insurances etc. could reduce the risk and encourage farmers towards socio-economic development. While formulating the insurance schemes, the socio-economic characteristics of flood-affected rural farm households within riverine ecosystems and their risk perceptions and attitudes should be carefully considered.

11

Conclusions and Recommendations for future work

11.1 A brief overview of work done

The research primarily encompasses the life around the riverine ecosystem, the services it provides and the competence of the dwellers, farmers and people to utilize it in the best possible way. In Assam, sandbars locally known as chars, developed within the Brahmaputra River and its tributaries are an important part of the landscape and ecology. They emerge from sandy alluvial deposits across floodplains and within the rivers through the process of aggradation and degradation providing numerous essential services. To understand the utilization capability of these riverine sandbars for crop growth and other income generating activities, it is essential to study its characteristics. In this research, the land-use change over the decades, agricultural and farming practices during different seasons as well as mapping the agricultural activities and their variations over time using geospatial techniques was studied within the Brahmaputra River in Assam. In addition to satellite studies, questionnaire surveys and data collection were performed. Lastly, an optimization model was developed along with a damage estimation model to estimate the actual benefit, potential economic losses, and evaluated the crop risk assessment through frequency analysis.

11.2 General discussion and conclusions

The study presented the scope of utilization of the riverine ecosystem and addressed the challenges faced during its utilization. Agriculture and farming activities being the most important provisioning services, an in-depth analysis of those services for the benefit of humankind is necessary. Agriculture not only contributes to essential ecological services but also changes and modifies other services in addition to delivering significant ecosystem benefits. Therefore, a detailed analysis of the riverine ecosystem has been carried out in the present work. The work was divided into different components. In the initial stage, the spatiotemporal variation of the land use land cover within the Brahmaputra River was analysed using satellite imageries. The work was initiated by carrying out a satellite-based study, followed by field investigations and questionnaire surveys that provided details about the crop type cultivated, the cropping pattern, age of farmers, duration, profit, production, etc. It was found that the percentage of dry sandbars remained more or less unchanged while the croplands and vegetation increased over the years. From the analysis, it could be inferred that dry sandbars within the riverine ecosystem were utilized for cropping and other agricultural activities. The spectral analysis provided information on different crop growth stages, i.e., sowing, plantation, harvesting, etc., with the interannual variation of NDVI showing the practice of double cropping within the sandbars. However, no specific planning of crops can be seen cultivated. The study envisaged the necessity to make people understand the need for such studies for their development and the socio-economic development of society.

To develop a framework for suggesting optimal cropping patterns, the field observations and questionnaire responses were integrated to derive potential economic benefits. Unorganized agriculture is traditionally practiced in these sandbars. Using the mathematical models, the dynamic behaviour and sandbar area available within the study reach could be specified. The study's findings revealed new insights into the flow dynamics within the sandbars, a broad understanding of food production in barren yet fertile sandbars, income and asset generation, increased food consumption, improved nutrition, and alternative risk management strategies during lean periods. From the simulated water depth, the sandbar area available during different seasons was determined for planning agricultural activities. The study on nutrient analysis has shown the potential of sandbars for agricultural purposes with the presence of both macronutrients and micronutrients essential

for plant growth. This analysis has also given a good insight into the soil characteristics of different sandbars. The cultivated sandbars contained less silt and clay as compared to vegetated sandbars and were well-graded, while the newly developed sandbars were poorly graded.

The use of short-term or seasonal forecast information could benefit the farmers in crop planning; however, it depends on how well these parameters could be predicted and how much this information helps in the actual decision-making process. The study demonstrated the usefulness of short-term flow forecasting in deriving optimal agricultural planning in a riverine ecosystem. The method used contains the historical information of the recent past events and uses that information to predict the future flow. The results obtained from the monthly streamflow trend analysis showed a significant increasing trend in the month of December-February. The findings of the study showed that the knowledge of both forecasting and optimization together could deal with the near future events in the agricultural sector accurately, which in turn could help tackle the associated damages and provide a judgment of selective cropping in such a riverine environment. By comparing the net economic benefits derived from the optimal cropping pattern and the existing cropping pattern, an increase in the net benefit of ~26% was found. Furthermore, in many real-world situations, uncertainties exist in the system components that could affect the decision-making processes. Moreover, uncertainties in the riverine ecosystem are unavoidable and frequent depending on various climatic and hydrological factors and human-induced impreciseness and fuzziness. Therefore, such vagueness was very well handled by the optimization framework, and the solutions derived could provide room for the decision maker with different levels of satisfaction.

With the increase in water level in rivers and streams, the cultivable area decreases, demanding selective crop planning. A damage estimation model was developed to assess crop damages at fluctuant water levels. The advantages of the model are its simplicity in terms of applicability and tuning it with few parameters. Integrating an agricultural damage estimation model with an optimization framework can help policymakers plan crop planning more efficiently, thereby increasing food supply and improving socio-economic status. With the practice of sandbar cropping and farming in riverine environments, farmers and dwellers need to understand risk and have risk management skills to anticipate problems better and reduce consequences. The study's findings implied that most farmers residing within the riverine environment perceived high risk and also confronted erosions,

which worsened during the monsoon season due to the braided nature of the Brahmaputra River. It was observed that the loss varied differently under different depth stages, which did not vary linearly. The adaptation measures, such as using drought and flood-resistant varieties of crops, optimal cropping patterns, crop diversification, shifting of planting periods, willingness to pay for insurance, etc., could reduce the risk and encourage farmers towards socio-economic development. Therefore, this study presents an overall understanding of the agricultural practices and the derived benefits and associated losses in riverine sandbars through a conceptual framework.

11.3 Scope of future work

This study provides a framework for integrating modelling techniques with optimization approaches in an agricultural system under uncertainties within the riverine ecosystem. The study also classified various sandbar types for the suitability of different crops. Although activities within the river involves the risk of crop damage due to water level fluctuations, adaptation strategies were suggested in the current research.

As a future extension of the current research, the scope of the study is discussed as follows:

- Satellite imageries from Landsat 7 and 8 provide information about the changes and phenological characteristics of crops grown in the sandbars. However, to distinguish between different crop types finer resolution imageries are needed, that could provide detailed information on crop health as well.
- The study was carried out in the Brahmaputra River; however, the study could be extended to different rivers around the world, as the sediment characteristics could vary widely.
- The damage estimation model developed in the study could handle the crop damage suffered due to water level fluctuations during different seasons. However, there is scope to improve the model by incorporating the maximum number of flood or dry days and determining the extent of crop damage suffered.
- In the optimization model, economic benefits through agricultural practices in sandbars were considered. However, maximizing benefit by incorporating the profit earned through sand mining used as a construction material could be considered as a scope for future work.

- The downstream impact of the potential risk of using fertilizer on water quality and the self-purification capacity of rivers is necessary to understand. An ecological model could be developed and linked with the optimization model to better understand the future impacts on the aquatic species.
- River ecosystems could become more vulnerable to climate change. Understanding the climate change impact on the aquatic habitats, as how various species would react to agriculture within sandbars, is necessary. Will the fertilizers serve as nutrients for the species, or is it declining its habitats leading to its extinction?

References

Aerts, J. C., Eisinger, E., Heuvelink, G., and Stewart, T. J. (2003). Using linear integer programming for multi-site land-use allocation. Geographical Analysis, 35(2), 148-169.

Aggarwal, P. K., Kalra, N., Chander, S., and Pathak, H. (2006). InfoCrop: a dynamic simulation model for the assessment of crop yields, losses due to pests, and environmental impact of agro-ecosystems in tropical environments. I. Model description. Agricultural systems, 89(1), 1-25.

Akhtar, M. P. (2011). 2-d depth averaged modelling for curvilinear braided stretch of Brahmaputra River.

Alhassan, H. (2020). Farm households' flood adaptation practices, resilience and food security in the Upper East region, Ghana. Heliyon, 6(6), e04167. https://doi.org/10.1016/j.heliyon.2020.e04167

Al-talib, G. A., and Ahmed, E. Z. (2013). Land Cover Classification Using Hidden Markov Models. International Journal of Computer Networks and Communications Security, 1(4), 165–172.

Anderson, C. C., and Renaud, F. G. (2021). A review of public acceptance of nature-based solutions: The 'why','when', and 'how'of success for disaster risk reduction measures. Ambio, 50(8), 1552-1573. https://doi.org/10.1007/s13280-021-01502-4

Anderson, R., Bayer, P. E., and Edwards, D. (2020). Climate change and the need for agricultural adaptation. Current opinion in plant biology, 56, 197-202.

Anderson, R., Bayer, P. E., and Edwards, D. (2020). Climate change and the need for agricultural adaptation. Current opinion in plant biology, 56, 197-202.

Anwar, A. A., and Haq, Z. U. (2013). Genetic algorithms for the sequential irrigation scheduling problem. Irrigation Science, 31(4), 815–829.

Apel, H., Aronica, G. T., Kreibich, H., and Thieken, A. H. (2009). Flood risk analyses—how detailed do we need to be?. Natural hazards, 49(1), 79-98.

Arciniegas, G., Janssen, R., and Omtzigt, N. (2011). Map-based multicriteria analysis to support interactive land use allocation. International Journal of Geographical Information Science, 25(12), 1931-1947.

Bahrami, S., Ardejani, F. D., and Baafi, E. (2016). Application of artificial neural network coupled with genetic algorithm and simulated annealing to solve groundwater inflow problem to an advancing open pit mine. Journal of Hydrology, 536, 471-484. https://doi.org/10.1016/j.jhydrol.2016.03.002

Bai, Y., Chen, Z., Xie, J., and Li, C. (2016). Daily reservoir inflow forecasting using multiscale deep feature learning with hybrid models. Journal of hydrology, 532, 193-206. https://doi.org/10.1016/j.jhydrol.2015.11.011

Banerjee, C., and Kumar, D. N. (2018). Analysing large-scale hydrologic processes using GRACE and hydrometeorological datasets. Water Resources Management, 32(13), 4409-4423.

Barbour, E. J., Holz, L., Kuczera, G., Pollino, C. A., Jakeman, A. J., and Loucks, D. P. (2016). Optimisation as a process for understanding and managing river ecosystems. Environmental Modelling and Software, 83, 167-178. https://doi.org/10.1016/j.envsoft.2016.04.029

Barik, B., Ghosh, S., Saheer Sahana, A., Pathak, A., and Sekhar, M. (2017). Water-food-energy nexus with changing agricultural scenarios in India during recent decades. Hydrology and Earth System Sciences, 21(6), 3041–3060. https://doi.org/10.5194/hess-21-3041-2017

Barman, B., Kumar, B., and Sarma, A. K. (2019). Impact of sand mining on alluvial channel flow characteristics. Ecological Engineering, 135, 36-44.

Barman, S., and Bhattacharjya, R. K. (2020). ANN-SCS-based hybrid model in conjunction with GCM to evaluate the impact of climate change on the flow scenario of the River Subansiri. Journal of Water and Climate Change, 11(4), 1150-1164.

Barnett, B. J., Barrett, C. B., and Skees, J. R. (2008). Poverty traps and index-based risk transfer products. World Development, 36(10), 1766-1785. https://doi.org/10.1016/j.worlddev.2007.10.016

Baruah, A., and Sarma, A. K. (2021). Ecological flow assessment using hydrological and hydrodynamic routing model in Bhogdoi river, India. Modeling Earth Systems and Environment, 7(4), 2453-2462.

Bates, P. D., and De Roo, A. P. J. (2000). A simple raster-based model for flood inundation simulation. Journal of Hydrology, 236(1–2), 54–77. https://doi.org/10.1016/S0022-1694(00)00278-X

Benfield, A. (2016). 2016 annual global climate and catastrophe report.

Bishop, Y. M. M., Fienberg, S. E., Holland, P. W., Light, R. J., and Mosteller, F. (1977). Book Review : Discrete Multivariate Analysis: Theory and Practice. Applied Psychological Measurement, 1(2), 297–306. https://doi.org/10.1177/014662167700100218

Bouma, J. J., François, D., and Troch, P. (2005). Risk assessment and water management. Environmental Modelling and Software, 20(2), 141-151.

Bradford, R.A., O'Sullivan, J.J., Van der Craats, I.M., Krywkow, J., Rotko, P., Aaltonen, J., Bonaiuto, M., De Dominicis, S., Waylen, K. and Schelfaut, K. (2012). Risk perception–issues for flood management in Europe. Natural hazards and earth system sciences, 12(7), 2299-2309. https://doi.org/10.5194/nhess-12-2299-2012

Brémond, P., and Grelot, F. (2013). Review Article: Economic evaluation of flood damage to agriculture - Review and analysis of existing methods. Natural Hazards and Earth System Sciences, 13(10), 2493–2512. https://doi.org/10.5194/nhess-13-2493-2013

Brown, J. D., and Damery, S. L. (2002). Managing flood risk in the UK: towards an integration of social and technical perspectives. Transactions of the institute of British Geographers, 27(4), 412-426. https://doi.org/10.1111/1475-5661.00063

Buchecker, M., Ogasa, D. M., and Maidl, E. (2016). How well do the wider public accept integrated flood risk management? An empirical study in two Swiss Alpine valleys. Environmental Science and Policy, 55, 309-317. https://doi.org/10.1016/j.envsci.2015.07.021

Cai, X., Wallington, K., Shafiee-Jood, M., and Marston, L. (2018). Understanding and managing the food-energy-water nexus–opportunities for water resources research. Advances in Water Resources, 111, 259-273.

Chakraborty, G. (2013). Assam's hinterland: Society and economy in the Char areas.

Chakravarty, D.N., Sehgal, J.L. and Dev, G. (1978) Influence of climate and topography on the pedogenesis of alluvium-derived soils of Assam. Indian J. Agric. Chem 11: 77-97

Chamling, M., and Bera, B. (2020). Spatio-temporal patterns of land use/land cover change in the Bhutan–Bengal foothill region between 1987 and 2019: study towards geospatial applications and policy making. Earth Systems and Environment, 4(1), 117-130.

Chausson, A., Turner, B., Seddon, D., Chabaneix, N., Girardin, C. A., Kapos, V., ... and Seddon, N. (2020). Mapping the effectiveness of nature-based solutions for climate change adaptation. Global Change Biology, 26(11), 6134-6155. https://doi.org/10.1111/gcb.15310

Chen, D., Huang, J., and Jackson, T. J. (2005). Vegetation water content estimation for corn and soybeans using spectral indices derived from MODIS near- and short-wave infrared bands. Remote Sensing of Environment, 98(2–3), 225–236. https://doi.org/10.1016/j.rse.2005.07.008

Chen, W., Carsjens, G. J., Zhao, L., and Li, H. (2014). A spatial optimization model for sustainable land use at regional level in China: A case study for Poyang Lake Region. Sustainability, 7(1), 35-55.

Cihlar, J. (2000). Land cover mapping of large areas from satellites: status and research priorities. International journal of remote sensing, 21(6-7), 1093-1114. https://doi.org/10.1080/014311600210092

Cohen, J. (1960). A coefficient of agreement for nominal scales. Educational and psychological measurement, 20(1), 37-46. https://doi.org/10.1177/001316446002000104

Conner, J. T., and Tonina, D. (2014). Effect of cross-section interpolated bathymetry on 2D hydrodynamic model results in a large river. Earth Surface Processes and Landforms, 39(4), 463-475. https://doi.org/10.1002/esp.3458

Corey, R. B., and Schulte, E. E. (1973). Factors affecting the availability of nutrients to plants. Soil testing and plant analysis, 23-33.

Costanza, R., R. d'Arge, R. de Groot, S. Farber, M. Grasso, B. Hannon, K. Limburg, S. Naeem, R.V. Oneill, J. Paruelo, R. G. Raskin, P. Sutton, and M. van den Belt. 1997. The value of the world's ecosystem services and natural capital. Nature 387 (6630): 253–260.

Coulthard, T. J., and Van De Weil, M. J. (2012). Modelling river history and evolution. Philosophical transactions of the royal society, Phil. Trans. R. Soc. A (2012) 370, 2123–2142.

Cunge, J. A., Holly, F. M., and Verwey, A. (1980). Practical aspects of computational river hydraulics.

Daghighi, A., Nahvi, A., and Kim, U. (2017). Optimal cultivation pattern to increase revenue and reduce water use: Application of linear programming to Arjan plain in Fars province. Agriculture (Switzerland), 7(9). https://doi.org/10.3390/agriculture7090073

Dancey, C. P., and Reidy, J. (2007). Statistics without maths for psychology. Pearson education.

de Groot, R., L. Brander, S, van der Ploeg, R. Costanza, F. Bernard, L. Braat, M. Christie, N. Crossman, A. Ghermandi, L. Hein, S. Hussain, P. Kumar, A. McVittie, R. Portela, L.C. Rodriguez, P. ten Brink, and P. van Beukering. 2012. Global estimates of the value of ecosystems and their services in monetary units. Ecosystem Services 1: 50–61.

DEFRA (Department for Environment, Food and Rural), 2000. Guidelines for environmental risk assessment and management. London

Dhanya, P., and Ramachandran, A. (2015). Farmers' perceptions of climate change and the proposed agriculture adaptation strategies in a semi-arid region of south India. Journal of Integrative Environmental Sciences, 13(1), 1-8.

DHI, M. (2007). A Modelling System for Rivers and Channels. Reference Manual. DHI Water and Environment, Denmark.

Di Baldassarre, G., Castellarin, A., Montanari, A., and Brath, A. (2009). Probability-weighted hazard maps for comparing different flood risk management strategies: a case study. Natural Hazards, 50(3), 479-496. https://doi.org/10.1007/s11069-009-9355-6

Ding, Y., Hayes, M. J., and Widhalm, M. (2011). Measuring economic impacts of drought: a review and discussion. Disaster Prevention and Management: An International Journal. Vol. 20 No. 4, pp. 434-446. https://doi.org/10.1108/09653561111161752

Doulgeris, C., Georgiou, P., Papadimos, D., and Papamichail, D. (2012). Ecosystem approach to water resources management using the MIKE 11 modelling system in the Strymonas River and Lake Kerkini. Journal of environmental management, 94(1), 132-143.

Downton, M. W., and Pielke, R. A. (2005). How accurate are disaster loss data? The case of US flood damage. Natural Hazards, 35(2), 211-228.

Dutta, D., Herath, S., and Musiake, K. (2003). A mathematical model for flood loss estimation. Journal of Hydrology, 277(1–2), 24–49. https://doi.org/10.1016/S0022-1694(03)00084-2

Dutta, P., and Sarma, A. K. (2021). Hydrological modeling as a tool for water resources management of the data-scarce Brahmaputra basin. Journal of Water and Climate Change, 12(1), 152-165.

El-Gafy, I., Grigg, N., and Waskom, R. (2017). Water-Food-Energy: Nexus and Non-Nexus Approaches for Optimal Cropping Pattern. Water Resources Management, 31(15), 4971–4980. https://doi.org/10.1007/s11269-017-1789-0

Endo, A., Burnett, K., Orencio, P. M., Kumazawa, T., Wada, C. A., Ishii, A., … Taniguchi, M. (2015). Methods of the water-energy-food nexus. Water (Switzerland), 7(10), 5806–5830. https://doi.org/10.3390/w7105806

Enggrob, H. and Tjerry, S. (1999) Simulation of morphological characteristics of a braided river. Proceedings of RCEM, IAHR symp. on River, Coastal and Estuarine Morphodynamics, Genova, Italy.

Fahad, S., Wang, J., Hu, G., Wang, H., Yang, X., Shah, A.A., Huong, N.T.L. and Bilal, A., (2018). Empirical analysis of factors influencing farmers crop insurance decisions in Pakistan: Evidence from Khyber Pakhtunkhwa province. Land use policy, 75, 459-467.

Fahimi, F., Yaseen, Z. M., and El-shafie, A. (2017). Application of soft computing based hybrid models in hydrological variables modeling: a comprehensive review. Theoretical and applied climatology, 128(3), 875-903. https://doi.org/10.1007/s00704-016-1735-8

FAO. (2015) Lakes and rivers key to livelihoods of millions, https://www.fao.org/news/story/en/item/276122/icode/

Fathian, F., Mehdizadeh, S., Sales, A. K., and Safari, M. J. S. (2019). Hybrid models to improve the monthly river flow prediction: Integrating artificial intelligence and non-linear time series models. Journal of Hydrology, 575, 1200-1213. https://doi.org/10.1016/j.jhydrol.2019.06.025

Fedele, G., Donatti, C. I., Harvey, C. A., Hannah, L., and Hole, D. G. (2019). Transformative adaptation to climate change for sustainable social-ecological systems.

Environmental Science and Policy, 101, 116-125. https://doi.org/10.1016/j.envsci.2019.07.001

Fisher, B., R.K. Turner, and P. Morling. (2009). Defining and classifying ecosystem services for decision making. Ecological Economics 68 (3): 643–653. https://doi.org/10.1016/j.ecolecon.2008.09.014.

Food and Agricultural Organization (FAO),1993. Guidelines for Land Use Planning; Food and Agricultural Organization of the United Nations: Rome, Italy,

FSIN, A. (2020). 2020 Global report on food crises: Joint analysis for better decisions. Rome, Italy and Washington, DC: Food and Agriculture Organization (FAO); World Food Programme (WFP); and International Food Policy Research Institute (IFPRI). https://www.fsinplatform.org/global-report-food-crises-2020

Fukue, K., Shimoda, H., Matumae, Y., Yamaguchi, R., and Sakata, T. (1988a). Evaluations of unsupervised methods for land-cover/use classifications of landsat TM data. Geocarto International, 3(2), 37–44. https://doi.org/10.1080/10106048809354147

Gandhi, G. M., Parthiban, B. S., Thummalu, N., and Christy, A. (2015). Ndvi: Vegetation change detection using remote sensing and gis–A case study of Vellore District. Procedia computer science, 57, 1199-1210.

Ganji, A., Ponnambalam, K., Khalili, D., and Karamouz, M. (2006). A new stochastic optimization model for deficit irrigation. Irrigation Science, 25(1), 63–73.

Gao, B. (1996). NDWI—A normalized difference water index for remote sensing of vegetation liquid water from space. Remote Sensing of Environment, 58(3), 257–266. https://doi.org/https://doi.org/10.1016/S0034-4257(96)00067-3

Gao, Y., Skutsch, M., Paneque-Gálvez, J., and Ghilardi, A. (2020). Remote sensing of forest degradation: a review. Environmental Research Letters, 15(10), 103001. https://doi.org/10.1088/1748-9326/abaad7

Garg, N. K., and Dadhich, S. M. (2014). Integrated nonlinear model for optimal cropping pattern and irrigation scheduling under deficit irrigation. Agricultural Water Management, 140, 1–13. https://doi.org/10.1016/j.agwat.2014.03.008

Girbaciu, A., Girbaciu, C., and Rosu, S. E. R. B. A. N. (2016). Water quality modeling of Bega River using MIKE 11. Materiale Plastice, 53(3), 533-536.

Government of Assam (GoA) Assam Human Development Report 2014 Guwahati http://niti.gov.in/writereaddata/files/human-development/Assam_HDR_30Sep2016.pdf

Govindaraju Rao S. (2000). Artificial Neural Networks in Hydrology. Journal of Hydrologic Engineering, 5(April), 124–137. https://doi.org/10.1007/978-94-015-9341-0

Greger, M., Landberg, T., and Vaculík, M. (2018). Silicon influences soil availability and accumulation of mineral nutrients in various plant species. Plants, 7(2), 41.

Groot, J. C. J., Oomen, G. J. M., and Rossing, W. A. H. (2012). Multi-objective optimization and design of farming systems. Agricultural Systems, 110, 63–77.

Grossberg Stephen. (1988). Nonlinear Neural Networks: Principles, Mechanisms, and Architectures. Nonlinear Neural Networks: Principles, Mechanisms, and Architectures, 1, 17–61. https://doi.org/10.1016/0893-6080(88)90021-4

Gu, Y., Hunt, E., Wardlow, B., Basara, J. B., Brown, J. F., and Verdin, J. P. (2008). Evaluation of MODIS NDVI and NDWI for vegetation drought monitoring using Oklahoma Mesonet soil moisture data. Geophysical Research Letters, 35(22), 1–5. https://doi.org/10.1029/2008GL035772

Guiteras, R. (2009). The impact of climate change on Indian agriculture. Manuscript, Department of Economics, University of Maryland, College Park, Maryland.

Guo, P., Chen, X., Li, M., and Li, J. (2014). Fuzzy chance-constrained linear fractional programming approach for optimal water allocation. Stochastic Environmental Research and Risk Assessment, 28(6), 1601–1612. https://doi.org/10.1007/s00477-013-0810-2

Gupta, U. C. (1968). Relationship of total and hot-water soluble boron, and fixation of added boron, to properties of podzol soils. Soil Science Society of America Journal, 32(1), 45-48.

Hafner, B. (2006). Energy dispersive spectroscopy on the SEM: a primer. Characterization Facility, University of Minnesota, 1–26.

Haines-Young R, Potschin M. (2010). “The links between biodiversity, ecosystem services and human well-being,”in ecosystem ecology: a new synthesis, eds. D. Raffaelli and C. Frid. Cambridge UniversityPress, Cambridge).

Hallouin, T., Bruen, M., Christie, M., Bullock, C., and Quinn, M. K. (2018). Challenges in Using Hydrology and Water Quality Models for Assessing Freshwater Ecosystem Services: A Review. geosciences, 8, 45; doi:10.3390/geosciences8020045.

Hamed, K. H., and Rao, A. R. (1998). A modified Mann-Kendall trend test for autocorrelated data. Journal of hydrology, 204(1-4), 182-196.

Hanna, D. E., Tomscha, S. A., Ouellet Dallaire, C., and Bennett, E. M. (2018). A review of riverine ecosystem service quantification: Research gaps and recommendations. Journal of Applied Ecology, 55(3), 1299-1311. https://doi.org/10.1111/1365-2664.13045

Hassan, I., and Raza, M. A. (2005). Use of linear programming model to determine the optimum cropping pattern, production and income level: A case study from Dera Ghazi Khan division. Journal of Agriculture and Social Sciences, 1 (1), 32-34.

Hassan, K. I., and Dibike, Y. B. (2000). Two-dimensional morphological modeling at the confluence of the Ganges and the Jamuna Rivers for dredging and navigation. In Proc. 4th Intl. Conf. Hydroinformatics. Iowa City, Iowa: University of Iowa, Iowa Institute of Hydraulic Research.

Hazaa, Y. M. H., Almaqtari, F. A., and Al-Swidi, A. (2021). Factors Influencing Crisis Management: A systematic review and synthesis for future research. Cogent Business and Management, 8(1), 1878979.

Hazarika, J., and Sarma, A. K. (2017). Assessment of climate change impact on Temperature and Rainfall of Guwahati. 22nd International Conference on Hydraulics, Water Resources and Coastal Engineering, 21-23 December 2017, L D College of Engineering Ahmedabad, India.

Hernandez-Apaolaza, L. (2014). Can silicon partially alleviate micronutrient deficiency in plants? A review. Planta, 240(3), 447-458.

Hirel, B., Tétu, T., Lea, P. J., and Dubois, F. (2011). Improving nitrogen use efficiency in crops for sustainable agriculture. Sustainability, 3(9), 1452-1485.

Holstead, K. L., Kenyon, W., Rouillard, J. J., Hopkins, J., and Galán-Díaz, C. (2017). Natural flood management from the farmer's perspective: criteria that affect uptake. Journal of Flood Risk Management, 10(2), 205-218. https://doi.org/10.1111/jfr3.12129

Horritt, M. S., and Bates, P. D. (2001). Predicting floodplain inundation: raster-based modelling versus the finite-element approach. Hydrological processes, 15(5), 825-842.

Hossain, M. I., Siwar, C., Mokhtar, M. Bin, Dey, M. M., Jaafar, A. H., and Alam, M. M. (2013). Water productivity for boro rice production: Study on floodplain Seels in Rajshahi, Bangladesh. Journal of Bio-Science, 21(May 2015). https://doi.org/10.3329/jbs.v21i0.22526

Hu, D., Zhong, D., Zhu, Y., and Wang, G. (2015). Prediction–Correction Method for Parallelizing Implicit 2D Hydrodynamic Models. II: Application. Journal of Hydraulic Engineering, Volume 141, Issue 8.

Huang, Y., Li, Y. P., Chen, X., and Ma, Y. G. (2012). Optimization of the irrigation water resources for agricultural sustainability in Tarim River Basin, China. Agricultural Water Management, 107, 74–85. https://doi.org/10.1016/j.agwat.2012.01.012

Islam, A., and Saha, R. C. (1969). Effects of silicon on the chemical composition of rice plants. Plant and Soil, 30(3), 446-458.

Jang, C. L., and Shimizu, Y. (2007). Numerical analysis of braided rivers and alluvial fan deltas. Engineering Applications of Computational Fluid Mechanics, 1(1), 15-24.

Jayaraman, V., Chandrasekhar, M. G., and Rao, U. R. (1997). Managing the natural disasters from space technology inputs. Acta Astronautica, 40(2-8), 291-325.

Ji, Z. G., Hamrick, J. H., and Pagenkopf, J. (2002). Sediment and Metals Modeling in Shallow River. Journal of Environmental Engineering, Volume 128, Issue 2 (105 - 119).

Jørgensen, P. V., and Edelvang, K. (2000). CASI data utilized for mapping suspended matter concentrations in sediment plumes and verification of 2-D hydrodynamic modelling. International Journal of Remote Sensing, 21(11), 2247-2258.

Kadam, P., and Sen, D. (2012). Flood inundation simulation in Ajoy River using MIKE-FLOOD. ISH Journal of Hydraulic Engineering, 18(2), 129-141.

Kalita, H. M., and Sarma, A. K. (2018). An Implicit Scheme for Shallow Water Flow with Wet Dry Interface. Water resources, 45(1), 61-68.

Kandali, G. G. A. M. I., Tary, A. B., and Das, A. K. (2009). Crop suitability for Char areas of Nalbari District , Assam. 19(1).

Kanga, S., Meraj, G., Das, B., Farooq, M., Chaudhuri, S., and Singh, S. K. (2020). Modeling the spatial pattern of sediment flow in lower Hugli estuary, West Bengal, India by quantifying suspended sediment concentration (SSC) and depth conditions using geoinformatics. Applied Computing and Geosciences, 8, 100043.

Karmakar,R.M (1985) Genesis and classification of soils of Northern Brahmaputra Valley of Assam . PH.D. Thesis; IARI, New Delhi

Karmaker, T., Medhi, H., and Dutta, S. (2017). Study of channel instability in the braided Brahmaputra river using satellite imagery. Current Science, 1533-1543.

Karthikeyan, L., Chawla, I., and Mishra, A. K. (2020). A review of remote sensing applications in agriculture for food security: Crop growth and yield, irrigation, and crop losses. Journal of Hydrology, 586(March), 124905. https://doi.org/10.1016/j.jhydrol.2020.124905

Kendall, M. G. (1948). Rank correlation methods.

Khalil, M. I., Khan, M. N. I., Kabir, M. Z., Majumder, R. K., Ali, M. I., Paul, D., and Islam, S. M. A. (2016). Heavy Minerals in Sands along Brahmaputra (Jamuna) River of Bangladesh. International Journal of Geosciences, 07(01), 47–52. https://doi.org/10.4236/ijg.2016.71005

Khatun, M., Rashid, M. A., Miah, M. A. M., Khandoker, S., and Islam, M. T. (2017). Profitability of sandbar cropping method of pumpkin cultivation in char land areas of northern Bangladesh. Bangladesh Journal of Agricultural Research, 42(4), 647–663.

Kilimani, N., Van Heerden, J., Bohlmann, H., and Roos, L. (2018). Economy-wide impact of drought induced productivity losses. Disaster Prevention and Management: An International Journal, 27(5), 636-648.

Klug, H.P. and L.E. Alexander (1974) X-ray difraction procedures. John Wiley and Sons, New York, pages 58-119.

Kreibich, H., Bubeck, P., Van Vliet, M., and De Moel, H. (2015). A review of damage-reducing measures to manage fluvial flood risks in a changing climate. Mitigation and adaptation strategies for global change, 20(6), 967-989. https://doi.org/10.1007/s11027-014-9629-5

Kuhlmann, B., 2010. Schäden in der Landwirtschaft (damages in agriculture). In: Thieken, A.H., Seifert, I., Merz, B. (Eds.), Hochwasserschäden – Erfassung, Abschätzung und Vermeidung, oekom, Munich, pp. 223–234 (in German).

Kumar, N. N., and Narayanaswamy, B. K. (2000). Entrepreneurial behavior and socio-economic characteristics of farmers who adopted sustainable agriculture in India. Karnataka Journal of Agricultural Sciences, 13(1), 83-90.

Kumari, Sangeeta, and P. P. Mujumdar (2017). "Fuzzy set–based system performance evaluation of an irrigation reservoir system." Journal of Irrigation and Drainage Engineering 143, no. 5: 04017002. https://doi.org/10.1061/(ASCE)IR.1943-4774.0001155

Kundzewicz, Z. W. (1999). Flood protection—sustainability issues. Hydrological Sciences Journal, 44(4), 559-571. https://doi.org/10.1080/02626669909492252

Kuriqi, A., Ali, R., Pham, Q.B., Montenegro Gambini, J., Gupta, V., Malik, A., Linh, N.T.T., Joshi, Y., Anh, D.T., Nam, V.T. and Dong, X. (2020). Seasonality shift and streamflow flow variability trends in central India. Acta Geophysica, 68(5), 1461-1475.

Lambin, E. F. (1997). Modelling and monitoring land-cover change processes in tropical regions. Progress in Physical Geography, 21(3), 375–393. https://doi.org/10.1177/030913339702100303

Laura, R. A., and Wang, J. D. (1984). Two-dimensional flood routing on steep slopes. Journal of Hydraulic Engineering, 110(8), 1121-1135.

Lavorel S, Locatelli B, Colloff MJ, Bruley E. (2020) Co-producing ecosystem services for adapting to climate change. Phil. Trans. R. Soc. B 375, 20190119. (doi:10.1098/rstb.2019.0119)

Lavorel, S., Locatelli, B., Colloff, M. J., and Bruley, E. (2020). Co-producing ecosystem services for adapting to climate change. Philosophical Transactions of the Royal Society B, 375(1794), 20190119.

Li, F. F., Shoemaker, C. A., Qiu, J., and Wei, J. H. (2015). Hierarchical multi-reservoir optimization modeling for real-world complexity with application to the Three Gorges system. Environmental Modelling and Software, 69, 319-329.

Li, X., Kang, S., Niu, J., Du, T., Tong, L., Li, S., and Ding, R. (2017). Applying uncertain programming model to improve regional farming economic benefits and water productivity. Agricultural Water Management, 179, 352–365. https://doi.org/10.1016/j.agwat.2016.06.030

Lick, W. (2008). Sediment and contaminant transport in surface waters. CRC press. https://doi.org/10.1201/9781420059885

Lien, H. C., Hsieh, T. Y., Yang, J. C., and Yeh, K. C. (1999). Bend-flow simulation using 2D depth-averaged model. Journal of Hydraulic Engineering, 125(10), 1097-1108.

Ligmann-Zielinska, A., Church, R. L., and Jankowski, P. (2008). Spatial optimization as a generative technique for sustainable multiobjective land-use allocation. International Journal of Geographical Information Science, 22(6), 601-622.

Luyckx, M., Hausman, J. F., Lutts, S., and Guerriero, G. (2017). Silicon and plants: current knowledge and technological perspectives. Frontiers in plant science, 8, 411. https://doi.org/10.3389/fpls.2017.00411

Maas, A. L., Hannun, A. Y., and Ng, A. Y. (2013). Rectifier nonlinearities improve neural network acoustic models. In ICML Workshop on Deep Learning for Audio, Speech and Language Processing, 28.

Maaß A-L (2019) Looking back, looking forward: Human impacts on fluvial morphodynamics since the Industrial Revolution and the return to a natural morphological river state, Dissertation. https:// doi. org/ 10. 18154/RWTH-2019-08256

Macian-Sorribes, H., Tilmant, A., and Pulido-Velazquez, M. (2017). Improving operating policies of large-scale surface-groundwater systems through stochastic programming. Water Resources Research, 53(2), 1407-1423.

Mahmoodi-Eshkaftaki, M., and Rafiee, M. R. (2020). Optimization of irrigation management: A multi-objective approach based on crop yield, growth, evapotranspiration, water use efficiency and soil salinity. Journal of Cleaner Production, 252. https://doi.org/10.1016/j.jclepro.2019.119901

Maibangsa, S., Borah, N., Maibangsa, M., Sharma, K. K., and Chowdhury, D. (2015). Characterization of sand-silt deposition in agricultural land of Dhemaji and Lakhimpur districts of Assam, India and evaluation for crop suitability. Journal of Science and Environment Today, 1, 33-41.

Malhi, Y., Franklin, J., Seddon, N., Solan, M., Turner, M. G., Field, C. B., and Knowlton, N. (2020). Climate change and ecosystems: Threats, opportunities and solutions. Philosophical Transactions of the Royal Society B, 375(1794), 20190104.

Malik, S., Pal, S. C., Das, B., and Chakrabortty, R. (2019). Intra-annual variations of vegetation status in a sub-tropical deciduous forest-dominated area using geospatial approach: a case study of Sali watershed, Bankura, West Bengal, India. Geology, Ecology, and Landscapes, 00(00), 1–12. https://doi.org/10.1080/24749508.2019.1633219

Mann, H. B. (1945). Nonparametric tests against trend. Econometrica: Journal of the econometric society, 245-259.

Maoh, H., and Kanaroglou, P. (2009). A tool for evaluating urban sustainability via integrated transportation and land use simulation models. Environnement Urbain/Urban Environment, (Volume 3).

Martin-Ortega, J., González-Eguino, M., and Markandya, A. (2012). The costs of drought: the 2007/2008 case of Barcelona. Water Policy, 14(3), 539-560. https://doi.org/10.2166/wp.2011.121

McFeeters, S. K. (1996). The use of the Normalized Difference Water Index (NDWI) in the delineation of open water features. International journal of remote sensing, 17(7), 1425-1432. https://doi.org/10.1080/01431169608948714

Meena, V. D., Dotaniya, M. L., Coumar, V., Rajendiran, S., Ajay, Kundu, S., and Subba Rao, A. (2014). A case for silicon fertilization to improve crop yields in tropical soils. Proceedings of the National Academy of Sciences India Section B - Biological Sciences, 84(3), 505–518. https://doi.org/10.1007/s40011-013-0270-y

Memmah, M. M., Lescourret, F., Yao, X., and Lavigne, C. (2015). Metaheuristics for agricultural land use optimization. A review. Agronomy for sustainable development, 35(3), 975-998.

Merz, B., Kreibich, H., Schwarze, R., and Thieken, A. (2010). Review article "assessment of economic flood damage." Natural Hazards and Earth System Science, 10(8), 1697–1724. https://doi.org/10.5194/nhess-10-1697-2010

Messner, F., and Meyer, V. (2006). Flood damage, vulnerability and risk perception–challenges for flood damage research. In Flood risk management: hazards, vulnerability and mitigation measures (pp. 149-167). Springer, Dordrecht.

Millenium Ecosystem Assessment (MEA) (2005). Ecosystems and Human Well-Being: Biodiversity Synthesis. World Resource Institute, Washington, DC.

Ming, B., Chang, J., Huang, Q., Wang, Y., and Huang, S. (2015). Optimal operation of multi-reservoir system based-on cuckoo search algorithm. Water Resources Management, 29(15), 5671–5687.

Morianou, G. G., Kourgialas, N. N., Karatzas, G. P., and Nikolaidis, N. P. (2016). Hydraulic and sediment transport simulation of Koiliaris River using the MIKE 21C model. Procedia engineering, 162, 463-470. https://doi.org/10.1016/j.proeng.2016.11.089

Morianou, G. G., Kourgialas, N. N., Karatzas, G. P., and Nikolaidis, N. P. (2016). Assessing hydro-morphological changes in Mediterranean stream using curvilinear grid modeling approach-climate change impacts. Earth Science Informatics, 11(2), 205-216. https://doi.org/10.1007/s12145-017-0326-2

Mujumdar, P. P. (2008). Implications of climate change for sustainable water resources management in India. Physics and Chemistry of the Earth, Parts A/B/C, 33(5), 354-358.

Mutlu, E., Chaubey, I., Hexmoor, H., and Bajwa, S. . (2008). Comparison of artificial neural network models for hydrologic predictions at multiple gauging stations in an agricultural watershed. Hydrological Processes, 22(September 2008), 5097–5106. https://doi.org/0.1002/hyp.7136

Nahar, S. L., Akteruzzaman, M., and Al-Amin, A. K. M. A. (2016). Sweet gourd production under sandbar cropping practices: a case study in Sundorganj of Gaibandha District in Bangladesh. Progressive Agriculture, 27(3), 320-326.

Nandy, S., Sahu, R. B., Das, M. K., and Barman, B. C. (2020). A quantitative assessment of hydrodynamic impacts due to variable discharges on the backwater deposits of Durgapur

Barrage over River Damodar in India using MIKE 11. In River Flow 2020 (pp. 1239-1245). CRC Press.

Nascimento, N., Baptista, M., Silva, A., Léa Machado, M., de Lima, J. C., Gonçalves, M., ... and Machado, É. (2006). Flood-damage curves: Methodological development for the Brazilian context. Water Practice and Technology, 1(1).

Nguyen, N. Y., Ichikawa, Y., and Ishidaira, H. (2017). Establishing flood damage functions for agricultural crops using estimated inundation depth and flood disaster statistics in data-scarce regions. Hydrological Research Letters, 11(1), 12-18.

Nicholls, R. J., Hutton, C. W., Adger, W. N., Hanson, S. E., Rahman, M., and Salehin, M. (2018). Ecosystem services for well-being in deltas: integrated assessment for policy analysis. Springer Nature.

Nigussie, T.A., Altunkaynak, A. Modeling the effect of urbanization on flood risk in Ayamama Watershed, Istanbul, Turkey, using the MIKE 21 FM model. Nat Hazards 99, 1031–1047 (2019). https://doi.org/10.1007/s11069-019-03794-y

Noman, M. R. A., Huda, K. S., and Rahman, M. S. (2014). Constraints and scope for practicing sandbar cropping technology in riverine areas of Bangladesh. International Journal of Agricultural Extension, 2(3), 169-176.

Noorivandi, A. N., Ajili, A., Chizari, M., and Bijani, M. (2009). The socio-economic characteristics of wheat farmers regarding adoption of sustainable soil management (SSM). Journal of Human Ecology, 27(3), 201-205.

Oladosu, Yusuff, Mohd Y. Rafii, Fatai Arolu, Samuel C. Chukwu, Ismaila Muhammad, Isiaka Kareem, Monsuru A. Salisu, and Ibrahim W. Arolu (2020). "Submergence Tolerance in Rice: Review of Mechanism, Breeding and, Future Prospects" Sustainability 12, no. 4: 1632. https://doi.org/10.3390/su12041632.

Osaki, M., and Batalha, M. O. (2014). Optimization model of agricultural production system in grain farms under risk, in Sorriso, Brazil. Agricultural Systems, 127, 178-188.

Osman, K. T. (2013). Plant nutrients and soil fertility management. In Soils (pp. 129-159). Springer, Dordrecht.

Ozesmi, S. L., and Bauer, M. E. (2002). Satellite remote sensing of wetlands. Wetlands Ecology and Management, 10(5), 381–402. https://doi.org/10.1023/A:1020908432489

Panda, A. (2010). Climate induced migration from Bangladesh to India: issues and challenges.

Panda, R. K., Pramanik, N., and Bala, B. (2010). Simulation of river stage using artificial neural network and MIKE 11 hydrodynamic model. Computers and Geosciences, 36(6), 735-745.

Pape, L., Kuriyama, Y., and Ruessink, B. G. (2010). Models and scales for cross-shore sandbar migration. Journal of Geophysical Research: Earth Surface, 115(F3).

Pathan, S. A., Ashwini, K., and Sil, B. S. (2021). Spatio-temporal variation in land use/land cover pattern and channel migration in Majuli River Island, India. Environmental Monitoring and Assessment, 193(12), 1-17.

Paton, D., McClure, J., and Bürgelt, P. T. (2006). Natural hazard resilience: The role of individual and household preparedness. Disaster resilience: An integrated approach, 105, 27.

Patowary, S., and Sarma, A. K. (2017). A modified hydrodynamic model for routing unsteady flow in a river having piedmont zone. Journal of Hydrology and Hydromechanics, 65(1), 60.

Patra, B., Pal, R., Paulraj, R., Pradhan, S. N., and Meena, R. (2020). Mineralogical composition and C/N contents in soil and water among betel vineyards of coastal Odisha, India. SN Applied Sciences, 2(6), 1-17.

Patro, S., Chatterjee, C., Mohanty, S., Singh, R., and Raghuwanshi, N. S. (2009). Flood inundation modeling using MIKE FLOOD and remote sensing data. Journal of the Indian Society of Remote Sensing, 37(1), 107-118. https://doi.org/10.1007/s12524-009-0002-1

Peña, M. A., and Brenning, A. (2015). Assessing fruit-tree crop classification from Landsat-8 time series for the Maipo Valley, Chile. Remote Sensing of Environment, 171, 234–244. https://doi.org/10.1016/j.rse.2015.10.029

Piao, S., Fang, J., Zhou, L., Guo, Q., Henderson, M., Ji, W., Li, Y. and Tao, S. (2003). Interannual variations of monthly and seasonal normalized difference vegetation index

(NDVI) in China from 1982 to 1999. Journal of Geophysical Research: Atmospheres, 108(D14).

Pietroniro, A., Leconte, R., Peters, D. L., and Prowse, T. D. (2000). Application of a hydrodynamic model in a freshwater delta using remote sensing. Remote Sensing and Hydrology 2000, IAHS Publ. no. 267, 2001.

Pistrika, A. (2010). Flood damage estimation based on flood simulation scenarios and a GIS platform. European Water, 30, 3-11.

Prashnani, M., Qadir, A., Goswami, J., and Raju, P. L. N. (2019). Spatio-temporal study of Brahmaputra River Islands (CHARS) for agriculture expansion in Assam, India. International Archives of the Photogrammetry, Remote Sensing and Spatial Information Sciences - ISPRS Archives, 42(3/W6), 429–433. https://doi.org/10.5194/isprs-archives-XLII-3-W6-429-2019

Raghuvanshi, R., and Ansari, M. A. (2017). A Study of Farmers' Awareness about Climate Change and Adaptation Practices in India. Young (Less than 45), 45, 40-90.

Rahman, K. A. U., and Reza, I. (2011). Accessing and Retaining Access to the Sandbars by the Extreme Poor: Experience from the Practical Action Project. Shiree, House, 5.

Rahman, M. A., and Rahman, M. M. (2012). Char formation process and livelihood characteristics of char dwellers of alluvial river in Bangladesh. ICSE, 6, 27–31.

Raju, K. S., and Kumar, D. N. (1999). Multicriterion decision making in irrigation planning. Agricultural Systems, 62(2), 117–129. https://doi.org/10.1016/S0308-521X(99)00060-8

Ramasamy, V., Rajkumar, P., and Ponnusamy, V. (2009). Depth wise analysis of recently excavated Vellar river sediments through FTIR and XRD studies. Indian Journal of Physics, 83(9), 1295–1308.

Rampini, C. (2017). Environmental and climate justice along the Brahmaputra River in Northeast India. Lessons in Conservation, 7, 24.

Rao, Y., Zhou, M., Ou, G., Dai, D., Zhang, L., Zhang, Z., Nie, X. and Yang, C. (2018). Integrating ecosystem services value for sustainable land-use management in semi-arid

region. Journal of Cleaner Production, 186, 662-672. https://doi.org/10.1016/j.jclepro.2018.03.119

Regulwar, D. G., and Gurav, J. B. (2012). Sustainable Irrigation Planning with Imprecise Parameters under Fuzzy Environment. Water Resources Management, 26(13), 3871–3892. https://doi.org/10.1007/s11269-012-0109-y

Robinson, S., Kerven, C., Behnke, R., Kushenov, K., and Milner-Gulland, E. J. (2016). The changing role of bio-physical and socio-economic drivers in determining livestock distributions: A historical perspective from Kazakhstan. Agricultural Systems, 143, 169–182.

Rouse, J. W., Hass, R. H., Schell, J. A., and Deering, D. W. (1973). Monitoring vegetation systems in the great plains with ERTS. Third Earth Resources Technology Satellite (ERTS) Symposium, 1, 309–317. https://doi.org/citeulike-article-id:12009708

Sadeghi, S. H., Sharifi Moghadam, E., Delavar, M., and Zarghami, M. (2020). Application of water-energy-food nexus approach for designating optimal agricultural management pattern at a watershed scale. Agricultural Water Management, 233(August 2019). https://doi.org/10.1016/j.agwat.2020.106071

Salunkhe, S. S., Rao, S. S., Prabu, I., Venkataraman, V. R., Murthy, Y. K., Sadolikar, C., and Deshpande, S. (2018). Flood Inundation Hazard Modelling Using CCHE2D Hydrodynamic Model and Geospatial Data for Embankment Breaching Scenario of Brahmaputra River in Assam. Journal of the Indian Society of Remote Sensing, 1-11.

Santillan, J. R., Makinano, M. M., and Paringit, E. C. (2010). Integrating remote sensing, GIS and hydrologic models for predicting land cover change impacts on surface runoff and sediment yield in a critical watershed in Mindanao, Philippines. International Archives of the Photogrammetry, Remote Sensing and Spatial Information Science, 38(8), 436-441.

Sanz Scovino, J. I., and Rowell, D. L. (1988). The use of feldspars as potassium fertilizers in the savannah of Colombia. Fertilizer research, 17(1), 71-83.

Sarkar, A., Garg, R. D., and Sharma, N. (2012). RS-GIS Based Assessment of River Dynamics of Brahmaputra River in India. Journal of Water Resource and Protection, 04(02), 63–72. https://doi.org/10.4236/jwarp.2012.42008

Sarker, M. H., Koudstaal, R., and Alam, M. (2003). Rivers, chars and char dwellers of Bangladesh. International Journal of River Basin Management, 1(1), 61–80. https://doi.org/10.1080/15715124.2003.9635193

Sarker, R., and Ray, T. (2009). An improved evolutionary algorithm for solving multi-objective crop planning models. Computers and Electronics in Agriculture, 68(2), 191–199.

Sarma, A. K., and Hazarika, J. (2014). GCM based fuzzy clustering to identify homogeneous climatic regions of north-east India. International Journal of Environmental and Ecological Engineering, 8(12), 807-814.

Sarma, A. K., and Hazarika, J. (2014). GCM based fuzzy clustering to identify homogeneous climatic regions of north-east India. International Journal of Environmental and Ecological Engineering, 8(12), 807-814.

Sarma, J. N., and Acharjee, S. (2018). A study on variation in channel width and braiding intensity of the Brahmaputra River in Assam, India. Geosciences, 8(9), 343. https://doi.org/10.3390/geosciences8090343

Sen, P. K. (1968). Estimates of the regression coefficient based on Kendall's tau. Journal of the American statistical association, 63(324), 1379-1389.

Sethi, L. N., Panda, S. N., and Nayak, M. K. (2006). Optimal crop planning and water resources allocation in a coastal groundwater basin, Orissa, India. Agricultural Water Management, 83(3), 209–220. https://doi.org/10.1016/j.agwat.2005.11.009

Seto, K. C., and Kaufmann, R. K. (2003). Modeling the drivers of urban land use change in the Pearl River Delta, China: Integrating remote sensing with socioeconomic data. Land Economics, 79(1), 106-121.

Shahid, Z., Piracha, A. (2016). Awareness of Climate Change Impacts and Adaptation at Local Level in Punjab, Pakistan. In: Maheshwari, B., Thoradeniya, B., Singh, V.P. (eds) Balanced Urban Development: Options and Strategies for Liveable Cities. Water Science and Technology Library, vol 72. Springer, Cham. https://doi.org/10.1007/978-3-319-28112-4_25

Sharma, A., and Goyal, M. K. (2018). Assessment of ecosystem resilience to hydroclimatic disturbances in India. Global Change Biology, 24(2), e432–e441. https://doi.org/10.1111/gcb.13874

Shirur, M., Shivalingegowda, N. S., Chandregowda, M. J., and Rana, R. K. (2017). Entrepreneurial behaviour and socio economic analysis of mushroom growers in Karnataka. Indian Journal of Agricultural Sciences, 87(6), 840-845.

Shrestha, R. R., and Nestmann, F. (2009). Physically Based and Data-Driven Models and Propagation of Input Uncertainties in River Flood Prediction. Journal of Hydrologic Engineering, Volume 14, Issue 12 (1309 - 1319).

Singh, A. (2012). An overview of the optimization modelling applications. Journal of Hydrology, 466, 167–182. https://doi.org/10.1016/j.jhydrol.2012.08.004

Singh, A. K., Singh, L., and Kumar, S. (2020). Impact of COVID-19 on agriculture and allied sectors. Journal of Community Mobilization and Sustainable Development Vol. 15(1), 8-16, January-April, 2020. ISSN 2231 – 6736

Singh, A., and Panda, S. N. (2012). Development and application of an optimization model for the maximization of net agricultural return. Agricultural Water Management, 115, 267–275. https://doi.org/10.1016/j.agwat.2012.09.014

Singh, L. K., Jha, M. K., and Chowdary, V. M. (2017). Multi-criteria analysis and GIS modeling for identifying prospective water harvesting and artificial recharge sites for sustainable water supply. Journal of Cleaner Production, 142, 1436-1456.

Singh, R. K., Villuri, V. G. K., Pasupuleti, S., and Nune, R. (2020). Hydrodynamic modeling for identifying flood vulnerability zones in lower Damodar river of eastern India. Ain Shams Engineering Journal, 11(4), 1035-1046.

Smakhtin, V. U. (2001). Low flow hydrology: a review. Journal of hydrology, 240(3-4), 147-186.

Sole, A., and Zuccaro, G. (2005). New urban area flood model: a comparison with MIKE11-quasi2d. Advances in Geosciences, 2, 279-284.

Solin, L., and Skubincan, P. (2013). Flood risk assessment and management: review of concepts, definitions and methods. Geographical Journal, 65(1), 23-44.

Somes, N. L., Bishop, W. A., and Wong, T. H. (1999). Numerical simulation of wetland hydrodynamics. Environment International, 25(6-7), 773-779.

Sonneveld, B. G., Merbis, M. D., Alfarra, A., Ünver, O., and Arnal, M. F. (2018). Nature-based solutions for agricultural water management and food security. FAO Land and Water Discussion Paper, (12).

Sravanthi, N., Ramakrishnan, R., Rajawat, A. S., and Narayana, A. C. (2015). Application of Numerical Model in Suspended Sediment Transport Studies along the Central Kerala, West- coast of India. Aquatic Procedia, 4, 109-116.

Stanford, J. A., Alexander, L. C., and Whited, D. C. (2017). Riverscapes. In Methods in Stream Ecology, Volume 1 (pp. 3-19). Academic Press.

Steinberg, R. A., Specht, A. W., and Roller, E. M. (1955). Effects of Micronutrient Deficiencies on Mineral Composition, Nitrogen Fractions, Ascorbic Acid and Burn of Tobacco Grown to Flowering in Water Culture. Plant Physiology, 30(2), 123. https://doi.org/10.1104/pp.30.2.123

Stronska, K., Borowicz, A., Kitowski, K., Michalik, G., Jørgensen, G., Van Kalken, T., and Butts, M. (1999). MIKE 11 as a flood management and flood forecasting tool for the Odra River, Poland. In Proceeding of the 3rd DHI Software Conference Helsingør, Denmark, http://www.dhigroup.com/upload/publications/mike11/Stronska_MIKE_11_as_flood.pdf

Sugirtharam, M., and Venuthasan, T. Farmers' Awareness on Climate Change Related Issues at Some Irrigable Areas of Batticaloa District, Sri Lanka, I. Res. J. Environmen Sci, 1(2), 29- 32.

Sulis, A., and Sechi, G. M. (2013). Comparison of generic simulation models for water resource systems. Environmental Modelling and Software, 40, 214–225.

Surminski, S., and Oramas-Dorta, D. (2014). Flood insurance schemes and climate adaptation in developing countries. International Journal of Disaster Risk Reduction, 7, 154-164. https://doi.org/10.1016/j.ijdrr.2013.10.005

Talukdar, G., Swain, J.B. and Patra, K.C. (2021). Flood inundation mapping and hazard assessment of Baitarani River basin using hydrologic and hydraulic model. Nat Hazards 109, 389–403. https://doi.org/10.1007/s11069-021-04841-3

Talukdar, N. C., Bhattacharyya, D., and Hazarika, S. (2004). Soils and agriculture. In The Brahmaputra basin water resources (pp. 35-71). Springer, Dordrecht. https://doi.org/10.1007/978-94-017-0540-0_4

Tandon, S. K., and Sinha, R. (2007). Geology of large river systems. Large rivers: geomorphology and management, 7-28.

Terpstra, T. (2011). Emotions, trust, and perceived risk: Affective and cognitive routes to flood preparedness behavior. Risk Analysis: An International Journal, 31(10), 1658-1675. https://doi.org/10.1111/j.1539-6924.2011.01616.x

Thakuriah, G., and Saikia, R. (2018). Short Review Paper RS and GIS based assessment of Bank Erosion in Goalpara District part of Brahmaputra River , Assam , India. 6(3), 1–8.

Thorslund, J., Jarsjo, J., Jaramillo, F., Jawitz, J. W., Manzoni, S., Basu, N. B., ... and Destouni, G. (2017). Wetlands as large-scale nature-based solutions: Status and challenges for research, engineering and management. Ecological Engineering, 108, 489-497. https://doi.org/10.1016/j.ecoleng.2017.07.012

Touchton, J. T., and Boswell, F. C. (1975). Effects of B Application on Soybean Yield, Chemical Composition, and Related Characteristics 1. Agronomy Journal, 67(3), 417-420. https://doi.org/10.2134/agronj1975.00021962006700030035x

Tripathi, A., and Mishra, A. K. (2017). Knowledge and passive adaptation to climate change: An example from Indian farmers. Climate Risk Management, 16, 195-207.

Tucci, C. E., Collischonn, W., Clarke, R. T., Paz, A. R., and Allasia, D. (2008). Short-and long-term flow forecasting in the Rio Grande watershed (Brazil). Atmospheric Science Letters, 9(2), 53-56. https://doi.org/10.1002/asl.165

Twisa, S., and Buchroithner, M. F. (2019). Land-use and land-cover (LULC) change detection in Wami River Basin, Tanzania. Land, 8(9), 136.

Vanwambeke, S. O., Meyfroidt, P., and Nikodemus, O. (2012). From USSR to EU: 20 years of rural landscape changes in Vidzeme, Latvia. Landscape and Urban Planning, 105(3), 241-249.

Verhoeven, J. T., and Setter, T. L. (2010). Agricultural use of wetlands: opportunities and limitations. Annals of botany, 105(1), 155-163. https://doi.org/10.1093/aob/mcp172

Wairimu, E., Obare, G., and Odendo, M. (2016). Factors affecting weather index-based crop insurance in Laikipia County, Kenya. Journal of agricultural extension and rural development, 8(7), 111-121.

Wang, R., Li, Y., and Tan, Q. (2015). A review of inexact optimization modeling and its application to integrated water resources management. Frontiers of earth science, 9(1), 51-64.

Wardlow, B. D., Egbert, S. L., and Kastens, J. H. (2007). Analysis of time-series MODIS 250 m vegetation index data for crop classification in the U.S. Central Great Plains. Remote Sensing of Environment, 108(3), 290–310. https://doi.org/10.1016/j.rse.2006.11.021

Warren, I. R., and Bach, H. (1992). MIKE 21: a modelling system for estuaries, coastal waters and seas. Environmental Software, 7(4), 229-240.

Webb, B. W. (1995). Regulation and thermal regime in a Devon river system. Sediment and Water Quality in River Catchments. John Wiley and Sons, Chichester, UK, 65-94.

Wilby, R. L., Wedgbrow, C. S., and Fox, H. R. (2004). Seasonal predictability of the summer hydrometeorology of the River Thames, UK. Journal of Hydrology, 295(1-4), 1-16. https://doi.org/10.1016/j.jhydrol.2004.02.015

Wu, C., Chen, B., Huang, X., and Wei, Y. D. (2020). Effect of land-use change and optimization on the ecosystem service values of Jiangsu province, China. Ecological Indicators, 117, 106507. https://doi.org/10.1016/j.ecolind.2020.106507

Wu, S., and Huang, G. H. (2007). An interval-parameter fuzzy approach for multiobjective linear programming under uncertainty. Journal of Mathematical Modelling and Algorithms, 6(2), 195–212. https://doi.org/10.1007/s10852-006-9042-5

Xie, D., Gao, S., Wang, Z. B., Pan, C., Wu, X., and Wang, Q. (2017). Morphodynamic modeling of a large inside sandbar and its dextral morphology in a convergent estuary: Qiantang Estuary, China. Journal of Geophysical Research: Earth Surface, 122(8), 1553-1572.

Xu, B., Wang, N., Chen, T., and Li, M. (2015). Empirical Evaluation of Rectified Activations in Convolutional Network. http://arxiv.org/abs/1505.00853

Yaseen, Z. M., El-Shafie, A., Jaafar, O., Afan, H. A., and Sayl, K. N. (2015). Artificial intelligence based models for stream-flow forecasting: 2000–2015. Journal of Hydrology, 530, 829-844. https://doi.org/10.1016/j.jhydrol.2015.10.038

Ying, X., Khan, A. A., and Wang, S. S. Y. (2004). An upwind conservative scheme for Saint Venant equations. Journal of Hydraulic Engineering, 130(10), 977–987.

Yue, S., and Wang, C. (2004). The Mann-Kendall test modified by effective sample size to detect trend in serially correlated hydrological series. Water resources management, 18(3), 201-218.

Zeleňáková, M., Gaňová, L., and Diaconu, D. C. (2020). Flood damage assessment and management. Springer International Publishing.

Zeng, X., Kang, S., Li, F., Zhang, L., and Guo, P. (2010). Fuzzy multi-objective linear programming applying to crop area planning. Agricultural Water Management, 98(1), 134–142.

Zhai, W., Ding, J., An, X., and Wang, Z. (2020). An optimization model of sand and gravel mining quantity considering healthy ecosystem in Yangtze River, China. Journal of Cleaner Production, 242, 118385. https://doi.org/10.1016/j.jclepro.2019.118385

Zhang, H. H., Zeng, Y. N., and Bian, L. (2010). Simulating multi-objective spatial optimization allocation of land use based on the integration of multi-agent system and genetic algorithm. International Journal of Environmental Research, 4(4), 765-776.

Zhang, H., Chen, L., and Singh, V. P. (2021). Flood frequency analysis using generalized distributions and entropy-based model selection method. Journal of Hydrology, 595, 125610.

Zhang, J., Zhu, Y., Zhang, X., Ye, M., and Yang, J. (2018). Developing a Long Short-Term Memory (LSTM) based model for predicting water table depth in agricultural areas. Journal of Hydrology, 561, 918-929. https://doi.org/10.1016/j.jhydrol.2018.04.065

Zhang, L. D., Guo, P., Li, M., and Fang, S. Q. (2014). Deficit irrigation optimization model for crop area allocation under uncertainties in Shiyang River basin, China. Sensor Letters, 12(3–4), 867–875. https://doi.org/10.1166/sl.2014.3120

Zheng, B., Myint, S. W., Thenkabail, P. S., and Aggarwal, R. M. (2015). A support vector machine to identify irrigated crop types using time-series Landsat NDVI data. International Journal of Applied Earth Observation and Geoinformation, 34(1), 103–112. https://doi.org/10.1016/j.jag.2014.07.002

Zimmermann, H. J. (1978). Fuzzy programming and linear programming with several objective functions. Fuzzy Sets and Systems, 1(1), 45–55. https://doi.org/10.1016/0165-0114(78)90031-3

Appendix

Format of survey Questionnaire on sandbar cultivation

Purpose of the questionnaire:

The purpose of this survey is for the work related to my research on riverine ecosystem. To study the different activities carried out by the dwellers/ farmers/local inhabitants on the sandbars of Brahmaputra River and to motivate them for optimal cropping pattern to increase their economy for better life.

Farmer's Details:

Name of the Farmer: _____

Age: _____

Education: _____

1. Have you done any kind of activity on sandbars?

☐ Yes ☐ No

If Yes, Specify

2. In which month the farmers start cultivation in the sandbars.

☐ Jan-Mar ☐ Apr-Jun

☐ Jul-Sep ☐ Oct-Dec

3. Other than crop production, is there any other activity that is practiced?

☐ Yes ☐ No

If Yes, Specify

4. What is your financial status?

☐ Below poverty line ☐ Lower middle class

☐ Upper middle class ☐ High income group

5. Profit earned (in Rupees)

☐ below 50000 ☐ 50000- 1 Lakh

☐ More than 1 Lakh ☐ Below 10 Lakh

6. From where do you get financial support?

☐ Govt. Banks ☐ Private / Co-operative Banks ☐ Others Specify: _____

7. Your opinion about the expenses in Agriculture?

☐ Very high ☐ Moderate ☐ Less

8. Do you get seeds and fertilizers in time?

☐ Yes ☐ No

9. Do you practice double cropping?

☐ Yes ☐ No

10. What factors affect your yield?

☐ Natural calamities ☐ Lack of knowledge

☐ Lack of finances ☐ Unavailability of resources

☐ Diseases ☐ Others:

11. How do you market your crops?

☐ Direct

☐ Through middle men

☐ Through agencies

12. Do you have storage place and market for your yield?

☐ Yes

☐ No

☐ Don't know

13. Are you aware of Government plans and facilities?

☐ Yes

☐ No

☐ Don't know

14. Does social evils like consumption of alcohol, smoking or lottery affect your life?

☐ Yes ☐ No

15. Are you benefitted from sandbar cultivation

☐ Yes ☐ No

16. How do you plan for your future?

☐ Insurance ☐ On property

☐ Fixed Deposits ☐ Any Other: _____

☐ Gold ☐ None

17. Does the cropping area /location of sandbars changes over time?

☐ Yes ☐ No

18. Did you encourage other dwellers/farmers for sandbar cultivation

☐ Yes ☐ No

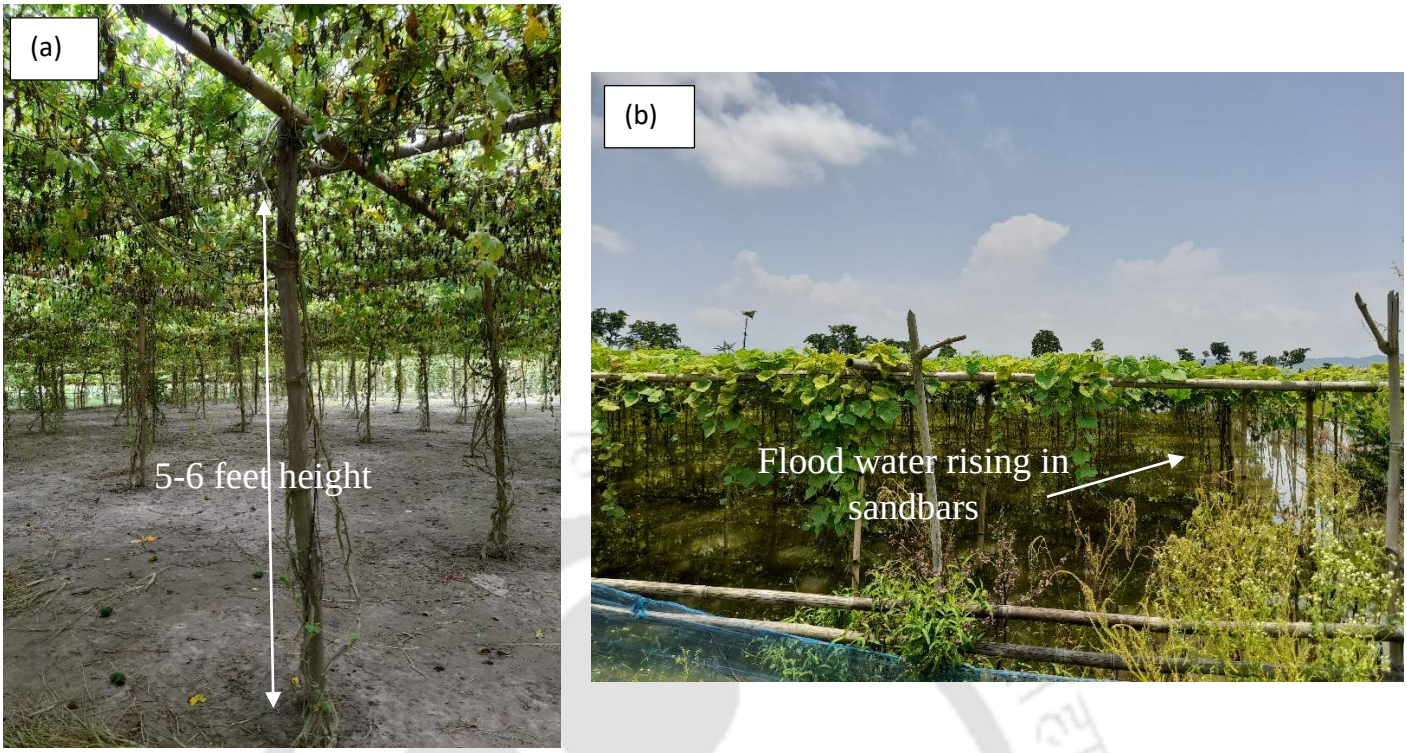

Figure S1: Pattern of vegetable grown during the onset of monsoon period in a sandbar within the Brahmaputra River to avoid damage due to flood (a) Before flooding condition (Farm 1) (b) during nominal flooding (Farm 2). The maximum depth of water measured was 0.4-0.5m. (*Location*: 26°14’37” N, 91°46’37” E, *Date*: 4th July 2021: 12.33 pm.)

Figure. S2: Probability density functions for different distributions

Distribution	Probability Density Function	Parameter
Log-Normal	$f(x) = \frac{exp\left(-\frac{1}{2}\left(\frac{\ln(x-\gamma-\mu)}{\sigma}\right)^2\right)}{(x-\gamma)\sigma\sqrt{2\pi}}$	σ: continuous parameter (σ > 0) μ: continuous parameter γ: continuous parameter (γ=0 for two parameter)
Exponential	$f(x) = \lambda \exp\left(-\lambda(x-\gamma)\right)$	λ: continuous scale parameter (λ>0) γ: continuous location parameter
Weibull (3P)	$f(x) = \frac{\alpha}{\beta}\left(\frac{x-\gamma}{\beta}\right)^{\alpha-1} exp\left(-\left(\frac{x-\gamma}{\beta}\right)^{\alpha}\right)$	α: continuous shape parameter (α>0) β: continuous scale parameter (β>0) γ: continuous location parameter
Gumbel Max	$f(x) = \frac{1}{\sigma} exp\left(-z - exp(-z)\right)$; $z=\frac{x-\mu}{\sigma}$	σ: continuous scale parameter (σ > 0) μ: continuous location parameter
Log Pearson (3P)	$f(x) = \frac{1}{x\lvert\beta\rvert\Gamma(\alpha)}\frac{(\ln(x)-\gamma)^{\alpha-1}}{\beta}\exp(-\frac{\ln(x)-\gamma}{\beta})$	α: continuous shape parameter (α>0) β: continuous scale parameter (β≠0) γ: continuous location parameter Γ: Gamma function

Table ST1: Velocity measurement at a section in the Brahmaputra river near Pandu, Assam

Northing	Easting	Depth	.2d			.8d		
			Rev.	Time (sec.)	Velocity(m/s)	Rev.	Time (sec.)	Velocity(m/s)
2899770	378781	1.1	22	60	0.252	17	60	0.196
2899823	378778.2	2.8	32	60	0.364	24	60	0.274
2899869	378758.2	3.8	40	60	0.453	34	60	0.386
2899911	378729.9	5.5	56	60	0.633	47	60	0.532
2899974	378792.7	7	68	60	0.767	50	60	0.565
2900015	378763.8	8.5	72	60	0.812	55	60	0.621
2900055	378734.7	9.2	76	60	0.857	57	60	0.644
290096.5	378705.8	8.5	71	60	0.801	53	60	0.599
2900137	378677.4	8.6	71	60	0.801	52	60	0.588
2900178	378648.3	8.3	70	60	0.789	50	60	0.565
2900218	378619.5	6.9	66	60	0.745	47	60	0.532
2900257	378589.8	6.3	62	60	0.7	46	60	0.521
2900299	378562.7	5.7	55	60	0.621	45	60	0.509
2900338	378532.7	5.1	49	60	0.554	38	60	0.431
2900379	378504.5	4.4	41	60	0.465	33	60	0.375
2900420	378476.3	3.8	39	60	0.442	30	60	0.341
2900461	378445.9	2.8	31	60	0.353	24	60	0.274
2900500	378418.5	2.6	29	60	0.33	22	60	0.252
2900541	378389.2	1.2	23	60	0.263	17	60	0.196
2900582	378359	0.9	13	60	0.151	11	60	0.129
2900621	378330.8	1	14	60	0.162	11	60	0.129
2900662	378305.3	1.4	16	60	0.185	13	60	0.151
2900707	378270	0.9	12	60	0.14	10	60	0.117
				Average	0.545			0.432

Table ST2: Area available in Zaid, Kharif and Rabi seasons for the years 1999-2015

ZAID PERIOD (Feb-May)																	
year	1999	2000	2001	2002	2003	2004	2005	2006	2007	2008	2009	2010	2011	2012	2013	2014	2015
Max Streamflow (cumecs)	10228	12235	9435	10411	10589	15146	11645	8829	12852	12007	10026	21788	10694	13869	12488	11627	11683
Dryland area	1893.1	1704	1970	1875	1858	1470	1755	2029.4	1559	1720	1912	955	1847	1197	1688	1757	1751
Area under 0-0.3m	56.61	70.84	49.68	57.42	58.2	59.6	62.8	43.3	71.3	64.7	55.7	61.1	58.6	57.1	76.53	62.7	63.1
Area under 0.3-0.6m	63.9	70.2	57.31	64.4	64.8	79.3	67.7	50.9	81.2	68.7	63.3	95.4	65.1	108.29	71.56	67.7	67.8
Area under 0.6-0.9m	55.21	73.32	49.97	57.14	59.1	85.3	70.1	46.8	78.8	73.8	53.1	101.1	60.1	95.43	72.83	70	70.5
Total area (Ha)	2068.8	1918.3	2126.9	2053.9	2040.1	1694.2	1955.6	2170.4	1790.3	1927.2	2084.1	1212.6	2030.8	1457.8	1908.9	1957.4	1952.4
KHARIF PERIOD (Jun-Sep)																	
year	1999	2000	2001	2002	2003	2004	2005	2006	2007	2008	2009	2010	2011	2012	2013	2014	2015
Max Streamflow (cumecs)	29146	31638*	29781	29149	33159*	40975*	34377*	26603	31875*	39876*	31769*	34656*	37349*	34737*	26089	26648	26627
Dryland area	797.95	-	792.41	797.93	-	-	-	827.2	-	-	-	-	-	-	838.91	826.17	826.65
Area under 0-0.3m	23.48	-	20.41	23.47	-	-	-	34.57	-	-	-	-	-	-	35.8	34.46	34.51
Area under 0.3-0.6m	33.21	-	30.25	33.2	-	-	-	47.43	-	-	-	-	-	-	52.24	47.01	47.2
Area under 0.6-0.9m	40.75	-	36.57	40.73	-	-	-	59.95	-	-	-	-	-	-	65.87	59.43	59.67
Total area (Ha)	895.39	0.00	879.64	895.33	0.00	0.00	0.00	969.15	0.00	0.00	0.00	0.00	0.00	0.00	992.82	967.07	968.03
RABI PERIOD (Oct-Jan)																	
year	1999	2000	2001	2002	2003	2004	2005	2006	2007	2008	2009	2010	2011	2012	2013	2014	2015
Max Streamflow (cumecs)	18019	14253	19683	14923	20745	19607	14500	13259	14998	15495	14585	20338	14620	21395	12151	13160	12549
Dryland area	1226.9	1563.2	1085.8	1511.4	1008.2	1092.2	1597.8	1413.9	1486.3	1440.9	1609.7	1035.6	1612.7	969.1	1710.0	1449.2	1666.9
Area under 0-0.3m	60.85	57.98	61.60	56.33	65.19	61.59	56.38	65.64	56.50	59.71	55.83	63.19	55.64	66.13	68.59	67.04	75.66
Area under 0.3-0.6m	93.11	81.98	101.0	75.33	102.0	100.73	69.26	92.11	78.28	81.00	64.88	102.49	63.44	99.96	69.61	89.47	73.18
Area under 0.6-0.9m	101.86	76.03	112.13	78.82	107.29	111.66	60.27	85.47	85.16	86.30	54.84	111.41	53.20	101.71	73.50	83.85	73.83
Total area (Ha)	1482.1	1779.20	1360.69	1721.94	1283.01	1366.26	1783.73	1657.21	1706.33	1668.00	1785.28	1312.73	1785.02	1237.05	1921.86	1689.62	1889.64

*Represents discharges above 30000 cumecs. Above this value the sandbar area were considered vulnerable to cropping due to risk of flooding and thus the areas were not calculated.

Table ST3: Cost of cultivation/production of crops/activities practiced in sandbars obtained during interview with farmers

Sl. No	Particulars	Approximate cost of cultivation/production (Rs.)
1.	**Vegetables* and potatoes**	
(a)	*Fixed cost*	
	Land on lease	Rs. 5000-6000/Bigha
(b)	*Operational cost*	
	Seeds	Rs. 500/Bigha
	Fertilizers	Rs. 3500/Bigha
	Medicine	Rs. 500/Bigha
	Human Labour	Rs. 6000-7000/Bigha (Sowing to Harvesting)
	Animal Labour	Rs. 500/Bigha
	Machine power	Nil
	Transportation	Rs. 1500
(c)	Total cost (a) + (b)	Rs.17000/Bigha
2.	**Dairy farming**	
(a)	*Fixed cost*	
	Land on lease	Rs. 5000-6000/Bigha
(b)	*Operational cost*	
	Human Labour	Rs. 350-400/day
	Cattle feed	Rs. 50/day/animal
	Medicine	Rs. 50/animal
(c)	Total cost (a) + (b)	Rs. 5500-6500
3.	**Paddy cultivation**	
(a)	*Fixed cost*	
	Land on lease	Rs. 5000-6000/Bigha
(b)	*Operational cost*	
	Seeds	Rs. 1000/Bigha
	Fertilizers	Rs. 3500/Bigha
	Medicine	Rs. 500/Bigha
	Human Labour	Rs. 6000-7000/Bigha (Sowing to Harvesting)
	Animal Labour	Rs. 500/Bigha
	Machine power	Nil
(c)	Total cost (a) + (b)	Rs.18000/- per Bigha
4.	**Cereals and Pulses cultivation****	
(a)	*Fixed cost*	
	Land on lease	Rs. 4000-6000/Bigha
(b)	*Operational cost*	
	Seeds	Rs. 1200/Bigha
	Fertilizers	Rs. 4500/Bigha
	Medicine	Rs. 500/Bigha
	Human Labour	Rs. 6000-7000/Bigha (Sowing to Harvesting)
	Animal Labour	Rs. 500/Bigha
	Machine power	Nil
(c)	Total cost (a) + (b)	Rs.17000/- per Bigha

Bigha is the unit of measurement of land in Assam (1 Bigha = 0.14 Hectare), Rupees (Rs.) unit of currency in India

* includes costs varies depending on the type of vegetables, demand and season of the year

** includes maize and wheat.

Table ST4: Flood tolerant varieties of crops

Crop	Flood tolerant crop varieties
Rice	CR Dhan 502, CR Dhan 505, Durga, Gayatri, Sarla, Hemavathi, Jaladhi 1, Jaladhi 2, JalaMani, , Jalnidhi, Neerja, Pooja, Prateeksha, Sambha Mahsuri, Sub-1Swarna Sub-1, Varshadhan
Maize	HM-5, Seed Tech-2324, HM-10, HTL lines, PMH-2, B73, SUS lines, Z. luxurians, and Z. mays ssp. huehuetenangensis Z. nicaraguensis
Barley	H. marinum and H. spontaneum
Wheat	Triticum macha L. or T. dicoccum cv., T. spelta
Rapeseed	B. juncea and B. carinata, GH01, Zhongshuang 9,
Jute	Bidhan Pat-1, JRC 321, JRC 532, JRC-517, JRC 7447, JRO 878, JRO 7835
Pulses	Pigeon pea (Asha (ICPL 87119)

List of Publications

Journals

Gaurav Talukdar, Arup Kumar Sarma, and Rajib Kumar Bhattacharjya. "Integrating optimization and damage estimation to increase economic benefit and ensure food security under seasonal land variability" Journal of Environmental Management, Elsevier, 320, 115872. https://doi.org/10.1016/j.jenvman.2022.115872

Gaurav Talukdar, Arup Kumar Sarma, and Rajib Kumar Bhattacharjya (2022). "Assessment of Land use change in riverine ecosystem and utilizing it for socio-economic benefit." Environmental Monitoring and Assessment, Springer, Manuscript No.: EMAS-D-21-04214. (*accepted*)

Gaurav Talukdar, Arup Kumar Sarma, and Rajib Kumar Bhattacharjya (2021). Sediment analysis and modelling based approach for optimal allocation of riverine sandbar for socio economic benefits. Ecological Engineering, Elsevier, 173, 106415. https://doi.org/10.1016/j.ecoleng.2021.1064152

Gaurav Talukdar, Arup Kumar Sarma, and Rajib Kumar Bhattacharjya (2020). Mapping agricultural activities and their temporal variations in the riverine ecosystem of the Brahmaputra River using geospatial techniques. Remote Sensing Applications: Society and Environment, Elsevier 20 (August), 100423. https://doi.org/10.1016/j.rsase.2020.100423

Submitted/communicated

Gaurav Talukdar, Rajib Kumar Bhattacharjya and Arup Kumar Sarma. "Understanding the effect of long-term and short-term hydrological components on landscape ecosystem" Ecological Information, Elsevier (Under Review). Manuscript No.- ECOINF-D-22-00708.

Gaurav Talukdar, Rajib Kumar Bhattacharjya, and Arup Kumar Sarma. "Optimal cropping pattern based on short-term streamflow forecasts to improve agricultural economic benefits and crop productivity under uncertainties" Hydrological Sciences Journal, Taylor and Francis (Under Review). Manuscript No.- HSJ-2022-0213

Under preparation

Gaurav Talukdar, Rajib Kumar Bhattacharjya, and Arup Kumar Sarma. "Agricultural risk assessment to estimate the potential economic loss in floodplains of Large Rivers"

Conference Presentations/proceedings

Gaurav Talukdar, Arup Kumar Sarma, and Rajib Kumar Bhattacharjya. Evaluating the Phytoplankton activities near Riverine Sandbars by estimating Chlorophyll-a Concentrations. AGU Fall meeting 2021, New Orleans, LA, USA, 13 - 17 December 2021

Gaurav Talukdar, Arup Kumar Sarma, and Rajib Kumar Bhattacharjya. "Riverine ecosystem for socio economic development" 15th IHE PhD Symposium for Collaborative Water Resources Management for a Water Secure World organized by IHE Delft Institute for Water Education, 14-15 October 2021, Netherlands

Gaurav Talukdar, Rajib Kumar Bhattacharjya and Arup Kumar Sarma, Effect of Long-Term and Short-Term Hydrological Components in Riverine Sandbars. AGU Fall meeting 2022, Chicago, IL, USA, 12 - 16 December 2022